TECHNISCHE UNIVERSITÄT MÜNCHEN

Lehrstuhl für Experimentelle Genetik

Characterization of RNF43, a novel negative regulator of the Wnt signaling pathway

Anke Loregger

Vollständiger Abdruck der von der Fakultät Wissenschaftszentrum Weihenstephan für Ernährung, Landnutzung und Umwelt der Technischen Universität zur Erlangung des akademischen Grades eines

Doktors der Naturwissenschaften

genehmigten Dissertation.

Vorsitzender:	Univ.-Prof. Dr. D. Haller
Prüfer der Dissertation:	1. Univ.-Prof. Dr. M. Hrabé de Angelis
	2. Univ.-Prof. Dr. M. Gerhard

Die Dissertation wurde am 26.09.2012 bei der Technischen Universität München eingereicht und durch die Fakultät Wissenschaftszentrum Weihenstephan für Ernährung, Landnutzung und Umwelt am 08.02.2013 angenommen.

I hereby confirm that I wrote this thesis at the Technical University of Munich suggested and guided by Prof. Dr. Markus Gerhard without external help and that I only applied to the listed literature references.

Munich, September 2012

_____

Anke Loregger

Acknowledgements

An dieser Stelle möchte ich die Gelegenheit nutzen mich bei jenen Menschen zu bedanken, die mich bei der Durchführung dieser Doktorarbeit begleitet und unterstützt haben, und ohne deren Hilfe die Durchführung dieser Arbeit nicht möglich gewesen wäre.

An erster Stelle geht mein besonderer Dank an den Betreuer meiner Arbeit, Prof. Dr. Markus Gerhard, für die Möglichkeit, ein breites Spektrum an Wissen und Arbeitstechniken zu erlernen, für die unzähligen interessanten Ideen, die Unterstützung meiner Arbeit durch wertvolle kritische Kommentare und nützliche Hinweise, das Korrekturlesen dieser Arbeit, sowie für die Möglichkeit, in seiner Arbeitsgruppe an diesem spannenden und vielseitigen Projekt zu arbeiten. Herzlichen Dank für die Betreuung während der letzten Jahre!

Darüber hinaus gilt mein besonderer Dank meinem Doktorvater, Prof. Dr. Hrabé de Angelis, für die Vertretung meiner Doktorarbeit vor dem Wissenschaftszentrum Weihenstephan der Technischen Universität München, sowie an Prof. Dr. Dirk Haller für die Übernahme des Vorsitzes der Prüfungskommission.

Darüber hinaus möchte ich mich bei Prof. Dr. Dirk Busch für die Möglichkeit, einen Teil dieser Arbeit in seinem Institut anfertigen zu dürfen, bedanken.

Für die Durchführung dieser Arbeit waren auch einige Kooperationspartner von großem Wert, bei denen ich mich nun an dieser Stelle bedanken möchte.

Herzlichen Dank an Dr. Ingrid Renner-Müller, Petra Renner sowie dem Mausstall-Team des Genzentrums der LMU München für die Einarbeitung und Unterstützung, sowie Hilfe bei Mausfragen, und an Dr. Maik Dahlhoff für die Durchführung der Embryonenspülungen. Mein besonderer Dank gilt auch Dr. Marlon Schneider für seine uneingeschränkte Hilfe.

Bei Dr. Dietmar Gradl möchte ich mich für die Durchführung der Xenopus-Versuche bedanken, und bei Dr. Gerhard Przemeck für die Hilfestellung bei der Durchführung der Whole Mount *In Situ* Hybridisierungen.

Herzlichen Dank auch an Prof. Dr. Klaus-Peter Janssen und Dr. Ulrich Nitsche für die Bereitstellung von cDNA aus Tumorproben, sowie an Prof. Dr. Klaus-Peter Janssen für seinen wertvollen fachlichen Input. Dafür möchte ich mich auch bei Dr. Pantelis Hatzis herzlich bedanken.

Mein besonderer Dank gilt auch meinen Kollegen der Arbeitsgruppe Gerhard. Für die große Unterstützung und Hilfsbereitschaft während meiner Promotionszeit, sowie für unzählige fachlich wichtige Diskussionen sowie die angenehme Zusammenarbeit möchte ich mich bei allen Kollegen der Arbeitsgruppe Gerhard herzlichst bedanken.

Vor Allem gilt mein besonderer Dank…

…der ursprüngliche Formation der AG Gerhard (Behnam, Florian, Jeannette, Kathi, Michael und Zohra), dafür, dass sie mir die Eingewöhnungszeit erleichtert haben.

…dem RNF43-Team (Martina, Kathrin und Raquel), für die vielen fachlich hilfreichen Diskussionen, die angenehme Zusammenarbeit und die uneingeschränkte Unterstützung in allen Bereichen.

…Eva, Kathi, Raphaela, Sarah, Florian, und vor allem Jeannette, für die geduldige Hilfe bei Maus-Angelegenheiten.

…Christian, Jeannette und Kathi, und natürlich besonders dem RNF43-Team, für die Unterstützung bei vielen Experimenten und technischen Fragestellungen.

…Behnam, für die kompetente und geduldige Beantwortung aller inhaltlichen und methodischen Fragen, für viele interessante Gespräche, für die Einarbeitung während der Anfangsphase sowie für Transportfahrten.

…Miriam, Esther, Martina und Kathrin, für den wertvollen Beitrag zum Projekt im Rahmen der Masterarbeit.

Herzlichen Dank auch an die 9-Uhr und 16-Uhr Kaffeetrinker, besonders an Eva, Ina, Jeannette, Kathi und Zohra, für die unzähligen Runden Kaffee sowie die vielen lustigen Zeiten in und vor allem auch außerhalb des Labors.

An dieser Stelle möchte ich mich auch herzlichst bei meinem privaten Umfeld bedanken. Mein besonderer Dank gilt meinen Eltern für die uneingeschränkte Unterstützung meines gewählten Lebensweges, sowie das Wissen, mich immer auf sie verlassen zu können.

Vor allem aber danke ich Frederik, der mich durch alle Phasen der Doktorarbeit mit unendlich viel Geduld und Verständnis begleitet hat, für seine 100 %ige Unterstützung sowie Motivation.

Index of Contents

Index of Figures

Index of Tables

Abbreviations

°C	Degree Celsius
µg	Microgram
µl	Micorliter
AFAP	Attenuated FAP
Amp	Ampicillin
AP axis	Anterior-posterior axis
APC	Adenomatosis polyposis coli
APS	Ammonium persulfate
ATCC	American type culture collection
bp	Basepairs
BSA	Bovine serum albumin
Ca^{2+}	Calcium
$CaCl_2$	Calcium chloride
CBC cell	Crypt base columnar cell
cDNA	Complementary DNA
CFP	Cyan fluorescent protein
CIN	Chromosomal instability
CO_2	Carbon dioxide
CRC	Colorectal cancer
d	Destilled
DAPI	4',6-Diamidinio-2-phenylindole
dd	Bidestilled
DMEM	Dulbecco's Modified Eagles Medium
DMSO	Dimethyl sulfoxide
DNA	Deoxyribonucleic acid
dNTP	Deoxyribonucleoside triphosphate
DOC	Sodium deoxycholate
DTT	Dithiothreitol
DV axis	Dorsoventral axis
E. coli	*Escherichia coli*
EDTA	Ethylenediaminetetraacetic acid
ER	Endoplasmatic reticulum

EtOH	Ethanol
FAP	Familiar adenomatous polyposis
FCS	Fetal calf serum
FITC	Fluorescein isothiocyanate
g	Gram
GFP	Green fluorescent protein
h	Hour
H_2O	Water
Hh	Hedgehog
HNPCC	Hereditary nonpolyposis colorectal cancer
HRP	Horseradish peroxidase
IF	Immunofluorescence
IP	Immunoprecipitation
ISC	Intestinal stem cell
KAc	Potassium acetate
KCl	Potassium chloride
kDa	Kilodalton
KH_2PO_4	Potassium phosphate
L	Liter
LB	Lucia broth
LiCl	Lithium chloride
LR axis	Left-right axis
LRC	Label retaining cell
M	Molar
mA	Milliampere
MEM	Minimum essential medium
MetOH	Methanol
mg	Milligram
MG132	Z-Leu-Leu-Leu-al
min	Minute
ml	Milliliter
mM	Millimolar
MMR	Mismatch repair
$MnCl_2$	Manganese chloride

mRNA	Messenger RNA
MSI	Microsatellite instability
MTT	Thiazolyl blue tetrazolium bromide
MW	Molecular weight
Na_2HPO_4	Disodium phosphate
NaCl	Sodium chloride
NaOAc	Sodium acetate
NaOH	Sodium hydroxide
ng	Nanogram
nM	Nanomolar
NPC	Nuclear pore complex
o.N.	Overnight
OD	Optical density
P/S	Penicillium/Streptomycin
PBS	Phosphate buffered saline
PCP	Planar cell polarity
PCR	Polymerase chain reaction
PFA	Paraformaldehyde
pH	Pondus Hydrogenii
qPCR	Quantitative PCR
RAD axis	Radial axis
RNA	Ribonucleic acid
RNase	Ribonuclease
rpm	Rounds per minute
RT	Room temperature
RT-PCR	Real-time PCR
S.D.	Standard deviation
SDS	Sodium dodecyl sulfate
SDS-PAGE	Sodium dodecyl sulfate polyacrylamide gel electrophoresis
sec	Second
siRNA	Small inhibitory RNA
TA cell	Transit amplifying cell
TCA	Trichloroacetic acid
TEMED	Tetramethyldiamine

Tris	Tris(hydroxymethyl)aminomethane
UV	Ultraviolet
V	Volt
v/v	Volume for volume
w/w	Weight for weight
WB	Western blot
Wg	Wingless
Zn^{2+}	Zinc

Summary

Colorectal cancer is one of the most commonly diagnosed cancers. Approximately 5 % of the Western population will develop colorectal malignancies during their lifetime. Since there is a continuous need for new therapeutic approaches, the identification of mechanisms underlying tumorigenesis is crucial.

The canonical Wnt signaling pathway plays a crucial role during embryonic development, maintains homeostasis of a variety of tissues, controls intestinal stem cell self-renewal, and regulates proliferation, morphology and motility. Deregulation of the canonical Wnt signaling pathway is tightly associated with several cancers, in particular carcinogenesis in the intestine. More than 90 % of colon cancers and a high percentage of other cancers evolve from activating mutations in the Wnt signaling pathway. Since elevated activation of the Wnt signaling pathway is involved in the development of most cases of colorectal carcinomas, new therapeutic approaches concentrate on antagonists of the Wnt signaling pathway in order to decrease elevated Wnt activity in tumors.

RNF43 was initially identified as an oncogene upregulated in colon cancer. It was recently shown to be a target gene of the Wnt signaling pathway, highly expressed in intestinal crypts at presumed stem cell positions and overexpressed in intestinal adenomas and carcinomas.

Nevertheless, the specific contribution of RNF43 to tumorbiological ascpects as well as its exact role in the Wnt signaling pathway remained elusive and should therefore be investigated in this study. Furthermore, the expression pattern of RNF43 in mice and humans should be characterized.

In this study, RNF43 was shown to be a highly conserved protein among different species, mainly expressed in endoderm-derived tissues, like stomach and intestine. RNF43 was found to be overexpressed in intestinal tumor samples, but RNF43 mRNA levels were low in colon cancer cell lines due to transcriptional repression involving epigenetic silencing.

The Ubiquitin E3-Ligase RNF43 exhibited a function as a strong negative regulator of Wnt signaling activity *in vitro* and *in vivo*, a function that was dependent on an active RING domain, since inactivation of the RING domain not only completely reversed the inhibitory effect of RNF43, but also transactivated Wnt signaling activity. The protein mainly localized

to the nuclear membrane, the ER and the Golgi apparatus, with small protein amounts detectable inside the nucleoplasm. RNF43 inhibited RNF43 downstream or at the level of ß-catenin in the Wnt signaling cascade, and was shown to strongly associate with Tcf4 and CTBP, suggesting a function of RNF43 at the transcription complex.

Analysis of RNF43 deletion mutants revealed an essential function of the N-terminus in the function of the protein in the Wnt signaling pathway, since deletion strongly diminished the inhibitory effect. The N-terminus was additionally found to mediate the localization of RNF43.

Investigation of tumor samples revealed a correlation of high RNF43 mRNA expression and poor prognosis of patients, and RNF43 was found to be frequently mutated in tumor cell lines and samples, indicating a function of RNF43 as a tumor suppressor. Since functionally inactive RNF43 strongly activated Wnt signaling *in vitro*, a function of mutated RNF43 in tumors in deregulating Wnt signaling and thus promoting tumorigenesis is likely. The novel inhibitory function of RNF43 may pave the way for the development of new therapeutic approaches.

Zusammenfassung

Kolorektaler Krebs ist einer der am häufigsten diagnostizierten Krebsarten. Ungefähr 5 % der westlichen Bevölkerung entwickeln im Laufe des Lebens kolorektale Malignome. Da dringend und ständig neue therapeutische Ansätze benötigt werden, ist die Identifizierung der Mechanismen, welche der Krebsentstehung zugrunde liegen, von großer Bedeutung.

Der kanonische Wnt Signalweg spielt eine entscheidende Rolle bei der Embryonalentwicklung, hält die Homöostase in verschiedenen Geweben aufrecht, kontrolliert die Selbsterneuerung von Stammzellen und reguliert Wachstum, Morphologie und Motiliät. Die Deregulierung des kanonischen Wnt Signalweges steht in einem engen Zusammenhang mit der Entstehung von Krebs im Darm. Mehr als 90 % aller Darmkrebserkrankungen und ein ein hoher Prozentsatz anderer Krebserkrankungen findet ihren Ursprung in Mutationen von Genen des Wnt Signalweges, welche zu einer erhöhten Aktivität des Wnt Signalweges führen. Da eine erhöhte Aktivität des Wnt Signalweges die Entwicklung und das Fortschreiten vieler kolorektaler Karzinome begünstigt, konzentrieren sich neue therapeutische Ansätze auf Antagonisten des Wnt Signalweges, welche erhöhte Wnt Signalaktivität in Tumoren senken sollen.

RNF43 wurde ursprünglich als ein in Darmkrebs hochreguliertes Onkogen identifiziert. Vor kurzem wurde gezeigt, dass es sich bei diesem Gen um ein Zielgen des Wnt Signalweges handelt, welches besonders in intestinalen Stammzellen und in intestinalen Adenomen und Karzinomen stark exprimiert ist. Der spezifische Beitrag von RNF43 zu tumorbiologischen Aspekten sowie die genaue Rolle dieses Gens im Wnt Signalweg sind aber bisher unbekannt und sollten deshalb im Rahmen dieser Studie untersucht werden. Darüber hinaus sollte das Expressionsmuster von RNF43 charakterisiert werden.

In dieser Studie wurde gezeigt, dass RNF43 ein evolutionär hochkonserviertes Protein ist, welches hauptsächlich in Geweben exprimiert wird, welche vom Endoderm abstammen, wie z.B. im Magen und im Darm. Zusätzlich wurde eine erhöhte Expression des Proteins in Proben aus intestinalen Tumoren festgestellt. Im Gegensatz dazu wurde RNF43 in Darmkrebszelllinien nur niedrig exprimiert, was auf eine Repression der Transkription durch epigenetische Mechanismen zurückgeführt werden konnte.

Die Ubiquitin E3-Ligase RNF43 zeigte sowohl *in vitro* als auch *in vivo* eine Funktion als negativer Regulator des Wnt Signalweges. Inaktivierung der RING-Domäne von RNF43 hob den inhibitorischen Effekt von RNF43 auf den Wnt Signalweg nicht nur komplett auf, sondern führte sogar zu einer signifikanten Erhöhung der Wnt Signalaktivität, was auf eine Abhängigkeit der Funktion von RNF43 von einer aktiven RING-Domäne schließen lässt.

RNF43 lokalisierte hauptsächlich an der Kernmembran, dem Endoplasmatischen Reticulum und dem Golgi Apparat. Geringe Mengen des Proteins waren zusätzlich im Kernplasma detektierbar. RNF43 inhibierte den Wnt Signalweg nach oder auf Höhe von ß-Catenin in der Wnt Signalkaskade. Außderdem konnte gezeigt werden, dass RNF43 mit Tcf4 und CTBP interagiert, was auf eine Funktion von RNF43 am Transkriptionskomplex hinweist.

Die Analyse von RNF43 Deletionsmutanten zeigte eine essentielle Funktion des N-terminalen Bereiches dieses Proteins bei der inhibitorischen Funktion auf den Wnt Signalweg. Darüber hinaus wurde eine entscheidende Rolle des N-terminalen Bereiches bei der Lokalisation von RNF43 festgestellt.

Untersuchungen von Tumorproben zeigten einen deutlichen Zusammenhang zwischen hoher RNF43 mRNA Expression und schlechter Prognose von Patienten. Es konnte darüber hinaus gezeigt werden, dass die *RNF43* Gensequenz in Tumorzelllinien und Tumorproben häufig mutiert ist, was auf eine Rolle von RNF43 als Tumorsuppressor hinweist. Da nicht-funktionelles RNF43 den Wnt Signalweg *in vitro* stark aktivierte, ist es sehr wahrscheinlich, dass mutiertes RNF43 den Wnt Signalwegs dereguliert, und somit die Tumorgenese fördert. Dieser Ansatz könnte neue therapeutische Möglichkeiten eröffnen.

1 Introduction

1.1 Intestinal development

In all vertebrates, the intestine evolves in a similar process and early in development from the endoderm (reviewed in de Santa Barbara, van den Brink et al. 2003). A process called gastrulation results in a group of undifferentiated cells, termed the epiblast. These cells form the three germ layers: ectoderm, mesoderm and endoderm (reviewed in Wells and Melton 1999). The intestine is composed of all three germ layers: the endoderm forms the epithelium, the mesoderm builds up the smooth muscle layers, and the ectoderm includes the enteric nervous system (reviewed in de Santa Barbara, van den Brink et al. 2003).

The intestine is organized into several axes early in embryonic development: the anterior-posterior (AP) axis, the dorsoventral (DV) axis, the left-right (LR) axis and the radial (RAD) axis. Differentiation along the AP axis and regional specific morphologic development give rise to three domains: the foreintestine, which will develop into the adult stomach, pharynx and esophagus, the midintestine, which will form the small intestines, and the hindintestine, which will give rise to the adult colon. The adult intestine has a very specific pattern in all four axes, both regarding morphology and functionality (reviewed in de Santa Barbara, van den Brink et al. 2003).

Resulting from the action of different transcription factors and signaling pathways during fetal development, cells mature (reviewed in de Santa Barbara, van den Brink et al. 2003) and in the small intestine, interactions between the epithelium and the mesenchyme induce an evagination of villi as well as a postnatal invagination of crypts (reviewed in Brabletz, Schmalhofer et al. 2009). Whereas villi are long and thin in the small intestine, they are wide and flat in the colon. In contrast to the small intestine, villi of the colon disappear at the time of birth in some species, including humans (reviewed in de Santa Barbara, van den Brink et al. 2003). Thus, in the end, the small intestine consists of crypts and villi (reviewed in Brabletz, Schmalhofer et al. 2009). In contrast, the colon carries no villi, but has a flat surface epithelium. The second histologically important difference between the epithelium of the small intestine and the colon is that Paneth cells are absent in the colon (reviewed in Scoville, Sato et al. 2008).

Both intestinal development as well as tissue homeostasis in adult organisms are based on a constant crosstalk between cells of the epithelium and the mesenchyme, which is mediated by pivotal signaling pathways, including the Wnt, Hedgehog (Hh), Notch, PI3K/Akt and BMP pathways. Deregulations in these interactions, which are tightly controlled, rapidly result in the development of tumors (Brabletz, Schmalhofer et al. 2009).

1.2 Architecture, function and homeostasis of the intestine

The gastrointestinal tract of vertebrates is a complex and specialized organ system. It is derived from an ordinary tubal structure. It includes the digestive system of the esophagus, stomach, intestines, and colon, as well as gastrointestinal tract derivatives, like the thyroid, lungs, pancreas and liver, which are structures that originally arise from the early intestine endoderm (reviewed in de Santa Barbara, van den Brink et al. 2003).

The intestine is divided into the small intestine, which can be subdivided into the duodenum, the jejunum and the ileum, and the colon (reviewed in van der Flier and Clevers 2009). The small intestine is composed of crypts and villi (reviewed in Brabletz, Schmalhofer et al. 2009), which enormously increase the surface of the epithelium. The villi are lined by a single layer of epithelial cells (reviewed in van der Flier and Clevers 2009). The function of the epithelium is to create a barrier between bacteria of the lumen and the rest of the body (reviewed in Abreu 2010) and to digest and adsorb nutrients and water (reviewed in van der Flier and Clevers 2009). Underlying the epithelium, the intestine consists of a layer of mesenchyme, which structurally supports the epithelium and provides it with growth signals. In addition, blood vessels, smooth muscles, neuronal cells as well as lymphocytes are embedded into the intestine (reviewed in Gregorieff, Pinto et al. 2005).

In the adult small intestine, a common pool of epithelial stem cells reside in crypts of Lieberkühn and give rise to the 4 differentiated cell types: Paneth cells, absorbing enterocytes, goblet cells and enteroendocrine cells (Cheng and Leblond 1974). In contrast to the other differentiated cell types, which populate the villi, Paneth cells are found exclusively at the base of the crypt. At cell positions 1 to 3, counting from the crypt base, Paneth cells make up 31 - 47 % of the epithelial cells, whereas they are rarely seen towards the upper part of crypts or villi. Together with crypt-base columnar (CBC) cells, which are located in between the Paneth cells in the crypts and exhibit features of undifferentiated cells, these two cell types

accomplish for most of the epithelial cells found in crypts (Cheng 1974; Cheng and Leblond 1974).

During the lifetime of an organism, most tissues are permanently renewed through substitution of differentiated cells by new cells which develop from stem cells, which exhibit tissue specificity (Nicolas, Kim et al. 2007). The intestinal epithelium is the most actively self-renewing tissue of adult mammals (Heath 1996). Thus, renewal occurs very rapidly, and the muCos7a of the intestine is reconditioned every few days. The various cell types present in the epithelium of the small intestine are renewed in about three days in the case of columnar, mucous and enteroendocrine cells, and in two to three weeks in the case of Paneth cells (Cheng and Leblond 1974). Therefore, the intestinal stem cells' immediate progeny form a rapidly cycling population of transit amplifying (TA) cells and replicate frequently (reviewed in Potten, Booth et al. 1997; Stappenbeck, Wong et al. 1998; Stappenbeck, Mills et al. 2003).

Three of the four epithelial lineages that have been given rise by the stem cells, namely the absorptive enterocytes, mucus-producing goblet cells, and enteroendocrine cells, mature and differentiate during they migrate upward towards the lumen. Since these cells continuously migrate towards the top of the villi, the location of a cell indicates its stage in the maturation process (Booth and Potten 2000; Scoville, Sato et al. 2008). Migration is a well-organized and very rapid process. Cells reach the top of the villi after 2 - 5 days, where they are removed by apoptosis and/or extrusion and shed into the lumen (reviewed in Stappenbeck, Wong et al. 1998). The amount of removed cells is not random, but maintenance of tissue homeostasis requires a balance between cell loss and the newly produced cells. (Hall, Coates et al. 1994).

In contrast, Paneth cells differentiate as they move in the opposite direction, hence towards the base of the crypt, where they stay for about 20 days before being subjected to phagocytosis by their adjacent cells (reviewed in Stappenbeck, Wong et al. 1998). Thus, Paneth cells represent the only differentiated cells that do not migrate upwards, but settle at the bottom of crypts, where they perform a function in innate immunity and antibacterial defense through secretion of antibacterial peptides (reviewed in van der Flier and Clevers 2009). Figure 1 illustrates a model of the architecture of the small intestinal epithelium and its different cell lineages.

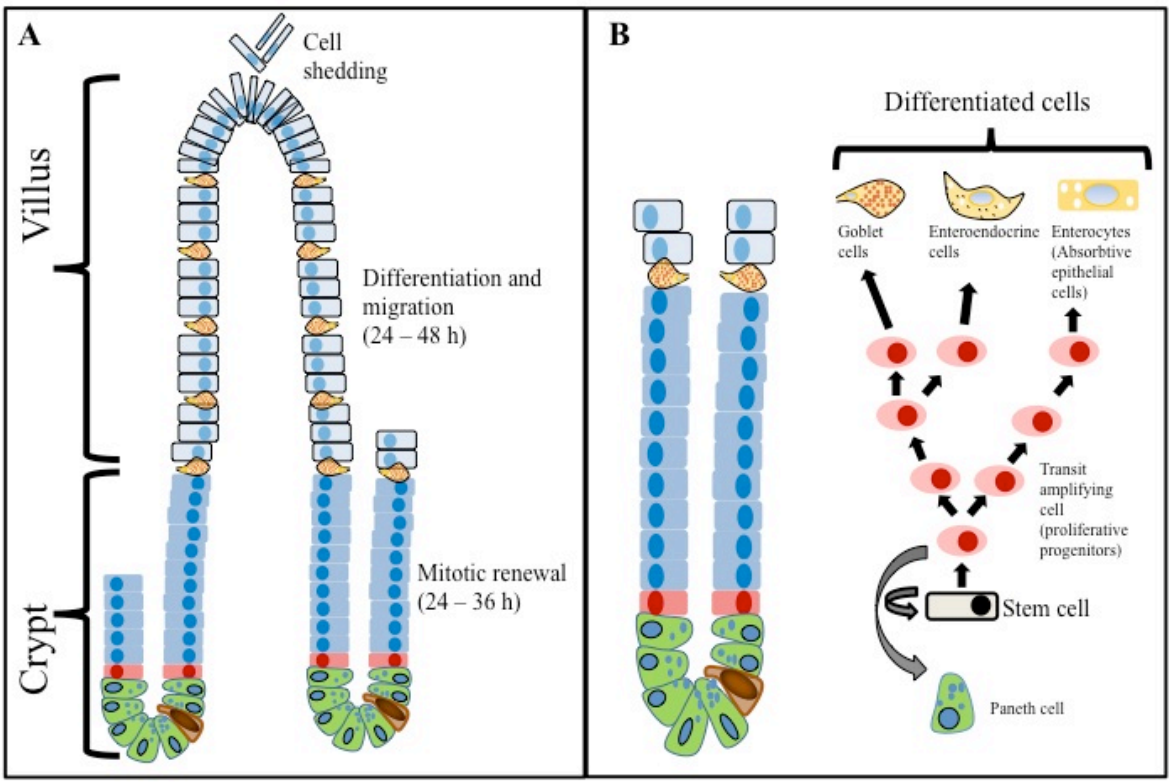

Figure 1 Model of the architecture of the small intestinal epithelium.
(adapted from Radtke and Clevers 2005) (A) The epithelial monolayer lines crypts and villi. (B) The scheme illustrates the stem cells, the transit-amplifying cells, and the four resulting differentiated cell lineages, divided into Paneth cells, the secretory lineage (goblet cells and enteroendocrine cells) and the enterocyte lineage (absorptive cells).

1.3 Intestinal stem cells

1.3.1 Stem cell properties

The epithelium of the intestine is an excellent model for studying the biology of stem cells as well as lineage specification, and it is probably the simplest mammalian model for the investigation of the self-renewal of tissue (Radtke and Clevers 2005).

Several studies showed that intestinal crypts are monoclonal. Thus, each crypt is derived from a monoclonal cell population derived from a single stem cell (Roth, Hermiston et al. 1991; Hermiston, Green et al. 1993; Bjerknes and Cheng 1999; Novelli, Cos7su et al. 2003), and each villus is provided with cells of several monoclonal crypts (reviewed in Hermiston, Green et al. 1993).

It turned out to be difficult to find a specific molecular fingerprint for stemness. The difficulties in finding a single common genetic program prevalent in different stem cells raised the question whether stem cells have common properties that are unique compared to other cells, hence whether there is a unique definition of stem cells.

Potten et al. defined stem cells as undifferentiated cells, which are capable of proliferation, self-maintenance, the production of a large number of undifferentiated functional progeny, tissue regeneration after injury and flexibility in the use of these options (Potten and Loeffler 1990). Thus, according to Potten et al., two characteristics are the two important criteria for stemness: self-renewal and multipotency (reviewed in Snippert and Clevers 2011).

Thus, a defined adult stem cell signature is missing, and different types of adult stem cells in different tissues probably use variable mechanisms in order to achieve self-renewal and multipotency. Neither study could provide a unique transcriptional profile but only molecular similarities between stem cell populations (Ivanova, Dimos et al. 2002; Ramalho-Santos, Yoon et al. 2002; Fortunel, Otu et al. 2003; Wong, Liu et al. 2008), indicating that a combination of many genes rather than a few individual genes may be responsible for controlling the characteristics of stem cells. Nevertheless, it is possible that genes, which are unique for all stem cells and expressed at a low level, exist (Fortunel, Otu et al. 2003).

1.3.2 Different models of intestinal stem cells

Approximately six intestinal stem cells (ISCs) are thought to be present in every crypt. The identity of these stem cells remains controversial, with two schools of thought dominating the literature, namely the classic model and the stem cell zone model (reviewed in van der Flier and Clevers 2009). The two models are illustrated in Figure 2.

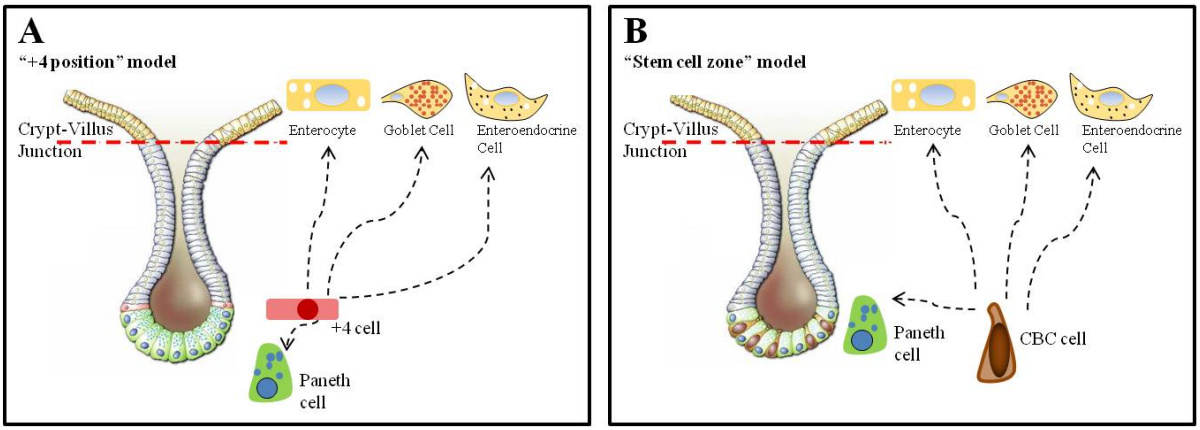

Figure 2 The two opponent models illustrating the identity of intestinal stem cells.
(adapted from Barker, van de Wetering et al. 2008) (A) The "+4 position model", or "classical model", proposed by Potten and colleagues, suggested that stem cells of the small intestine occupy position +4, the fourth cell position counting from the crypt bottom. (B) The "stem cell zone model" proposed by Leblond and colleagues, suggested that undifferentiated, actively cycling crypt columnar cells, which are located intermingled with Paneth cells, are the stem cells of the intestine.

The "+4 position model", or "classical model", which was proposed by Potten and colleagues in 1974, suggested that stem cells of the small intestine occupy position +4, the fourth cell position counting from the crypt bottom. Positions 1 to 3 are occupied by differentiated Paneth cells. In the colon, where Paneth cells are absent, stem cells directly reside at the bottom of crypts (Potten, Kovacs et al. 1974). Due to the absence of specific molecular markers for the identification of stem cells, the localizations of putative intestinal stem cells could only be identified by indirect means (reviewed in Brabletz, Schmalhofer et al. 2009). Thus, Potten et al. used the long-term label retaining technique to mark putative intestinal stem cells, and detected long-term DNA label-retaining cells (LRCs) at the +4 position (+4 LRCs) (Potten, Kovacs et al. 1974; Marshman, Booth et al. 2002; Potten, Owen et al. 2002). Furthermore, they have unrevealed these +4 LRCs as cells which are especially sensitive to radiation, a property which is suggested to protect stem cells from damage (Potten 1977). The +4 label retaining cells were considered as ISCs for a long time (reviewed in Brabletz, Schmalhofer et al. 2009).

The second model, the stem cell zone model, originated more than 30 years ago, with the identification of crypt base columnar (CBC) cells. CBC cells are small, undifferentiated, cycling cells that are located in between the Paneth cells at the base of crypts. Cheng, Leblond and Bjerknes suggested that CBC cells may represent stem cells of the intestine (Cheng and Leblond 1974; Cheng and Leblond 1974; Bjerknes and Cheng 1981; Bjerknes and Cheng 1981; Bjerknes and Cheng 1999; Stappenbeck, Mills et al. 2003).

Recently, Barker and colleagues identified a Wnt target gene, *Lgr5/GPR49*, which is exclusively expressed in CBC cells in the crypt base interspersed between Paneth cells. Their finding was based on the observation that Wnt signaling is an important factor of intestinal stemness (reviewed in Brabletz, Schmalhofer et al. 2009). To investigate the stem cell potential of these Lgr5-expressing cells, (also called Lgr5 positive cells), Barker et al. generated a mouse model with an EGFP-ires-CreERT expression cassette downstream of the transcription start site of the endogenous *Lgr5* promoter. In lineage-tracking experiments using mice generated from an Lgr5-GFP-ires-CreERT x RosaLacZ cross, they showed that CBCs expressing Lgr5 fulfill all criteria of stemness. They self-renew, are pluripotent and can persist for a long time (Barker, van Es et al. 2007). In contrast to the current assumption that adult stem cells are maintained in a quiescent state and cycle very slowly, the intestinal stem cells marked by Lgr5 are rapidly cycling with an average cycling time of about a day (Barker, van Es et al. 2007).

Scoville et al. suggested that there are two types of intestinal stem cells that coexist: the +4 LRCs, which provide a "reserve" pool of ISCs in a quiescent state, and the actively cycling CBCs, which are ready to be regulated by factors released from the underlying cells of the stroma (reviewed in Scoville, Sato et al. 2008).

Despite the compelling work of Barker et al., a new study by Sangiorgi and Capecchi added another twist to the debate on the localization and identity of intestinal stem cells. They suggested that another pool of stem cells is present in the epithelium of the small intestine, which is characterized by expression of the marker *Bmi1*. In their study, they characterized the progeny of Bmi1-expressing cells using the same lineage-tracing approach that was used to characterize Lgr5 positive cells. They showed that the activation of the Cre recombinase expressed in Bmi1-expressing cells marks long-lived cell clones of all cell types, thus Bmi1-expressing cells are another pool of stem cells. Furthermore, loss of Bmi1, which is located near the bottom of crypts in the small intestine, above and occasionally between the Paneth cells (among the +4 position), results in depletion of the epithelium of the whole crypt units (Sangiorgi and Capecchi 2008).

A recent study of Tian *et al.* suggested that the quiescent Bmi1-expressing cells are acting upstream of rapidly cycling Lgr5-expressing stem cells and replenish the pool of active Lgr5 stem cells, in order to avoid exhaustion of the actively cycling stem cell pool. Furthermore, they demonstrated that homeostasis of the epithelium is not affected upon loss of Lgr5

positive cells, but in the case of loss of these cells, the production of progeny by cells expressing Bmi1 is enhanced, and Bmi1-expressing cells can constitute an alternative pool of intestinal stem cell (Tian, Biehs et al. 2011).

Further studies will be required in order to understand how different stem cell populations influence the activities of each other, how stem cell populations can substitute each other, and whether additional until now undiscovered stem cell populations exist.

1.3.3 Localization and maintenance of intestinal stem cells

The localization of stem cells within crypts and the loss of stemness in their progeny that migrate towards the top of the villi suggest that the surrounding area is perfect for their maintenance of stemness. Extracellular signals that are crucial for maintaining this environment are found at an optimal concentration at stem cell positions and diluted as cells move away. Some factors probably control the properties of stem cells, but impair the migration of stem cells towards the top of the villi as well as their differentiation (reviewed in Booth and Potten 2000). Thus, the stemness of stem cells is most likely an extrinsic characteristic (reviewed in van der Flier and Clevers 2009), and is determined by extracellular factors and the microenvironment, which constitute a niche for stem cells (reviewed in Nusse 2008).

In the niche, present stem cells compete for restricted amounts of growth factors, thus sustaining a balance between self-renewal and differentiation. In addition to small molecules such as retinoic acid, these factors are members of several signaling pathways, including BMP, Hedgehog (Hh), FGF and Wnt pathway (reviewed in Nusse 2008). In order to adequately regulate the behavior and important functions of stem cells, the niche must be flexible (reviewed in Voog and Jones 2010).

On the other hand, in order to maintain tissue homeostasis and to avoid degeneration of tissue and growth of tumors, intestinal stem cells have to be tightly controlled. Therefore, a fine-tuned interaction between epithelial and underlying stromal cells, which can be achieved by controlled production of limited concentration of ligands and their associated receptors, is necessary (reviewed in Brabletz, Schmalhofer et al. 2009).

Several interacting signaling pathways substantially contribute to the regulation of intestinal stem cells as well as to tissue development and homeostasis. Nevertheless, although all

interacting pathways are crucial regulators, Wnt signaling is the most dominant force in controlling intestinal stem cells (reviewed in Brabletz, Schmalhofer et al. 2009). In stem cells of various lineages, Wnt signaling and Wnt proteins are especially important for their maintenance (reviewed in Nusse 2008). For example, the transcription factor Tcf4 is particularly required for maintenance of the undifferentiated crypt cell compartment. In the intestine, loss of the transcription factor Tcf4 leads to the depletion of stem cells (Korinek, Barker et al. 1998). In contrast, elevated Wnt signaling activity, resulting from e.g. mutations in *APC* or *ß-catenin*, leads to an increase in size of the crypt compartment, resulting in an abnormal architecture of the tissue, thus polyp formation (Bienz and Clevers 2000).

1.4 Colon cancer

1.4.1 Epidemiology of colon cancer

Worldwide, colorectal cancer is the third most commonly diagnosed cancer in males and the second in females. More than 1.2 million new cancer cases and over 600 000 cases of death have occurred in 2008 (Jemal, Bray et al. 2011). There is a huge geographical variation in incidence, which is at least 25-fold. The highest incidence and mortality rates are observed in North America, Australia/New Zealand, Western and Eastern Europe, and the lowest rates are in Africa and Asia. Rates are intermediate in southern parts of South America (Parkin 2004) These large geographic differences most likely correlate with environmental exposures, especially diet (Parkin 2004), since risk factors for development of colorectal cancer include obesity, overconsumption of energy, physical inactivity, heavy alcohol consumption, smoking, a diet high in red or processed meats, and inadequate consumption of fruits and vegetables (Giovannucci 2002; Botteri, Iodice et al. 2008).

Approximately 5 % of the Western population will develop colorectal malignancies during their lifetime (Bienz and Clevers 2000). While colorectal cancer death rates have been decreasing in several Western countries due to early detection and advanced therapies, rates continue to increase in many countries with restricted health infrastructure, especially in Eastern Europe as well as in Central and South America (Jemal, Bray et al. 2011). Fortunately, progress has been made in identifying mechanisms of tumorigenesis (Ahmed 2005).

Colorectal cancer is traditionally divided into sporadic and familial (hereditary) cases (reviewed in Moran, Ortega et al. 2010).

1.4.2 Hereditary colon cancer

About 20 - 25 % of all colorectal cancer cases are an inherited form of disease (reviewed in Moran, Ortega et al. 2010). In approximately 1/5 of these cases, there is an association with well-characterized inherited mutations, whereas the reasons for the remaining cases of inherited colorectal cancers remain elusive so far (Jasperson, Tuohy et al. 2010).

The "Lynch syndrome", also called "hereditary nonpolyposis colorectal cancer (HNPCC) syndrome", is the most common type of hereditary colorectal cancer. Individuals with Lynch syndrome are predisposed to different types of cancer, especially colorectal cancer (Lynch and de la Chapelle 2003). The syndrome accounts for about 3 - 5 % of all colorectal cancer cases (reviewed in Stoffel, Mukherjee et al. 2009) and develops as a consequence of defective mismatch (MMR) repair associated with germline mutations in the DNA mismatch repair genes *MLH1*, *MSH2*, *MSH6* and *PMS2* (reviewed in Hampel, Frankel et al. 2008). The lifetime colorectal cancer risk is estimated to be about 50 - 80 % (Stoffel, Mukherjee et al. 2009; Jasperson, Tuohy et al. 2010), and HNPCC patients develop colon cancers and polyps at a younger age than patients with sporadic neoplasms (reviewed in Jasperson, Tuohy et al. 2010).

The second frequently inherited colorectal cancer syndrome is called "familial adenomatous polyposis (FAP)". It affects 1 in 10 000 individuals. From early adolescence on, patients develop hundreds to thousands of colonic adenomas, and the risk of developing colorectal cancer during lifetime is 100 % (reviewed in Jasperson, Tuohy et al. 2010). A less severe form of FAP, with about 69 % lifetime risk of developing colorectal cancer and a smaller number of colonic adenomatous polyps of about 30, is called "attenuated FAP (AFAP)" (Burt, Leppert et al. 2004). The disease-causing mutation in both FAP and AFAP was found to reside in the tumor suppressor gene *APC* (Groden, Thliveris et al. 1991; Kinzler, Nilbert et al. 1991; Nishisho, Nakamura et al. 1991; Joslyn, Richardson et al. 1993; Spirio, Olschwang et al. 1993).

Other hereditary colorectal cancer syndromes are called "MUTYH-associated polyposis", "Peutz-Jeghers syndrome", "juvenile polyposis syndrome" and "hyperplastic polyposis".

They are also associated with a high risk of colon cancer development, but they are less prevalent than the Lynch syndrome or FAP (Jasperson, Tuohy et al. 2010).

1.4.3 Sporadic colon cancer

About 75 - 80 % of colorectal cancers have sporadic origin. Sporadic colorectal cancers can originate from at least two different pathways. The two pathways can be distinguished by molecular differences, as well as distinct histopathological properties and clinical behaviors (reviewed in Moran, Ortega et al. 2010).

The traditional pathway, which involves chromosomal instability (CIN), is called "suppressor pathway" (reviewed in Moran, Ortega et al. 2010), and follows the model of Fearon and Vogelstein. Fearon and Vogelstein proposed a multi-step genetic model of colorectal carcinogenesis. According to this model, colorectal cancer (CRC) originates and progresses through the adenoma-to-carcinoma sequence, which is a series of well-defined histological stages with each of the stages characterized by specific mutations in oncogenes and tumor suppressor genes (Fearon and Vogelstein 1990). At least four genetic mutations are necessary in order to guarantee the development of colorectal cancer (reviewed in Fodde, Smits et al. 2001). In the overwhelming majority of cases of sporadic CRC, the initiating event is a constitutive activation of the Wnt signaling pathway (reviewed in Fodde, Smits et al. 2001), leading to the formation of benign adenomas (reviewed in van der Flier and Clevers 2009). The mutations in the Wnt signaling cascade either occur at the level of the tumor suppressor gene *APC* (Miyoshi, Ando et al. 1992; Powell, Zilz et al. 1992; Miyaki, Konishi et al. 1994), *AXIN2* (Liu, Dong et al. 2000), or the *CTNNB1* gene, coding for ß-Catenin, resulting in increased levels of Wnt signaling activity (Morin, Sparks et al. 1997; Rubinfeld, Robbins et al. 1997). Further mutations, e.g. in the classical oncogenes and tumor suppressor genes such as *KRAS*, *SMAD4* and *P53*, finally lead to the formation of metastasizing carcinomas (Fearon and Vogelstein 1990).

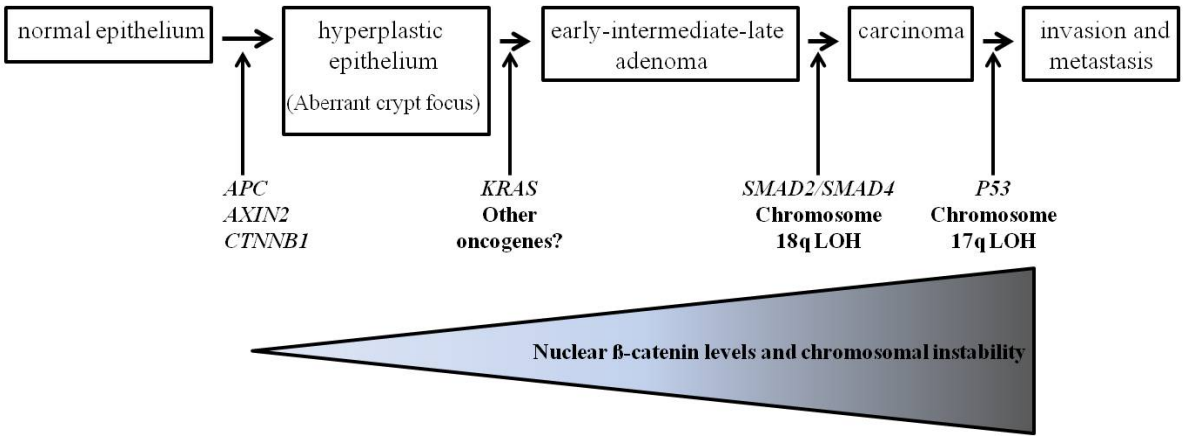

Figure 3 Schematic representation of the tumor progression model according to the model of Fearon and Vogelstein.
(adapted from Fodde, Smits et al. 2001) The earliest alterations in the formation of colorectal tumors are mutations leading to an activation of the Wnt signaling cascade, mainly in the *APC* gene. Further mutations, e.g. in the genes *KRAS*, *SMAD4* and *P53*, lead to progression of the tumor.

The other main colorectal carcinogenesis pathway, which is called "mutator pathway" or "microsatellite instability (MSI) pathway" is present in nearly 15 - 20 % of all cases of sporadic colorectal cancer (reviewed in Moran, Ortega et al. 2010). A defect in DNA mismatch repair genes results in mutations in the microsatellite sequences. Microsatellites are short sequences repeated in tandem (Ionov, Peinado et al. 1993; Thibodeau, Bren et al. 1993; Moran, Ortega et al. 2010). Throughout the genome, they are abundant. They exhibit polymorphism among individuals, but in each person, they have exactly the same length in every tissue (reviewed in Boland and Goel 2010). Tumors with Mismatch Repair (MMR) deficiency harbor a huge number of mutations. Mutation rates in these tumor cells are 100 - 1000- fold higher than in normal cells (Peltomaki 2001).

Since elevated activation of the Wnt signaling pathway is involved in most cases of colorectal carcinomas, new therapeutical approaches concentrate on proteins of the Wnt signaling pathway in order to decrease elevated Wnt activity. Components of the Wnt pathway could be alternative therapeutic targets, but it will first be important to understand the molecular and cellular biological function in detail (Daniels, Eklof Spink et al. 2001; Moon, Kohn et al. 2004). Since Wnt signaling performs essential functions like maintenance of homeostasis in the intestine (Pinto, Gregorieff et al. 2003), and a complete inhibition of Wnt signaling activity would result in the loss of the intestinal epithelium due to an absent proliferating crypt department (Korinek, Barker et al. 1998), a long way remains in order to generate new clinically applicable chemotherapeutics.

1.5 Wnt signaling pathway

The Wnt signaling pathway is an ancient and evolutionarily conserved pathway in metazoan animals (reviewed in Komiya and Habas 2008). In addition to its important function in the maintenance of stem cells (1.3.3), it plays a crucial role in various biological processes (reviewed in Logan and Nusse 2004; Clevers 2006; White, Nguyen et al. 2007). It regulates important developmental processes including cell-fate determination, proliferation, motility and the establishment of the primary body axis during vertebrate embryogenesis (reviewed in Harland and Gerhart 1997; Wodarz and Nusse 1998; Logan and Nusse 2004).

The first Wnt gene, mouse Wnt1, was discovered in 1982 as a proto-oncogene (Nusse and Varmus 1982). As a result, the main focus of research in the 1980s was targeted on the potential involvement of Wnt genes in cancer (reviewed in Nusse and Varmus 1992). In 1987, the Drosophila segment polarity gene *Wingless* (*Wg*) was identified as the homologue of Wnt1 (Cabrera, Alonso et al. 1987; Rijsewijk, Schuermann et al. 1987). Furthermore, several studies on the phenotypic analysis of *Wnt1* mutations in mice in 1990 (McMahon and Bradley 1990; Thomas and Capecchi 1990) demonstrated the importance of Wnt genes as important regulators of many developmental decisions (reviewed in Nusse and Varmus 1992; Parr and McMahon 1994; Cadigan and Nusse 1997).

In the following years, nearly 100 Wnt genes have been isolated from various different species, including humans. These Wnt genes encode for proteins harboring a conserved pattern of 23 cysteines and a signal sequence (reviewed in Wodarz and Nusse 1998).

Wnt proteins comprise a large family of secreted proteins, which perform their functions through cell surface receptors either on the producing or on the vicinal cells (reviewed in Wodarz and Nusse 1998). The extracellular Wnt proteins stimulate intracellular signal transduction cascades, including the canonical or Wnt/ß-catenin-dependent pathway and the non-canonical or ß-catenin-independent pathway (reviewed in Komiya and Habas 2008).

Wnt signaling regulates the transcription of several specific genes, which mainly determine cell fate and regulate proliferation (reviewed in Giles, van Es et al. 2003). In *Xenopus laevis* embryos, it is responsible for dorso-ventral axis specification, and ectopic expression of Wnt can induce the formation of a secondary body axis (Sokol 1999). In the fruit fly *Drosophila melanogaster*, the homologous Wingless (Wg) pathway is important for segment polarity and wing formation (reviewed in Cadigan and Nusse 1997). In mice, different phenotypes are

induced by depletion of different isoforms of Wnt proteins. For instance, lack of Wnt1 leads to depletion of most of the midbrain (McMahon and Bradley 1990), and removal of Wnt4 affects the kidneys (Stark, Vainio et al. 1994). Since Wnt7a is a dorsalizing factor, it is required for anterior-posterior patterning. In mice lacking Wnt7a, limb development is affected (Parr and McMahon 1995). In addition, there is a requirement for Wnt3a, since Wnt 3a depleted mice are deficient in the formation of the primary axis (Liu, Wakamiya et al. 1999).

In addition to its role in development, Wnt signaling controls proliferation and differentiation of healthy and malignant cells in the intestinal epithelium (van de Wetering, Sancho et al. 2002), as well as in stem cells of the intestinal epithelium (Korinek, Barker et al. 1998; Lin, Xu et al. 2008), the skin (Alonso and Fuchs 2003), muscles (Polesskaya, Seale et al. 2003) and the blood (Reya, Duncan et al. 2003).

1.5.1 The non-canonical Wnt signaling pathways

Vertebrate non-canonical Wnt signaling is involved in various diverse processes like gastrulation, convergent extension, cochlear hair cell morphology, heart induction, dorsoventral patterning, neuronal migration, and cancer. There are different mechanisms of non-canonical Wnt signaling transduction, including signaling through the release of calcium, JNK (c-Jun N-terminal kinase) and through G proteins (reviewed in Wallingford, Fraser et al. 2002; Veeman, Axelrod et al. 2003). The protein Dishevelled, with its PDZ and DEP domain, is crucial for the transduction of the signal (reviewed in Komiya and Habas 2008).

The non-canonical, or ß-catenin-independent Wnt signaling pathway, can be divided into the Planar Cell Polarity (PCP) pathway and the Wnt/Ca^{2+} pathway (reviewed in Komiya and Habas 2008).

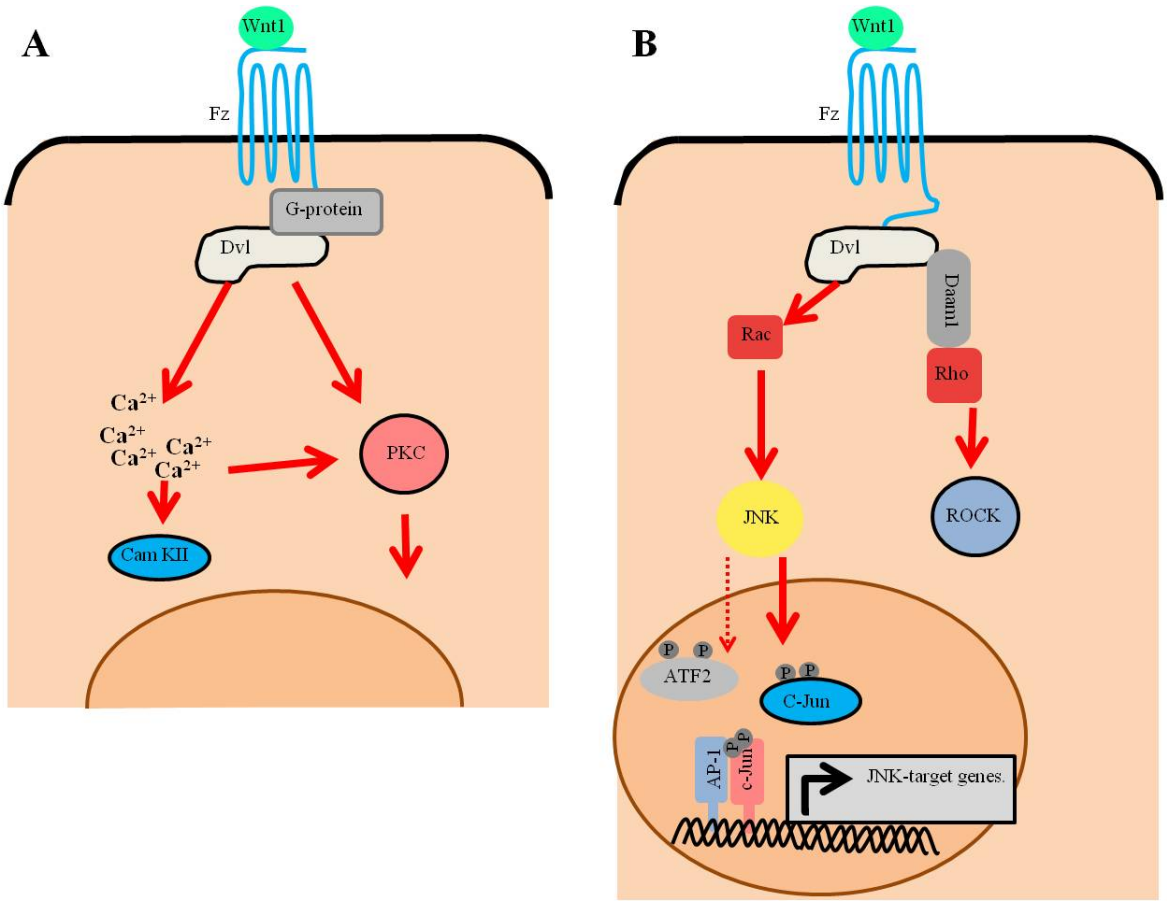

Figure 4 Schematic overview of the non-canonical Wnt signaling pathway components.
(adapted from Saadeddin, Babaei-Jadidi et al. 2009) (A) In the Wnt/Ca^{2+} pathway, Wnt signaling is mediated through heterotrimeric G-proteins, and involves different other factors, like the initiation factor Dishevelled (Dvl), PKC (protein kinase C) and CamK2 (calcium-calmodulin-dependent kinase 2). (B) In the planar cell polarity pathway, the activation of Rho and Rac small GTPases is mediated by two independent pathways, which are both initiated by Dishevelled (Dvl).

1.5.1.1 The polar cell polarity (PCP) pathway

The PCP pathway (Figure 4B) regulates important functions of the cell during various processes, such as gastrulation (reviewed in Wallingford, Fraser et al. 2002; Veeman, Axelrod et al. 2003), a complex morphogenetic developmental process that sets up the basic plan of the body. During this process, cell polarity, movement and adhesion need to be tightly controlled. (Habas, Dawid et al. 2003). In vertebrates, the so-called convergent extension (CE) movement, in which cells polarize, elongate along the mediolateral axis and intercalate towards the midline (convergence), leads to the extension of the anterior-posterior axis (reviewed in Shih and Keller 1992; Wallingford, Fraser et al. 2002; Habas, Dawid et al. 2003). The non-canonical Wnt signaling pathway, induced by Wnt11, is responsible for

correct CE movements during gastrulation (Heisenberg, Tada et al. 2000; Smith, Conlon et al. 2000; Wallingford, Rowning et al. 2000; Adler 2002).

In the PCP pathway, two signaling cascades lead to the activation of the small GTPases of the Rho family, Rho and Rac, and activation of Rho and Rac both are dependent on different domains of the cytoplasmic protein Dishevelled (Dvl). Rho and Rac activation by Dishevelled occurs independently (Habas, Dawid et al. 2003).

In order to activate Rho, Dvl forms a complex with Rho, a process that is mediated by the protein Daam1. Daam1 binds to both proteins and mediates Wnt-induced Dvl-Rho complex formation, resulting in an activation of the Rho-associated kinase ROCK, which mediates re-organization of the cytoskeleton, thus indicating a role for ROCK in cell motility (Habas, Kato et al. 2001; Winter, Wang et al. 2001; Marlow, Topczewski et al. 2002).

In contrast to the activation of Rho, Rac activation is independent of Daam1, but only requires Dvl in order to stimulate JNK activity (Boutros, Paricio et al. 1998; Habas, Dawid et al. 2003; Veeman, Axelrod et al. 2003). In addition to activation by Wnt signals, JNK is activated in response to growth factors, inhibition of DNA and protein synthesis, environmental stress and inflammatory cytokines. It is a key regulator of many cellular events and regulates motility, cell proliferation, differentiation and programmed cell death (Liu and Lin 2005; Johnson and Nakamura 2007; Saadeddin, Babaei-Jadidi et al. 2009).

1.5.1.2 **The Wnt/Ca^{2+} pathway**

Wnt/Ca^{2+} signaling plays an important role during gastrulation, in processes like cell adhesion and cell movements (reviewed in Wallingford, Fraser et al. 2002; Habas and Dawid 2005).

In the Wnt/Ca^{2+} pathway, signaling is mediated through the release of intracellular Ca^{2+}, initiated through activation of heterotrimeric G-proteins by Frizzled receptors. Other molecules that are mediators known to be involved in signaling include PKC (protein kinase C) and CamK2 (calcium-calmodulin-dependent kinase 2) (reviewed in Miller, Hocking et al. 1999; Kuhl, Sheldahl et al. 2000; Kuhl 2002).

There is an overlap between the Wnt/Ca^{2+} pathway and the other Wnt pathways. The Wnt/Ca^{2+} pathway is suggested to influence both the canonical and PCP pathways (reviewed in Habas and Dawid 2005). The extent of overlap between the PCP and the Wnt/Ca^{2+} pathway is still unclear (reviewed in Wallingford, Fraser et al. 2002).

1.5.2 The canonical ß-catenin dependent Wnt signaling pathway

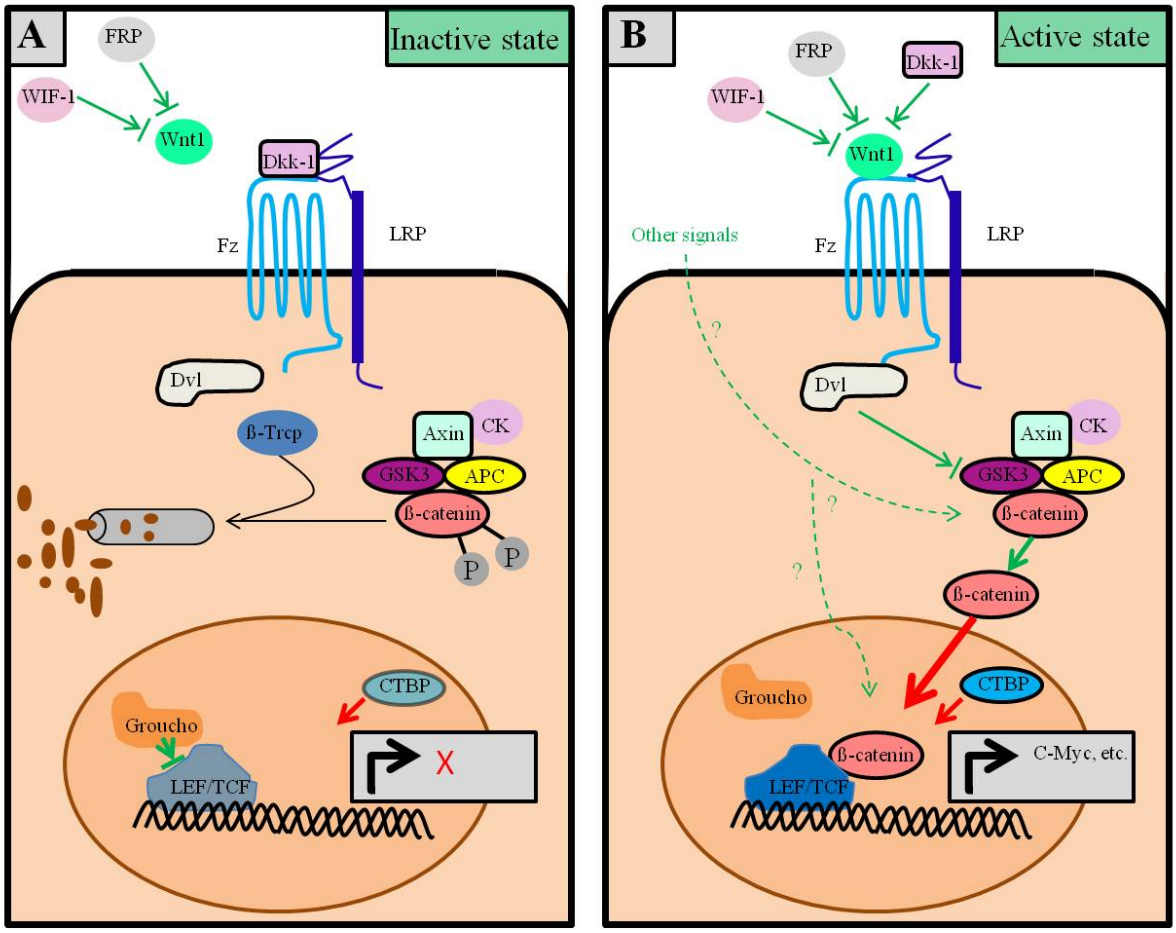

Figure 5 Scheme of the canonical Wnt signaling pathway.
(adapted from Luo, Chen et al. 2007) (A) In the absence of a Wnt ligand, ß-catenin is marked for degradation by phosphorylation by GSK3, followed by ubiquitination of phosphorylated ß-catenin and subsequent degradation by the proteasome. Together with co-repressors, TCF/LEF represses transcription of downstream Wnt target genes. (B) The presence of a Wnt ligand bound to a Frizzled receptor and LRP co-receptor results in a series of events leading to the disruption of the APC/Axin/GSK3 complex. Thus, ß-catenin is not degraded and leads to the transcription of Wnt target genes in the nucleus. Several negative regulators inhibit the interactions between Wnt ligands and receptors (see text for details).

In the non-activated state, the levels of ß-catenin in the cytoplasm remain low through phosphorylation of the protein by Glycogen Synthase Kinase 3ß (GSK3), followed by ubiquitination of phosphorylated ß-catenin and subsequent degradation by the proteasome (reviewed in Gordon and Nusse 2006). In this inactive state, TCF/LEF factors in the nucleus act as transcriptional repressors of Wnt-responsive genes. T cell-specific transcription factor 4/ lymphoid enhancer-binding factor 1 (TCF/LEF) are transcription factors that mediate Wnt signaling by recruitment of ß-catenin. In the non-active state of Wnt signaling, TCF/LEF physically interact with co-repressors of the Groucho family in order to fully repress the

transcription of Wnt target genes (Molenaar, van de Wetering et al. 1996; Cavallo, Cox et al. 1998; Levanon, Goldstein et al. 1998; Roose, Molenaar et al. 1998; Gordon and Nusse 2006).

For activation of the Wnt signaling pathway, Wnt proteins bind to a Frizzled/LRP receptor complex, which is composed of LDL-(low density lipoprotein)-receptor-related proteins (LRP) and of members of the Frizzled (Fz) family of seven transmembrane, serpentine receptors (reviewed in Gordon and Nusse 2006).

This initializing binding event leads to a series of happenings that result in the disruption of a complex consisting of APC, Axin, and Glycogen Synthase Kinase 3 (GSK3). This complex is required for ß-catenin phosphorylation by GSK and subsequent destruction (reviewed in Gordon and Nusse 2006). Upon impaired ß-catenin phosphorylation, ß-catenin accumulates in the cytoplasm and translocates into the nucleus, where it leads to the expression of target genes through interaction with the TCF/LEF family of transcription factors (Molenaar, van de Wetering et al. 1996).

Additionally, in the presence of Wnt proteins that activate the canonical Wnt signaling pathway, LRP5 and LRP6 homologues (LRP), which have multiple modular Casein Kinase 1 (CK1) phosphorylation sites and are associated with CK1, are phosphorylated by CK1. In addition to LRP phosphorylation by CK1, which is initiated upon binding of a canonical Wnt ligand, LRP phosphorylation is mediated by a membrane-associated form of GSK. Phosphorylation of LRP results in the recruitment of the scaffold protein Axin to the plasma membrane, which then binds to a conserved sequence at the cytoplasmic tail of LRP (Mao, Wang et al. 2001; Davidson, Wu et al. 2005; Zeng, Tamai et al. 2005). Before recruitment of Axin to LRP (Mao, Wang et al. 2001), the phosphorylated LRP proteins form aggregates that are associated to the membrane. These phospho-LRP aggregates occur as a rapid response to Wnt stimulation (Bilic, Huang et al. 2007).

Both the phosphorylation of LRP, followed by the recruitment of Axin to LRP at the plasma membrane, as well as subsequent internalization of LRP, which is (like the recruitment of Axin to LRP) dependent on the protein caveolin, are necessary for the accumulation of ß-catenin and thus for the activation of the canonical Wnt signaling pathway (Yamamoto, Komekado et al. 2006; Yamamoto, Sakane et al. 2008).

An important protein that is required for phosphorylation and aggregation of LRP is the scaffold protein Dishevelled (Dvl). Upon activation of Wnt signaling, aggregates of Dvl form

at the plasma membrane, where they co-cluster LRP with other components of the Wnt signaling pathway including Frizzled receptor, Axin and GSK3, a cluster called the "LRP-signalosome" (Bilic, Huang et al. 2007).

Dvl is known to bind to Axin and the Fz receptors and it is still unclear how it becomes activated or communicates with Fz receptors. It is phosphorylated by various kinases, and it is suggested to be the core of a large multiprotein complex, which ensures correct Wnt signaling through effectors as well as control through feedback regulation (Kishida, Yamamoto et al. 1999; Wharton 2003; Wong, Bourdelas et al. 2003; Komiya and Habas 2008).

Dvl directly binds to Axin, and it inhibits phosphorylation of ß-catenin through GSK3, a process promoted by Axin. The DIX domain of Dvl is required for the inhibitory activity (Kishida, Yamamoto et al. 1999). Thus, once Dvl is activated, it inhibits GSK3ß activity through inhibition of Axin, and activates a complex series of events, leading to inhibition of ß-catenin degradation and as a consequence ß-catenin stabilization and cytoplasmic accumulation (Kishida, Yamamoto et al. 1999).

Stabilized ß-catenin then translocates into the nucleus by a poorly understood mechanism. It is imported into the nucleus by a mechanism that is independent of NLS and importin/karyopherin proteins or the Ran-mediated nuclear import, but by directly binding to the nuclear pore machinery (Fagotto, Gluck et al. 1998). It was suggested that the distribution of ß-catenin between the nucleus and cytoplasm is regulated by Axin, which shuttles between the nucleus and the cytoplasm and acts as a molecular chaperone for ß-catenin (Cong and Varmus 2004). In addition, ß-catenin can be transported back to the cytoplasm as a cargo of APC, a protein that also shuttles between the cytoplasm and the nucleus. APC contains nuclear export signals, which are highly conserved. Since they are located 3' adjacent to the mutation cluster region, the ability to exit from the nucleus is lost in APC mutant cancer cells. As a result, ß-catenin accumulates in the nucleus, indicating that the ability to exit from the nucleus is an important function of APC as a tumor suppressor (Henderson 2000; Rosin-Arbesfeld, Townsley et al. 2000).

Upon translocation of ß-catenin into the nucleus, ß-catenin interacts with the N-terminus of the transcription factors TCF (Molenaar, van de Wetering et al. 1996; van de Wetering, Cavallo et al. 1997) and LEF (Behrens, von Kries et al. 1996). TCF/LEF factors transduce the Wnt signals (van de Wetering, Cavallo et al. 1997). By displacement of Groucho, a

transcriptional repressor, from TCF/LEF, TCF is transiently converted into a transcriptional activator, an event that is mediated by ß-catenin (Daniels and Weis 2005).

ß-catenin acts as a strong co-activator of TCF-driven transcription (van de Wetering, Cavallo et al. 1997). It has several binding partners that contribute to its function. The co-activator function of ß-catenin mainly depends on two domains: The amino-terminal activating arm (NTAA), which recruits Bcl9 and Pygopus, and the carboxy-terminal activating arm (CTAA), which binds to TATA-binding protein (TBP), Brahma-related gene-1 (Brg-1), CREB-binding protein (CBP) and the closely related p300, Mediator subunit 12 (MED12) and Parafibromin. Thus, through binding to co-activators such as CBP, a histone acetylase, and Brg-1, a component of the SWI/SNF chromatin remodeling complex, the recruitment of ß-catenin to TCF affects local chromatin in several ways (reviewed in Stadeli, Hoffmans et al. 2006).

Additionally, TCF proteins have been shown to bind to CTBP proteins (C-terminal Binding Proteins) (Brannon, Brown et al. 1999; Valenta, Lukas et al. 2003; Hamada and Bienz 2004; Cuilliere-Dartigues, El-Bchiri et al. 2006). Hamada et al. suggested that APC acts as an adaptor protein between ß-catenin and CTBP, and that CTBP prevents binding of nuclear ß-catenin to TCF4 and thus activation of transcription by decreasing the availability of free nuclear ß-catenin. Furthermore, in their study, they showed that in contrast to ß-catenin, CTBP proteins do not bind to TCF in mammalian cells (Hamada and Bienz 2004). They are transcriptional co-repressors which can interact with histone deacetylases (HDACs), and binding of CTBP proteins represses TCF-mediated transcription either in a way dependent of HDAC or in an independent manner (reviewed in Chinnadurai 2002). In addition, CTBP also functions as an activator of the transcription of Wnt target genes (Fang, Li et al. 2006).

After the release of the Groucho and CTBP repressor systems from the TCF complex, nuclear ß-catenin can fully develop its function as a transcriptional activator. Nevertheless, it is not clear how the repressor effect of CTBP on the TCF complex is handled by Wnt signaling and whether ß-catenin actively contributes to this process (reviewed in Stadeli, Hoffmans et al. 2006).

To summarize, the activation of Wnt target genes is an inter-coordinated and well balanced process, which dynamically coordinates the action of transcriptional modulators at the central scaffold protein ß-catenin in a sequential manner (reviewed in Stadeli, Hoffmans et al. 2006).

1.5.3 Wnt target genes

In several studies, various different target genes of the Wnt signaling pathway have been identified in biological systems. Especially the target genes involved in cancer, like *c-Myc* and *CCND1* (coding for CyclinD1), are in the focus of studies. Cell type specificity was observed for most of the Wnt target genes, and it remains elusive whether non-cell type specific Wnt target genes exist (reviewed in Clevers 2006).

At many levels of Wnt signaling, auto-regulation can be observed. The expression of a huge amount of positive as well as negative modulators of the Wnt signaling pathway is tightly controlled by feedback loops, thus Wnt signaling activity controls the expression of regulators and proteins of the Wnt signaling pathway, such as Frizzled, Axin and TCF/LEF (reviewed in Logan and Nusse 2004; Clevers 2006).

1.5.4 Inhibitors of the Wnt signaling pathway

Several endogenous inhibitors of the Wnt signaling pathway have been identified till now. Extra-cellular inhibitors, which are active at the cell surface, are important for fine-tuning of the spatial and temporal patterns of Wnt activity. They can be divided into two classes regarding their mechanisms, namely the sFRP class, comprising the sFRP family, WIF-1 and Cerberus, and the Dickkopf (Dkk) class (reviewed in Kawano and Kypta 2003).

Members of the sFRP class directly bind to Wnt molecules or Fz receptors, thus they can inhibit both canonical and non-canonical Wnt signaling, whereas members of the Dkk class bind to LRP receptors, resulting in LRP endocytosis and inhibition of the Fz/LRP complex. Thus, Dkk proteins can only inhibit canonical Wnt signaling (reviewed in Kawano and Kypta 2003).

Frizzled Related Proteins (sFRP proteins) are proteins which share sequence similarity to the Frizzled receptor CRD (cysteine rich domain), but lack the transmembrane and intracellular domains. sFRPs inhibit Wnt signaling either by binding to Wnt ligands, by inhibiting interactions of Wnt proteins with Fz receptors, or by forming complexes with Fz, which are not functional (Finch, He et al. 1997; Leyns, Bouwmeester et al. 1997; Wang, Krinks et al. 1997; Kawano and Kypta 2003).

WIF-1 (Wnt-Inhibitory-Factor 1) is a secreted antagonist of the Wnt signaling pathway that binds to Wnt proteins and inhibits their activities in order to fine-tune the spatial and temporal

patterns of Wnt signaling activity. It has been implicated in the regulation of several developmental processes (Hsieh, Kodjabachian et al. 1999).

Dickkopf1 (Dkk1) belongs to a family of secreted proteins, which are structurally unrelated to Wnt or Frizzled (Glinka, Wu et al. 1998; Fedi, Bafico et al. 1999). It antagonizes Wnt signaling through binding to LRP proteins (Bafico, Liu et al. 2001; Mao, Wu et al. 2001). Thus, it inhibits the association of Fz and LRP, resulting in inhibition of only the canonical Wnt signaling pathway. These results indicate that Fz/LRP complex formation, but not Wnt/Fz interaction, triggers canonical Wnt signaling (Semenov, Tamai et al. 2001).

Dkk1 forms a complex with the transmembrane proteins Kremen1 and Kremen2, which are high-affinity receptors for Dkk1. They bind to Dkk1 and functionally cooperate with Dkk1 to inhibit canonical Wnt signaling through induction of endocytosis and thus removal of LRP from the plasma membrane (Bafico, Liu et al. 2001; Mao, Wu et al. 2002).

Antagonists of Wnt signaling are illustrated in Figure 6.

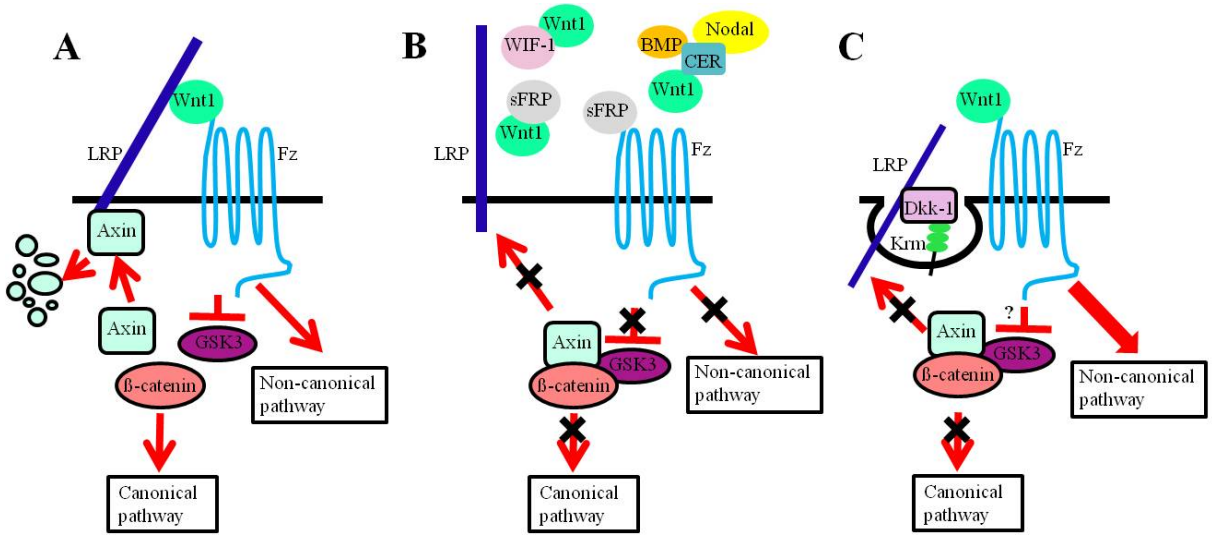

Figure 6 Inhibitors of the Wnt signaling pathway.
(adapted from Kawano and Kypta 2003) (A) In the normal state of Wnt signaling, a Wnt ligand binds to Fz/LRP, followed by recruitment of Axin to LRP and Axin degradation. Further events lead to an activation of Wnt signaling. (B) Wnt antagonists of the sFRP class inhibit both the canonical and the non-canonical Wnt pathway. sFRP family proteins, WIF-1 and CER, prevent Wnt proteins from binding to their receptors. Members of the sFRP class can also form inactive complexes with Fz receptors in order to inhibit the binding of Wnt proteins. (C) Dkk1 inhibits only canonical Wnt signaling. It interacts with LRP and Kremen 1/2, resulting in impaired LRP/Fz complex formation and endocytosis of LRP.

However, since acting upstream of the oncogenic mutations found in colon cancer, like *APC* or the gene coding for ß-catenin (*CTNNB1*), such proteins are not able to block the Wnt signaling pathway in cancer cells.

Since there is a continuous need for the development of chemotherapeutic agents useful for the prevention or treatment of cancer, or for use in combination with other known cancer therapies. Therefore, components that are involved in or that affect the Wnt signaling pathways, especially those that comprise inhibitory function downstream of the oncogenic mutations found in colon cancer, like in *APC* or the ß-catenin gene *CTNNB1*, need to be uncovered, in order to allow more accurate and effective diagnosis and treatment of diseases.

1.5.5 The role of Wnt signaling in cancer development

Although many genes involved in the Wnt signaling pathway were originally described to have a function in development, they later turned out to operate as oncogenes and tumor suppressors upon deregulation in human cancer (reviewed in Klaus and Birchmeier 2008).

In 1993, an overlap was found between research on Wnt signaling and human cancer. The Wnt pathway component ß-catenin was found to biochemically interact with the tumor suppressor APC as well as the truncated mutant forms of APC (Rubinfeld, Souza et al. 1993; Su, Vogelstein et al. 1993).

Deregulation of the canonical Wnt-signaling pathway has been shown to be causally involved in several cancers, in particular carcinogenesis in the intestine (reviewed in Polakis 2000). More than 90 % of colon cancers and a high percentage of other cancers evolve from activating mutations in the Wnt signaling pathway (reviewed in Klaus and Birchmeier 2008). Canonical Wnt signaling promotes tumorigenesis by maintaining a proliferative state of intestinal epithelial cells, thus any mutation that results in stabilized nuclear ß-catenin und in activated canonical Wnt signaling represents an early event of intestinal oncogenesis (reviewed in Pinto and Clevers 2005).

Since elevated activation of the Wnt signaling pathway is involved in most cases of colorectal carcinoma, new therapeutical approaches concentrate on antagonists of the Wnt signaling pathway in order to decrease elevated Wnt activity. Components of the Wnt pathway could be alternative therapeutic targets, but it will first be important to understand the mechanisms of their functions in detail (Daniels, Eklof Spink et al. 2001; Moon, Kohn et al. 2004). Nevertheless, it is likely that in future inhibiting the Wnt pathway could considerably contribute to cancer therapy (reviewed in Klaus and Birchmeier 2008).

1.6 Ubiquitination

Post-translational modifications of proteins by conjugation of the conserved 8 kDA polypeptide ubiquitin to lysine residues on a target protein are central to most aspects of eukaryotic life. Since they are reversible, they are a valuable tool for the regulation of cellular processes (reviewed in Weissman 2001; Bergink and Jentsch 2009). They have been implicated in various different biological processes, including signal transduction pathways, cell cycle progression, transcriptional regulation, immune response, endocytosis, development and apoptosis. Deregulations have been shown to correlate with pathological conditions, including malignant transformation (reviewed in Hochstrasser 1996; Hershko and Ciechanover 1998).

The ubiquitination process is dependent on ATP and requires the cooperation of three enzymes: the ubiquitin-activating enzyme (E1), the ubiquitin-conjugating enzyme (E2) and ubiquitin-ligases (E3). ATP-dependent formation of a thiol ester with a cysteine residue of the activating enzyme (E1) activates ubiquitin, which is then transferred to a cysteine residue of a conjugating enzyme (E2), and subsequently to a ubiquitin-ligase (E3), which is the enzyme that mediates specific substrate recognition and catalyzes the transfer of ubiquitin to a lysine residue of the substrate (reviewed in Hochstrasser 1996; Varshavsky 1997; Hershko and Ciechanover 1998; Pickart 2000; Pickart 2001; Pickart 2001). The ubiquitin conjugation cascade is illustrated in Figure 7.

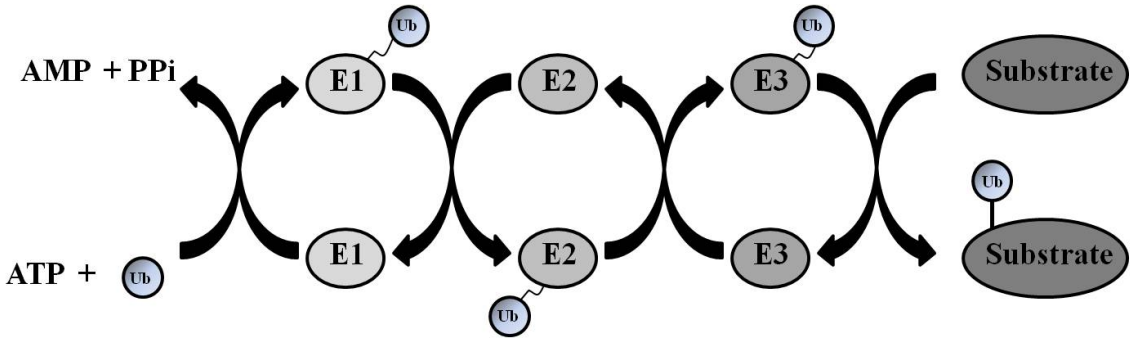

Figure 7 Scheme of the Ubiquitin conjugation cascade.
(adapted from Pickart 2001) Ubiquitin is activated by an E1 enzyme, transferred to an E2 enzyme, and subsequently the Ubiquitin E3-Ligase catalyzes the transfer of ubiquitin to an E3-specific substrate.

Protein fates upon monoubiquitination are diverse. The target proteins can exhibit various altered activities and signaling functions (reviewed in Pickart 2001), as illustrated in Figure 8.

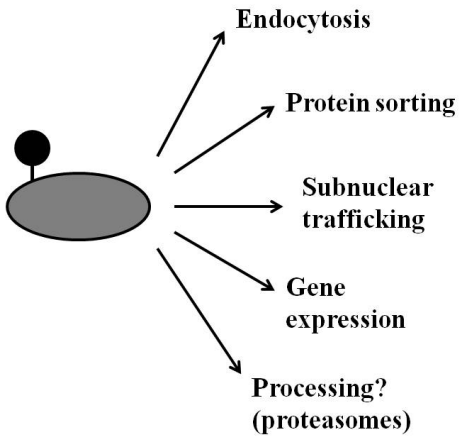

Figure 8 Schematic representation of functions of proteins upon monoubiquitination.
(adapted from Pickart 2001)

In contrast, upon multiubiquitination, the target proteins are typically substrates for degradation by the proteasome (Chau, Tobias et al. 1989; Finley, Sadis et al. 1994). Nevertheless, it was described that chains of ubiquitin, which are linked through different lysine residues, may be distinct signals. K48-linked chains and K29-linked chains are signals for proteasomal degradation (reviewed in Pickart 2000), but K63-linked chains mediate various other biological functions, like for instance DNA repair (Spence, Sadis et al. 1995; Hofmann and Pickart 1999), response to stress (Arnason and Ellison 1994), mitochondrial DNA inheritance (Fisk and Yaffe 1999), and protein targeting for endocytosis (Galan and Haguenauer-Tsapis 1997) (Figure 9).

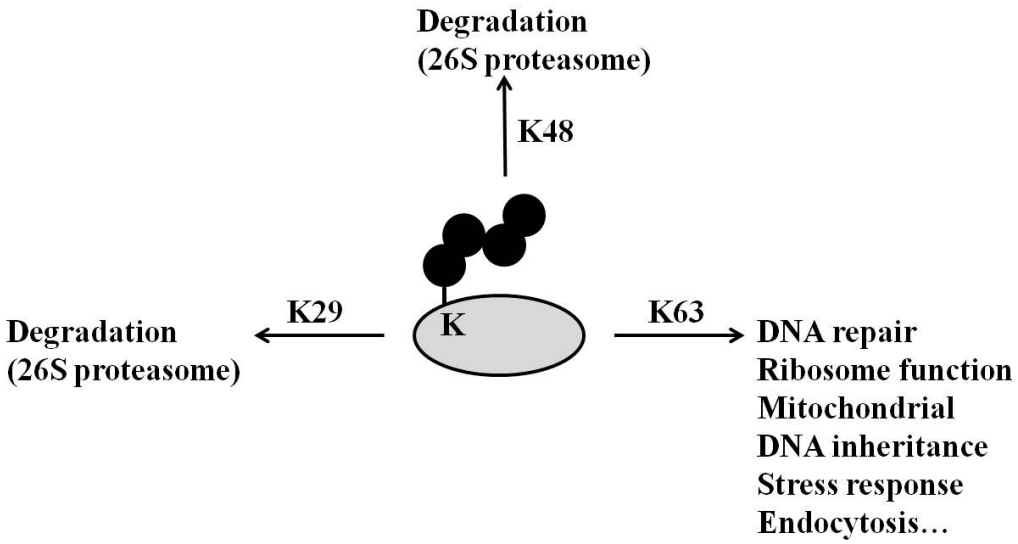

Figure 9 Scheme representing functions determined by polyubiquitin chains.
(adapted from Pickart 2000) K48-linked chains are the most important signal for degradation of the proteasome. In addition, K29-linked chains can also be a signal for the same way of degradation. In contrast, K63-linked chains mediate other biological functions.

1.7 RING finger proteins and ubiquitination

1.7.1 Structure of RING finger proteins

The RING finger motif was first identified 1991 in a protein encoded by the *Ring1* (*R*eally *I*nteresting *N*ew *G*ene 1) gene. It is a cysteine-rich amino acid sequence motif that can be described as **C**-X-(I,V)-**C**-X(11-30)-**C**X-**H**-X-(F,I,L)-**C**-X(2)-**C**-(I,L,M)-X(10-18)-**C**-P-X-**C** (X can be any amino acid), a pattern that is highly specific (Freemont, Hanson et al. 1991) and similar to well-known zinc finger motifs (Berg 1990). However, several differences were observed, which suggested a novel three-dimensional structure for the motif (Freemont, Hanson et al. 1991).

The RING finger domain contains cysteine/histidine residues for metal-binding (Freemont 1993; Lovering, Hanson et al. 1993; Freemont 2000)). In contrast to zinc finger domains, they coordinate two zinc atoms in a "cross-braced" fashion (Freemont 2000), as illustrated in Figure 10.

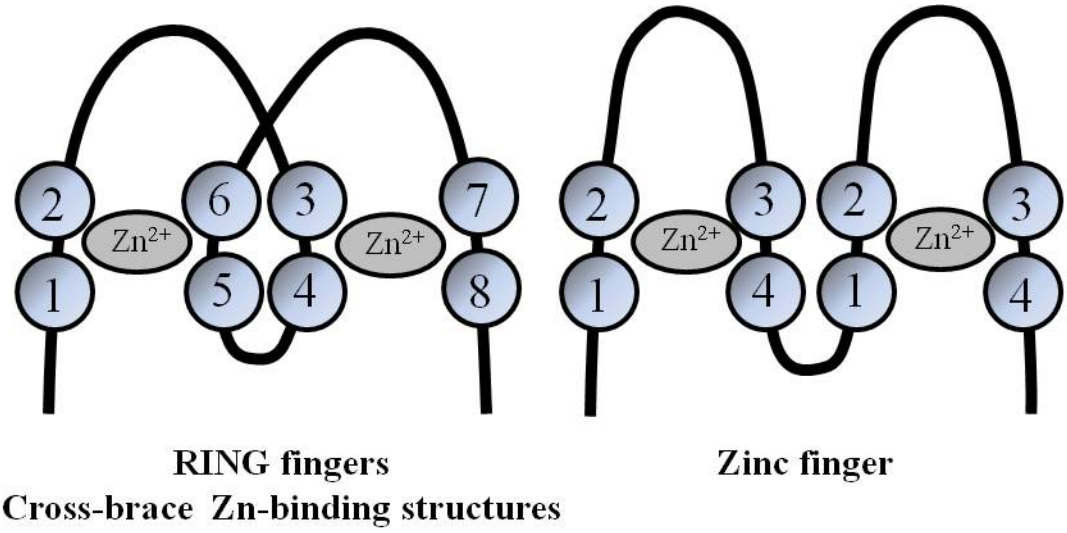

Figure 10 **Schematic representation of RING fingers.**
(adapted from Fang, Lorick et al. 2003). Scheme illustrating RING fingers (left) and classical zinc fingers (right). The eight zinc-coordinating residues are numbered.

The first and third pair of metal-binding Cys/His residues form "site I" and bind the first zinc atom, and the second and fourth pair form "site II" and bind the second zinc atom (reviewed in Borden 2000). The coordination of zinc is required for folding as well as for biological functions (Capili, Edghill et al. 2004).

Dependent on whether the fifth Zn-coordinating residue is a histidine (-H2) or cysteine (-HC), RING fingers are subcategorized into RING-HC and RING-H2 RING fingers (reviewed in Joazeiro and Weissman 2000).

1.7.2 Function of RING finger proteins

In contrast to classical zinc fingers, whose localization is restricted to the nucleus and which function in binding to nucleic acids, RING domains are present in the whole cell, where they are involved in various protein-protein interactions. In some cases, they are responsible for the coordination of multi-protein complexes, wherefore other proteins and/or protein domains may be necessary (Saurin, Borden et al. 1996).

No general, but various different biochemical functions have been attributed to RING domains (Capili, Edghill et al. 2004). For example, a large number of RING finger proteins function as Ubiquitin E3-Ligases in the ubiquitin pathway, where they catalyze the transfer of activated ubiquitin residues from an E2 ubiquitin conjugating enzyme to a substrate, thus they mediate E2-dependent ubiquitination (reviewed in Joazeiro and Weissman 2000).

Important roles in various cellular processes have been ascribed to RING finger-containing E3-Ligases. They are implicated in having a role in cell cycle and in contribute to disease (reviewed in Joazeiro and Weissman 2000). Furthermore, levels of plasma membrane proteins are regulated by ubiquitination through proteasomal degradation (Levkowitz, Waterman et al. 1999; Yokouchi, Kondo et al. 1999), as well as by facilitating endocytosis and lysosomal/vacuolar targeting of proteins (reviewed in Joazeiro and Weissman 2000).

RING finger E3-Ligases also have a function in the secretory pathway. They play an important role in quality control of proteins in the ER (Kikkert, Doolman et al. 2004). In addition, they can influence the balance between proliferation and apoptosis (Yang, Fang et al. 2000), and several RING finger proteins, like BRCA1, are directly associated with deregulated growth and malignancy (reviewed in Joazeiro and Weissman 2000). Since RING finger-containing E3-Ligases provide substrate specificity, they play important regulatory roles and thus represent putative targets for new therapies of diseases. Nevertheless, it remains elusive by which molecular mechanism the RING finger proteins mediate ubiquitination (Fang, Lorick et al. 2003).

1.8 RING finger protein 43

RNF43 (registered sequence: NM_017763) is a gene with a coding nucleotide sequence of 2352 bp length. In humans, it consists of 10 exons and codes for a 783 aa long RING finger protein with a molecular mass of approximately 85 kDa.

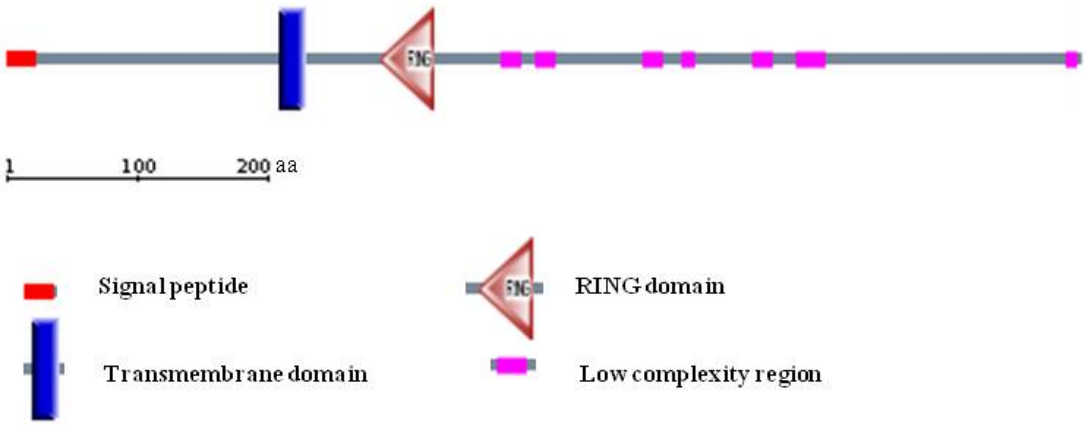

Figure 11 Schematic representation of the RNF43 protein sequence
according to the SMART (Simple Modular Architecture Research Tool)[1] analysis of domain architectures.

According to the "SMART" (Simple Modular Architecture Research Tool) program, the RNF43 protein consists of an N-terminal signal peptide (aa 1 - 23), a transmembrane domain (aa 199 - 218), a RING domain (aa 272 - 312) and seven regions of low complexity (aa 360 - 374, 385 - 399, 464 - 478, 494 - 503, 544 - 558, 576 - 597, 772 - 780).

Although the predicted molecular weight of RNF43 was approximately 85 kDa, bands with larger sizes are observed upon detection in Western blot analysis, suggesting post-translational modifications of the protein, like glyCos7ylation or phosphorylation (Yagyu, Furukawa et al. 2004).

Sequential analysis revealed that two potential methionines for the initiation of translation are present in the sequence of RNF43. The majority of RNF43 is translated from the first methionine upstream in the sequence. Nevertheless, translation of RNF43 can also be initiated at the methionine at position 128, but less efficiently (Sugiura, Yamaguchi et al. 2008).

RNF43 was initially identified as an oncogene upregulated in colon cancer (Takemasa, Higuchi et al. 2001; Uchida, Tsunoda et al. 2004; Yagyu, Furukawa et al. 2004; Sugiura,

[1] http://smart.embl-heidelberg.de/

Yamaguchi et al. 2008). Sugiura et al. showed that RNF43 expression is already increased in precancerous colon adenomas (Sugiura, Yamaguchi et al. 2008).

Based on the finding that RNF43 is upregulated in colon cancer, RNF43 was identified as a tumor-associated antigen (TAA) for use in cancer immunotherapy, a therapy based on CD8 cytotoxic T lymphocytes (CTLs) that recognize epitope peptides derived from TAAs. Identifications of new TAAs that induce potent and specific antitumor immune responses are important for further development of peptide vaccinations for various types of cancers (Uchida, Tsunoda et al. 2004).

Yagyu et al. suggested that RNF43 is growth-related, since overexpression of RNF43 exhibits growth-promoting activity, whereas its knockdown retards cell growth (Yagyu, Furukawa et al. 2004). These findings suggested a role for RNF43 in colorectal carcinogenesis.

Since lysates of cells expressing RNF43 showed high molecular smear band, an evidence typical for ubiquitination, it was suggested that RNF43 is ubiquitinated in intact cells. RNF43 mutated in the RING finger domain (at positions 290 and 292) was also found to be ubiquitinated *in vivo* (Sugiura, Yamaguchi et al. 2008).

When looking at the subcellular localization, RNF43 was found to localize in the Endoplasmatic reticulum (ER) and around the nuclear rim in the nuclear membrane, with occasional staining in the nucleoplasm (Sugiura, Yamaguchi et al. 2008). In contrast, Yagyu et al. suggested that RNF43 is a secretory protein (Yagyu, Furukawa et al. 2004).

One of the principle functions of RING finger proteins is to act as Ubiquitin E3-Ligases (Lorick, Jensen et al. 1999). The presence of the RING finger domain in RNF43 suggested that RNF43 is an Ubiquitin E3-Ligase, and indeed, RNF43 was shown to exhibit Ubiquitin E3-Ligase activity. It is a RING finger-dependent Ubiquitin E3-Ligase, with selectivity for UbcH5b and UbcH5c as E2 enzymes (Sugiura, Yamaguchi et al. 2008).

Although a chromatin-associated protein, HAP95, which faces the nuclear envelope, was shown to be a RNF43 interaction partner, it does not serve as a substrate for ubiquitination. However, the protein level of HAP95 decreased upon co-expression of RNF43. Since the reduction of the HAP95 protein level could not be restored upon MG132 treatment, HAP95 degradation is not mediated by the proteasome (Sugiura, Yamaguchi et al. 2008).

Additionally, RNF43 was shown to interact with the tumor suppressor PSF, which is part of the PSF/p54nrb heterodimer, but as observed for HAP95, RNF43 did not ubiquitinate PSF (Miyamoto, Sakurai et al. 2008).

In a recent study, Shinada et al. showed that RNF43 interacts with NEDL1, a protein that binds and regulates p53, and additionally with p53. p53 is one of the important tumor suppressors since it induces G1 cell cycle arrest in order to facilitate DNA repair during replication, or apoptosis. They showed that RNF43 not only interacts with these two proteins, but RNF43 overexpression also suppresses the transcriptional activity of p53 as well as apoptosis induced by UV. Shinada et al. suggested that in colorectal carcinogenesis, RNF43 may regulate cell growth and apoptosis via NEDL1 and p53 (Shinada, Tsukiyama et al. 2011).

Van der Flier et al. found RNF43 to be upregulated in GFP-positive epithelial cells from crypts isolated from LGR5-GFP-ires-CreERT mice, indicating that RNF43 is part of the transcriptome of Lgr5 positive intestinal stem cells (van der Flier, van Gijn et al. 2009). These data suggest that RNF43 is upregulated in intestinal stem cells, making it an interesting candidate for further research.

Furthermore, in addition to its increased expression in intestinal Lgr5 positive stem cells, the *RNF43* gene was shown to exhibit inactivating mutations in several forms of neoplastic cysts in the pancreas, which are IPMNs (intraductal papillary mucinous neoplasms) and MCNs (mucinous cystic neoplasms). Both types of mucinous cysts are benign, but they have the potential to progress into invasive tumors. *RNF43* was shown to be the most commonly mutated gene in IPMNs. Several mutations were base pair substitutions resulting in nonsense codons, and several IPMNs exhibited loss of heterozygosity (LOH) of the region on chromosome 17q containing the *RNF43* gene. Since inactivating mutations are characteristic for tumor suppressor genes, the inactivating mutations in the *RNF43* gene suggest that RNF43 suppresses neoplasia in ductal epithelial cells of the pancreas (Wu, Jiao et al. 2011).

Nevertheless, the detailed molecular mechanism of RNF43 function remained elusive.

1.9 Previous work on RNF43

Previous work on RNF43 done in our laboratory concentrated on the investigation of the physiological expression of RNF43 in the intestine of mice.

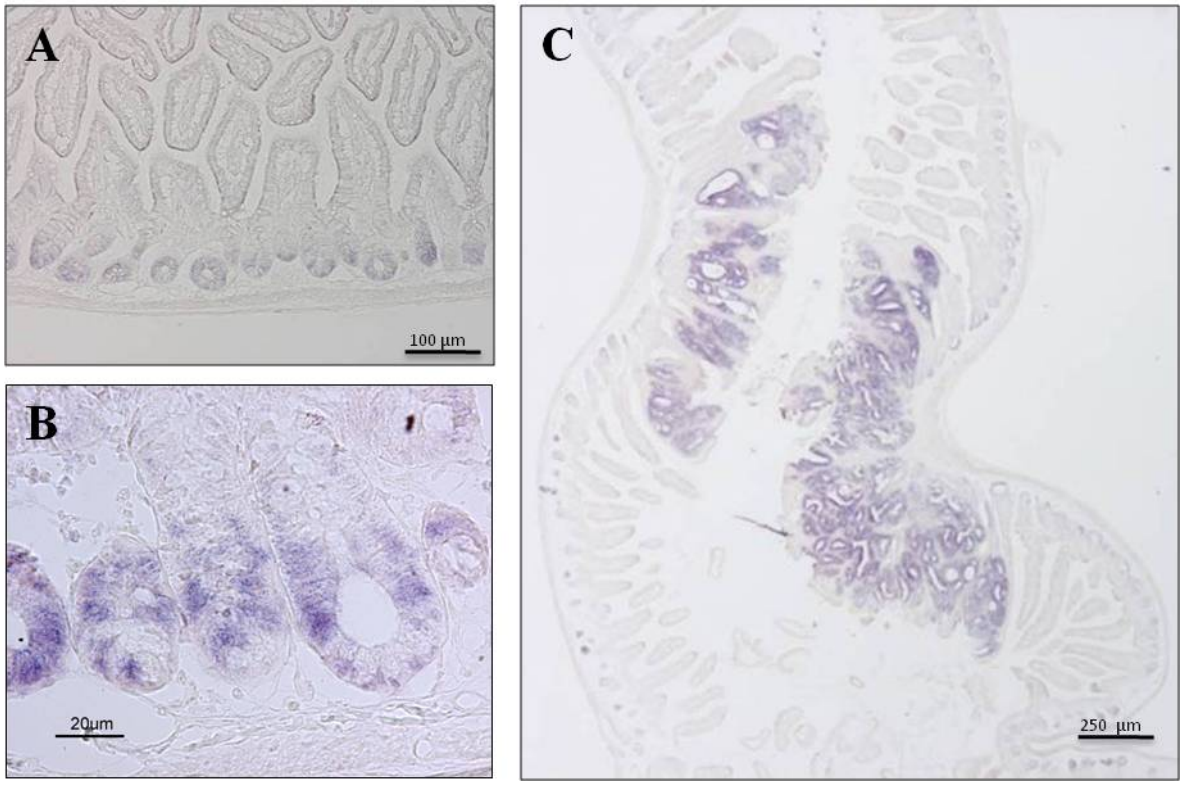

Figure 12 *In situ* hybridization analyses for RNF43 in the small intestine of adult mice using DIG-labeled probes for RNF43.
(A, B) In the small intestine, RNF43 was exclusively expressed in epithelial cells at the base of crypts. (B) Magnified image of a crypt. (C) RNF43 expression in intestinal adenomas.

In situ hybridizations for RNF43 revealed an expression of RNF43 restricted to a limited number of cells located at the base of crypts. The expression of RNF43 was strong at the so-called "+4 position" (see 1.3.2), and additionally, the expression pattern was similar to the expression pattern of Lgr5, which is known to be a marker for long-lived, pluripotent stem cells (Barker, van Es et al. 2007). Thus, in *in situ* hybridizations, RNF43 expression was restricted to presumed stem cell positions in intestinal crypts. Additionally, *in situ* hybridizations showed a strong overexpression of RNF43 in intestinal adenomas in mice (Gerhard et al., unpublished data).

The increased RNF43 mRNA expression levels at sites of high Wnt signaling indicated a link to the Wnt signaling pathway and therefore suggested further investigating whether RNF43 is a direct or indirect target of the Tcf-/ß-catenin transcription factor complex. Therefore, chromatin-IP (ChIP)-coupled DNA microarray analysis (ChIP- on ChIP), which couples the IP of transcription factors bound to chromatin with the identification of the bound DNA sequences through hybridization on DNA microarrays, was performed. Seven evolutionarily

conserved regions of the *RNF43* gene sequence were found to contain Tcf4 binding sites. They were located in the promoter region and in the introns of the *RNF43* gene. Thus, *RNF43* is a direct target gene of Tcf4-mediated Wnt signaling (Gerhard et al., unpublished).

In order to test whether there is a possible function of RNF43 mediated by the active RING domain, a functionally inactive RNF43 mutant, termed "RNF43mut", was generated. Therefore, two point mutations (A→G) were introduced into the sequence of the *RNF43* gene, resulting in amino acid exchanges from histidine to arginine at the amino acids at positions 292 and 295. These two amino acids are essential for the function of the RING domain, since they are responsible for zinc coordination.

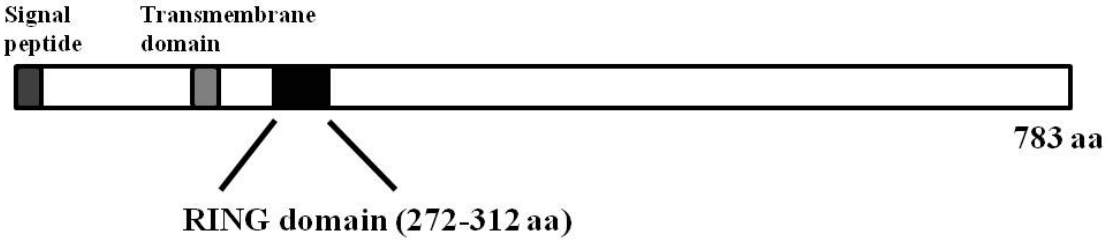

Figure 13 Schematic diagram of the *RNF43* gene.
Exons 7 and 8 code for the RING domain of the human RNF43 protein. For generation of a functionally inactive mutant, two point mutations resulting in amino acid exchanges at positions 292 and 295were introduced into the sequence of the *RNF43* gene.

RNF43 was shown to be a target gene of the Wnt signaling pathway. In order to identify a possible effect of wildtype or mutant RNF43 on the Wnt signaling pathway, TOP/FOP Luciferase reporter assays were performed.

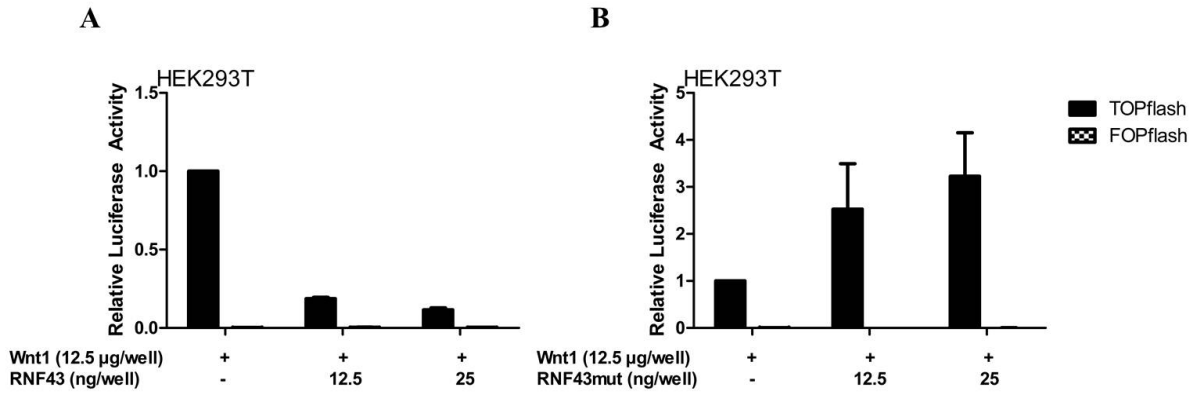

Figure 14 Wildtype, (but not mutant) RNF43 inhibits Wnt signaling in HEK293T cells.
HEK293T cells were transfected with pTOPflash or the control pFOPflash reporter plasmids as well as the indicated amounts of an RNF43 wildtype (A) or mutant (B) expression construct. Wnt signaling was activated by transfection with the indicated amounts of a plasmid expressing Wnt1. Results were normalized to Renilla values and to the Wnt1-transfected sample. Data are means + S.D. of one representative experiment, which was performed in duplicates.

As illustrated in Figure 14, co-transfection of the indicated amounts of a plasmid expressing RNF43 resulted in a dose-dependent decrease of Tcf4-mediated Wnt signaling activity in HEK293T cells stimulated by co-transfection of Wnt1. In contrast, RNF43mut exhibited the opposite effect and strongly increased Wnt signaling. Thus, in HEK293T cells, RNF43 negatively regulated Wnt1-induced Wnt signaling activity *in vitro* (Gerhard et al., unpublished). The preliminary results suggested further investigating the effect of RNF43 on the Wnt signaling pathway, as well as a possible function of the protein in tumorigenesis.

1.10 Objectives

The aim of this project was the characterization of RNF43, a protein mainly expressed at sites of high Wnt signaling, regarding its function and localization. Therefore, this study aimed to

- Get an insight into the expression pattern of RNF43
- Unravel a possible effect of the Wnt target gene *RNF43* on the Wnt signaling pathway by using *in vivo* and *in vitro* methods
- Investigate the mechanism(s) of function of RNF43
- Generate several deletion mutants of RNF43 and the previously generated RNF43 RING dead mutant, analyze them and compare them with full length proteins
- Evaluate the role of RNF43 in tumors

2 Materials and Methods

2.1 Materials

2.1.1 Consumables

Blotting paper	GB46	Hartenstein
Cell culture flasks, sterile, 175 cm^2	734-2315	VWR International
Cell culture flasks, sterile, 25 cm^2	734-2311	VWR International
Cell culture flasks, sterile, 75 cm^2	734-2313	VWR International
Cell scrapers, 30 cm	99003	TPP
Cellstar centrifuge tubes, 15 ml	188271	Greiner Bio-one
Cellstar centrifuge tubes, 50 ml	227261	Greiner Bio-one
Cryogenic vial, 1 ml	LW3332	Alpha Laboratories
Cryogenic vial, 2 ml	LW3334	Alpha Laboratories
DNA Pick-Tips	03DNA65	SLG
Drigalski spatulas	RSGA354.165	VWR
Inoculation spreader	612-1561	VWR International
LightCycler®480 multiwell plate 96, white	04 729 692 001	Roche
Medical X-ray film (Super RX)	47410 08389	Fujifilm
MicroAmp™ fast optical 96-well reaction plate	4346906	Applied Biosystems
MicroAmp® optical 384-well reaction plate	4309849	Applied Biosystems
Microcentrifuge tubes, 1.5 ml	T9661-1000EA	Eppendorf
Microscope cover glasses, 18 x 18 mm	0101030	Marienfeld Superior
Microscope slides	ISO8037/1	Thermo Scientific
Novax® gel cassettes	NC2010	Invitrogen
Novax® gel combs 10-, 12-, 15 wells	NC3010,-12,-15	Invitrogen
PCR tubes	6003-SF	Kisker
Plastic embedding device	07-7100	Bio-Optica
Protan nitrocellulose transfer membrane,0.45µm	NC04	Whatman
Round-bottom assay plate, 96 well	3789	Cos7tar
Serological pipettes, 10 ml	607 180/10ml	Greiner Bio-one

Serological pipettes, 25 ml	706 180/25ml	Greiner Bio-one
Serological pipettes, 5 ml	606 180/5ml	Greiner Bio-one
Superfrost plus microscope slides	J1800AMNZ	Thermo Scientific
TipOne graduated filter tips, 10 µl	S1121-3810	Starlab
TipOne bevelled filter tips, 20 µl	S1121-1810	Starlab
TipOne graduated filter tips, 1000 µl	S1122 1830	Starlab
TipOne graduated filter tips, 1 - 200 µl	S1120-8810	Starlab
Tips, 10 µl	732-0561	VWR International
Tips, 1 - 200 µl	732-0539	VWR International
Tips, 1000 µl	732-0532	VWR International
Tissue culture dish, 100 mm	353003	BD Bioscience
Tissue culture dish, 150 mm	353025	BD Bioscience
Tissue culture plate, 6 well	353046	BD Bioscience
Tissue culture plate, 12 well	353043	BD Bioscience
Tissue culture plate, 24well	353047	BD Bioscience
Tissue culture plate, 48 well	353078	BD Bioscience
XCell II™ blot module	EI9051	Invitrogen
XCell SureLock™ mini-cell chambers	EI0001	Invitrogen

2.1.2 Chemicals and reagents

2-Propanol	67523	Roth
30 % Acrylamid/Bis solution	161-0158	Bio-Rad
5-Aza-2´-Deoxycytidine	A3656	Sigma-Aldrich
Aceton	9372	Roth
Acetic acid	A3738.4	Roth
AG 501-X8 Resin	143-6424	Bio-Rad
Anti-digoxigenin-AP conjugate, Fab frag.	11093274910	Roche
Agar-Agar	5210	Roth
Agarose	A9539-5009	Sigma-Aldrich
Albumin Fraction V (BSA)	A1391,0500	AppliChem
Ammoniumpersulfat, APS	A2941,0100	AppliChem
Ampicillin	K029.3	Roth
Aqua ad iniectabilia Diaco	2034374	Serag-Wiessner KG

Bench Top 1kb DNA Ladder	G7541	Promega
Beta-Mercaptoethanol	M3148	Sigma-Aldrich
Blocking reagent	11096176001	Roche
BM Purple AP substrate solution	11442074001	Roche
Bromophenol blue	8122	Merck
Calcium chloride	2388.1000	Merck
Cell Titer-Glo® substrate	G755A	Promega
Complete protease inhibitor cocktail tablets	04693159001	Roche
Disodium hydrophosphate, $Na_2HPO_{4x}2H_2O$	119753	Merck
Dithiothreitol, DTT	A3668,0050	AppliChem
DMSO	A3672,0250	AppliChem
DNA-free DNase treatment and removal kit	AM1906	Ambion
Dual Luciferase reporter assay system	E1960	Promega
Dulbecco´s Modified Eeagle Medium, DMEM	41965	GIBCO®, Invitrogen
Ethanol, abs.	A3678,1000	AppliChem
Ethylenediaminetetraacetic acid, EDTA	A2937,0500	AppliChem
Fetal calf serum, FCS	F7524-500ML	Sigma-Aldrich
FideliTaq™ PCR Master Mix (2x)	71182	USB
Formamide	A1682,1000	AppliChem
GenElute™ mammalian total RNA miniprep kit	RTN70-1KT	Sigma-Aldrich
Glycerin	A2926,1000	AppliChem
Glycine	3790.3	Sigma-Aldrich
GoTaq® Green Master Mix (2x)	M7112	Promega
Hydrochloric acid, HCl	1090631000	Merck
Heparin sodium salt	H3149	Sigma-Aldrich
IGEPAL (NP-40)	I8896	Sigma-Aldrich
Illustra GFX PCR and gel band purification kit	28-9034-70	GE Healthcare
Ponceau S	14119-4	Sigma-Aldrich
Potassium acetate, KAc	T874.2	Roth
Potassium chloride, KCl	4936.1000	Merck
KAPA SYBR® FAST qPCR Universal Master Mix	07-KK4600-03	PeqLab
LB Agar	75851	USB
LB Broth	75852	USB

Levamisole hydrochloride	196142	Sigma-Aldrich
Lipofectamine 2000	11668	Invitrogen
Lithium chloride, LiCl	A490875	Merck
Maleic acid	11585762001	Roche
Manganese chloride, $MnCl_2$	T881.2	Roth
Maxima^{TM} SYBR Green/ROX qPCR MasterMix (2x)	K0221	Fermentas
Methanol	4627.4	Roth
Milk Powder	T145.2	Roth
M-MLV reverse transcriptase, RNase H(-)	M3682	Promega
Monopotassium phosphate, KH_2PO_4	1048730250	Merck
Opti-MEM	51985	GIBCO®, Invitrogen
Orange G	O3756	Sigma-Aldrich
Penicillin/Streptomycin (P/S) 100x Solution	15140	GIBCO®, Invitrogen
peqGOLD protein marker V	27-2210	PeqLab
Paraformaldehyde	0335.1	Roth
Phosphate buffered saline, PBS, 1x	14190	GIBCO®, Invitrogen
Pierce ECL Western blotting substrate	32106	Thermo Scientific
Protein A agarose	05015979001	Roche
Protein G agarose	05015952001	Roche
PureYield^{TM} plasmid midiprep system	A2492	Promega
Restore Western blot stripping buffer	21059	Thermo Scientific
Ribonuclease A (RNase A)	R4875	Sigma-Aldrich
RNF43 (human) siRNA	SR310324	OriGene
Rothi®-Safe	3865.1	Roth
Saponine	4185.1	Roth
SDS-Pellets	CN30.2	Roth
siTran 1.0; siRNA transfection reagent	TT300002	OriGene
Sodium chloride, NaCl	3957.1	Roth
Sodium acetate, NaOAc	6779.2	Roth
Sodium citrate	567446	Merck
Sodium deoxycholate, DOC	3484.2	Roth
Sodium hydroxide, NaOH	A4422,5000	AppliChem
Sodium hydroxide, NaOH, pellets	106462	Merck

SP6 RNA Polymerase	P1085	Promega
T4 DNA Ligase	M0202S	NewEnglandBioLabs
T4 DNA Ligase	M180	Promega
T7 RNA Polymerase	P2075	Promega
Tetramethylethylenediamine, TEMED	A1148,0025	AppliChem
Thiazolyl blue tetrazolium bromide (MTT)	M5655	Sigma-Aldrich
Trichloroacetic acid solution 20 %	7437.1	Roth
Tris	9090.3	Roth
Triton X-100	A1388,0500	AppliChem
Trypan blue 0.4 %	15250	GIBCO®, Invitrogen
Trypsin/EDTA	41010	PromoCell
Tryptone	A1553,1000	AppliChem
Tween 20	A1389,0500	AppliChem
Vectashield mounting medium with DAPI	H-1200	Vector Laboratories
Wizard® SV gel and PCR clean-up system	A9282	Promega
Wizard® SV minipreps plus DNA purification system	A1460	Promega
Yeast extract	212750	BD Bioscience
Z-Leu-Leu-Leu-al, MG132	C2211	Sigma-Aldrich

2.1.3 Buffers, media and solutions

All buffers, media and solutions were prepared using ddH_20.

1x PBS:
- 137 mM NaCl
- 2.7 mM KCl
- 4.3 mM Na_2HPO_{4x} $2H_2O$
- 1.4 mM KH_2PO_4
- pH 7.4

1x TBS:
- 50 mM Tris
- 150 mM NaCl
- pH 7.5

1x TBS-T:	1x TBS 0.1 % (v/v) Tween 20
1x TAE:	40 mM Tris 20 mM Acetic acid 1 mM EDTA
6x Orange G loading dye:	30 % (v/v) Glycerin 0.4 % (w/v) Orange G in 1x TAE
TfB-I buffer:	30 mM KAc 5 mM $MnCl_2$ 10 mM KCl 10 mM $CaCl_2$ 15 % (v/v) Glycerin
TfB-II buffer:	10 mM $MnCl_2$ 75 mM $CaCl_2$ 10 mM KCl 15 % (v/v) Glycerin

TfB buffers were prepared and autoclaved without $MnCl_2$ and Glycerin. These two components were added to the autoclaved buffers under sterile conditions.

Solutions for Immunofluorescence stainings

Fixation solution:	Methanol/Acetone (same amounts), storage: -20 °C
IF blocking and permeabilization:	3 % (w/v) BSA 1 % (w/v) Saponine 0.5 % (v/v) Triton X-100 in 1x PBS

Wash solution 1:	3 % (w/v) BSA
	1 % (w/v) Saponine
	in 1x PBS
Wash solution 2:	1 % (w/v) Saponine
	in 1x PBS

Buffers for SDS-PAGE and Western blot analysis

Running Buffer:	25 mM Tris
	0.2 M Glycin
	0.1 % (w/v) SDS
Transfer Buffer:	190 mM Glycin
	25 mM Tris
	0.01 % (w/v) SDS
	20 % Methanol
1x SDS-PAGE Stacking gel buffer:	0.4 % (w/v) SDS
	0.5 M Tris
	pH 6.8
1x SDS-PAGE Separation gel buffer:	0.4 % (w/v) SDS
	1.5 M Tris
	pH 8.8
Stacking gel (1 cassette):	1.06 ml H_2O
	0.39 ml 30 % Acrylamide/Bis solution
	0.49 ml Stacking gel buffer
	0.01 ml 10 % APS
	0.01 ml TEMED

Separation gel (1 cassette):	2.43 ml H_2O
	2.02 ml 30 % Acrylamide/Bis solution
	1.5 ml Separation gel buffer
	0.02 ml 10 % APS
	0.01 ml TEMED
4x SDS sample buffer:	240 mM Tris/HCl pH 6.8
	40 % (v/v) Glycerol
	8 % (w/v) SDS
	5 % ß-Mercaptoethanol
	0.004 % (w/v) Bromophenol Blue
Ponceau S staining solution:	0.1 % (w/v) Ponceau S
	5 % (v/v) Acetic acid

Buffers for cell lysis

1x SDS lysis buffer:	62.4 mM Tris pH 6.8
	2 % (w/v) SDS
	10 % (v/v) Glycerol
	50 mM DTT
	0.01 % (w/v) Bromphenol blue
NP-40 lysis buffer (for IP):	50 mM Tris
	150 mM NaCl
	1 % (v/v) NP-40
	Complete protease inhibitor cocktail tablet
	pH 8.0
RIPA buffer (for IP):	50 mM Tris-HCl pH 7.4
	150 mM NaCl
	1 % (v/v) Triton X-100
	1 % (w/v) Sodium deoxycholate
	0.1 % (w/v) SDS

1 mM EDTA
Complete protease inhibitor cocktail tablet

Buffers for whole mount *in situ* hybridizations

Since all solutions used for and before hybridization needed to be RNase-free, DEPC was used for preparation of these solutions. In addition, they were autoclaved.

DEPC-H_2O:	H_2O 0.01 % (v/v) DEPC
4 % PFA/PBS:	4 % (w/v) PFA 1x PBS-DEPC for dissolving, add a few drops of 10 N NaOH and heat at 55 °C cool on ice pH 7.0
PBT:	PBS-DEPC 0.1 % (v/v) Tween20
tRNA:	10 µg/µl in DEPC-H_2O
RIPA buffer:	0.05 % (w/v) SDS 150 mM NaCl 1 % (v/v) Igepal (NP-40) 0.5 % (w/v) Deoxycholate 1 mM EDTA 0.05 M Tris-HCl pH 8.0 in DEPC-H_2O Do not autoclave!
20x SSC:	3 M NaCl 0.3 M Sodium citrate

	in DEPC-H_2O
	pH 7.0
Deionized formamide:	10 % (w/v) AG 501-X8 Resin in formamide
	Stir for 1 h
	Filtration
Hybe-buffer (10 ml):	5 ml deionized formamide
	2.5 ml 20x SSC
	5 µl heparin solution (100 mg/ml in DEPC-H_2O)
	10 µl Tween 20
	2.05 ml DEPC-H_2O
	Adjust to pH 6.0 with 1 M Citric acid (~ 0.45 ml/10ml)
SSC/FA/Tween 20:	2x SSC
	50 % (v/v) formamide (deionized is not necessary)
	0.1 % Tween 20
	in DEPC-H_2O
10x TBST (use: 1x):	8 % (w/v) NaCl
	0.2 % (w/v) KCl
	0.25 M Tris-HCl pH 7.5
	10 % (v/v) Tween 20
	DEPC-H_2O to 100 ml
RNase solution:	0.5 M NaCl
	0.01 M Tris-HCl pH 7.5
	0.1 % (w/v) Tween 20
	in DEPC-H_2O
RNaseA:	10 µg/µl in 0.01 M Sodium acide (pH 5.2)
	Heat to 100 °C for 15 min
	Cool slowly to RT

	adjust pH by adding 0.1 vol. of 1 M Tris-HCl pH 7.4
MAB:	0.1 M Maleic acid 0.15 M NaCl in DEPC-H_2O pH 7.5 (adjust with solid NaOH)
MABT:	MAB 0.1 % (v/v) Tween 20
Blocking solution:	10 % (w/v) Blocking reagent MAB (for dissolving, shake and heat!) after dissolving, add 0.1 % (v/v) Tween 20
Alkaline phosphatase buffer:	0.1 M NaCl 0.05 M $MgCl_2$ 0.1 % (v/v) Tween 20 0.1 M Tris-HCl pH 9.5 4.8 mg Levamisole in DEPC-H_2O (final volume: 10 ml)
Staining solution:	BM purple AP substrate solution 2 mM Levamisole 0.1 % (v/v) Tween 20 Centrifuge, don't use pellet!

Media

LB (Luria-Broth) medium:	1 % (w/v) NaCl 0.5 % (w/v) Yeast extract 1 % (w/v) Tryptone pH 7.4

Before addition of antibiotics (Ampicillin, 100 µg/ml), LB medium was autoclaved and cooled to 50 - 60 °C. LB medium was stored at 4 °C.

LB agar:	0.5 % (w/v) NaCl
	0.5 % (w/v) Yeast Extract
	1 % (w/v) Tryptone
	1.5 % (w/v) Agar
	pH 7.4

LB agar was autoclaved and cooled to 50 - 60 °C before addition of antibiotics (Ampicillin, 100 µg/ml) and transfer to plates. After cooling to room temperature, LB agar plates were stored at 4 °C.

Cell culture medium:	500 ml DMEM
	50 ml FBS
	5 ml Penicillin/Streptomycin (100x solution)

2.1.4 Bacterial strains

E.coli DH5α

Escherichia coli DH5α is a highly transformable, widely used strain for DNA manipulation (Hanahan 1983). It enables the selection by α-complementation.

The genotype is defined as F^-, Φ80d*lacZ*ΔM15, Δ(*lacZYA-argF*)U169, *deoR*, *recA*1, *endA*1, *hsdR*17(rk^-, mk^+), *phoA*, *supE*44, λ^-, *thi*-1, *gyrA*96, *relA*1.

2.1.5 Cell lines

The cell lines used in this study, as well as their origins are listed in Table 1.

Name	Origin	Purchased from
DLD1	Human colorectal adenocarcinoma	ATCC no.: CCL-221
Cos7	African green monkey kidney fibroblast-like cells	ATCC no.: CRL-1651
CaCo2	Human colorectal adenocarcinoma	ATCC no.: HTB-37
HCT116	Human colorectal carcinoma	ATCC no.: CCL-247
HEK293T	Human embryonic kidney	ATCC no.: CCL-11268
HT29	Human colorectal adenocarcinoma	ATCC no.: HTB-38
SW480	Human colorectal adenocarcinoma	ATCC no.: CCL-228
LS174T	Human colorectal adenocarcinoma	ATCC no.: CCL-188
Mcf7	Human breast mammary gland adenocarcinoma	ATCC no.: HTB-22

Table 1 Cell lines used in this study.

2.1.6 Antibodies

Tables 1, 2 and 3 list the antibodies used in this study.

Primary antibodies:

Name	Produced in	Implemented concentration	Manufacturer
Anti-flag (M2)	mouse (monoclonal)	WB: 1:1000, IF: 1:200	Sigma-Aldrich F3165
Anti-flag	rabbit (monoclonal)	WB: 1:1000, IF: 1:200	Sigma-Aldrich F7425
Anti-ß-actin	mouse (monoclonal)	WB: 1:5000	Sigma-Aldrich A1978
Anti-ß-catenin	mouse (monoclonal)	WB: 1:1000, IF: 1:200	BD Biosciences 610154
Anti-Tcf4 (C9B9)	rabbit (monoclonal)	WB: 1:1000, IP: 1:170	Cell Signaling 2565S
Anti-CTBP (E-12)	mouse (monoclonal)	WB: 1:1000, IF: 1:200, IP: 1:170	Santa Cruz sc-17759
Anti-CTBP (H-440)	rabbit (polyclonal)	WB: 1:1000, IP: 1:170	Santa Cruz sc-11390

Anti-HA	mouse (monoclonal)	WB: 1:1000, IF: 1:200	Sigma-Aldrich H3663
Anti-HA	rabbit (polyclonal)	WB: 1:1000, IF: 1:200	Sigma-Aldrich H6908
Anti-Golgin 97	mouse (monoclonal)	IF: 1:200	Invitrogen A21270
Anti-Lamin B Receptor	rabbit (monoclonal)	IF: 1:200	Abcam Ab32535
Anti-Calnexin (H-70)	rabbit (polyclonal)	IF: 1:200	Santa Cruz sc-11397
Anti-PSF (clone B92)	mouse (monoclonal)	IF: 1:200	Sigma-Aldrich P2860
Anti-rabbit normal IgG	rabbit	IP: 1:850	Santa Cruz Sc-2027
Anti-mouse normal IgG	mouse	IP: 1:850	Santa Cruz Sc-2025
Anti-RNF43	rabbit (polyclonal)	WB: 1:1000, IF: 1:100	LifeSpan Biosciences LS-C102008
Anti-Histidine tag	mouse (monoclonal)	WB: 1: 2000	AbD Serotec MCA 1396
Anti-K63-linked Poly-Ubiquitin (D7A11)	rabbit (monoclonal)	WB: 1:500	Cell Signaling 5621 S

Table 2 Primary antibodies used in this study.

Secondary antibodies for Western blot analysis:

Name	Implemented concentration	Manufacturer
Anti-mouse IgG (H&L) HRP conjugate	1:2500	Promega W402B
Anti-rabbit IgG (H&L) HRP conjugate	1:2500	Promega W401B

Table 3 Secondary antibodies used for Western blot analysis.

Secondary antibodies for Immunofluorescence stainings:

Name	Implemented concentration	Manufacturer
AlexaFlour488 goat anti-mouse IgG	1:200	Invitrogen A11001
AlexaFlour594 chicken anti-rabbit IgG	1:200	Invitrogen A21442

Table 4 Secondary antibodies used for Immunofluorescence stainings.

2.1.7 Restriction enzymes

The used restriction endonucleases were all stored at -20 °C and purchased from Promega. The conditions for enzymatic activity as well as the buffers were chosen according to the manufacturer's instructions. The enzymes are listed in Table 5.

Name	Sites	Genomic source
*Eco*RV (10 U/µl)	GAT▼ATC CTA▲TAG	*E.coli* J62 pLG74
*Not*I (10 U/µl)	GC▼GGCCGC CGCCGG▲CG	*Nocardia otitidiscaviarum*
*Eco*RI	G▼AATTC CTTAA▲G	*E.coli RY13*
*Xba*I	T▼CTACA AGATC▲T	*Xanthomonas campestris pv. poorrii*

Table 5 Restriction enzymes used in this study.

2.1.8 Vectors

For the *Xenopus laevis* double axis formation assay, human wildtype and mutant RNF43 sequences (NCBI reference number: NM_017763) were cloned into pCS2myc using *Eco*RI and *Xba*I restriction enzymes. pCS2myc is a vector commonly used for mRNA expression and subsequent injection into embryos. It was kindly provided by Dr. Dietmar Gradl.

For mammalian expression, the plasmids RNF43-flag and RNF43-HA were constructed by Markus Gerhard using pcDNA^{TM}4/TO (Invitrogen) as a backbone. pcDNA^{TM}4/TO (pcDNA4TO) contains a hybrid promoter consisting of the human cytomegalovirus immediate-early (CMV) promoter and 2 tetracycline operator (TetO2) sites for tetracycline-

regulated expression in mammalian cells. In addition, it harbors a Zeocin™ resistance gene for selection of transfected cells and generation of stable cell lines. The RNF43 open reading frame was amplified by PCR using the primers listed in 2.1.9 and cloned into pcDNA4TO using *Evo*RV and *Not*I restriction sites. The flag- or HA-tag was added at the C-terminus of the RNF43 sequence.

The mutant RNF43-flag and RNF43-HA constructs were generated by Markus Gerhard using a QuickChange Site-Directed Mutagenesis Kit (Stratagene). These mutants harbor two point mutations (A→G) at nucleotides 875 and 884 of the *RNF43* gene resulting in two amino acid exchanges from histidine to arginine at the amino acids at positions 292 and 295.

The plasmids expressing RNF43 and RNF43mut derivates lacking different N- or C-terminal parts of RNF43 were cloned by inserting PCR-amplified *RNF43* gene fragments into *Eco*RV and *Not*I restriction sites of the expression vector pcDNA^{TM}4/TO (Invitrogen). The flag-tag was added at the C-terminus of the truncated RNF43 sequences.

RNF43(245-783) and RNF43mut(245-783) was constructed by Miriam Bognar, exactly like the other derivates lacking different parts of RNF43 (Wehrle 2010).

The plasmids RNF43-CFP and RNF43-Cherry were constructed by using the Gateway® recombination cloning technology (Invitrogen) according to the manufacturer's instructions. The RNF43 sequence was amplified by PCR using the Primers listed in 2.1.9, cloned into the pDONR^{TM}207 vector and afterwards cloned into pDest-Cherry and pDest-CFP vectors, which were all kindly provided by Dr. Ludger Hengst (Biocenter, Division of Medical Biochemistry, Innsbruck).

The Wnt-responsive, TCF-dependent luciferase constructs, pTOPflash and the control plasmid pFOPflash, containing mutated TCF binding sites, as well as an S33-ß-catenin expression construct (in which Ser33 is mutated) and a Wnt1 expression construct were kindly provided by Prof. Hans Clevers (Utrecht University, Utrecht, The Netherlands) and have been described previously (Morin, Sparks et al. 1997). pRL-TK Renilla plasmid, which was used to evaluate the transfection efficiency, was purchased from Promega.

The plasmid PSF-HA (pCR3.1 backbone) was kindly provided by Prof. Philip Tucker (University of Texas, Austin), Tcf4-HA (pcDNA3 backbone) was kindly provided by Dr. Jaw-Jou Kang (National Taiwan University, Taiwan), and the plasmid his-Ubiquitin (pCR3.1

backbone) was kindly provided by Dr. Kanaga Sabapathy (National Cancer Centre, Singapore).

For generation of probes for *in situ* hybridizations, the RNF43 sequence was amplified by PCR and cloned into the cloning vector pGEM®-T vector (Promega).

2.1.9 Primers

Primers used for amplifying specific targets are listed in Table 6.

Amplified target	Vector	Primer name	Primer sequence 5′→3′	Product size
RNF43/RNF43mut	pcDNA4TO	RNF_ EcoRV_se	GCAGATATCGCCATGAG TGGTGGCCACCAGCTGC	
		RNF43 NotI FLAG as	GCAGCGGCCGCTCACTTATC GTCGTCATCCTTGTAATCCA CAGCCTGTTCACACAGCTC	2399 bp
		RNF43 NotI HA as	GCAGCGGCCGCTCAAGCGT AATCTGGAACATCGTATGG GTAACCCACAGCCTGTTCAC ACAGCTC	2405 bp
RNF43(62-783)/ RNF43mut(62-783)	pcDNA4TO	RNF oTM1 se	GCAGATATCGCCACCATG AATCTCACTTTGGAAGGTGT GTT	
		Esther6 as= RNF2flagrev	GCAGCGGCCGCTCACTTATC GTCGTCATCCTTGTAATCCA CAGCCTGTTCACACAGCT	2216 bp
RNF43(121-783)/ RNF43mut(121-783)	pcDNA4TO	RNF oTM2 se	GCAGATATCGCCACCATGTC ACTGGCTAGCAAGGCTC	
		Esther6 as= RNF2flagrev	GCAGCGGCCGCTCACTTATC GTCGTCATCCTTGTAATCCA CAGCCTGTTCACACAGCT	2039 bp
RNF43(184-783)/ RNF43mut(184-783)	pcDNA4TO	RNF oTM3 se	GCAGATATCGCCACCATGG TGAGGATTGAGCTGAAGGA G	

		Esther6 as= RNF2flagrev	GCAGCGGCCGCTCACTTATC GTCGTCATCCTTGTAATCCA CAGCCTGTTCACACAGCT	1868 bp
RNF43(229-783)/ RNF43mut(229-783)	pcDNA4TO	RNF oTM4 se	GCAGATATCGCCACCATGC CGGATCCGCTTCAGCAG	
		Esther6 as= RNF2flagrev	GCAGCGGCCGCTCACTTATC GTCGTCATCCTTGTAATCCA CAGCCTGTTCACACAGCT	1715 bp
RNF43(245-783)/ RNF43mut(245-783)	pcDNA4TO	Esther4 se	GCAGATATCGCCATGACCA GGAGGTACCAGGCC	
		Esther6 as= RNF2flagrev	GCAGCGGCCGCTCACTTATC GTCGTCATCCTTGTAATCCA CAGCCTGTTCACACAGCT	1670 bp
RNF43(229-783)+sp/ RNF43mut(229-783)+sp	pcDNA4TO	OTM4+ SP_se	GCAGATATCGCCACCATG AGTGGTGGCCACCAGCTGC AGCTGGCTGCCCTCTGGCCC TGGCTGCTGATGGCTACCCT GCAGGCACCGGATCCGCTT CAGCAG	
		Esther6 as= RNF2flagrev	GCAGCGGCCGCTCACTTATC GTCGTCATCCTTGTAATCCA CAGCCTGTTCACACAGCT	1781 bp
RNF43(245-783)+sp/ RNF43mut(245-783)+sp	pcDNA4TO	pcTO+ 7/8+SP_ se	GCAGATATCGCCATG AGTGGTGGCCACCAGCTGC AGCTGGCTGCCCTCTGGCCC TGGCTGCTGATGGCTACCCT GCAGGCAACCAGGAGGTAC CAGGCC	
		Esther6 as= RNF2flagrev	GCAGCGGCCGCTCACTTATC GTCGTCATCCTTGTAATCCA CAGCCTGTTCACACAGCT	1737 bp
Part A for overlap PCR for RNF43(Δ191-228)/ RNF43(Δ 191-228)		PCR_A_ se	GCAGATATCGCCACCATGA GTGGTGGCCACCAGCTG	

		PCR_A_ as	CTGCTGAAGCGGATCCGGC TCCTTCAGCTCAATCCTCAC	603 bp
Part B for overlap PCR for RNF43(Δ191-228)/ RNF43(Δ 191-228)		PCR_B_ se	CCGGATCCGCTTCAGCAG	
		Esther6 as= RNF2flagrev	GCAGCGGCCGCTCACTTATC GTCGTCATCCTTGTAATCCA CAGCCTGTTCACACAGCT	1704 bp
RNF43(Δ191-228)/ RNF43(Δ 191-228) (generated by overlap PCR)	pcDNA4TO	PCR_A_ se	GCAGATATCGCCACCATGA GTGGTGGCCACCAGCTG	
		Esther6 as= RNF2flagrev	GCAGCGGCCGCTCACTTATC GTCGTCATCCTTGTAATCCA CAGCCTGTTCACACAGCT	2289 bp
pcDNA4TO+Venus	pcDNA4TO	Venus_se	GCAGATATCGCCATGGTGA GCAAGG GCGAGG	
		Venus_as	GCA GCG GCC GCT TAC TTG TAC AGC TCG TCC ATG	743 bp
Mouse RNF43 (for *in situ* hybridization)	pGEM®-T	insitu_ long_sens	CAGAGGTTCATCCATTGATG TTC	
		insitu_ as	ACATAGTGCCTGATTCAAGC ATC	1567 bp
Human RNF43 (for sequence analysis of N-terminus)	pGEM®-T	Esther1 se= RNF1for	GCAGATATCGCCATGAGTG GTGGCCACCAGC	
		Esther2 se= RNF1flagrev	TGGGACCCTCTCGATCTTAC TACCCATACGATGTTCCAGA TTACGCTGCGGCCGCTGC	1036 bp
Human RNF43 (for sequence analysis of C-terminus)	pGEM®-T	700se	GAGAACAGCCTGGGCCATC	

		Esther6 as= RNF2flagrev	GCAGCGGCCGCTCACTTATC GTCGTCATCCTTGTAATCCA CAGCCTGTTCACACAGCT	1689 bp
RNF43 (for Gateway-cloning)	pDONR^{TM} 207	RNF-Gateway_ se	GGGGACAAGTTTGTACAAA AAAGCAGGCTTTACCATGA GTGGTGGCCACCAGC	
		RNF-Gateway_ as	GGGGACCACTTTGTACAAG AAAGCTGGGTCCTTATCGTC GTCATCCTTGTAAT	2439 bp

Table 6 Primers for cloning.

Primers used for RT-PCR are listed in Table 7.

Amplified target	Primer	Primer sequence 5′→3′	Product size
Human RNF43	hRNF43 for	CCTGTGTGTGCCATCTGTCT	
	hRNF43 rev	GCAAGTCCGATGCTGATGTA	120 bp
Human GAPDH	hGAPDH for	GAAGGTGAAGGTCGGAGT	
	hGAPDH rev	GAAGATGGTGATGGGATTTC	226 bp
Mouse RNF43	mRNF43 for	CCCGTGTGTGCCATCTGTCT	
	mRNF43 rev	GCAAGTCCGATGCTGGTATAG	120 bp
Mouse GAPDH	mGAPDH for	GCACAGTCAAGGCCGAGAAT	
	mGAPDH rev	GCCTTCTCCATGGTGGTGAA	151 bp

Table 7 Primers for Real-time PCR.

Primers used for sequencing are listed in Table 8.

Vector	Primer	Primer sequence 5′→3′
pcDNA4TO	CMV for	CGCAAATGGGCGGTAGGCGTG
pcDNA4TO	BGH rev	TAGAAGGCACAGTCGAGG
pGEM®-T	T7	TAATACGACTCACTATAGGG
pGEM®-T	SP6	ATTTAGGTGACACTATAG
RNF43/RNF43mut	RNF 400 se	CTGTCCTCTTTGACATCACTG
RNF43/RNF43mut	RNF 700 se	GAG AAC AGC CTG GGC CAT C
RNF43/RNF43mut	RNF 1000 se	GAACCAGGTCGAAGACTCCAC
RNF43/RNF43mut	RNF 1410 se	CCTGTCATGGCTCTTCCAGTGAC
RNF43/RNF43mut	RNF 1530 se	GTGTACTGCAGCCCTAAAGG
RNF43/RNF43mut	RNF 2200 se	CCAGCCCCTGGAACCACATCCAC
RNF43/RNF43mut	RNF 750 as	CTGATGGCCCAGGCTGTTC
RNF43/RNF43mut	RNF 815 as	CGCAGCACCGAAGCCAGG
RNF43/RNF43mut	RNF 1700 as	GTTTCTGGGCCAGGCTTCCTGCC
RNF43/RNF43mut	RNF 1391 as	TCCAGATCCACTGCTGTCAG

Table 8 Primers for sequencing.

2.1.10 Instruments

Agarose Electrophoresis Chambers	Bio-Rad
AxioVert 40 Microscope	Zeiss
Biofuge Pico Centrifuge	Heraeus, Thermo Scientific
Biofuge Primo R Centrifuge	Thermo Scientific
Cell Culture Incubator, HeraCell, 240	Heraeus, Thermo Scientific
Centrifuge 5415D	Eppendorf
Centrifuge 5424	Eppendorf
Centrifuge Micro 200R	Hettich
Confocal Microscope, Leica SP5	Leica microsystems
Developing Machine (Curix60)	AGFA
Electronic Pipet Filler, Easypet®	Eppendorf
Electrophoresis Power Supply PowerPac300	Bio-Rad

Fluorescence Microscope, DMRB	Leica
Freezer -20°C	Liebherr
Heatable Magnetic Stirrer	IKAMAG RET-G
HERAFreeze Basic -86°C Freezer	Thermo Scientific
Hybridization Oven OV3	Biometra
Ice Machine	Ziegra
iCycler	Bio-Rad
Innova 2100 Platform Shaker	New Brunswick Scientific
Keyence BZ-9000 Microscope	Keyence
Laboratory Precision Scale XB120A Precisa	Precisa
Laboratory Scale	Kern
Laminar Airflow Cabinet, HeraSafe	Heraeus, Thermo Scientific
Leica DMRB Microscope	Leica microsystems
LightCycler480	Roche
Mithras LB9440	Berthold
Multifuge 3 S-R	Heraeus, Thermo Scientific
NanoDrop 1000	Thermo Scientific
Neubauer Hemocytometer Cell Counting Chamber	Marienfeld
Orion Microplate Luminometer	Berthold
pH-Meter	WTW inoLab
Power Supply PowerPac Basic (for SDS gels)	Bio-Rad
Refrigerator 4°C	Liebherr
Shaker, Titramax 100	Heidolph
Single Channel Pipettor, 0.5-10 µl	Corning
Single Channel Pipettor, 200-1000 µl	Corning
Single Channel Pipettor, 20-200 µl	Corning
Single Channel Pipettor, 2-20 µl	Corning
Sonoplus HD60	Bandelin
Spectrophotometer NanoDrop 1000	Thermo Scientific
StepOnePlus™ Real-Time PCR System	Applied Biosystems
T10 Basix ULTRA-TURRAX Disperser	IKA
T3000 Thermocycler	Biometra
Thermomixer Compact	Eppendorf

UV Transilluminator, Eagle Eye Gel Doc	Bio-Rad
Applied Biosystems 7900HT system	Applied Biosystems
Vortex Genie 2	Schultheiss
Waterbath Julabo	Julabo
Waterbath	GFL
XCell IITM Blot Module	Invitrogen
XCell SureLock® Mini-Cell	Invitrogen

2.1.11 Software

Adobe Photoshop	Adobe
AxioVision Rel. 4.8.	Zeiss
GraphPad Prism	GraphPad
LAF-AS	Leica
LightCycler® 480 software (V1.5.0)	Roche Applied Science
Molecular Imager Gel Doc XR+ System	BioRad
NCBI/BLAST	National Center for Biotech Information
NEBcutter (V2.0)	New England BioLabs
OligoCalc	Northwestern University Chicago
ORF Finder	National Center for Biotech Information
SMART; Simple Modular Architecture research tool	EMBL Heidelberg
Subnuclear Compartments Prediction System (V 2.0)	Laboratory of Computational Functional Genomics, Department of Bioengineering, University of Illinois Chicago
PSORT II	Human Genome Center, Institute for Medical Science, University of Tokyo, Japan
Euk-PLoc 2.0	Chou and Shen; Gordon Life Science Institute San Diego California; Institut of Image Processing and

	Patterning, Shanghai Jiaotong University, China
TargetP 1.1	Technical University of Denmark
DAS Transmembrane Prediction Server	Stockholm University, Sweden
TMHMM Server v. 2.0	Center for Biological Sequence analysis, CBS, Technical University of Denmark
TMPred	European Molecular Biology Network, Swiss node
Split Membrane Protein Transmembrane Secondary Structure Prediction Server	University of Split, Croatia
PRALINE multiple sequence alignment	IBIVU, University of Amsterdam
TANTIgen version 1.0	Bioinformatics Core at Cancer Vaccine Center, Dana-Faber Cancer Institute
NeXtProt	Swiss Institute of Bioinformatics (SIB) and GeneBio SA

2.2 Methods

For sterilization, all heat stable consumables, media and solutions were autoclaved at 121 °C and 2 bar for 20 min. Non-heat stable consumables, media and solutions were sterilized using mechanical filters (size 0.2 µm for removal of bacteria, size 20 nm for removal of viruses).

2.2.1 Microbiological Methods

2.2.1.1 Culture and storage of *E.coli* DH5α

The *E.coli* DH5α strain was cultured at 37 °C in LB medium (on a thermoshaker) or on LB agar plates. For long-term storage of bacteria, glycerin stocks were prepared.

2.2.1.2 Preparation of glycerin stocks

For long-term storage of bacteria, 2 ml of culture were pelleted, resuspended in 0.5 ml LB medium (without antibiotics) and mixed with 0.5 ml Glycerin (87 %). Subsequently, the glycerin stocks were rapidly frozen in liquid nitrogen and stored at -80 °C.

2.2.1.3 Generation of chemically competent *E.coli* DH5α

For generation of chemically competent *E.coli* DH5α, 250 ml TYM medium were inoculated to OD_{600} of 0.1 with an overnight culture. The culture was incubated at 37 °C on a thermoshaker. When OD_{600} of 0.5 - 0.7 was reached, the bacteria were incubated on ice for 30 min. Afterwards they were pelleted (5 min, 4000 rpm, 4 °C). The obtained cell pellets were resuspended in 10 ml TfB-I buffer, followed by centrifugation (8 min, 4000 rpm, 4 °C). The resulting cell pellets were then resuspended in 10 ml TfB-II buffer. Aliquots of 100 µl of the final suspension were quickly frozen in liquid nitrogen and stored at -80 °C.

2.2.1.4 Transformation of chemically competent *E.coli* DH5α

For transformation of bacteria, 100 ng of plasmid DNA or 10 µl of ligation mix were added to an aliquot of chemically competent *E.coli* DH5α, upon thawing of the bacteria on ice. After incubation of the DNA-bacteria-mixture on ice for 10 min, the cells were subjected to heat shock (42 °C, 45 sec). Afterwards, they were again incubated on ice for 5 min. Subsequently,

900 µl of pre-heated (37 °C) LB medium were added to the cells, followed by incubation at 37 °C for 30 min. The bacteria were then pelleted (5 min, 5000 rpm), the supernatant was discarded and the cells were plated on agar plates using disposable Drigalski spatulas.

2.2.1.5 Culture and storage of transformed *E.coli* DH5α

After transformation of a respective plasmid, single clones were picked from the agar plate and transferred to LB medium containing the appropriate antibiotics (e.g. Ampicillin: 1 µg/ml final concentration). The bacteria harboring the plasmid were subsequently cultured on a shaker at 37 °C overnight. For long time storage of bacteria, glycerin stocks were prepared.

2.2.2 Molecular biological methods

2.2.2.1 Amplification of DNA by PCR

In this study, conventional PCR was used for the construction of vector inserts as well as for screening purposes. PCR conditions were dependent on the GC content/melting temperatures of the respective primers, and on the size of the expected DNA fragment. The annealing temperature, which was dependent on the melting temperature of the respective primers, was ~ 56 - 58 °C.

2.2.2.2 Isolation of plasmid DNA

For small amounts of plasmid DNA, e.g. for analytical purposes, plasmid DNA isolation was performed from 4 ml of *E.coli* DH5α overnight culture using the Wizard® SV Minipreps Plus DNA purification system (Promega) according to the manufacturer's instructions.

For obtaining larger amounts of plasmid DNA, isolation was performed from 100 ml of *E.coli* DH5α overnight culture using a PureYield™ Plasmid Midiprep system (Promega) following the manufacturer's instructions. Both plasmid DNA isolation systems provide a rapid method for purification of plasmid DNA of high quality for use in eukaryotic *in vitro* expression experiments. The elution was performed in 50 µl (Minipreps) or 500 µl (Midipreps) nuclease-free H_2O, and isolated plasmid DNA was stored at 4 °C.

2.2.2.3 Determination of concentration and purity of DNA and RNA

The concentrations of RNA and DNA were determined by the use of UV spectrophotometry. Both RNA and DNA absorb UV light efficiently, thus even low amounts can be detected. In this study, DNA and RNA concentrations were quantified using the spectrophotometer NanoDrop 1000. Concentrations were measured at 260 nm (A_{260}) using 1.5 µl of DNA or RNA, and purities were assessed by the A_{260}/A_{280} ratio. The ratio for pure DNA or RNA, without any protein contaminations, is ~ 1.8 for DNA and ~ 2.0 for RNA.

2.2.2.4 Digestion of DNA using restriction endonucleases

DNA was digested with restriction enzymes purchased from Promega according to the manufacturer's instructions. The digestions were performed in a total volume of 10 µl or 20 µl. All digests were analyzed by agarose gel electrophoresis.

2.2.2.5 Agarose gel electrophoresis

Agarose gel electrophoresis was used for the determination of the size of DNA fragments, either after PCR amplification of DNA fragments, digestion of DNA, for verification of lengths of DNA fragments, or for determination of purity of DNA or RNA. Negatively charged nucleic acid fragments are forced to migrate through a cross-linked agarose gel matrix by voltage application. Since smaller fragments can migrate faster through the gel matrix, a separation between smaller and larger fragments in the gel is achieved. Larger fragments become entangled and run more slowly.

Agarose gels were prepared by dissolving 1 - 2 % (w/v) of agarose in 1x TAE buffer through heating in a microwave for ~ 5 min. After cooling down to room temperature, 5 µl of Rhoti® – Safe were added per 100 ml of agarose solution. The solution was subsequently poured into a gel chamber. A comb for the generation of sample pockets was placed. After hardening of the gel, the comb was removed and the gel chamber with the gel was placed into an electrophoresis chamber, where it was completely covered with 1x TAE buffer. Afterwards, each sample was mixed with an appropriate amount of 6x Orange G loading dye and filled into the sample pockets of the gel. Electrophoresis was performed at 95 V for 30 - 45 min. The separated nucleic acid fragments were then visualized by UV illumination (λ = 302 nm) and documented using a Molecular Imager Gel Doc XR+ System.

2.2.2.6 DNA extraction from agarose gels

After agarose gel electrophoresis and visualization of nucleic acids, DNA fragments that were needed for further experiments, (e.g. ligations into plasmids) were recovered from the gel by picking with a pipette and DNA Pick-tips (SLG). Pieces of gel containing the desired DNA were placed into 1.5 ml tubes and DNA was eluted from the gel using the Wizard® SV Gel and PCR Clean Up Kit (Promega) or Illustra GFX PCR and Gel Band Purification Kit (GE Healthcare) according to the manufacturers' instructions. The DNA was eluted in 15 - 25 µl nuclease-free H_2O.

2.2.2.7 Ligation of DNA fragments into plasmids

Ligation was achieved by using T4 DNA ligase (Promega; New England Biolabs) according to the manufacturer's instructions. The T4 DNA ligase catalyzes the joining of DNA strands between adjacent nucleotides. Therefore, a cloning vector, e.g. pGEM®-T (Promega), which is suitable for direct cloning of the insert of interest into the vector, can be used. For ligation of an insert into an expression vector, the vector was opened by restriction endonucleases generating appropriate ends before ligation. In addition, the insert was cut by restriction enzymes in order to generate suitable ends for cloning into the specific vector. After ligation, the products were transformed into chemically compentent *E.coli* DH5α.

2.2.2.8 Sequencing of DNA

All cloned constructs were sent to MWG Eurofins for sequencing with the appropriate primers in order to verify the DNA sequences of inserts, tags and restriction sites, and to identify possible point mutations. Each sample sent for sequencing contained 750 - 1000 ng of plasmid DNA in a total volume of 15 µl H_2O. 3 µl of a specific primer of 10 µM concentration were either added directly or the DNA was sequenced using a universal primer added by the company.

2.2.3 Cell culture methods

2.2.3.1 Culture of cell lines

All cell lines used in this study were purchased from ATCC and are listed in Table 1. Cell lines were cultured in 25 cm^2, 75 cm^2 or 175 cm^2 cell culture flasks in 5 ml, 10 ml or 25 ml

Dulbecco's Modified Eagle's Medium (DMEM; GIBCO®). All media were supplemented with 10 % fetal calf serum (FCS; Sigma-Aldrich) and 1x penicillin/streptomycin (P/S; GIBCO®). All cells were maintained in a humidified 5 % CO_2 atmosphere at 37 °C. Cells were subcultured by removing the medium, washing the cells with 5 ml PBS and incubating them with 1 ml of 0.25 % Trypsin-EDTA (GIBCO®) at 37 °C and 5 % CO_2 for approximately 5 min in order to detach the adherent cells from the bottom of the flask. After incubation, 10 ml of DMEM + 10 % FCS + 1x P/S were added in order to stop the trypsinization reaction. The cell suspension was transferred to a 15 ml tube and centrifuged at 1200 rpm for 5 min. The supernatant was discarded and the cell pellet was resuspended in 5 ml DMEM + 10 % FCS + 1x P/S. Cells were either split (1:3 - 1:10) or seeded in cell culture plates or dishes for experiments at an appropriate density. All cell lines were regularly checked for the presence of mycoplasma.

2.2.3.2 Treatment of cells

For experiments with 5-Aza-2'-Deoxycytidine, cells were treated with 5 µM of 5-Aza-2'-Deoxycytidine (5-Aza-2'-dCyt; Sigma-Aldrich, freshly prepared in water) for up to 96 h prior to cell lysis. Fresh drug was added every 24 h after the medium was changed.

The proteasome inhibitor MG132 (Z-Leu-Leu-Leu-al; Sigma-Aldrich) was dissolved in DMSO, and cells were treated with 10 µM MG132 for up to 12 h prior to cell lysis.

For induction of Wnt signaling activity in HEK293T cells and Cos7 cells, cells were treated with Lithium chloride. Treatments were performed 24 h after transfections for 24 h, with the amounts indicated in the figure legends.

For blue staining of colonies in Colony formation assays, cells were treated with a final concentration of 120.5 µg/ml of MTT for 1 - 2 h.

2.2.3.3 Freezing and thawing of cells

For long-term storage, cells were frozen. Therefore, cryotubes containing 500 µl of freezing medium (90 % FCS + 10 % DMSO) were prepared. Cells were trypsinized (2.2.3.1) and the cell pellet was resuspended in DMEM +10 % FCS + 1x P/S. 500 µl of the obtained cell suspension were added to each of the prepared cryotubes. After incubation of the tubes at -80 °C for 24 - 72 h, they were transferred to liquid nitrogen and stored at -190 °C.

For thawing of cells, 30 ml of pre-warmed DMEM +10 % FCS + 1x P/S were prepared in 50 ml centrifugation tubes. Cells were then thawed by incubating the cryotube in a waterbath at 37 °C for a short period. Upon thawing, the cell suspension was rapidly transferred to the prepared medium and centrifuged at 1200 rpm for 5 min at room temperature. The supernatant was discarded and the cell pellet was resuspended in 5 ml DMEM +10 % FCS + 1x P/S and transferred to a 25 cm^2 flask.

2.2.3.4 Determination of cell number

The number of living cells per unit volume of a suspension was determined by using a Neubauer hemocytometer cell counting chamber and a microscope.

One quarter of a counting chamber represents the area of 1 mm^2 and the height of 0.1 mm. Thus, the cell number of one quarter represents 0.1 µl of cell suspension. For counting, 10 µl of cell suspension were diluted 1:5 in Trypan blue (GIBCO®), which is a vital dye used to selectively stain dead cells blue, whereas the dye does not penetrate the cell membrane of viable cells. After diluting the cell suspension with Trypan blue (GIBCO®), a special coverslip was placed on the counting surface. Then, 10 µl of the Trypan blue-diluted cell suspension was introduced into one of the wells. After the area under the coverslip filled by capillary action, the counting chamber was positioned on the microscope stage and the counting grid was brought into focus.

For calculation of the number of living cells, the viable cells in each of the four quarters were counted. Then, the mean cell number per quarter was calculated. Finally, the mean was multiplied by the dilution factor 5 and then multiplied by 10^4 to include the volume of the chamber. The resulting value represented cells per ml.

2.2.3.5 Transfection of cells with plasmid DNA

Transfections of cells with plasmid DNA were performed in 6-well plates for Immunofluorescence stainings, mRNA extractions and colony formation assays, in 12-well plates for SDS lysates (for Western blot analysis), in 24-well plates for TOP/FOP Luciferase Reporter assays, in 48-well plates for proliferation assays and in 10 cm^2 dishes for IPs. Cells were seeded approximately 24 h before transfections at an appropriate density. Transfections with the respective plasmid DNA were performed using Lipofectamine 2000 (Invitrogen)

according to the manufacturer's instructions. After transfections, cells were incubated at 37 °C and 5 % CO_2 for 24 - 48 h, depending on the experiment.

2.2.3.6 Transfection of cells with siRNA

For specific knockdown of the *RNF43* gene, a set of three siRNAs (A, B and C) targeting *RNF43* was obtained from OriGene (SR310324) and tested regarding their effct on RNF43 mRNA levels in qRT-PCR. The target sequences of the RNF43 siRNAs were as follows: siRNA A 5′-GGGAATAAACTTTAGAGAAAGGAAG-3′, siRNA B 5′-TCAATCACAAGCAAAGUUGGAAATT-3′, and siRNA C 5′-GGTAGCCAGGTGTTACAAAGGTGCT-3′.

Cell transfections with siRNA were performed in 6-well plates for mRNA extraction and subsequent cDNA synthesis and RT-PCR analysis, and in 48-well plates for proliferation assays. The siRNA was delivered as a powder (2 nmol) and thus diluted in 200 µl siRNA duplex resuspension buffer (OriGene), which was supplied together with the siRNAs, in order to obtain an siRNA stock solution with a final concentration of 10 µM.

For experiments, a final concentration of 10 nM or 20 nM siRNA was used. Transfections with the respective siRNAs (OriGene) were performed using siTran transfection reagent (OriGene) according to the manufacturer's instructions.

For siRNA transfections and RT-PCR analysis, cells were seeded approximately 24 h before transfections in a volume of 2.5 ml (6-well plates) at an appropriate density. Per well, 20 µl siTran transfection reagent (OriGene) were diluted with 120 µl Opti-MEM (GIBCO®) without serum and added to 2.65 µl of siRNA stock solution (10 µM; in order to obtain a final concentration of 10 nM) or 5.30 µl of siRNA stock solution (in order to obtain a final concentration of 20 nM) in total. The transfection mix was incubated at RT for 10 min before added to the cells. After transfection, cells were incubated at 37 °C and 5 % CO_2 for 48 h or 72 h.

For siRNA transfections and proliferation assays, cells were seeded approximately 24h before transfections at a density of 10 000 cells per well (48-well plates) in a volume of 250 µl per well. Per well, 3 µl siTran transfection reagent (OriGene) were diluted with 17 µl Opti-MEM (GIBCO®) without serum and added to 0.54 µl of siRNA stock solution (10 µM; in order to obtain a final concentration of 20 nM). The transfection mix was incubated at RT for 10 min

before added to the cells. After transfection, cells were incubated at 37 °C and 5 % CO_2 for 48 h or 72 h.

For siRNA transfections and TOP/FOP Luciferase reporter assays, cells were seeded approximately 24 h before transfections at a density of 100 000 cells per well (24-well plates) in a volume of 500 µl per well. On the next day, cells were transfected in duplicates with 100 ng pTOPflash or pFOPflash plasmid (per well) and 10 ng Renilla plasmid (per well), as described in 2.2.5. On the following day, per well, 6 µl siTran transfection reagent (OriGene) were diluted with 34 µl Opti-MEM (GIBCO®) without serum and added to 1.08 µl of siRNA stock solution (10 µM; in order to obtain a final concentration of 20 nM). The transfection mix was incubated at RT for 10 min before added to the cells. After transfection with siRNA, cells were incubated at 37 °C and 5 % CO_2 for 72 h.

2.2.4 Protein biochemical methods

2.2.4.1 Co-Immunoprecipitation

The Co-Immunoprecipitation (Co-IP) method was used in order to identify possible protein-protein interactions. Therefore, target protein specific antibodies were used for precipitation of proteins bound to the specific target protein.

For each Co-IP, cells were seeded in two 10 cm^2 dishes at an appropriate density. The next day, cells were transfected using Lipofectamine 2000. Therefore, 6 µg of plasmid DNA (per plasmid and dish) were diluted in 150 µl Opti-MEM (GIBCO®) without serum. In parallel, 150 µl Lipofectamine mix were prepared by diluting Lipofectamine 2000 1:10 in Opti-MEM (GIBCO®) without serum and incubating at RT for 5 min. The Lipfectamine mix was subsequently added to the plasmid mix and incubated at RT for 25 min before adding the mixture (300 µl) to a dish. Cells were incubated at 37 °C and 5 % CO_2 for 48 h, before washed with 1x PBS once and subjected to lysis for non-denaturating or denaturating IPs.

For investigation of protein interactions, non-denaturating IPs were performed. Therefore, cells were lysed with 900 µl of NP-40 lysis buffer (2.1.3) per dish. Cell scrapers were used for removing the attached cells from the dishes. Cell lysates (900 µl per dish) were transferred to 1.5 ml tubes and put on ice.

For investigation of ubiquitination, denaturating IPs were performed. Therefore, cells were treated with 10 µM MG132 for 12 h prior to cell lysis with 100 µl RIPA buffer (2.1.3) per dish. Cell scrapers were used for removing the attached cells from the surface. Cell lysates (100 µl per dish) were transferred to 1.5 ml tubes and SDS was added to a final concentration of 1 %. The lysates were boiled for 5 min (95 °C), before 900 µl of NP-40 buffer were added to each tube. Lysates were incubated on ice for 5 min, before resuspended thoroughly.

In both denaturating and non-denaturating IPs, cell lysates were subjected to pre-clearing by incubation with 50 µl Protein A agarose beads (for precipitation with anti-rabbit antibody) or Protein G agarose beads (for precipitation with anti-mouse antibody) for 2 h at 4 °C on a rotating wheel. Cell lysates where then centrifuged at 13 000 rpm for 2 min at 4 °C. The pre-clearing step was repeated once.

After the two pre-clearing steps, 10 % of the raw lysates were transferred to 1.5 ml tubes and 4x SDS sample buffer was added to a final concentration of 1x SDS sample buffer. Raw lysate samples were frozen at -20 °C.

The remaining lysates were transferred to fresh 1.5 ml tubes and incubated with a specific antibody (Table 2) overnight at 4 °C on a rotating wheel. As a negative control, lysates were incubated with anti-mouse or anti-rabbit IgGs (Santa Cruz).

The following monoclonal antibodies were used: rabbit monoclonal anti-Tcf4 antibody (Cell signaling), mouse monoclonal anti-CTBP antibody (Santa Cruz), and anti-mouse or anti-rabbit IgG (Santa Cruz) as a negative control (Table 2). The concentrations of the antibodies were chosen according to the manufacturer's instructions.

After incubation of the pre-cleared lysates with a specific antibody overnight at 4 °C, 70 µl of Protein A agarose beads (when precipitating with a rabbit antibody), or Protein G agarose beads (when precipitating with a mouse antibody) were added and incubated on a rotating wheel for 4 h at 4 °C. Beads were collected by centrifugation and washed five times with 1x PBS. For recovering of the proteins attached to the beads, 100 µl of 1x SDS sample buffer were added to the beads and samples were incubated at 95 °C for 5 min.

The obtained Co-IP protein samples as well as the raw lysates were subjected to Western Blot analysis (2.2.4.2).

2.2.4.2 Western blot

Transfections for Western blot

For Western blot analysis, cells were seeded in 12-well plates at an appropriate density. Transfections were performed approximately 24 h after seeding (see 2.2.3.5). Therefore, 1 µg of plasmid DNA was diluted in 50 µl Opti-MEM (GIBCO®) without serum. In parallel, 50 µl Lipofectamine mix were prepared by diluting Lipofectamine 1:100 in Opti-MEM (GIBCO®) without serum. The Lipofectamine mix was incubated for 5 min at RT before it was added to the DNA mix and incubated at RT for 25 min. The DNA-Lipfectamine mix was subsequently added to the cells and incubated for 24 - 48 h at a humidified atmosphere and 5 % CO_2 at 37 °C.

Cell lysis for Western blot

Cells were lysed 24 - 48 h post-transfection. Therefore, the medium was removed and cells were washed with 1x PBS. Cells were lysed with 200 µl 1x SDS lysis buffer (2.1.3) per well (12-well plate) on ice. Cell scrapers were used for removing the attached cells from the surface. Cell lysates were transferred to 1.5 ml tubes and put on ice. In order to reduce sample visCos7ity, lysates were sonicated for 25 sec at 50 % of maximal intensity for shearing of DNA. After denaturation (95 °C, 5 min) and short centrifugation (13 000 rpm, 2 min), cell lysates were directly implemented for Western Blot analysis or stored at -20 °C.

SDS-Polyacrylaminde Gel Electrophoresis (SDS-PAGE)

SDS-PAGE was used for separating proteins according to their molecular weight. During this study, 8 % polyacrylamide (PAA) gels were used. The composition of separation and stacking gels are listed in section 2.1.3.. At first, the separation gel was prepared, and transferred into gel cassettes. Afterwards, the gel solution was covered with 100 µl Isopropanol, which was removed after polymerization. After polymerization, the stacking gel was prepared on top of the separation gel. In order to generate pockets for the samples, combs with 10 - 15 pockets were quickly placed into the stacking gel before polymerization. After 30 - 45 min at RT, the polymerized gels were either used directly or wrapped into wet paper towels for storage in a plastic bag at 4 °C.

For gel electrophoresis, gels were fixed in XCell SureLock^{TM} mini-cell chambers (Invitrogen) and filled with 1x SDS running buffer (2.1.3). Equal amounts of protein samples were loaded into the gel pockets, and subjected to electrophoresis at 170 V for 60 - 65 min.

Wetblot and X-ray development

For Western blot analysis, proteins separated according to their molecular weights were blotted onto nitrocellulose transfer membranes using XCell II^{TM} blot modules (Invitrogen). Blotting was performed at 230 mA for 95 min in transfer buffer (2.1.3). Afterwards, membranes were blocked for at least 1 h in 1x TBS-T (2.1.3) containing 5 % milk powder at RT. Alternatively, membranes were blocked overnight at 4°C. After blocking, membranes were incubated with the primary antibodies, which are indicated in the figure legends, in 1x TBS-T containing 1 % milk powder for 1.5 h at RT or overnight at 4 °C. The appropriate antibody dilutions are listed in Table 2. After washing of the membranes 3 - 5 times with 1x TBS-T, they were incubated with the secondary anti-mouse or anti-rabbit HRP-conjugated antibodies (Table 3) for 1 h. Membranes were again washed with 1x TBS-T (3 - 5 times, 10 min each). Each membrane was then covered with 2 ml of Pierce ECL Western Blotting Substrate (Thermo Scientific) before detection with X-ray films (Fujifilm) and the Curix60 developing machine.

Staining of membranes with Ponceau S

For staining of proteins on membranes, membranes were stained with Ponceau S. Therefore, the membranes were incubated in Ponceau S staining solution for 5 min with gentle agitation. For destaining, membranes were washed with ddH_2O several times.

TCA preciptiation of proteins

For precipitation of proteins, samples were mixed with 20 % Trichloroacetic acid (TCA) to a final volume of 10 % before incubated at 4 °C overnight. The next day, samples were centrifuged (10 min, full speed), and pellets were washed 2 times with Acetone. Pellets were dried and resuspended in 1x SDS sample buffer for subsequent Western blot analysis.

2.2.5 TOP/FOP Luciferase reporter assay

The TOP/FOP Luciferase reporter assay is a dual luciferase reporter system that allows the measurement of two individual reporter luciferases, which are simultaneously expressed, within a single system. Typically, the experimental reporter luciferase, the Firefly luciferase (*Photinus pyralis*), is correlated with the effect of specific conditions, whereas the activity of the co-transfected control reporter luciferase, the Renilla luciferase (*Renilla reniformis*), provides an internal control for experimental variations such as differences in transfection efficiencies. Since Firefly and Renilla luciferases have dissimilar enzyme structures, they have different substrate requirements, allowing a selective differentiation between their respective bioluminescence reactions. The luminescence from the firefly luciferase reaction can be quenched, while the luminescence from the Renilla luciferase is concurrently activated. Thus, the activity of the experimental Firefly reporter luciferase can be normalized to the activity of the internal control Renilla luciferase. Consequently, experimental variations caused by differences in cell viability or transfection efficiency can be reduced.

The TOP/FOP Luciferase reporter assay, which is based on the dual luciferase system, was developed as a readout for TCF/LEF transcriptional activity allowing the measurement of canonical Wnt signaling activity. The used luciferase reporter constructs were pTOPflash, which contains eight copies of the optimal TCF/LEF binding sites (CCTTTGATC) upstream of a promoter driving luciferase expression, and pFOPflash, which contains mutated TCF/LEF binding sites and serves as a negative control (Korinek 1997).

TOP/FOP Luciferase reporter assays were performed in order to investigate the effect of different expression constructs on the canonical Wnt signaling pathway. Therefore, cells were seeded in 24-well plates at an appropriate density according to their growth rate. On the next day, they were transiently transfected in duplicates with 100 ng pTOPflash or pFOPflash plasmid (per well), 10 ng Renilla plasmid (per well), and different amounts of other expression constructs, whose effects on the Wnt signaling pathway wanted to be determined. The amount of DNA used per well was kept constant by addition of empty vector (pcDNA4TO). For one duplicate, plasmids were diluted in 50 µl Opti-MEM (GIBCO®) without serum. In parallel, 50 µl of Lipofectamine mix were prepared (per duplicate) by diluting Lipofectamine 2000 1:25 in Opti-MEM (GIBCO®) without serum and incubating at RT for 5 min. The Lipofectamine mix was subsequently added to the plasmid mix and incubated at RT for 25 min before adding 50 µl of the mixture to each well of the duplicate.

Treatments of cells with Lithium chloride were performed 24 h after transfections for 24 h, as indicated in the figure legends.

After incubation at 37 °C and 5 % CO_2 for 48 h, cells were washed with 1x PBS and lysed with 100 µl of 1x Passive lysis buffer (Promega) per well, which was included in the Dual Luciferase reporter assay system kit (Promega). After cell lysis and shaking of the plates for 30 min on a shaking platform, lysates were either measured directly or frozen at -20 °C. For measurement of the luciferase activities, 20 µl of each of the lysates were transferred to a white round-bottom 96-well plate. The reagents of the Dual Luciferase Reporter assay system kit (Promega) were prepared according to the manufacturer's instructions and the samples were measured using an Orion Microplate Luminometer (Berthold).

Values were expressed as the -fold increase in luciferase activity relative to the level of activity obtained by transfection of the reporter plasmids only (HCT116 and SW480 cells), by transfection of the reporter plasmids and additional activation of Wnt signaling activity by treatment with LiCl (HEK293T and Cos7) or by transfection of the reporter plasmids and control siRNA (HT29 cells).

2.2.6 mRNA extraction, DNaseI treatment and cDNA preparation

mRNA of cells and tissues was isolated with a GenElute^{TM} Mammalian Total RNA Miniprep Kit (Sigma-Aldrich) according to the manufacturer's instructions. For extraction of mRNA of cells, cells were washed once with 1x PBS, followed by addition of the lysis buffer. For extraction of mRNA of tissues, tissues were put into lysis buffer followed by homogenization using a T10 basix ULTRA-TURRAX Disperser for at least 30 sec on ice. To effectively release RNA from tissues, tissues were treated with Proteinase K (5 µl of 5 mg/ml stock solution) for 10 min. The total RNA was eluted in 50 µl ddH_2O and the concentration of the RNA was measured using a NanoDrop 1000 spectrophotometer.

In order to remove genomic DNA, the total RNA extracts were subjected to DNaseI treatment using a DNase treatment kit (Ambion) according to the manufacturer's instructions. Therefore, all samples prepared for one PCR run were adjusted to the same mRNA concentration (between 100 and 250 ng/µl) in a total volume of 25 µl ddH_2O. Following addition of 2.5 µl of DNase buffer and 1 µl of DNaseI, the samples were incubated at 37 °C for 25 min. The reaction was stopped by addition of 2.5 µl inactivation buffer and incubation

at RT for 2 min. Afterwards samples were subjected to centrifugation (10 000 g, 1 min, RT). The supernatant (~27 µl) was transferred to a new 1.5 ml tube.

RNA was transcribed into complementary DNA using the M-MLV reverse transcriptase RNase H(-) point mutant kit (Promega) following the manufacturer's protocol. For each sample, 2 reaction mixtures were set up, each containing 12 µl total RNA (DNaseI treated), 5.75 µl ddH_2O and 1 µl random primers (150 ng/µl). The reaction mixtures were incubated at 70 °C for 5 min, and subsequently rapidly chilled on ice. Then, 5 µl 5x M-MLV buffer and 1.25 µl dNTPs were added to each tube. In addition, 1 µl of reverse transcriptase was pipetted into one of the two tubes, and 1 µl of ddH_2O was added to the other tube, which served as a negative control for reverse transcription. The samples were then incubated at RT for 10 min, at 50 °C for 50 min and at 70 °C for 15 min. Afterwards, cDNAs were diluted 1:10 in ddH_2O and either directly used as templates for RT-PCR analysis or stored at -20 °C.

2.2.7 Real-Time PCR

For quantitative Real-Time PCR analysis, cDNAs were generated as described above (2.2.6). qRT-PCR gene expression analysis was always perfomed in at least duplicates, commonly using KAPA SYBR® FAST qPCR Universal 2x Master Mix (Peqlab), LightCycler®480 multiwell plates (96 wells) and a LightCycler®480 (Roche) PCR system.

For analysis of RNF43 expression in tumor stage II samples, Maxima™ SYBR Green/ROX qPCR 2x Master Mix (Fermentas), MicroAmp® optical 384-well reaction plates and a Applied Biosystems 7900HT cycler were used, since a bigger pool of samples was analyzed and this cycler was suitable for analysis of samples in 384-well format.

For analysis of RNF43 expression in embryos and organs of mice (Figure 17, Figure 18), Maxima SYBR Green/ROX qPCR 2x Master Mix (Fermentas), MicroAmp™ fast optical 96-well reaction plates and a StepOnePlus™ cycler (Applied Biosystems) were used.

Although different cyclers were used, the reaction and amplification conditions of all PCRs were the same and are illustrated in Table 9.

Reaction step	Temperature	Time
1. Initial denaturation	95°C	10 min
2. Amplification: Step 1	95°C	15 sec
Step 2	60°C	60 sec
Steps 1+2: repeated 40x		
3. Melting curve generation	95°C	15 sec
	60°C	60 sec
	95°C	15 sec

Table 9 Conditions for RT-PCR.

Primers used for RT-PCR analysis are listed in Table 7. Results were normalized to Glyceraldehye 3-phosphate dehydrogenase (GAPDH), which was used as an endogenous control. For analysis of the resulting data, the $2^{-\Delta\Delta Ct}$ method was used in order to calculate relative changes in gene expression.

When amplifications were performed using primers for the target gene *RNF43* and the internal control *GAPDH*, the -fold changes in expression of the *RNF43* target gene normalized to *GAPDH* and relative to the expression in a control sample, like normal muCos7a or untreated cells, was calculated as follows: the C_T values were calculated for both RNF43 and GAPDH, and the ΔC_T ($C_{T,RNF43} - C_{T,GAPDH}$) values were determined. The ΔC_T value from the control sample was then subtracted from the ΔC_T value of the non-control sample using the

$$\Delta\Delta C_T = (\Delta C_T)_{\text{non-control sample}} - (\Delta C_T)_{\text{control sample}}$$

formula, followed by the $2^{-\Delta\Delta Ct}$ calculation. Duplicates or triplicates were used for calculations. Means and standard deviations were determined from $2^{-\Delta\Delta Ct}$ calculations of at least three independent experiments.

The $2^{-\Delta\Delta Ct}$ method was not used if no relative changes in gene expression were determined. In this case, the C_T values were calculated for both RNF43 and GAPDH, and the ΔC_T ($C_{T,RNF43} - C_{T,GAPDH}$) values were determined, followed by conversion to the linear form using the term 2^-

$^{\Delta Ct}$, since converting the individual data to a linear form more precisely illustrates the variation among replicates (Livak and Schmittgen 2001).

2.2.8 Whole mount *in situ* hybridization

For whole mount *in situ* hybridizations, embryos were obtained from timed pregnancies and dissected at E 8.5 - E 9.5 dpc.

A mouse *RNF43* gene fragment (1567 bp), which is specific for hybridization with RNF43, was amplified from mouse cDNA (GenBank Accession number, NM_172448: nucleotides 2701 - 4267) and cloned into pGEM®-T vector (Promega) using the primers listed in Table 6. Sense and antisense RNA probes were generated using the DIG RNA labeling mix (Roche) according to the manufacturer's instructions. The antisense digoxigenin (DIG)-labeled complementary RNA probe was synthesized from linearized vectors with T7 RNA polymerase (Promega). The sense DIG-labeled RNA probe, which was used as a negative control for hybridization, was synthesized from linearized vectors with SP6 RNA polymerase (Promega).

Whole mount *in situ* hybridizations were performed as previously described (Sporle and Schughart 1998). All solutions are listed in 2.1.3. All (pre-) hybridization solutions contained 0.01 % DEPC.

Embryos were prepared in PBS, put into 2 ml cryogenic vials and fixed in 4 % PFA/PBS at 4 °C overnight. On the next day, they were dehydrated (on ice) through 25 %, 50 % and 75 % MetOH/PBS for at least 10 min, followed by two incubation steps with 100 % MetOH for 5 - 10 min each. Embryos were either directly implemented for whole mount *in situ* hybridizations or stored in 100 % MetOH at -20 °C.

For rehydration, embryos were incubated (on ice) in 75 %, 50 % and 25 % MetOH/PBS for 10 min each, followed by several washing steps with PBS (on ice; 2x10 min, 1x5 min). Subsequently, embryos were incubated for 10 min in RIPA buffer (without shaking) on ice. Embryos were then washed 2x5 min with PBT (without shaking) on ice. Afterwards, they were incubated in hybe-buffer/PBT (at same amounts) at RT for 10 min before washed with hybe-buffer (10 min, RT).

Pre-hybridization occurred in hybe-buffer + tRNA (100 µg/ml) at 68 °C for at least 3 h. The DIG-labeled sense and antisense RNA probes were denaturated (90 °C, 3 min) and

immediately put on ice. For hybridization, a 1:100 dilution of the DIG-labeled sense or antisense probe was added to the vial containing embryos, hybe-buffer and tRNA. Hybridization occurred in a hybridization oven at 68 °C overnight (under gentle agitation).

On the next day, the unbound probes were removed. Therefore, hybe-buffer and SSC/FA/Tween 20 were heated to 65 °C, and embryos were washed 2 times with hybe-buffer at 65 °C. They were subsequently cooled down to RT and washed 5 min at RT with hybe-buffer/RNase solution (at same amounts). Afterwards, they were washed 5 min with RNase solution and incubated with RNase solution containing 100 µg/ml RNaseA at 37 °C for 60 min. Embryos were then washed with RNase solution/(SSC/FA/Tween 20) (at same amounts) for 5 min at RT, before they were heated in SSC/FA/Tween 20 from RT to 65 °C, and washed 2x5 min, 3x10 min and at least 5x30 min at 65 °C with SSC/FA/Tween 20. Embryos were subsequently cooled down to RT and washed 5 min with (SSC/FA/Tween 20)/1xTBST (at same amounts) at RT, before washed 2x10 min in 1x TBST and 2x10 min in MABT.

For blocking, embryos were incubated in 10 % blocking solution for 1 h at RT. Meanwhile, the antibody solution was prepared. Therefore, DIG antibodies were incubated at 4 °C for 1 h in 1 % blocking solution/MABT (1:5000 dilution). Embryos were incubated in the antibody solution at 4 °C overnight.

For removal of the unbound antibody, embryos were washed 3x5 min and at least 8x1 h with TBST at RT. Alternatively, they were left in TBST at 4 °C on a shaker over the weekend.

Afterwards, the embryos were washed 2x5 min with freshly prepared alkaline phosphatase buffer at RT. They were stained using BM Purple AP Substrate (Roche) according to the manufacturer's instructions. The incubation time until development of strong staining was approximately 1 - 2 days. Embryos were post-fixed for at least 30 min with 4 % PFA in PBS.

For documentation, whole embryos were mounted on a thin layer of agarose. Pictures were adjusted for brightness and contrast in Adobe Photoshop (Adobe).

2.2.9 Proliferation assays

Cells were seeded in 48-well plates in 250 µl medium per well. The next day, cells were transfected with 20 nM siRNA or 250 ng plasmid DNA.

For siRNA transfections, cells were seeded approximately 24 h before transfections at a density of 10 000 cells per well (48-well plates) in a volume of 250 µl per well. Per well, 3 µl

siTran transfection reagent (OriGene) were diluted with 17 µl Opti-MEM (GIBCO®) without serum and added to 0.27 µl of siRNA stock solution (10 µM). The transfection mix was incubated at RT for 10 min before addition to a well. After transfection, cells were incubated at 37 °C and 5 % CO_2 for 48 h. Transfections were performed in triplicates.

For transfections with plasmid DNA, cells were also seeded at a density of 10 000 cells per well (48-well plates) in a volume of 250 µl per well. The next day, per well, 250 ng plasmid DNA were diluted in 25 µl Opti-MEM (GIBCO®) without serum. Lipofectamine (Invitrogen) was diluted 1:50 in 25 µl Opti-MEM (GIBCO®) without serum, incubated at RT for 5 min and subsequently added to the 25 µl of DNA mix. The 50 µl transfection mix was incubated at RT for 25 min before addition to one well. After transfection, cells were incubated at 37 °C and 5 % CO_2 for 48 h. Transfections were performed in triplicates.

48 h after transfection, proliferation was measured in triplicates using Cell Titer-Glo® substrate (Promega) according to the manufacturer's instructions using an Orion Microplate Luminometer (Berthold) or a Mithras 96 well plate reader (Berthold). Data were normalized to cells transfected with the control vector or control siRNA.

2.2.10 Immunofluorescence stainings

For immunofluorescence stainings, cells were seeded on cover glasses in 6-well plates at an appropriated density. Transfections were performed approximately 24 h after seeding (see 2.2.3.5). Therefore, 2 µg of plasmid DNA were diluted in Opti-MEM (GIBCO®) without serum in a volume of 100 µl. In parallel, 100 µl Lipofectamine mix were prepared by diluting Lipofectamine 1:25 in Opti-MEM (GIBCO®) without serum and the Lipofectamine mix was incubated for 5 min at RT. The Lipofectamine mix was then added to the DNA mix and incubated at RT for 25 min. The DNA-Lipofectamine mix was subsequently added to the cells, and cells were incubated for 24 - 48 h at a humidified atmosphere and 5 % CO_2 at 37 °C.

Cells were fixed 24 - 48 h post-transfection. Therefore, the medium was removed, cells were washed with cold PBS, incubated with ice-cold Methanol/Acetone (in same amounts) for 15 min at RT, and washed again with cold PBS (3x). The cells were then incubated with IF blocking and permeabilization solution (2.1.3) for 15 min at RT, followed by incubation with the primary antibody in the same solution in a humidified chamber in the dark for at least 90

min at RT, or overnight at 4°C. The used antibody dilutions are listed in 2.1.6. Afterwards, cells were washed 3x5 min with Wash solution 1 (2.1.3), followed by incubation with the secondary antibody diluted 1:200 in IF blocking and permeabilization solution for 1 h at RT in a humidified chamber in the dark. Afterwards, the stained cells on the cover glasses were washed 3x with Wash solution 2 (2.1.3) and mounted with Vectashield mounting medium containing DAPI (Vector Laboratories) on microscope slides before sealed with nail polish.

For visualization of RNF43-CFP and RNF43-Cherry, cells were fixed 24 h post-transfection. After washing with PBS, cells were directly mounted with Vectashield mounting medium containing DAPI (Vector Laboratories) on microscope slides and sealed with nail polish.

Subsequently, fluorescence microscopy was performed. Fluorescence microscopy of colocalizations of Tcf4 and full length wildtype and mutant RNF43 was performed using a Keyence BZ-9000 microscope. This fluorescence microscope harbors a Z-stack function, which means that the focal point of an objective lens can be moved through the Z-axis and thus this function enables capturing sets of images of planes of different depths within a single cell, which are called Z stacks. Fluorescence microscopy of all other stainings was performed using a Leica DMRB microscope.

Slides could be stored at -20 °C for approximately 3 days or at -80 °C for about a week, before the fluorescence intensity decreased.

2.2.11 Analyses of *RNF43* gene sequences

In order to search for mutations in the open reading frame of the N-terminal part of *RNF43* in colon cancer samples and cell lines, cDNA from different cell lines (HCT116, HT29, SW48, DLD1, Cos7, HEK293T, CaCO2) and 8 intestinal tumor samples (5 tumor stage II samples, 3 tumor stage IV samples) was amplified and investigated by sequencing analysis. Furthermore, the C-terminus of HT29 cells was included into the analysis. cDNA templates of the tumor samples were kindly provided by Prof. Dr. Janssen and Dr. Nitsche. Fragments of *RNF43* cDNA samples were amplified by PCR using the primers listed in Table 6 , subcloned into pGEM®-T vector and subsequently sequenced with T7 and SP6 primers.

The resulting sequences were compared to the annotated human *RNF43* sequence (NM_017763.4) using the "Blast 2 Sequences" software from NCBI[2].

2.2.12 Colony formation assays

For colony formation assays, HCT116 colon cancer cells were seeded in 6-well plates at an appropriate density. Transfections were performed approximately 24 h after seeding (see 2.2.3.5).

In order to have a control plasmid for the assay, Venus was amplified from a plasmid containing the Venus ORF and cloned into the pcDNA4TO vector, which is also the backbone of all RNF43 and RNF43mut constructs. Expression of Venus was verified by Immunofluorescence microscopy.

Transfections were performed in 6-well plates approximately 24 h after seeding the cells at an appropriate density. Therefore, 2 µg of pcDNA4TO+Venus, RNF43-flag or RNF43mut-flag plasmid DNA were diluted in Opti-MEM (GIBCO®) without serum in a volume of 100 µl. In parallel, 100 µl Lipofectamine mix were prepared by diluting Lipofectamine 1:25 in Opti-MEM (GIBCO®) without serum and the Lipofectamine mix was incubated for 5 min at RT. The Lipofectamine mix was subsequently added to the DNA mix and incubated at RT for 25 min. The DNA-Lipofectamine mix was subsequently added to the cells and cells were incubated for 48 h at a humidified atmosphere and 5 % CO_2 at 37 °C. After incubation, cells were expanded into 10 cm^2 - or 15 cm^2 dishes and transfected cells were selected by addition of 1 µg/ml Zeocin™. The medium was changed every 3 - 4 days. After selection for 2 to 3 weeks, colonies were stained blue with thiazolyl blue tetrazolium bromide (MTT). Therefore, the MTT powder was solved in ddH_2O (5 mg/ml) and added to the medium to a final concentration of 120.5 µg/ml. After 1 h, the medium was removed, dishes were washed with 1x PBS and pictures of the blue stained colonies were taken. Furthermore, colonies were counted.

[2] http://blast.ncbi.nlm.nih.gov/Blast.cgi?PAGE_TYPE=BlastSearch&PROG_DEF=blastn&BLAST_PROG_DEF=megaBlast&BLAST_SPEC=blast2seq

2.2.13 *Xenopus laevis* axis duplication assays

Xenopus laevis axis duplication assays were performed by Dr. Dietmar Gradl at the Institute for Cell and Developmental Biology at the KIT (Karlsruhe Institute of Technology).

Therefore, wildtype and mutant RNF43 sequences were cloned into pCS2myc and sent to Dr. Gradl. In his lab, capped mRNAs were transcribed *in vitro* from linearized DNA templates. 5 pg Wnt-1 mRNA were co-injected with 500 pg RNF43 or RNF43mut mRNA in a total volume of 4 nl into the marginal zone of both ventral blastomeres of four-cell stage embryos. The embryos were staged according to (Nieuwkoop 1967) and scored for the appearance of secondary axes. Furthermore, pictures were taken.

2.2.14 Statistical analysis

Results are presented as means + standard deviation (S.D.). Differences were analyzed by student's t-test using GraphPad Prism 5 software. Statistical significance was defined as $p \leq 0.05$, and $p \leq 0.01$ was defined as very significant.

3 Results

RNF43 is a protein that was found to exhibit Ubiquitin E3-Ligase activity (1.8), but its detailed function in carcinogenesis and its functionally important domains remained elusive.

There is a strong correlation between the conservation of a protein and its function. Proteins that are conserved among species are often necessary for important or essential cellular functions, and conservation of proteins between species indicates functional similarities of proteins. In addition, highly conserved regions of a protein are of particular functional importance, since they often represent active sites of enzymes or binding sites for other proteins.

Thus, investigation of similarities in protein sequences by alignment is a valuable tool for the identification of evolutionary conserved elements of a protein, and thus the functional importance of a particular protein for the cell, as well as its functional important regions.

In order to identify whether the RNF43 protein sequence is evolutionarily conserved among different species and thus of functional importance, and in order to determine regions that are conserved and thus of particular importance for the function of RNF43, the RNF43 amino acid sequences of different species (*Homo sapiens*: AAI09029.1; *Mus musculus*: NP_766036.2; *Rattus norvegicus*: NP_001129393.1; *Bos taurus*: NP_001178123.1) as well as the predicted amino acid sequences of some other species (*Equus caballus*: XP_001503751.1; *Pan troglodytes*: XP_001172611.1, *Loxodonta africana*: XP_003414643.1) were compared by sequence alignment using the IBIVU PRALINE multiple sequence alignment program[3]. The RNF43 amino acid sequence of *Xenopus laevis* was not included into the analysis, since so far there are no annotations of the sequence available at NCBI.

[3] http://www.ibi.vu.nl/programs/pralinewww/

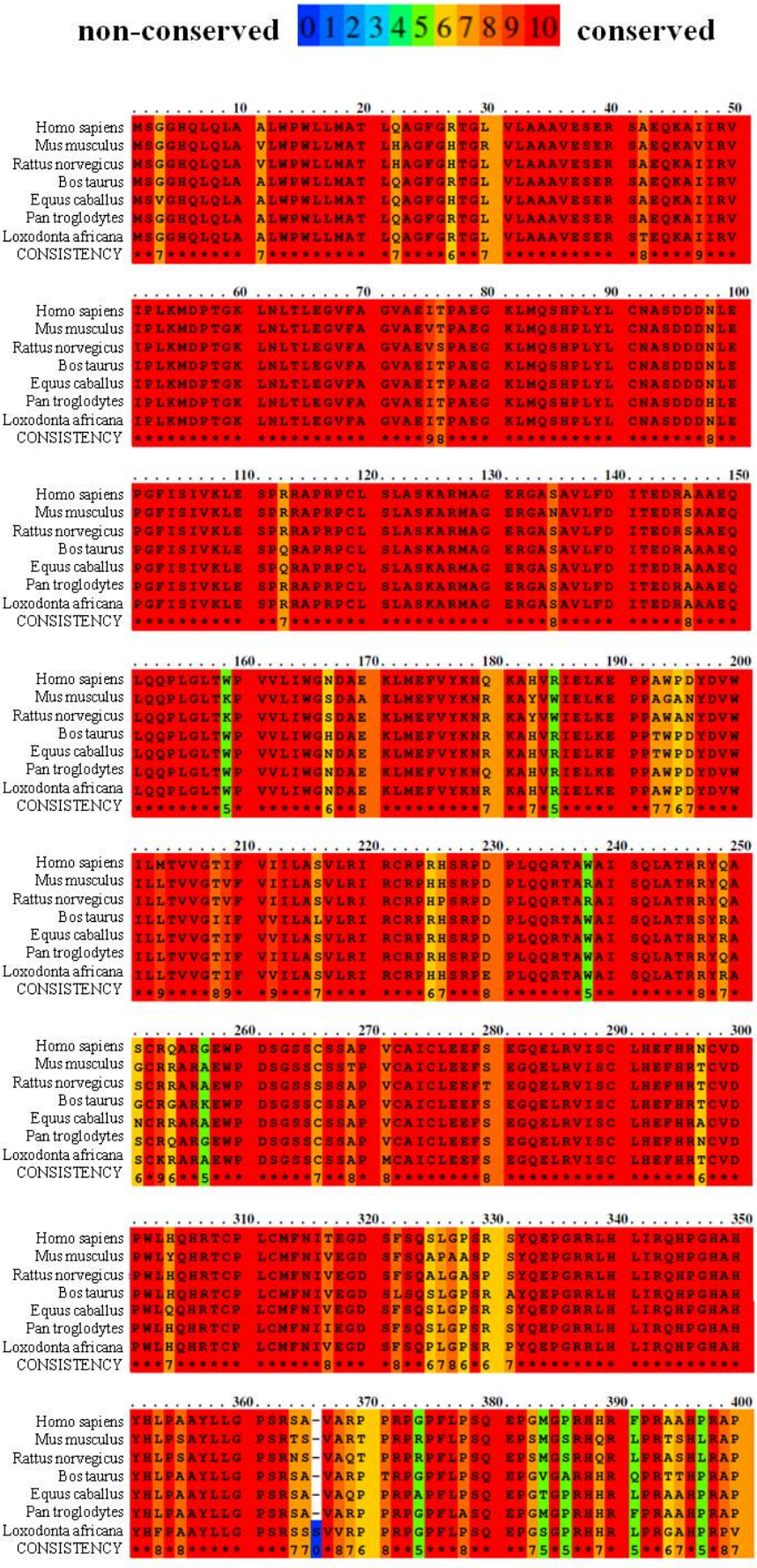
non-conserved 0 1 2 3 4 5 6 7 8 9 10 conserved
Homo sapiens
Mus musculus
Rattus norvegicus
Bos taurus
Equus caballus
Pan troglodytes
Loxodonta africana
CONSISTENCY

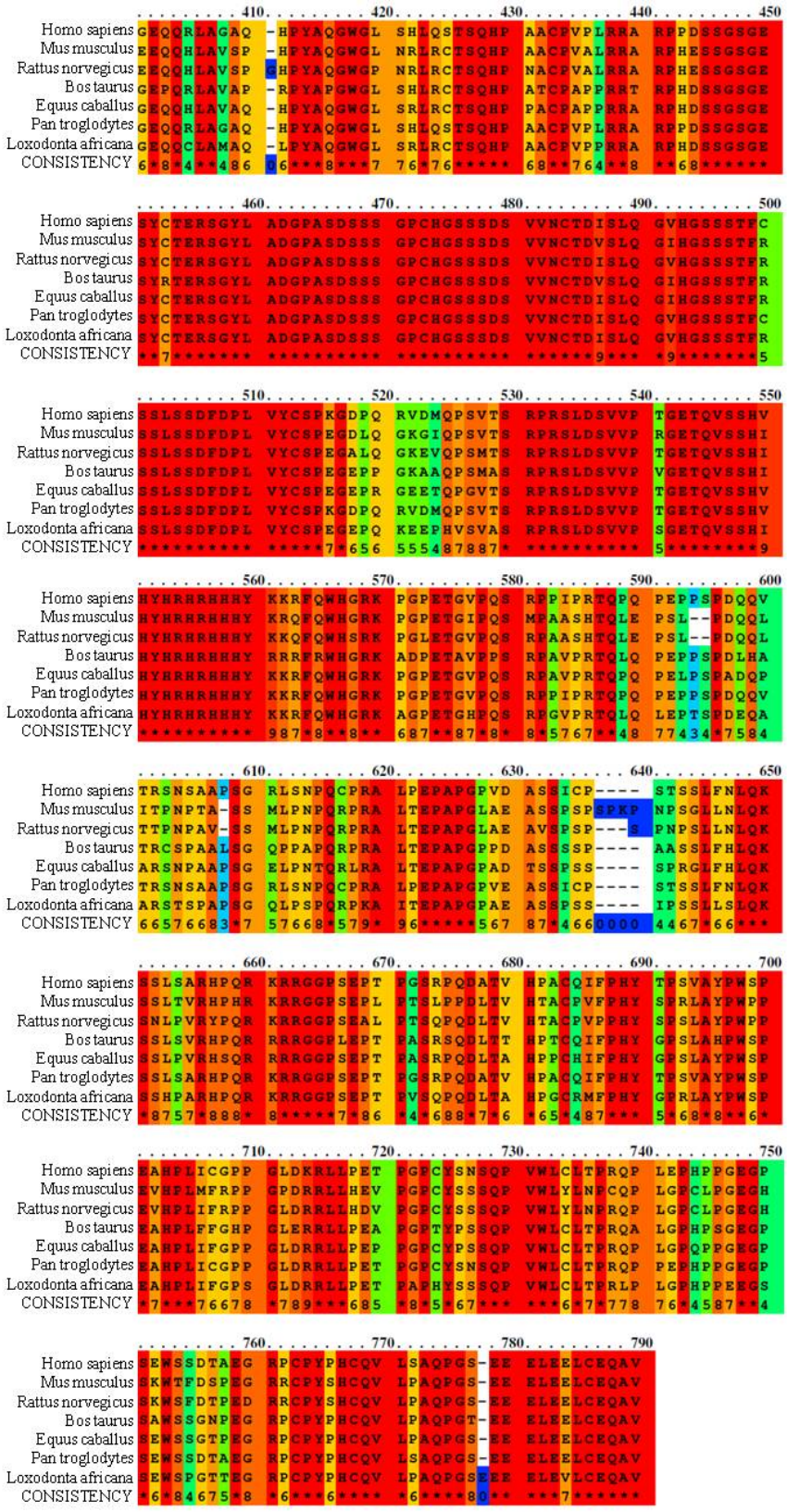

Figure 15 Amino acid sequence alignment of the RNF43 protein sequence of different species.
Sequence alignment of *Homo sapiens, Mus musculus, Rattus norvegicus, Bos taurus, Equus caballus, Pan troglodytes* and *Loxodonta Africana* amino acid sequences using the IBUVU PRALINE multiple sequence alignment program. Residues are highlighted in colors according to their extent of conservation. Identical residues are accentuated in red, similar residues in orange and green, and non-conserved residues in blue.

As illustrated in Figure 15, nearly all amino acid residues are highlighted in red, indicating that not only the RING domain (aa 272 - 312), but also the rest of the protein sequence of RNF43 is evolutionarily conserved among species to a very high extent. Thus, since there is a correlation between protein conservation and functional importance, RNF43 is likely to be an essential or at least crucial protein in various species.

3.1 Expression of RNF43

3.1.1 Expression of RNF43 in mice

In order to better understand the biological function of a gene of interest in embryology, determination of its expression pattern at different stages of development is essential.

To obtain detailed information about the expression of RNF43 in mouse embryos at mid-gestational stages, whole mount *in situ* hybridization analysis was performed. Therefore, as described in 2.2.8, an antisense RNA probe, which was complementary to the *RNF43* sequence, and a sense probe, which was used as a negative control, were generated. Embryos at 8.5 dpc and 9.5 dpc were probed with the generated riboprobes targeting the RNF43 mRNA sequence as described in 2.2.8.

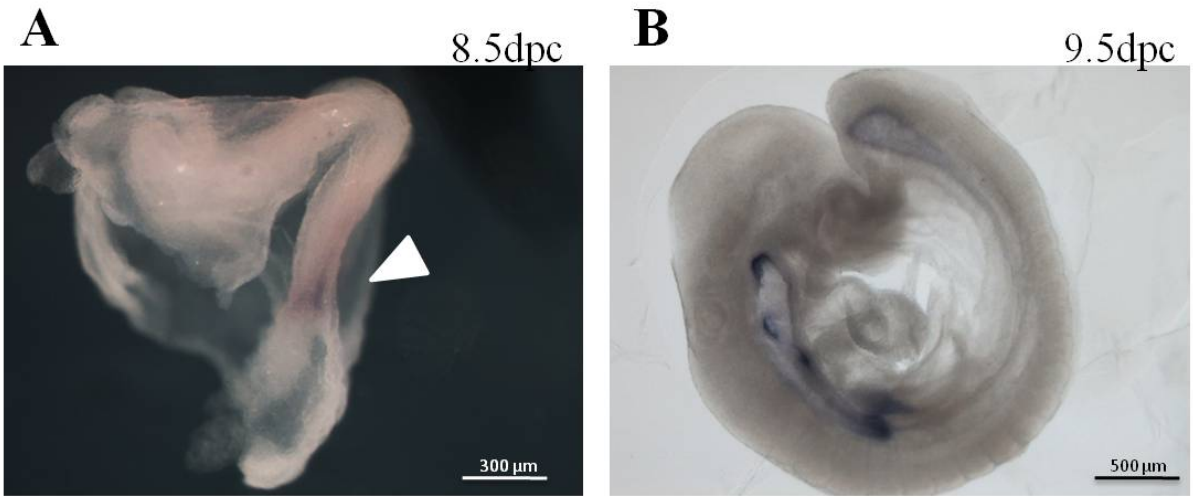

Figure 16 Whole mount *in situ* hybridization analysis for RNF43 in mouse embryos.
Embryos at a range of mid-gestational stages (E8.5 and E9.5) were hybridized with an antisense riboprobe to RNF43. (A, B) Whole embryos at 8.5 - 9.5 dpc revealed a strong posterior expression pattern. (B) Embryos at 9.5 dpc showed a strong expression of RNF43 in the endoderm derived tissues.

At 8.5 dpc, RNF43 exhibited a posterior expression pattern, which is typical for Wnt target genes (Figure 16A). At 9.5 dpc, RNF43 showed a strong expression throughout the endoderm-derived tissues, like the stomach and intestine. Furthermore, a remarkable staining of the trunk region was observed.

In situ hybridizations using the sense probe did not result in any signal (data not shown), indicating that the observed staining was specific.

In order to prove the expression of RNF43 mRNA in endoderm-derived tissues in embryos of mice, and in order to obtain more information about the expression of RNF43 in mouse embryos, quantitative RT-PCR analyses, using primers specific for the detection of RNF43, were performed. The expression of RNF43 in mouse embryos, stomach, intestine, skin and brain at 14.5 dpc and18.5 dpc was investigated. Results were normalized to GAPDH expression.

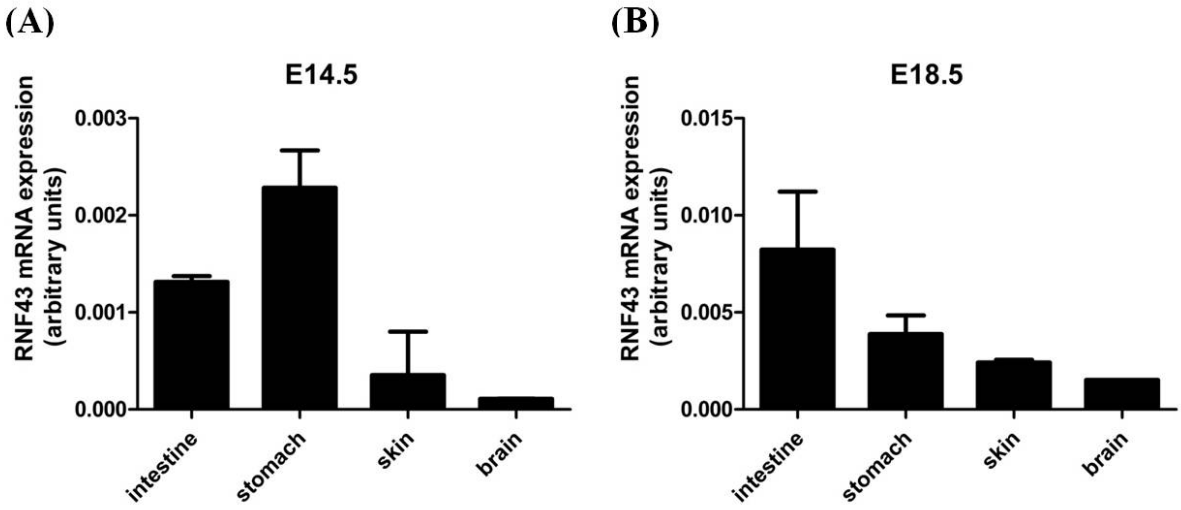

Figure 17 RNF43 mRNA expression of embryos of mice.
Expression of RNF43 mRNA in mouse organs of one mouse at (A) 14.5 dpc. and (B) at 18.5 dpc. RT-PCR was performed two times in duplicates. Data were normalized to GAPDH expression. Data shown are means +S.D. of duplicates of one representative RT-PCR.

Real-time PCR analysis revealed a high expression of RNF43 mRNA in the intestine and stomach of mouse embryos (Figure 17), supporting the data obtained by whole mount *in situ* hybridizations (Figure 16), which indicate that in mouse embryos, RNF43 is mainly expressed in endoderm-derived tissues.

In order to investigate whether the expression of RNF43 mRNA in tissues of adult mice is similar to the expression pattern found in mouse embryos, mRNA of adult mouse organs was isolated, reverse transcribed into cDNA and subjected to qRT-PCR analysis.

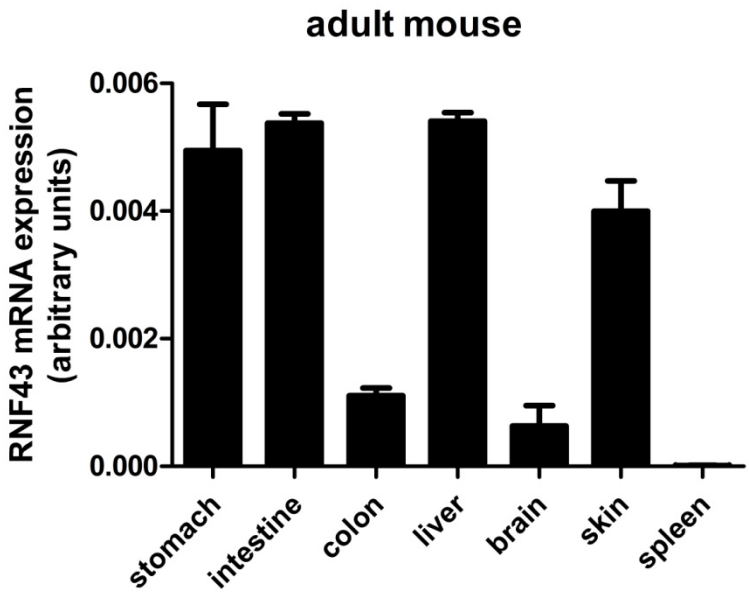

Figure 18 RNF43 mRNA expression in organs of adult mice.
RT-PCR was performed two times in duplicates. Data were normalized to GAPDH expression. Data shown are means +S.D. of duplicates of one representative RT-PCR.

In accordance with the obtained expression data of RNF43 in mouse embryos, in adult mice, RNF43 mRNA was also strongly expressed in the endoderm-derived tissues like the stomach, intestine and liver, whereas less RNF43 mRNA expression was detectable in the brain as well as in the spleen.

In addition to the strong expression in endoderm-derived tissues, RNF43 mRNA expression was also very high in the skin, which is derived from the ectoderm, suggesting that the expression of RNF43 is not limited to endoderm-derived tissues.

3.1.2 Expression of RNF43 in human colon cancer samples and cell lines

Since *in situ* hybridization analysis revealed a very high expression of RNF43 in intestinal crypts and intestinal adenomas (Figure 12), RNF43 mRNA levels of human intestinal tumors of different stages were investigated.

Therefore, several tumor samples of different tumor stages, in detail four tumor stage II samples and three tumor stage IV samples, as well as four normal intestinal muCos7a

samples, were subjected to qRT-PCR analysis using specific primers for the detection of RNF43. Results were normalized to GAPDH expression.

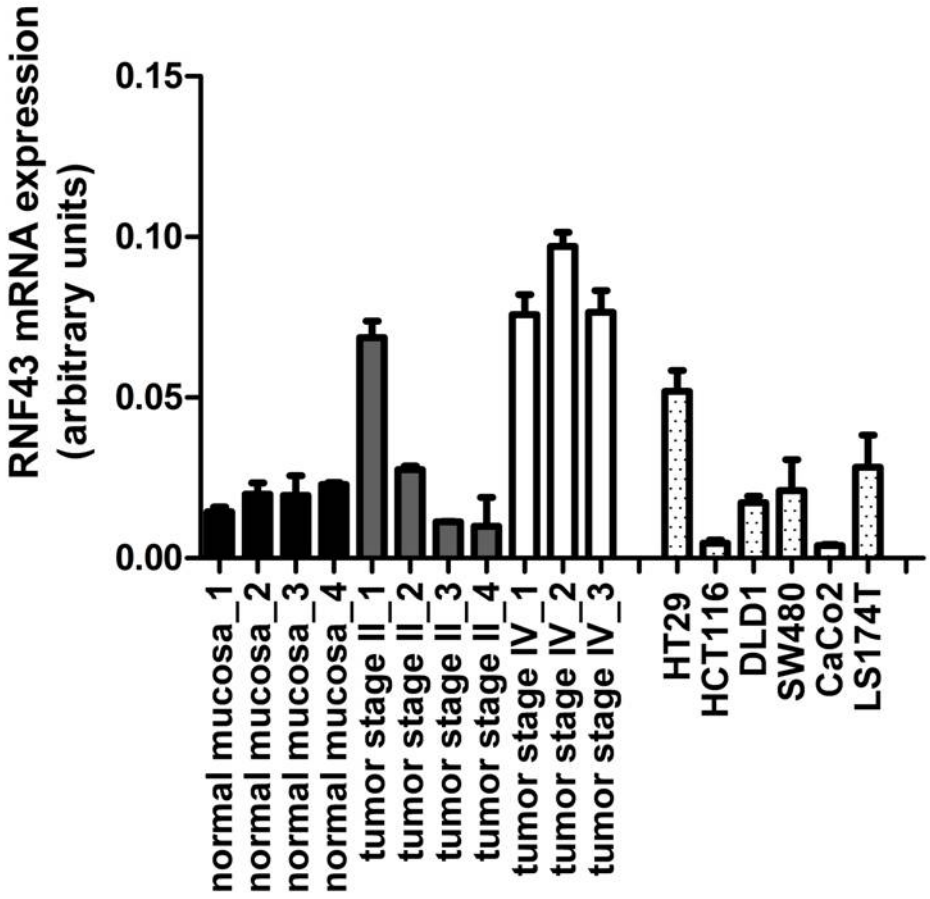

Figure 19 RNF43 mRNA expression in human intestinal cancer samples, normal muCos7a and colon cancer cell lines.
In the case of normal muCos7a samples and intestinal tumor stage II and IV samples, RT-PCR was performed two times in duplicates. Data were normalized to GAPDH expression. Data shown are means +S.D. of duplicates of one representative RT-PCR experiment. In the case of colon cancer cell lines, mRNA was extracted 3 times from cell lines and data shown represent means +S.D. of three independent experiments.

As visible in Figure 19, RNF43 mRNA expression was low in normal muCos7a as compared to intestinal tumor stage IV samples, which exhibited the highest levels of RNF43 mRNA expression. The expression of RNF43 mRNA in tumor stage II samples was variable and largely differed between the individual samples, indicating a more heterogeneous expression of RNF43 in tumor stage II samples.

To examine the expression of RNF43 mRNA in different colon cancer cell lines, RT-PCR analysis of total RNA was performed. In order to verify the comparability of the obtained results with the results of RNF43 mRNA expression in tumor and normal muCos7a samples, normal muCos7a sample nr. 3 was included into this experiment. Since values of these

independent RT-PCRs were comparable (data not shown), results of RNF43 mRNA expression in different colon cancer cell lines were included in Figure 19.

Even though RNF43 was characterized as a gene commonly up-regulated in colorectal tumors (Yagyu, Furukawa et al. 2004), RT-PCR analysis revealed very low RNF43 mRNA expression in most of the colorectal cancer cell lines tested (Figure 19). In contrast to the low levels observed in HCT116, DLD1, SW480, CaCo-2 and LS174T cells, RNF43 mRNA expression in HT29 adenocarcinoma cells was at a level comparable to the expression level observed in tumors.

Since Human Embryonic Kidney (HEK293T) and African Green Monkey Kidney (Cos7) cells did not express any RNF43 mRNA, or the expression was below the detection limit (data not shown), RNF43 mRNA expression was higher in colon cancer cell lines than in HEK293T and Cos7 cells.

In order to determine whether RNF43 protein is expressed in colon cancer cell lines, Western blot analysis with the anti-human polyclonal RNF43 antibody (produced in rabbit) provided by LS BioSciences was performed. HCT116 cells transfected with RNF43-HA were used as a positive control. Mcf7 breast cancer cells were also used as a positive control, since they were suggested to be used as a positive control by the provider. ß-actin was used as an internal loading control.

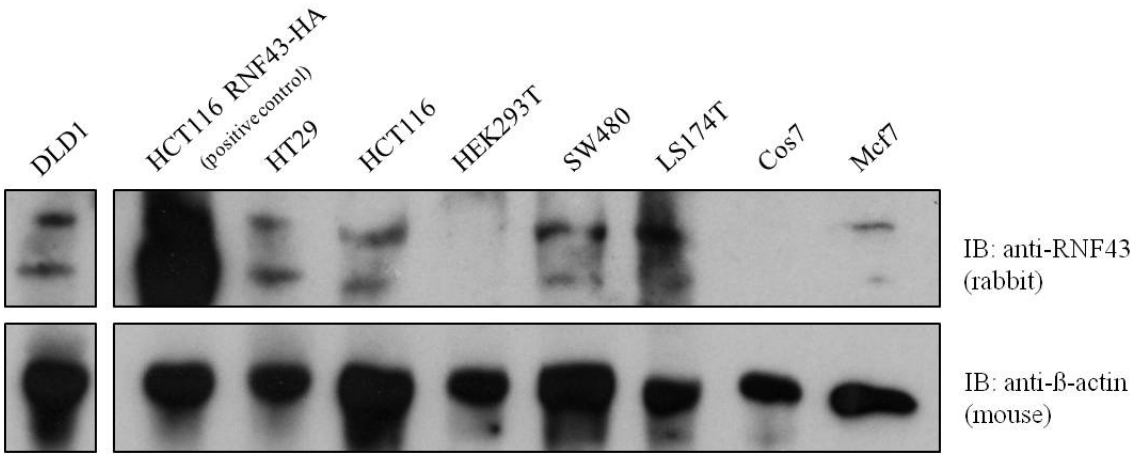

Figure 20 Endogenous RNF43 protein expression in different cell lines.
Endogenous RNF43 protein expression in colon cancer cell lines (HT29, HCT116, SW480, DLD1 and LS174T) as well as in HEK293T and Cos7 cells was detected by Western blot analysis with the anti-RNF43 polyclonal RNF43 antibody provided by LS Biosciences. Mcf7 breast cancer cells and HCT116 cells transfected with RNF43-HA were used as positive controls. ß-actin was used as a loading control. One representative Western blot is shown.

As illustrated in Figure 20, endogenous RNF43 could be detected in all investigated colon cancer cell lines (HT29, HCT116, SW480, DLD1 and LS174T) as well as in the positive controls (Mcf7 cells; HCT116 cells transfected with RNF43-HA). Several distinct bands were visible in the Western blot. Since four isoforms of the RNF43 protein were suggested to exist (by the online knowledge platform on human proteins, "NeXtProt"[4]), the bands are likely to represent different isoforms of RNF43.

In contrast, no endogenous RNF43 protein was detectable in HEK293T and Cos7 cells. Thus, neither RNF43 mRNA nor RNF43 protein was detectable in these two cell lines, indicating that in HEK293T and Cos7 cells, RNF43 is either not expressed or expressed at very low levels.

Since *RNF43* was previously shown to be a Wnt target gene (1.9) and since it exhibited an expression pattern typical for Wnt target genes (Figure 12, Figure 16), a possible correlation of RNF43 expression with endogenous Wnt signaling activity of the most commonly used cell lines was investigated. Therefore, TOP/FOP Luciferase reporter assays were performed (Figure 21).

[4] http://www.nextprot.org/db/entry/NX_Q68DV7

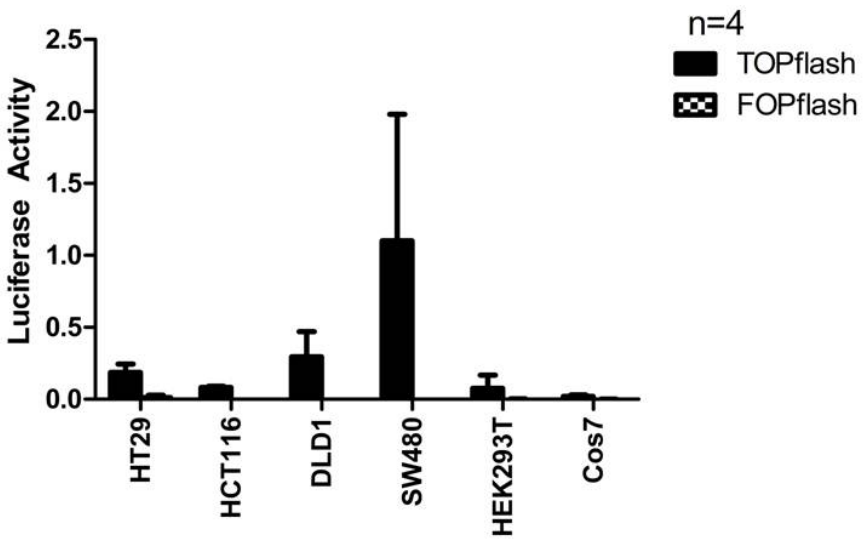

Figure 21 Endogenous Wnt signaling activities of different cell lines.
Endogenous Wnt signaling activities of the most commonly used cell lines were investigated by TOP/FOP Luciferase reporter assays. Cells were transfected with pTOPflash and pFOPflash reporter plasmids. Results were normalized to Renilla values. Data are means +S.D. of four independent experiments.

As illustrated in Figure 19 and Figure 21, no correlation between RNF43 mRNA expression and endogenous Wnt signaling activity in the investigated cell lines could be detected. Although HT29 cells exhibited very high levels of RNF43 mRNA expression, the endogenous Wnt signaling activity observed in these cells was very low. On the other hand, SW480 cells, which showed a very high endogenous Wnt signaling activity, exhibited intermediate RNF43 mRNA expression. HCT116 and DLD1 cell lines both revealed intermediate levels of RNF43 mRNA expression and Wnt signaling activity. Similarly, no correlation between RNF43 protein expression and endogenous Wnt signaling activity could be determined (Figure 20, Figure 21).

HEK293T and Cos7 exhibited very low levels of endogenous Wnt signaling activity. These cell lines do not harbor any described mutations in the Wnt signaling pathway. In our experiments, they did not express any RNF43 mRNA, or the expression was below the detection limit (data not shown). They also did not express RNF43 protein at detectable amounts. Thus, compared to HEK293T and Cos7 cell lines, the cancer cell lines HT29, HCT116, DLD1 and SW480 exhibited elevated levels of endogenous Wnt signaling activity. Nevertheless, no correlation between endogenous Wnt signaling activities of cell lines and the levels of RNF43 expression could be observed.

3.1.3 Model for investigation of effects on Wnt signaling activity

As a model system for the investigation of effects of specific proteins on Wnt signaling activities of cells, Cos7 and HEK293T cells were used.

Cos7 cells exhibit very low endogenous levels of Wnt signaling activity, since they do not harbor any activating mutations in the Wnt signaling cascade. Upon treatment of Cos7 cells with Lithium chloride (LiCl), the canonical Wnt pathway can be activated. LiCl inhibits Glycogen Synthase Kinase-3ß (GSK3ß), an enzyme that phosphorylates ß-catenin in the cytoplasm and targets it for ubiquitination, followed by proteasomal degradation. Inhibition of GSK3ß results in an increase in ß-catenin protein levels, leading to an activation of the canonical Wnt signaling pathway *in vivo* and *in vitro* (Klein and Melton 1996; Hedgepeth, Conrad et al. 1997; O'Brien, Harper et al. 2004).

The optimal concentration of Lithium chloride for treatment of Cos7 cell was determined by TOP/FOP Luciferase reporter assays. Therefore, Cos7 cells were treated with different concentrations of LiCl for 24 h prior to cell lysis.

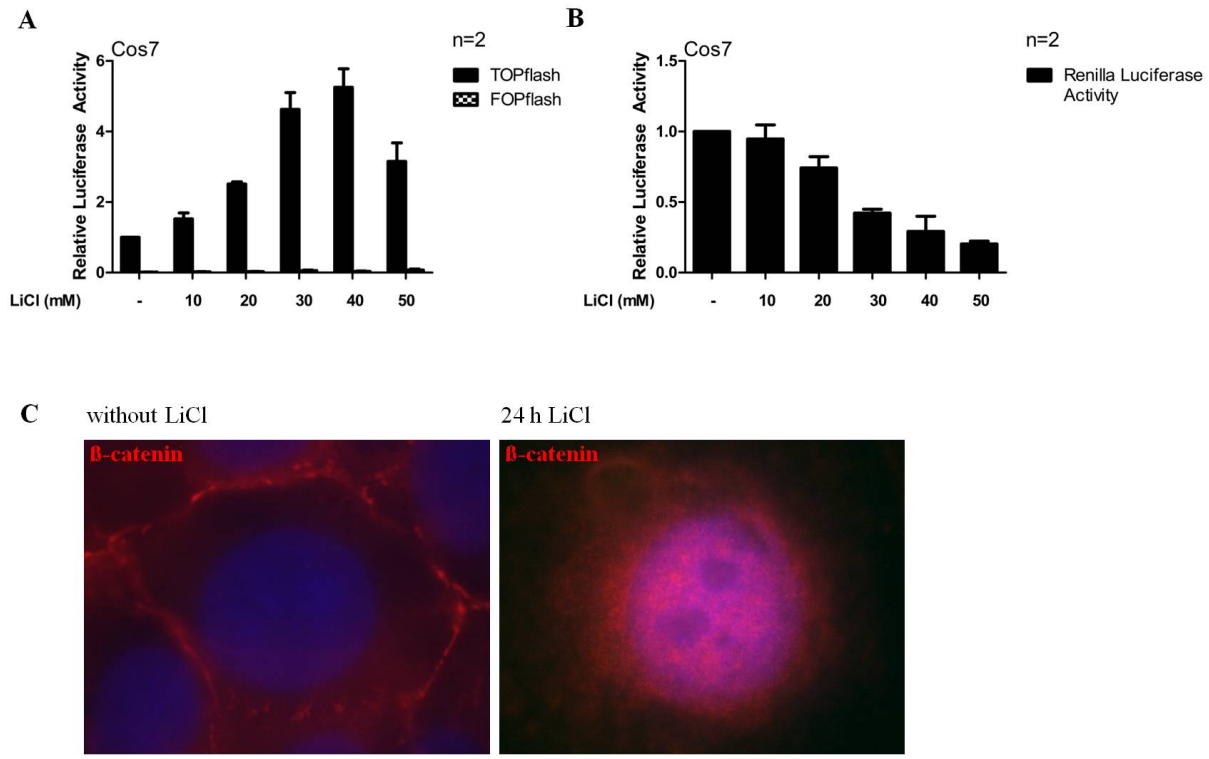

Figure 22 Activation of the Wnt signaling pathway by Lithium chloride in Cos7 cells.
(A) TOP/FOP Luciferase reporter assays of Cos7 cells transfected with pTOPflash and pFOPflash reporter plasmids and treated 24 h post-transfection with increasing amounts of LiCl for 24 h. Renilla luciferase was used as an internal control. Data were normalized to the untreated control and to Renilla values. Data are means + S.D. of two independent experiments. (B) Renilla values of the TOP/FOP Luciferase assays displayed in (A). Data were normalized to the untreated control. Data are means + S.D. of two independent experiments. (C) The effect of activation of the Wnt signaling pathway on ß-catenin. Immunofluorescence stainings of endogenous ß-catenin were performed in Cos7 cells. Pictures of Immunofluorescence stainings illustrate DAPI (blue) and anti-ß-catenin (red) stainings in untreated and 40 mM (24 h) LiCl treated Cos7 cells.

As shown in Figure 22A, treatment of Cos7 cells with LiCl resulted in an increase in luciferase activity, thus in an increase in Wnt signaling activity. The highest activation was achieved by treatment with 40 mM LiCl.

The increase in Wnt signaling activity in Cos7 obtained by treatment with 40 mM for 24 h was also apparent in Immunofluorescence stainings of ß-catenin (Figure 22C). Upon activation of Wnt signaling by LiCl in Cos7 cells, ß-catenin shuttled from the cytoplasm into the nucleus, resulting in a more pronounced nuclear ß-catenin staining. In addition, the red fluorescence intensity was elevated upon LiCl treatment, indicating an increase in ß-catenin protein levels, thus an accumulation of ß-catenin in the cells.

Treatment of Cos7 cells with LiCl resulted in a dose-dependent decrease in Renilla values (Figure 22B), indicating a negative effect of treatment with LiCl on Cos7 cells. Since treatment of Cos7 cells with 20 mM LiCl (for 24 h) resulted in an approximately 2-fold

increase in Wnt signaling activity without drastically decreasing Renilla values, this concentration was chosen for following experiments.

Similar results were obtained in HEK293T cells. Like Cos7 cells, HEK293T cells also exhibited very low basal levels of Wnt signaling activity, since they do not harbor any activating mutations in the Wnt signaling cascade. Like in Cos7 cells, the Wnt signaling pathway can also be activated by treatment with LiCl in HEK293T cells. Unlike observed in Cos7 cells, treatment of HEK293T cells with LiCl did not result in a dose-dependent decrease in Renilla values, but Renilla values remained constant upon treatment with LiCl. Thus, a concentration of 40 mM LiCl for activation of Wnt signaling in HEK293T was chosen for following experiments. Treatment with 40 mM LiCl (for 24 h) resulted in an approximately 3-fold increase in Wnt signaling activity.

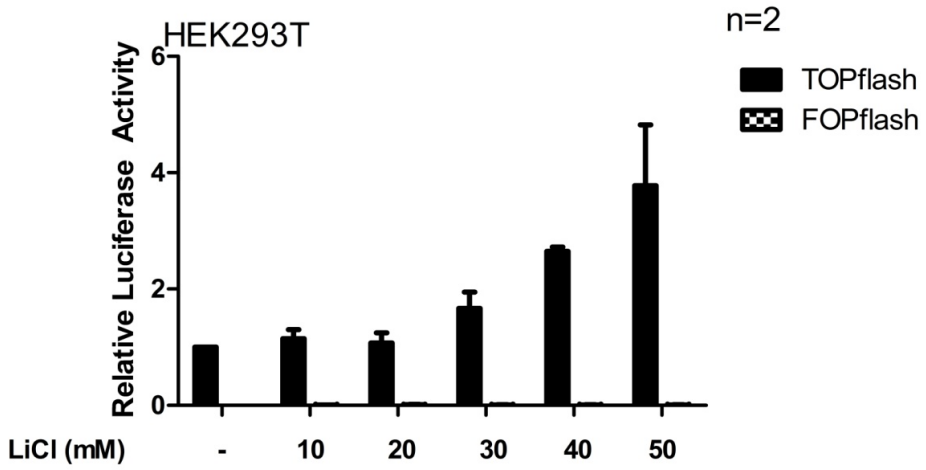

Figure 23 Activation of the Wnt signaling pathway by Lithium chloride in HEK293T cells.
TOP/FOP Luciferase assays of HEK293T cells transfected with pTOPflash and pFOPflash reporter plasmids and treated 24 h post-transfection with increasing amounts of LiCl for 24 h. Data were normalized to the untreated control and to Renilla values. Data are means + S.D. of two independent experiments.

Thus, treatment of both Cos7 and HEK293T cells with Lithium chloride provides a powerful method for activation of the Wnt signaling pathway in these cell lines. Hence, these cell lines can be used as a valuable model for further analyzing the effects of previously uncharacterized proteins on Wnt signaling activity *in vitro*.

3.2 RNF43 is a negative regulator of ß-catenin/Tcf4-mediated transcriptional activation

Since RNF43 was shown to be a Wnt target gene expressed at sites of high Wnt signaling, and since RNF43 was shown to inhibit Wnt1-induced Wnt signaling in HEK293T cells in preliminary experiments (1.9) the next aim was to examine the effect of RNF43 on Wnt-dependent transcription *in vitro* in detail.

Therefore, TOP/FOP Luciferase reporter assays were performed. pTOPflash or the control pFOPflash plasmids were co-transfected with a construct expressing RNF43-flag into Cos7 cells and HEK293T cells. The Wnt signaling pathway was stimulated by treatment with LiCl (20 mM in Cos7 cells, 40 mM in HEK293T cells) 24 h after transfection for 24 h prior to cell lysis. The levels of the ß-catenin/Tcf4-mediated transcription were determined.

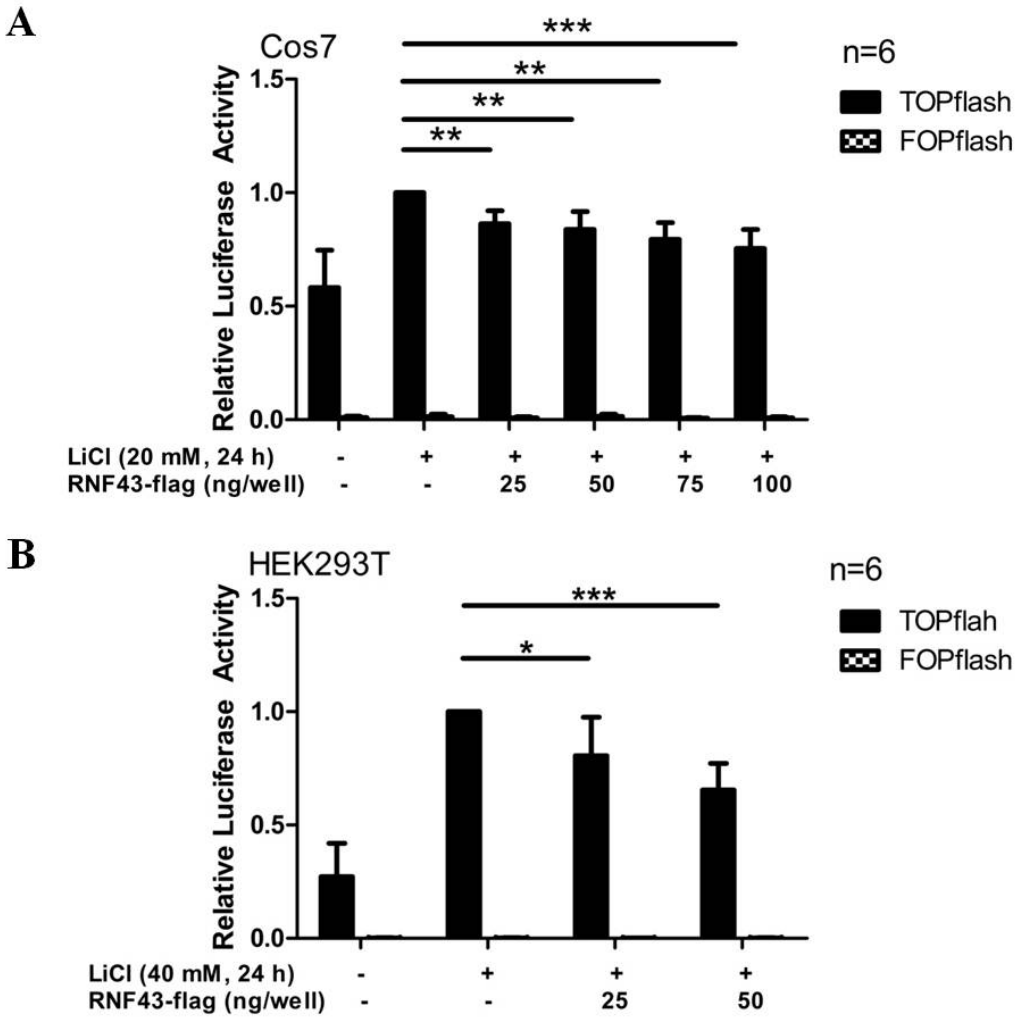

Figure 24 RNF43 inhibits Wnt signaling activity *in vitro*.
Cos7 cells (A) and HEK293T cells (B) were transfected with pTOPflash or the control pFOPflash reporter plasmids and the indicated amounts of the plasmid RNF43-flag. RNF43-flag was transfected at increasing amounts. Wnt signaling was activated by treatment with the indicated concentrations of LiCl. Results were normalized to Renilla values and to the LiCl-treated controls. Data are means + S.D. of six independent experiments.

In both cell lines, treatment with LiCl increased TOP/FOP Luciferase reporter activities, thus Wnt signaling activities, as compared to the basal Wnt signaling activities of untreated cells. Co-transfection of the indicated amounts of a construct expressing RNF43 resulted in a significant dose-dependent decrease of LiCl-induced Wnt signaling activity in both Cos7 and HEK293T cells (Figure 24).

Thus, RNF43 acts as a negative regulator of LiCl-induced Wnt signaling activity *in vitro*.

3.2.1 The RING domain of RNF43 is required for inhibition of Wnt/ß-catenin signaling

Wildtype RNF43 was shown to inhibit the canonical Wnt signaling pathway *in vitro* (Figure 23). Furthermore, mutated RNF43 was shown to inhibit Wnt1-induced Wnt signaling in HEK293T cells in preliminary experiments (1.9). Therefore, TOP/FOP Luciferase reporter assays were carried out in order to examine the effect of mutant RNF43 on the Wnt signaling pathway in detail. Assays were performed in HEK293T and Cos7 cells. The effects of mutant RNF43 on the LiCl-induced Wnt signaling activity observed in *in vitro* TOP/FOP Luciferase reporter assay experiments in Cos7 and HEK293T cells are illustrated in Figure 25.

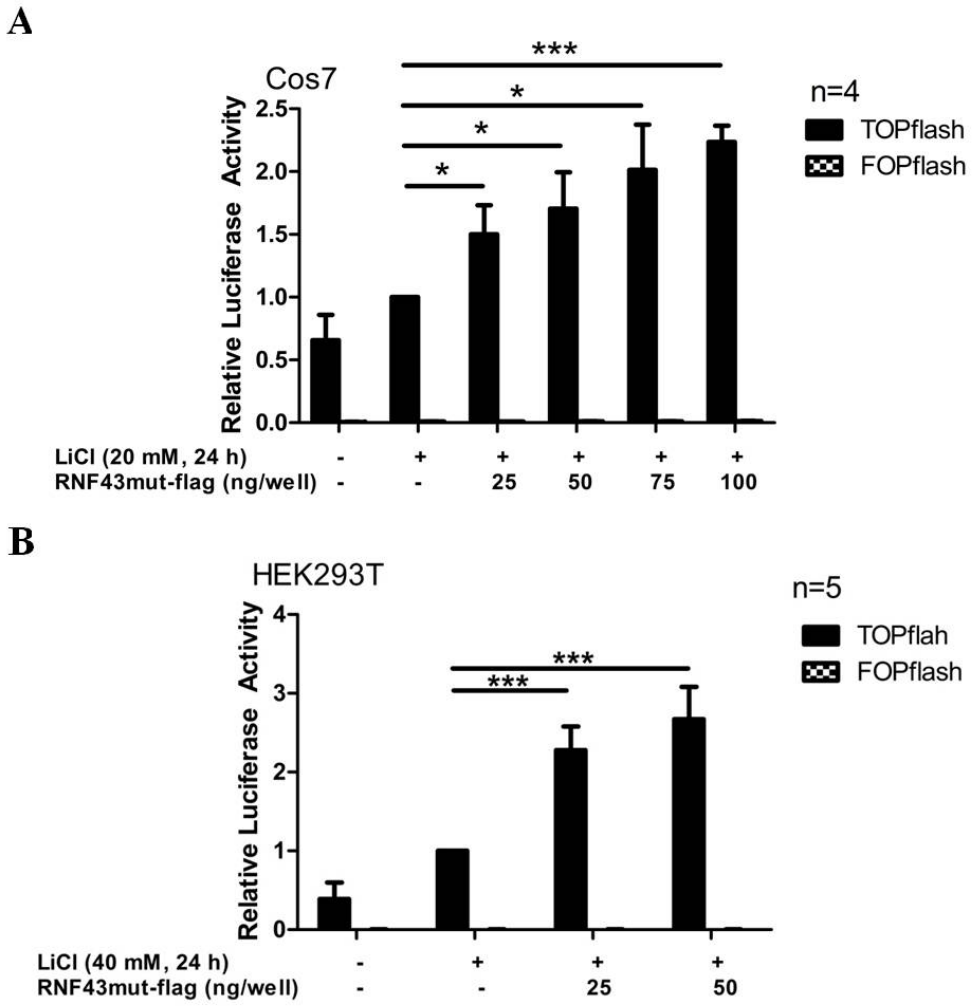

Figure 25 The inhibition of Wnt signaling by RNF43 is mediated by a functional RING domain.
(A) Cos7 cells and (B) HEK293T cells were transfected with pTOPflash or the control pFOPflash reporter plasmids and the indicated amounts of the plasmid RNF43mut-flag. RNF43mut-flag was transfected at increasing amounts. Wnt signaling was activated by treatment with the indicated concentrations of LiCl. Results were normalized to Renilla values and to the LiCl-treated control. Data are means + S.D. of four (A) or five (B) independent experiments.

In contrast to the inhibitory effect of wildtype RNF43 on the Wnt signaling pathway, co-transfection of the indicated amounts of mutant RNF43 not only reversed the inhibitory effect of wildtype RNF43 on Wnt signaling activity in TOP/FOP Luciferase reporter assays, but also resulted in a significant and dose-dependent increase in Tcf4-mediated Wnt signaling activity (Figure 25). Hence, functional inactivation of the RING domain of RNF43 by introduction of two point mutations resulting in amino acid exchanges at positions 292 and 295 transactivated Wnt signaling.

Thus, the functional RING domain of wildtype RNF43 is required for its inhibitory effect on the Wnt/ß-catenin signaling pathway.

3.2.2 RNF43 inhibits Wnt signaling *in vivo*

Since RNF43 was shown to inhibit canonical Wnt signaling *in vitro*, the next aim was to investigate its role *in vivo*. *Xenopus laevis* was used as a model system. In *Xenopus laevis*, Wnt signaling is essential for proper embryonic development. Wnt/ß-catenin signaling regulates the formation of different structures in developing *X. laevis* (reviewed in Moon, Brown et al. 1997), making it a useful model to investigate the *in vivo* role of previously uncharacterized modulators of the Wnt signaling pathway. In order to detect a possible *in vivo* function of RNF43, a *Xenopus laevis* axis duplication assay was carried out.

The main principle of the assay is that increased Wnt signaling induced by ectopic expression of Wnt1 in *Xenopus laevis* embryos results in body axis duplication. Thus, ventral injection of Wnt1 mRNA into the marginal zone of blastomeres of four-cell stage embryos activates the canonical Wnt pathway and induces the formation of a secondary body axis.

Xenopus laevis axis duplication assays were carried out by Dr. Dietmar Gradl. Therefore, wildtype and mutant RNF43 sequences were cloned into a pCS2myc plasmid and mRNA was generated. Since the *Xenopus laevis* RNF43 sequence is not annotated so far, und since the RNF43 sequence is conserved among species to a very high extent (Figure 15), the human RNF43 sequence was used as a template for cloning. mRNAs were co-injected with Wnt1 mRNA into *Xenopus laevis* embryos. Results obtained in the *Xenopus laevis* axis duplication assay are displayed in Figure 26.

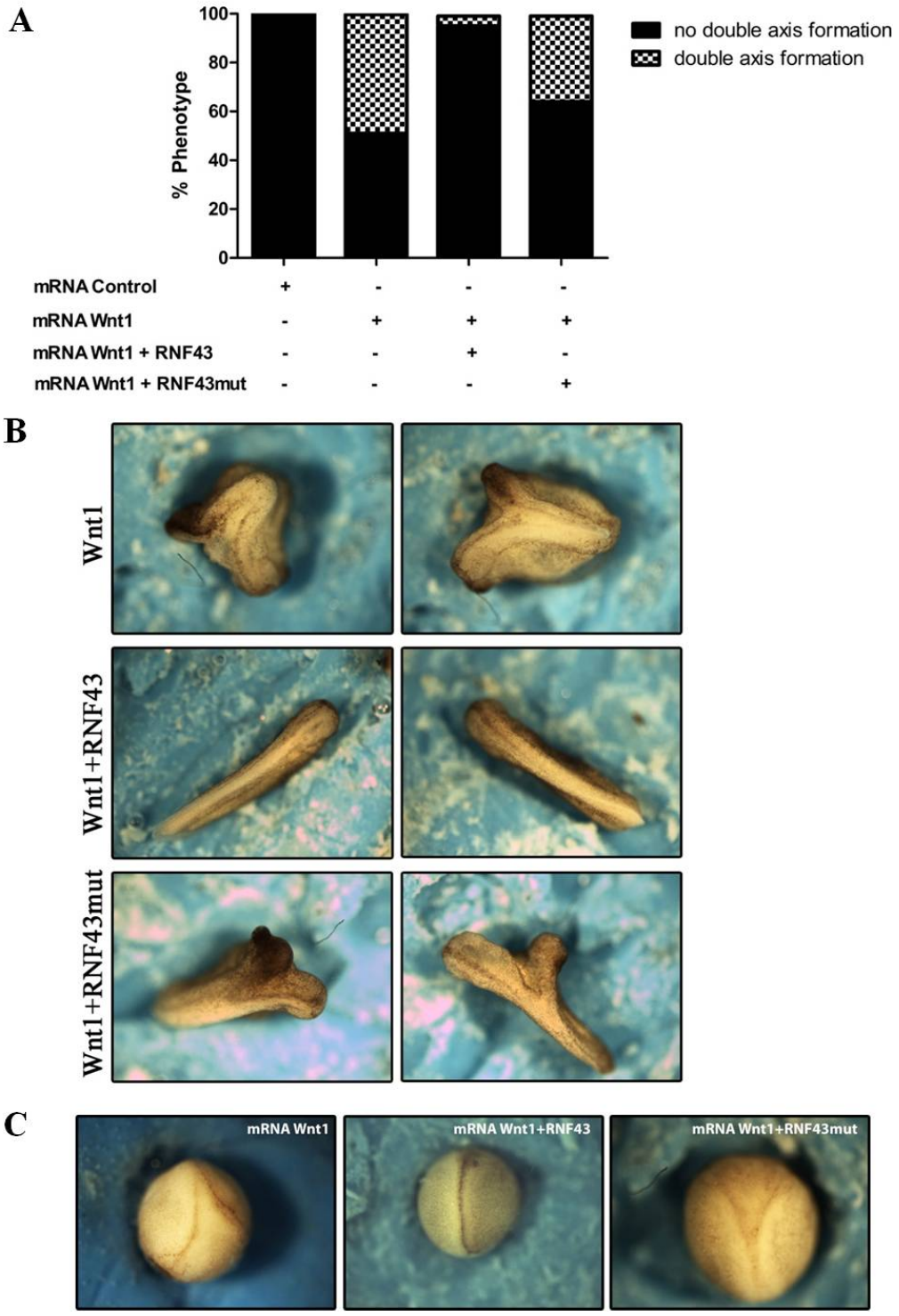

Figure 26 RNF43 inhibits Wnt signaling *in vivo*.
(A) Quantification of a *Xenopus laevis* axis duplication assay. *X. laevis* embryos were injected with control mRNA, Wnt1 mRNA (n = 198), Wnt1 mRNA in the presence of RNF43 mRNA (n = 142) or Wnt1 mRNA in the presence of RNF43mut mRNA (n = 106) by Dr. Dietmar Gradl. Injection of *X. laevis* embryos with Wnt1 mRNA into ventral blastomeres of 4-cell embryos resulted in an induction of the double axis phenotype. Co-expression of RNF43 mRNA rescued the Wnt1-induced double axis formation. (B) Two representative pictures of *Xenopus laevis* embryos injected with mRNA as indicated in the graph. (C) The effects of RNF43 and RNF43mut mRNA upon Wnt1 mRNA injection were already visible at a very early stage of gastrulation and body axis formation.

As illustrated in Figure 26, microinjection of 5 pg Wnt1 mRNA into ventral blastomeres of 4-cell *Xenopus laevis* embryos induced the formation of a secondary body axis in 48.7 % of all embryos (n = 198). Co-injection of RNF43 mRNA (500 pg) considerably reversed the effect of Wnt1 mRNA and nearly completely inhibited the double axis formation induced by Wnt1 mRNA. Upon RNF43 mRNA co-injection, only 4.9 % of all embryos still showed double axis formation, whereas co-injection of RNF43mut mRNA (500 pg) upon Wnt1 mRNA injection (5 pg) could not reverse the effect of Wnt1 mRNA. Therefore, 35.8 % of the *Xenopus laevis* embryos still exhibited the double body axis phenotype upon co-injection of RNF43mut.

As illustrated in Figure 26C, the effects of RNF43 and RNF43mut mRNA co-injection upon Wnt1 mRNA injection were already apparent at a very early stage of gastrulation and body axis formation.

These data are in accordance with *in vitro* TOP/FOP Luciferase reporter experiments, which indicated a function of RNF43 in negatively regulating the Wnt signaling pathway (Figure 25, Figure 26). *Xenopus laevis* axis duplication assays showed that RNF43 is not only an inhibitor of Wnt signaling *in vitro*, but also a bona fide inhibitor of canonical Wnt signaling *in vivo*, whereas the mutant form of RNF43 is not.

3.2.3 RNF43 acts at the level or downstream of ß-catenin

In mice, RNF43 was mainly expressed in intestinal tissues (Figure 17, Figure 18). In addition, RNF43 was shown do influence Wnt signaling activities in Cos7 and HEK293T cells (Figure 24). These data suggested further investigating the effect of RNF43 on Wnt signaling activities of colon cancer cells. Thus, in order to determine a possible effect of wildtype and mutant RNF43 on Wnt signaling activities of the colon cancer cell lines HCT116 and SW480, TOP/FOP Luciferase reporter assays were performed.

Both cell lines harbor mutations in the Wnt signaling cascade. HCT116 cancer cells harbor a mutation in the gene coding for ß-catenin (*CTNNB1*). In detail, a deletion of three basepairs results in the removal of one amino acid (Ser^{45}) (Morin, Sparks et al. 1997). Since Ser^{45} has been implicated in the down-regulation of ß-catenin through phosphorylation, ß-catenin mutants lacking this site are not degradable und thus more stable. Hence, cell lines harboring a form of ß-catenin mutated at Ser^{45} exhibit increased ß-catenin protein levels and thus higher

Wnt signaling activities than cell lines without mutations in this protein (Yost, Torres et al. 1996).

SW480 colon cancer cells exhibit a mutation in the *APC* gene, resulting in a functionally inactive, truncated APC protein. Since the ability of wildtype APC in inhibiting Wnt signaling is crucial for its function as a tumor suppressor, APC mutants that are defective in inhibiting Wnt signaling cause increased Wnt signaling activity (Morin, Sparks et al. 1997).

Thus, since HCT116 and SW480 cell lines harbor mutations, either in ß-catenin or in APC, an effect of wildtype and mutant RNF43 on Wnt signaling activity of these cell lines would indicate a function of RNF43 downstream or at the level of the mutated proteins, thus downstream or at the level of APC and ß-catenin. In order to investigate whether wildtype or mutant RNF43 affect the Wnt signaling activities in these two cell lines, TOP/FOP Luciferase reporter assays were performed.

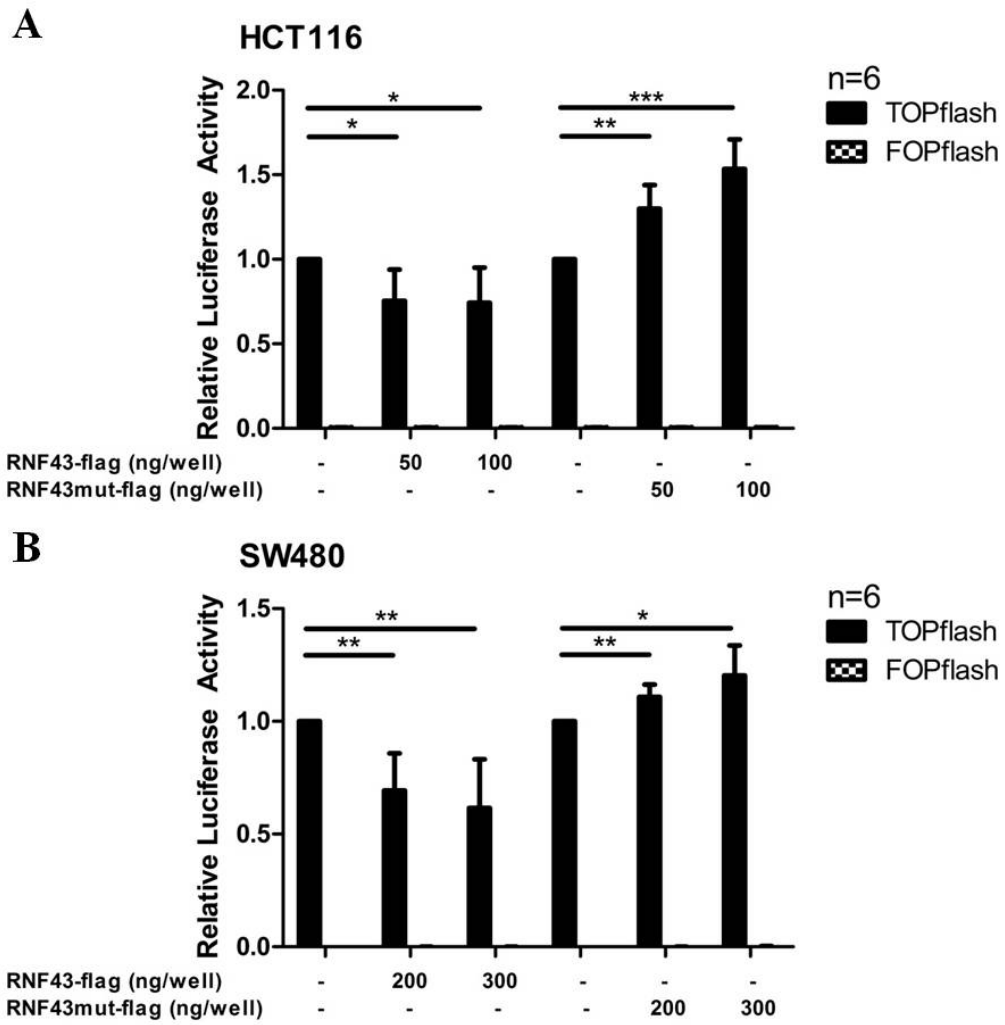

Figure 27 Function of RNF43 and RNF43mut on Wnt signaling activity of colon cancer cell lines.
HCT116 and SW480 colon cancer cells were transfected with pTOPflash or the control pFOPflash reporter plasmids and the indicated amounts of the plasmids RNF43-flag and RNF43mut-flag. Results were normalized to Renilla values and to the control without RNF43/RNF43mut. Data are means + S.D. of six independent experiments.

As illustrated in Figure 27, the function of wildtype and mutant RNF43 could still be observed in SW480 and HCT116 colon cancer cells in TOP/FOP Luciferase reporter assays.

RNF43 still inhibited Wnt signaling in SW480 cells (Figure 27), which carry mutations in the *APC* gene leading to elevated Wnt signaling activity, and mutant RNF43 still performed its activating function on Wnt signaling in SW480 cells. Thus, RNF43 performs its function downstream of APC in the Wnt signaling cascade.

In addition, in HCT116 cells, RNF43 also still performed its inhibitory function on Wnt signaling, and mutant RNF43 still elevated Wnt signaling in this cell line (Figure 27).

Thus, RNF43 performs its function not only downstream or at the level of APC, but also downstream or at the level of ß-catenin in the Wnt signaling cascade.

In the absence of Wnt signaling activity, ß-catenin levels are kept low through phosphorylation of ß-catenin and subsequent ubiquitination and degradation by the proteasome. In pathological situations, abnormal stabilization of ß-catenin is often caused by mutations in the ß-catenin gene (*CTNNB1*) itself. Usually, the mutations affect residues at amino acid positions 33 (S), 37 (S), 41 (T) or 45 (S). These residues are targets of phosphorylation. Priming phosphorylation by Casein Kinase 1 (CK1) occurs at serine 45 (S45), followed by subsequent consecutive phosphorylation events at S33, S37 and T41 residues by Glycogen Synthase Kinase 3 (GSK3). Impaired phosphorylation of ß-catenin and thus impaired degradation, as well as the resulting stabilization and nuclear translocation of the protein finally lead to an increase in Wnt signaling activity (reviewed in Austinat, Dunsch et al. 2008).

In addition to LiCl, which was shown to activate Wnt signaling in Cos7 cells and HEK293T cells (3.1.3), Wnt signaling can also be activated by transfection of a construct expressing a stabilized form of ß-catenin, s33-ß-catenin, which is a construct expressing ß-catenin harboring a mutation at the serine residue at position 33. Due to the mutation at the serine 33 residue in this ß-catenin mutant, the phosphorylation cascade is impaired. Hence, ß-catenin cannot be marked for proteasomal degradation, resulting in stabilized ß-catenin. Since increased levels of ß-catenin result in elevated Wnt signaling activity, the effect of s33-ß-catenin on Wnt signaling was investigated. The increase in canonical Wnt signaling activity upon transfection of s33-ß-catenin was investigated in TOP/FOP Luciferase reporter assays in Cos7 cells.

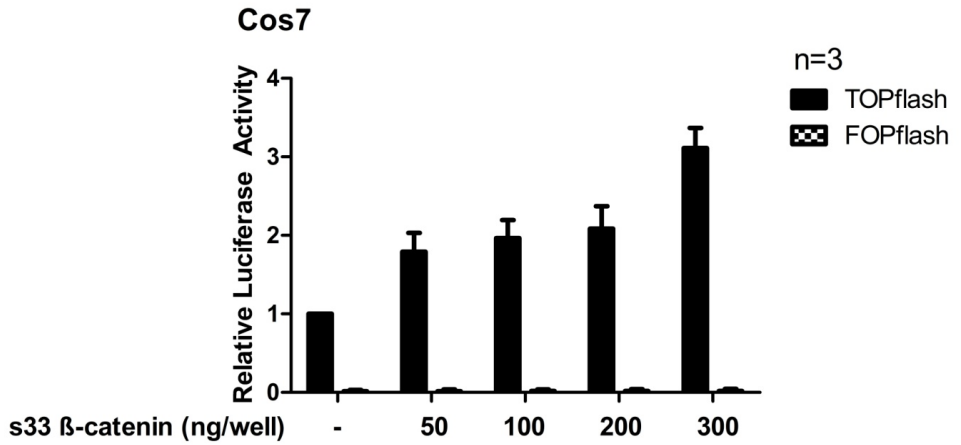

Figure 28 Dose-dependent activation of Wnt signaling activity by s33-ß-catenin.
Cos7 cells were transfected with pTOPflash or the control pFOPflash reporter plasmids as well as the indicated amounts of s33-ß-catenin plasmid. The stabilized form of ß-catenin, S33-ß-catenin, increased activation of ß-catenin/TCF-mediated transcription. Results were normalized to Renilla values and to the control without s33-ß-catenin. Data are means + S.D. of three independent experiments.

Transfection with increasing amounts of s33-ß-catenin resulted in a dose-dependent increase of Wnt signaling activity in TOP/FOP Luciferase reporter assays in Cos7 cells (Figure 28). Since transfection with 50 ng s33-ß-catenin per well already increased Wnt signaling activity around 2-fold, this concentration was chosen for the stimulation of the Wnt signaling pathway in the subsequent experiment.

In order to determine whether RNF43 also acts at the level or downstream of ß-catenin in Cos7 cells, as observed in HCT116 cells (Figure 27), TOP/FOP Luciferase reporter assays were performed in this cell line. Wnt signaling was activated by co-transfection of a construct expressing s33-ß-catenin, a stabilized form of ß-catenin.

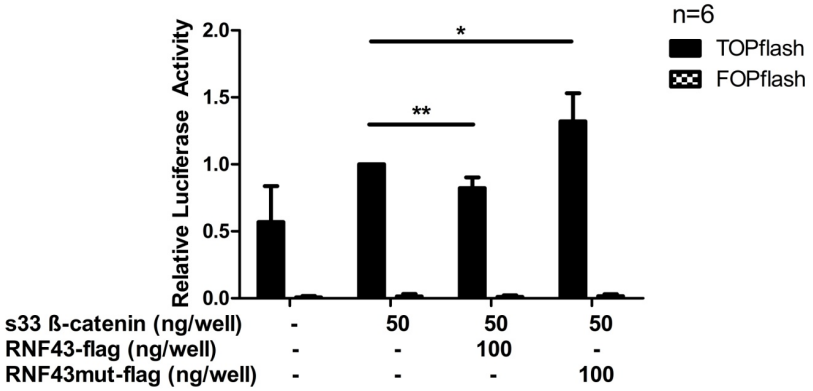

Figure 29 RNF43 inhibits Wnt signaling downstream or at the level of ß-catenin.
Cos7 cells were transfected with pTOPflash or the control pFOPflash reporter plasmids as well as the indicated plasmids. RNF43-flag repressed transcriptional activation of ß-catenin/TCF-mediated transcription induced by a stabilized form of ß-catenin, s33-ß-catenin, whereas RNF43mut-flag increased Wnt signaling. Results were normalized to Renilla values and to s33-ß-catenin transfected cells. Data are means + S.D. of six independent experiments.

In Cos7 cells, the activating effect on Wnt signaling mediated by a stabilized form of ß-catenin, s33-ß-catenin, could be reversed by wildtype RNF43 and further increased by mutant RNF43 (Figure 29).

Thus, in accordance with the effects of wildtype and mutant RNF43 shown in HCT116 colon cancer cells (Figure 27), the effects of both proteins were also visible in TOP/FOP Luciferase reporter assays performed in Cos7 cells. Wildtype RNF43 still exhibited its inhibiting function on the ß-catenin/TCF reporter activity driven by the ectopic expression of a degradation-resistant form of ß-catenin, and mutant RNF43 still further increased Wnt signaling under the same conditions. Hence, RNF43 acts at the level or downstream of ß-catenin in the Wnt signaling cascade.

3.3 Function of RNF43

3.3.1 Subcellular localization of RNF43

Many different biochemical functions have been attributed to proteins with RING domains (Capili, Edghill et al. 2004). Their localization is not restricted to a specific compartment but they are located throughout the whole cell (Saurin, Borden et al. 1996). Since there is often a correlation between function and localization of a protein, the next aim was to investigate the subcellular localizations of wildtype and mutant RNF43.

For a prediction of the subcellular localization of RNF43, protein localization tools were used. The protein localization tool "PSORTII"[5] suggested a nuclear localization of RNF43. In addition, the program found several nuclear localization sequences in the RNF43 protein sequence, which are located at positions 654 (RKRR) and 434 (PLRRARP). PSORTII did not identify any ER membrane retention signals, peroxisomal targeting signals or vacuolar targeting motifs in the RNF43 protein sequence, but a mitochondrial targeting sequence was found, and RNF43 was identified to be a type 1b membrane protein, which is a single-pass transmembrane protein without a cleaved signal peptide. Amino acids 201 - 217 were calculated to be the amino acids located inside the membrane. Amino acids 201 - 783 were calculated to build up the cytoplasmic tail and the other amino acids (1 - 200) were found to face towards the other side. According to PSORTII, type1b transmembrane proteins are often found in the ER.

Another protein localization program, "Euk-mPLoc 2.0"[6], predicted a localization of RNF43 inside the cytoplasm, the nucleus, and the ER. Unfortunately, no more details were mentioned.

In order to obtain more information about a potential localization of RNF43 in the nucleus, the "Subnuclear Compartments Prediction System (V2.0)"[7] was used, which suggested a localization of RNF43 in the nuclear lamina.

Yagyu et al. described RNF43 as a protein harboring a signal peptide at the N-terminus, which they identified using the protein motif finder "SMART (Simple Modular Architecture research tool)"[8]. The program predicted RNF43 to be a protein with a signal peptide (codons 1-27) and a RING finger motif (codons 272 - 312) (Yagyu, Furukawa et al. 2004). Due to the presence of a signal peptide, there were protein localization prediction tools, like e.g. "TargetP1.1"[9], that invariably predicted RNF43 to be a secreted protein.

[5] http://psort.hgc.jp/form2.html

[6] http://www.csbio.sjtu.edu.cn/bioinf/euk-multi-2/

[7] http://array.bioengr.uic.edu/subnuclear.htm

[8] http://smart.embl-heidelberg.de/

[9] http://www.cbs.dtu.dk/services/TargetP/

Yagyu et al. found RNF43 to be expressed in spotty granules inside the cytoplasm. In addition, they suggested that RNF43 is a secreted protein, since upon transfection of Cos7 cells with a construct expressing RNF43, they detected RNF43 not only in lysates but also in culture media (by Western Blot analysis) (Yagyu, Furukawa et al. 2004). This is in according with the calculations from the "TargetP1.1" protein localization prediction program.

In order to verify the results obtained by Yagyu et al., we aimed to investigate the subcellular localizations of wildtype and mutant RNF43 proteins by Immunofluorescence stainings using HCT116 and SW480 colon cancer cells, as well as Cos7 cells. Therefore, cells were transiently transfected with RNF43 and RNF43mut constructs, followed by Immunofluorescence stainings using anti-ß-catenin (mouse) and anti-flag (rabbit) antibodies as well as DAPI staining in order to visualize the nucleus.

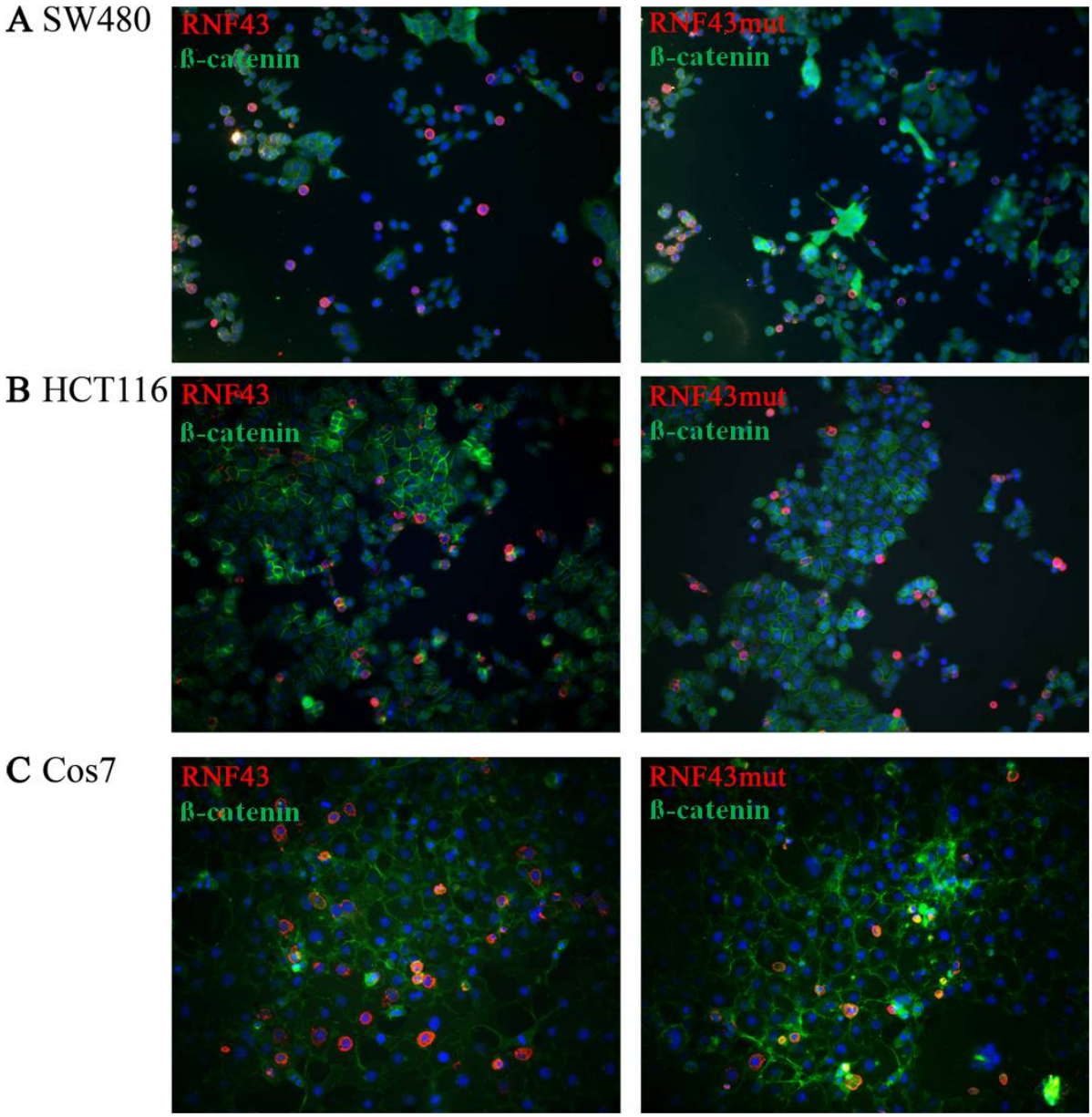

Figure 30 Overexpression of wildtype and mutant RNF43 in SW480, HCT116 and Cos7 cells.
SW480 (A), HCT116 (B) and Cos7 (C) cells were transiently transfected with RNF43-flag or RNF43mut-flag constructs. Pictures of Immunofluorescence stainings illustrate DAPI (blue), ß-catenin (green) and anti-flag (red) stainings (20x magnification).

As illustrated in Figure 30, both wildtype and mutant RNF43 constructs harboring a C-terminal flag-tag exhibited clear signals in Immunofluorescence microscopy upon staining with the indicated antibodies. Due to the fact that Cos7 cells are easier to transfect than colon cancer cells, transfection efficiencies were around 20 % in Cos7 cells and approximately 10 % in SW480 and HCT116 cells.

The subcellular localization of RNF43 and RNF43mut in the indicated cell lines was subsequently investigated more precisely (Figure 31).

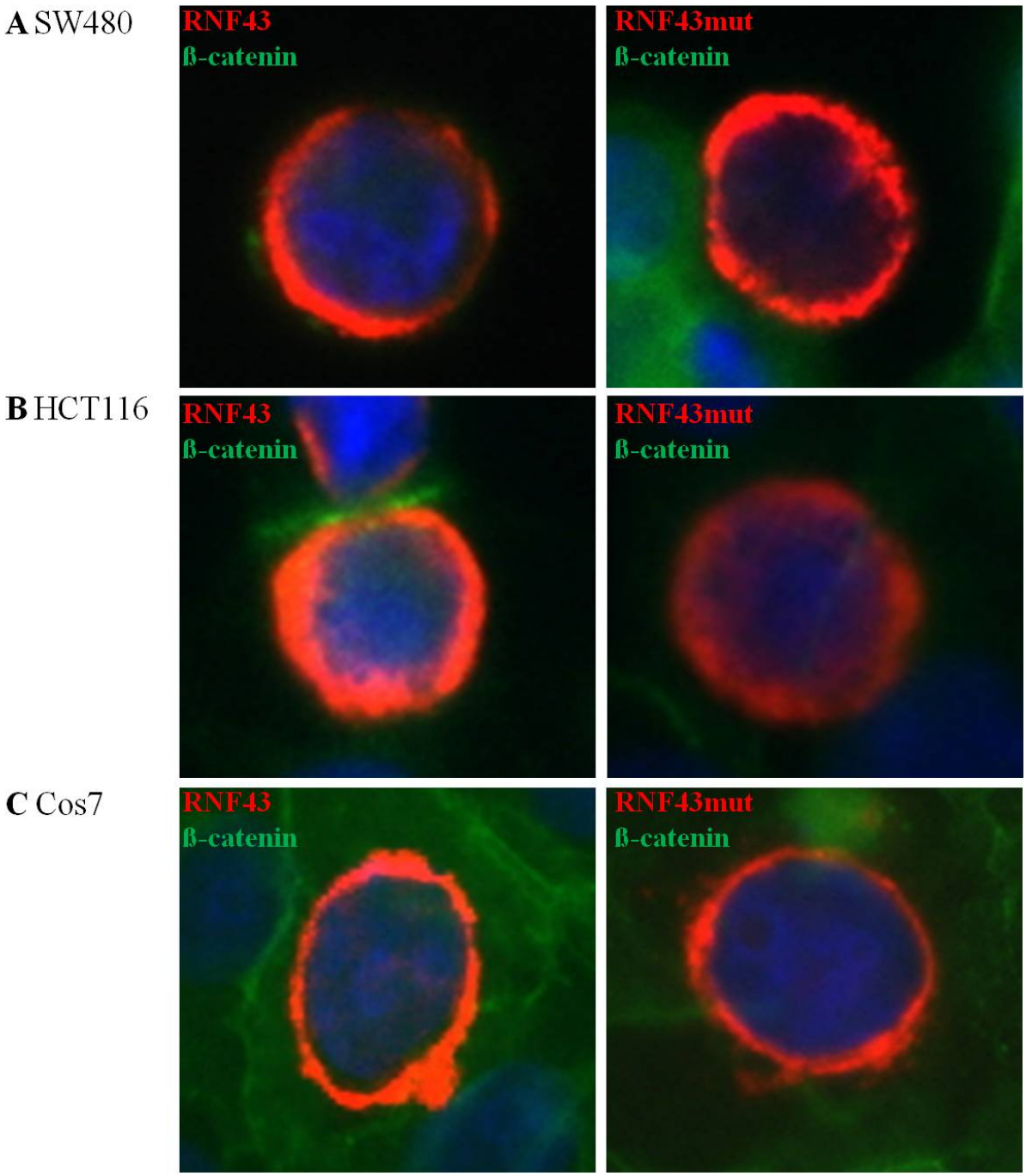

Figure 31 Overexpression of wildtype and mutant RNF43 in SW480, HCT116 and Cos7 cells.
SW480 (A), HCT116 (B) and Cos7 (C) cells were transiently transfected with RNF43-flag or RNF43mut-flag constructs. Pictures of Immunofluorescence stainings illustrate DAPI (blue), ß-catenin (green) and anti-flag (red) stainings.

ß-Catenin showed a strong staining of the cytoplasmic membrane, but small amounts of the protein were also detectable in the cytoplasm, and, as colon cancer cells exhibit endogenous Wnt signaling activity, small amounts of the protein were also detectable in the nucleoplasm in HCT116 and SW480 cells.

As illustrated in Figure 30 and Figure 31, RNF43 and RNF43mut were both located inside the cells. Wildtype as well as the mutant RNF43 exhibited a strong staining of the nuclear envelope. No differences between the localizations of RNF43 and RNF43mut were detectable. Small amounts of wildtype and mutant RNF43 were also visible inside the nucleoplasm. In contrast to the localization pattern suggested by Yagyu et al. (Yagyu, Furukawa et al. 2004), RNF43 was never detected in spotty granules inside the cytoplasm during this study.

In addition to the localization of RNF43 in spotty granules in the cytoplasm, Yagyu et al. suggested that upon transfection of Cos7 cells with constructs expressing RNF43, RNF43 is additionally detectable in the culture medium. Thus, they concluded that RNF43 is not only present in granules in the cytoplasm, but also is a secreted protein (Yagyu, Furukawa et al. 2004).

In order to investigate whether RNF43, in addition to its localization inside the cell, is a secreted protein, as suggested by Yagyu et al., the next aim was to examine a possible detectability of RNF43 in the supernatant. Therefore, HCT116 cells were transfected with RNF43-HA, RNF43mut-HA or a control plasmid, and 48 h post-transfection, the proteins of the supernatants were precipitated with TCA. In addition, adherent cells were lysed with 1x SDS lysis buffer. Proteins of the supernatant as well as of the crude extracts were subjected to Western blot analysis with anti-HA and anti-ß-actin antibodies. Since ß-actin is not secreted and thus does not serve as a loading control for proteins of the supernatant, the proteins on the membranes were stained with Ponceau S staining solution, in order to evidence the presence of proteins in the supernatant samples.

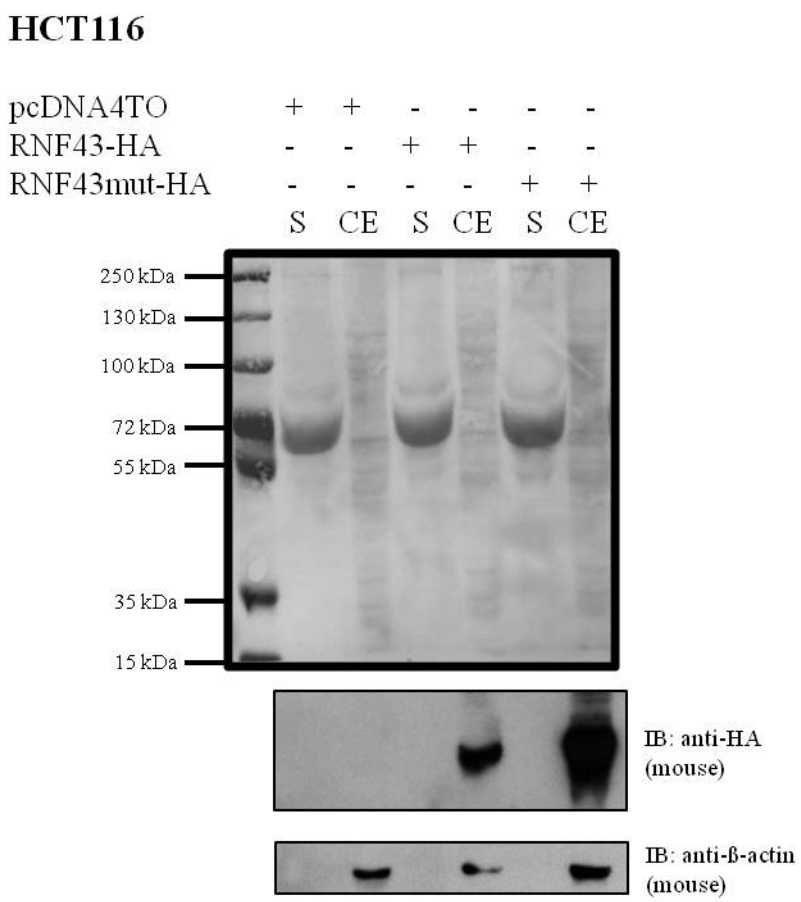

Figure 32 Wildtype and mutant RNF43 are not secreted.
HCT116 cells were transiently transfected with RNF43-flag, RNF43mut-flag or a control plasmid. 48 h after transfection, the proteins of the supernatant were precipitated with TCA. Adherent cells were lysed with 1x SDS lysis buffer. Proteins of the supernatants (S) as well as of the cell crude extracts (CE) were subjected to Western blot analysis with anti-HA and anti-ß-actin antibodies. The membrane was stained with Ponceau S in order to evidence the presence of proteins in all samples.

As visible in Figure 32, wildtype as well as mutant RNF43 were only detectable in cell lysates, but not in the supernatant of cells. Thus, in contrast to the data obtained by Yagyu et al., secreted forms of RNF43 were never detected during this study.

In order to determine whether RNF43 and RNF43mut localize to the inner nuclear membrane, Immunofluorescence co-stainings of RNF43, which was detected by an antibody recognizing the flag-tag, and Lamin B receptor, which was detected by an antibody recognizing endogenous protein, were performed. The Lamin B receptor, also referred to as LBR, is an integral membrane protein of the nuclear envelope that associates with the nuclear intermediate filament protein Lamin B, implicating this protein in the attachment of the nuclear lamina to the inner nuclear membrane in interphase (Worman, Yuan et al. 1988;

Worman, Evans et al. 1990). Lamin B receptor is a protein commonly used as a marker for the inner nuclear membrane.

As illustrated in Figure 33, Immunofluorescence co-stainings of wildtype and mutant RNF43 and Lamin B receptor exhibited a colocalization of both proteins with the marker protein, indicating a localization of both wildtype and mutant RNF43 at the inner nuclear membrane.

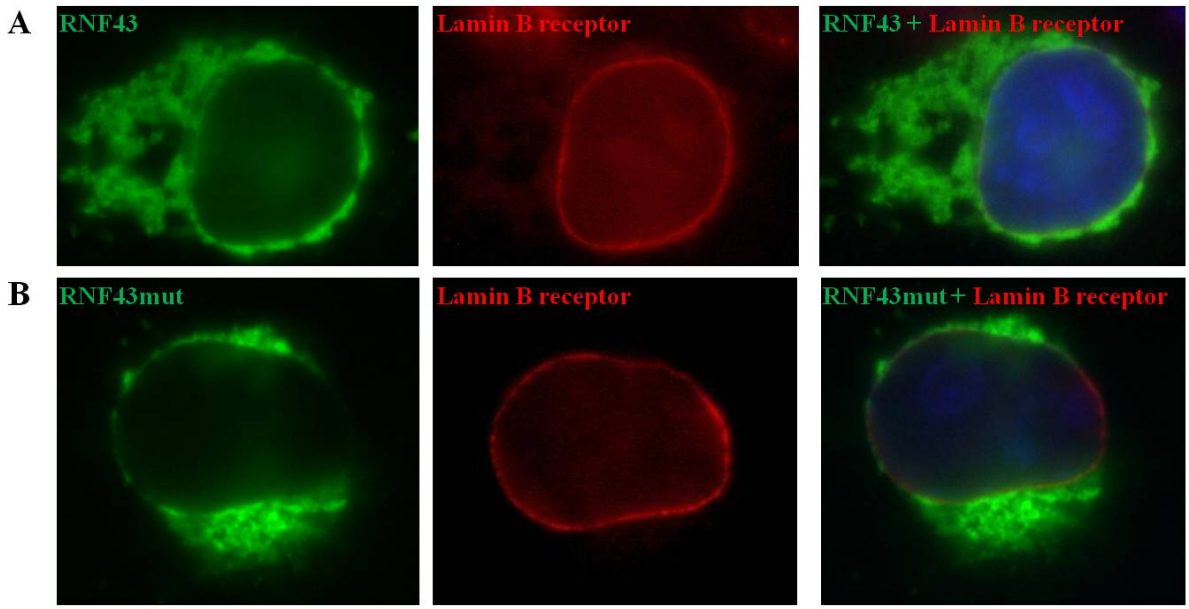

Figure 33 Immunofluorescence co-stainings of wildtype and mutant RNF43 and Lamin B receptor.
HCT116 cells were transiently transfected with (A) RNF43-flag or (B) RNF43mut-flag constructs. Pictures of Immunofluorescence stainings illustrate DAPI (blue), anti-flag (green) and anti-Lamin B receptor (red) stainings.

In addition to their localization in the nuclear membrane, both wildtype and mutant RNF43 sometimes localized to structures located on one side outside of the nucleus, indicating a localization of the proteins in the Endoplasmatic reticulum (ER) or the Golgi apparatus. Therefore, Immunofluorescence co-stainings of wildtype and mutant RNF43 and Calnexin, a marker for the ER, and Golgin 97, a marker for the Golgi apparatus, were performed in HCT116 cells (Figure 34, Figure 35).

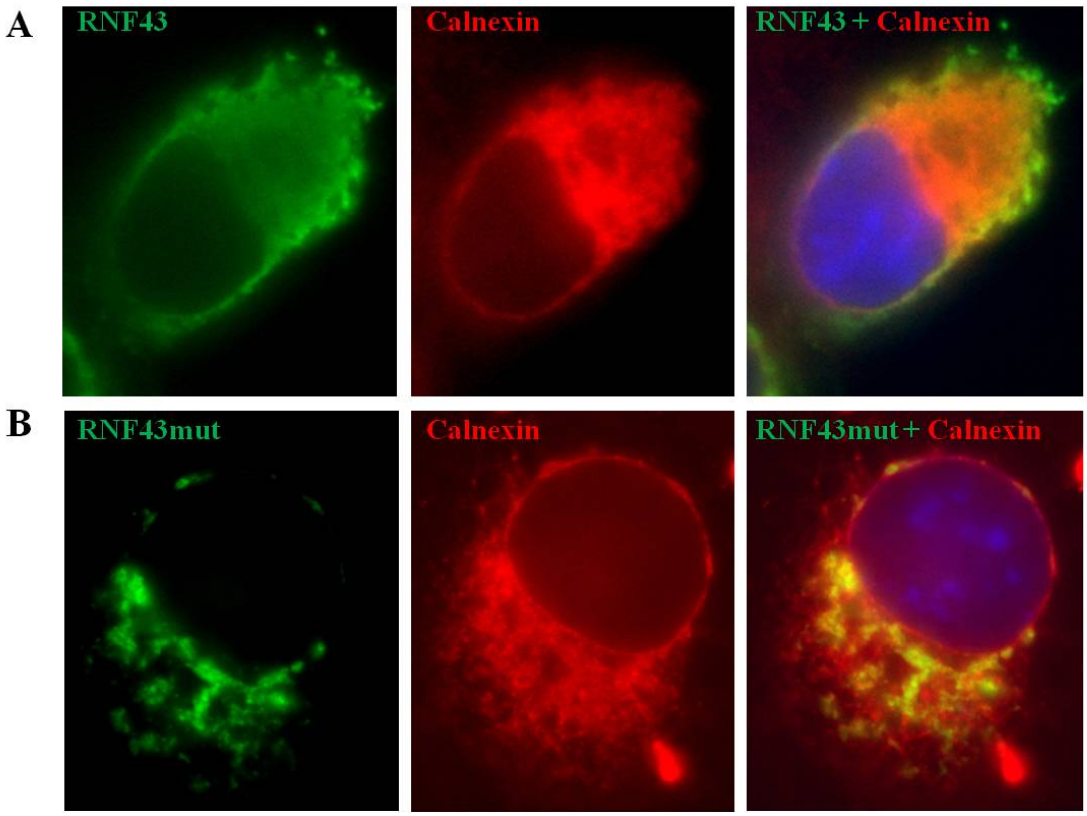

Figure 34 Immunofluorescence co-stainings of wildtype and mutant RNF43 and Calnexin.
HCT116 cells were transiently transfected with (A) RNF43-flag or (B) RNF43mut-flag constructs. Pictures of Immunofluorescence stainings illustrate DAPI (blue), anti-flag (green) and anti-Calnexin (red) stainings.

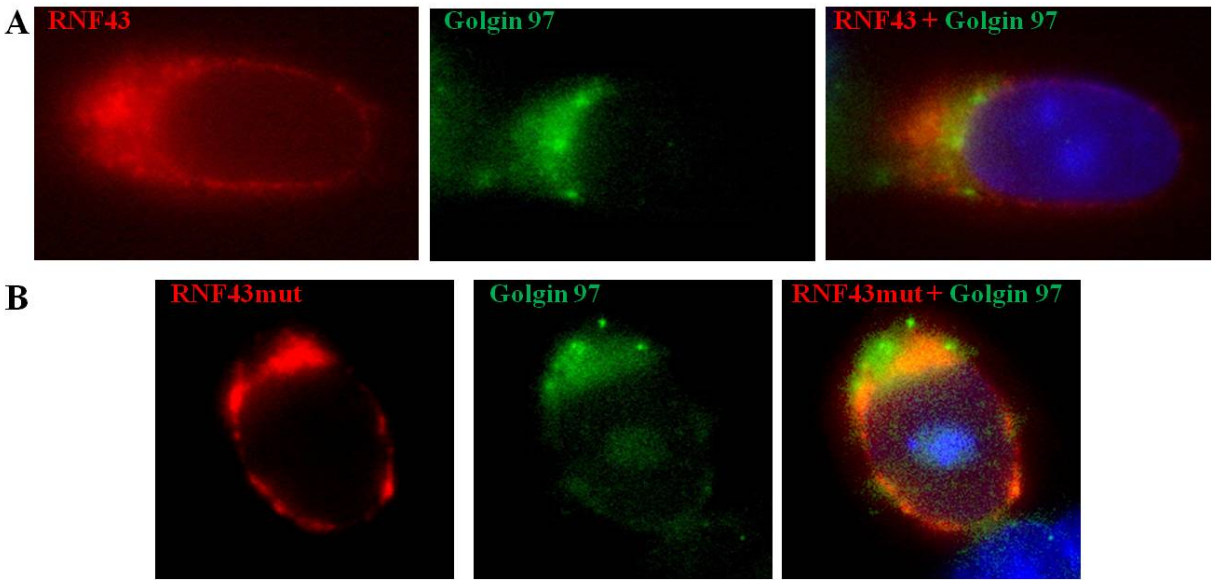

Figure 35 Immunofluorescence co-stainings of wildtype and mutant RNF43 and Golgin 97.
HCT116 cells were transiently transfected with (A) RNF43-flag or (B) RNF43mut-flag constructs. Pictures of Immunofluorescence stainings illustrate DAPI (blue), anti-flag (red) and anti-Golgin 97 (green) stainings.

In Immunofluorescence co-stainings, both wildtype and mutant RNF43 proteins colocalized with Calnexin, the ER marker, and Golgin 97, the marker for the Golgi apparatus, in HCT116 cells (Figure 34, Figure 35).

Thus, in all investigated cell lines (HCT116, SW480, Cos7), both wildtype and mutant RNF43 mainly localized to the inner nuclear membrane, the ER and the Golgi apparatus. Small amounts were also detectable inside the nucleoplasm.

3.3.2 Recently described function of RNF43

Recently, when this thesis was in preparation, a study of Hao et al. showed that ZNRF3, a homologue of RNF43, and LGR4 form a receptor complex for R-Spondin (Hao, Xie et al. 2012). R-spondin proteins are secreted proteins (Kazanskaya, Glinka et al. 2004) that strongly activate the Wnt signaling pathway (Kazanskaya, Glinka et al. 2004; Kim, Kakitani et al. 2005; Kim, Mao et al. 2007), and the stem cell marker Lgr5 and its homologue Lgr4 are receptors for R-spondin, which are essential for its function as an activator of Wnt signaling (Hao, Xie et al. 2012). Hao et al. suggested that in the absence of R-spondin, ZNRF3 ubiquitinates Frizzled and promotes the degradation of both LRP6 and Frizzled at the plasma membrane. As a result, Wnt signaling is inhibited. They also suggested that RNF43 is a functional homologue of ZNRF3, since activation of Wnt signaling induced by ZNRF3 siRNA could be inhibited by overexpression of wildtype RNF43 protein. When they used RNF43ΔRING instead of RNF43, they observed a transactivating effect on Wnt signaling activity.

They also found both RNF43 and ZNRF3 to be localized to the plasma membrane. Although they showed pictures of ZNRF3 Immunofluorescence stainings, they did not show any for RNF43. Since they observed identical localizations of RNF43 and ZNRF3, and since activation of Wnt signaling induced by ZNRF3 siRNA could be inhibited by overexpression of RNF43, they concluded that ZNRF3 and RNF43 are functional homologues, both acting as negative regulators of Wnt signaling at the plasma membrane responsible for the degradation of LRP6 and Frizzled in the absence of R-spondin (Hao, Xie et al. 2012).

In contrast, a localization of wildtype or mutant RNF43 at the plasma membrane upon ectopic expression was never observed during this study. Instead, a localization of RNF43 mainly at the nuclear membrane, the ER and in small amounts inside the nucleoplasm was observed

(3.3.1). Hao et al. used a plasmid expressing RNF43-GFP for their localization studies. Since attachment of big peptides or proteins often results in alterations in protein localizations, the localization pattern observed during their study could possibly be attributed to the attachment of GFP to RNF43.

During our study, RNF43-CFP and RNF43-Cherry expression constructs were generated using the Gateway recombinase system (2.1.8). The fluorescent proteins were attached to the C-terminus of RNF43, and the localization of both RNF43-CFP and RNF43-Cherry was investigated in HCT116 cells.

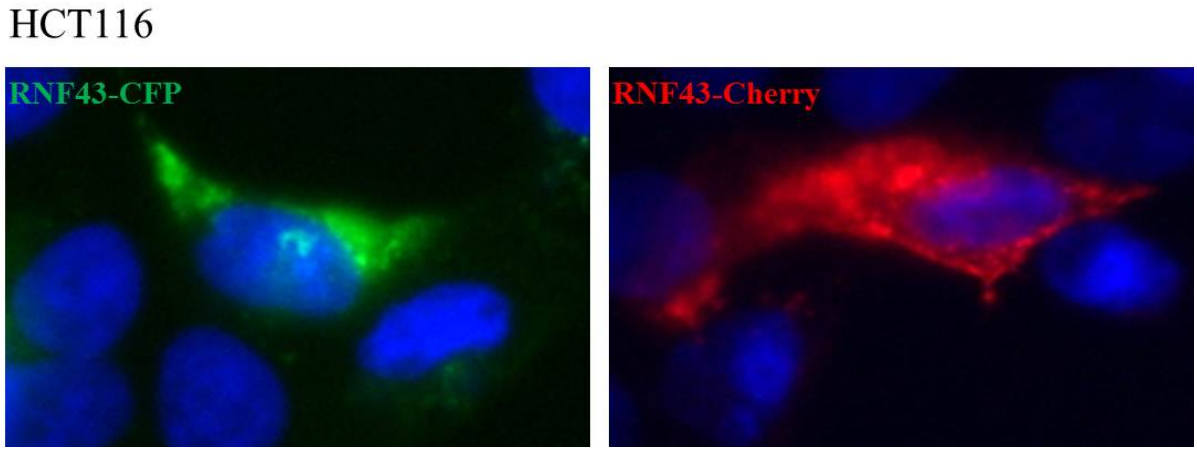

Figure 36 Localization of RNF43-CFP and RNF43-Cherry in HCT116 cells.
HCT116 cells were transiently transfected with constructs expressing RNF43-CFP or RNF43-Cherry. Immunofluorescence pictures illustrate DAPI (blue) staining, CFP (green) and Cherry (red) fluorescence.

As illustrated in Figure 36, both RNF43-CFP and RNF43-Cherry fusion proteins exhibited a localization pattern that was different from the localization pattern of RNF43 fused to a HA- or flag-tag. Thus, the attachment of a large tag like CFP or Cherry resulted in an altered localization pattern of RNF43. These data indicate that similarly to the results obtained by attachment of a CFP- or Cherry-tag, attachment of a GFP-tag may possibly also have influenced the localization of RNF43.

In order to determine whether the attachment of a large tag, which was shown to change the localization of RNF43 (Figure 36), also results in alterations in the function of RNF43, the effect of RNF43-CFP and RNF43-Cherry on the endogenous Wnt signaling activity of HCT116 cells was investigated.

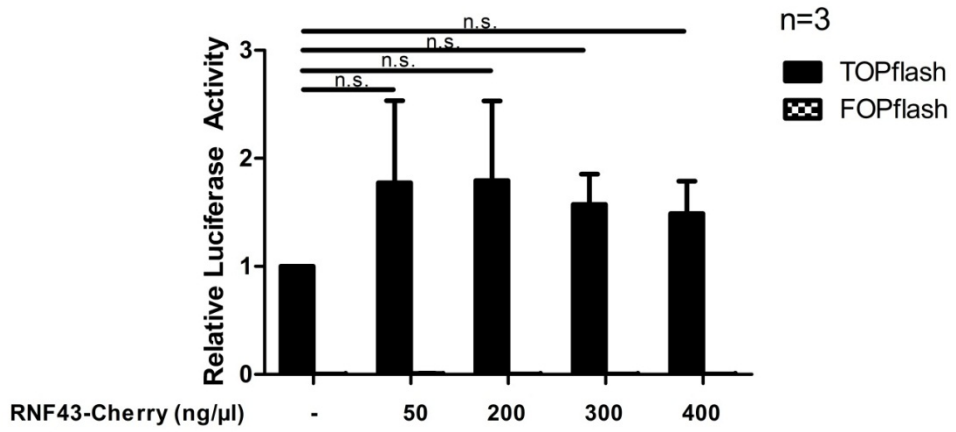

Figure 37 RNF43-Cherry does not inhibit Wnt signaling in HCT116 cells.
HCT116 cells were transfected with pTOPflash or the control pFOPflash reporter plasmids and the indicated amounts of a construct expressing RNF43-Cherry. Data were normalized to Renilla values as well as to the control without RNF43-Cherry. Data are means + S.D. of three independent experiments.

As visible in Figure 37, the function of RNF43 coupled to Cherry was completely lost. RNF43-Cherry was completely deficient in inhibiting Wnt signaling in HCT116 cells (Figure 37) as well as in LiCl-activated Cos7 cells (data not shown). The same results were obtained for RNF43-CFP (data not shown). Since RNF43 fused to smaller tags like flag significantly inhibited Wnt signaling in HCT116 cells (Figure 27), the loss of function of RNF43-CFP and RNF43-Cherry can be ascribed to the large tags, and is likely to correlate with the alterations in localizations of RNF43-CFP and RNF43-Cherry proteins as compared to RNF43 fused to smaller tags.

Similarly, the function of RNF43 coupled to GFP, which was used in the study of Hao et al., may also be impaired or altered. Thus, in addition to the localization of RNF43-GFP at the plasma membrane, the mechanism of the inhibitory function of RNF43-GFP on Wnt signaling activity, as proposed by Hao et al., seems questionable.

Since sequence similarities serve as evidence for functional conservation, the extent of conservation between the human ZNRF3 (precursor) protein sequence (NCBI reference sequence: NP_001193927.1) and the human RNF43 protein sequence (NCBI reference sequence: AAI09029.1) was investigated by alignment using the IBIVU PRALINE multiple sequence alignment program[10].

[10] http://www.ibi.vu.nl/programs/pralinewww/

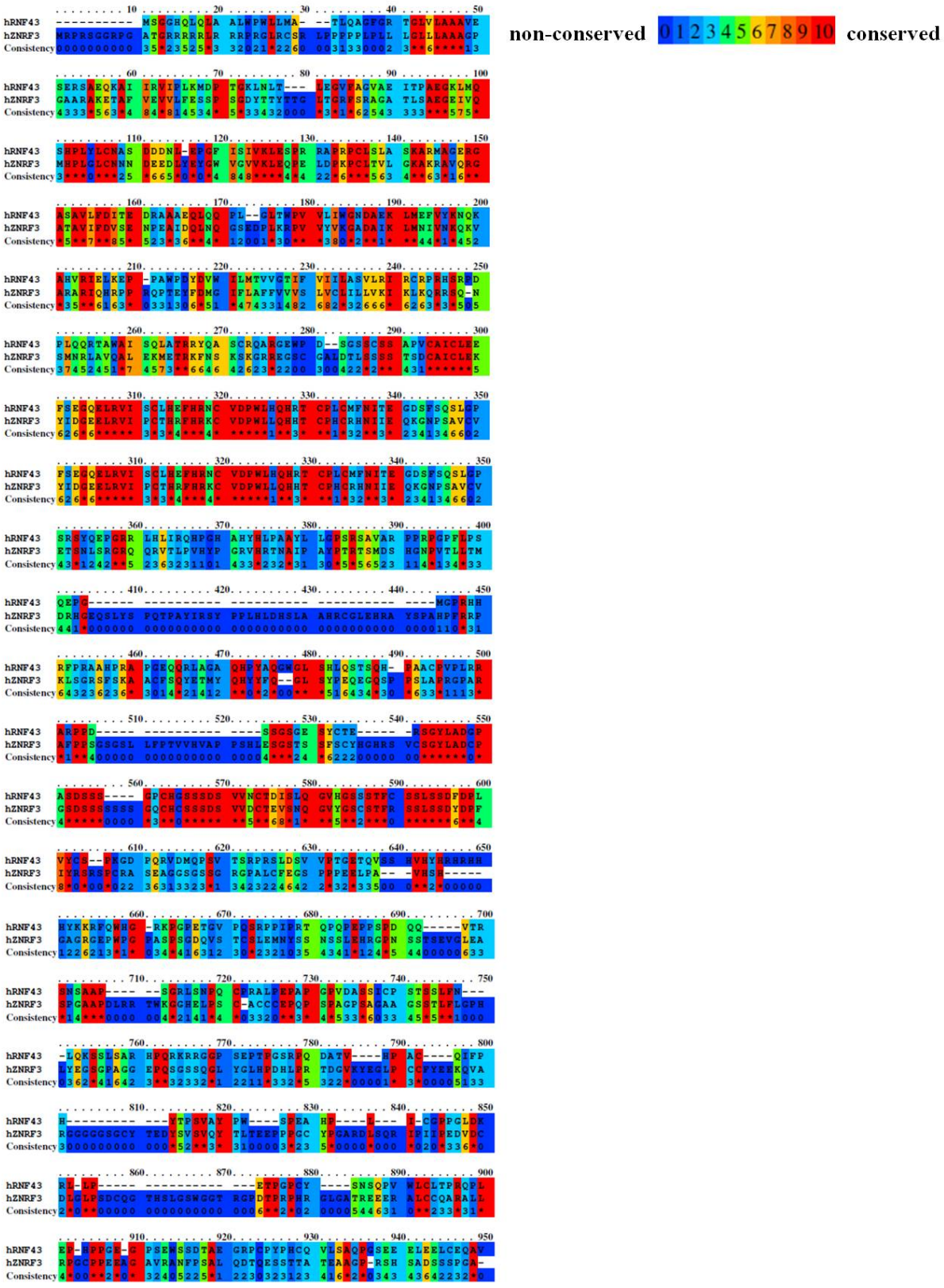

Figure 38 Amino acid sequence alignment of human ZNRF3 and human RNF43.
Residues are highlighted in colors according to their extent of conservation. Identical residues are accentuated in red, similar residues in orange and green, and non-conserved residues in blue.

As visible in Figure 38, with exception of the RING domain, which exhibited a high level of conservation between human RNF43 and human ZNRF3, the extent of conservation and thus homology between the sequences of the two proteins was very low. Thus, although RNF43 was described to be a homologue of ZNRF3, the function of the two proteins may not necessarily be the same. Other functions and localizations of RNF43 cannot be excluded.

3.3.3 Interaction of RNF43 and PSF

Miyamoto et al. identified the PSF/p54nrb heterodimer to interact with RNF43 (Miyamoto, Sakurai et al. 2008). PSF, (Polypyrimidine tract-binding protein (PTB)-associated splicing factor), a 100 kDa protein, was originally identified as a pre-mRNA splicing factor and an interaction partner of PTB (Patton, Porro et al. 1993). Meanwhile, the PSF/p54nrb heterodimer is known to play crucial roles in various other processes, like for instance transcriptional regulation and DNA replication, and the protein is known to be able to bind to RNA and DNA, as well as to proteins. These multifunctional proteins are expected to mediate various functions, and since they localize to several nuclear compartments (nuclear matrix, nucleoplasm, nuclear foci, nucleolus, nuclear membrane), their function may depend on the nuclear compartment. In addition, the PSF/p54nrb heterodimer is implicated in tumorigenesis, possibly by interacting with oncogenic proteins (reviewed in Shav-Tal and Zipori 2002).

In their study, Miyamoto et al. found RNF43 to localize to the nuclear rim and to the ER region, which is in accordance with the expression pattern observed during this study. Upon co-expression of PSF, Miyamoto et al. observed a movement of RNF43 from the perinuclear region to the cytoplasm, resulting in a profound colocalization of RNF43 and PSF in the nucleoplasm of Cos71 cells (Miyamoto, Sakurai et al. 2008).

In contrast to the data shown by Miyamoto et al., RNF43 did not relocalize from the nuclear membrane to the nucleoplasm upon transfection with a construct expressing PSF-HA in our experiments, neither in SW480 cells (Figure 39) or HCT116 cells, nor in Cos7 cells (data not shown), which are similar to Cos71 cells used by Miyamoto et al..

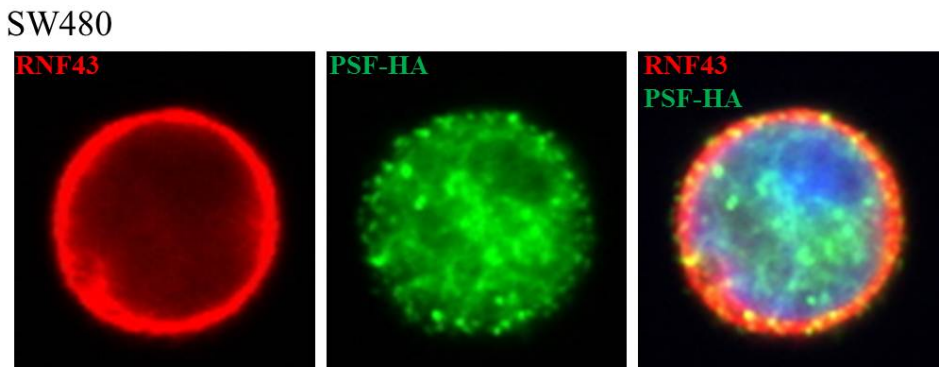

Figure 39 Co-expression of RNF43 with PSF.
SW480 cells were transiently transfected with RNF43-flag and PSF-HA constructs. Pictures of Immunofluorescence stainings illustrate DAPI (blue), anti-HA (green) and anti-flag (red) stainings.

As illustrated in Figure 39, co-expression of PSF-HA did not alter the localization of RNF43, and did not result in a more pronounced localization of RNF43 in the nucleoplasm. RNF43 mainly localized to the nuclear rim, and PSF mainly localized to small punctuate structures inside the nucleoplasm. Small amounts of PSF also resided in the nuclear membrane, where it colocalized with RNF43 (yellow dots in Figure 39). The same results were obtained upon co-expression of mutant RNF43 with PSF-HA (data not shown).

In contrast to the diverging data obtained by Immunofluorescence analysis, the interaction of PSF and RNF43 could be confirmed during this study. The existence of RNF43/PSF-complexes in mammalian cells was evidenced by Co-IP experiments. Therefore, HCT116 cells were co-transfected with RNF43-flag and PSF-HA constructs, and whole cell lysates were immunoprecipitated with a monoclonal flag (mouse) antibody or irrelevant mouse IgG as a control. Western Blot analysis revealed an interaction of RNF43 with PSF.

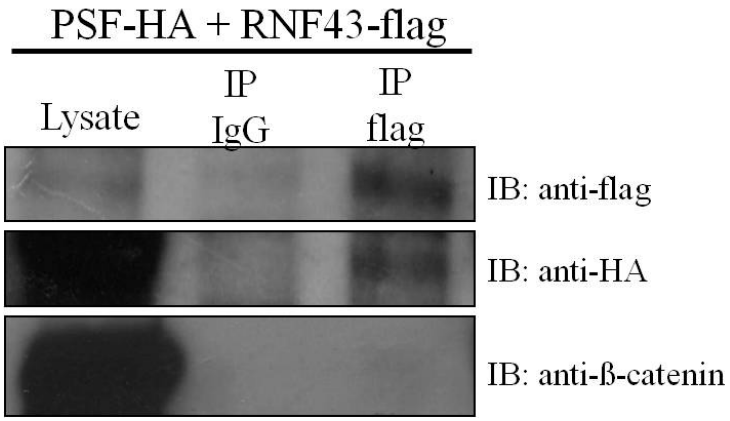

Figure 40 Association of RNF43 and PSF.
HCT116 cells were transfected with RNF43-flag and PSF-HA constructs. Whole cell lysates were subjected to Immunoprecipitation analysis with monoclonal flag antibody or mouse IgG as a control. The immunoprecipitates were analyzed by Western blot using the indicated antibodies.

As illustrated in Figure 40, PSF was detectable in precipitates of RNF43-flag (but not in the negative control) in Co-IP experiments. In contrast, ß-catenin was never observed to associate with RNF43. The same results were obtained upon Co-IP of PSF-HA with mutant RNF43 (data not shown).

Thus, the interaction of RNF43 with PSF, which was suggested by Miyamoto et al. (Miyamoto, Sakurai et al. 2008) could be confirmed during this study.

Since in addition to the nuclear rim staining of RNF43 very small amounts of RNF43 were also occasionally detected inside the nucleoplasm, and since PSF localized to the nuclear membrane as well as to the nucleoplasm, it remains elusive whether RNF43 and PSF interact at the nuclear membrane or inside the nucleoplasm.

In order to examine a possible effect of PSF on the canonical Wnt signaling activity, TOP/FOP Luciferase reporter assays were performed in HEK293T cells. The Wnt signaling pathway was stimulated by co-transfection of a construct expressing Wnt1, and the levels of Tcf4-mediated transcription were determined (Figure 41).

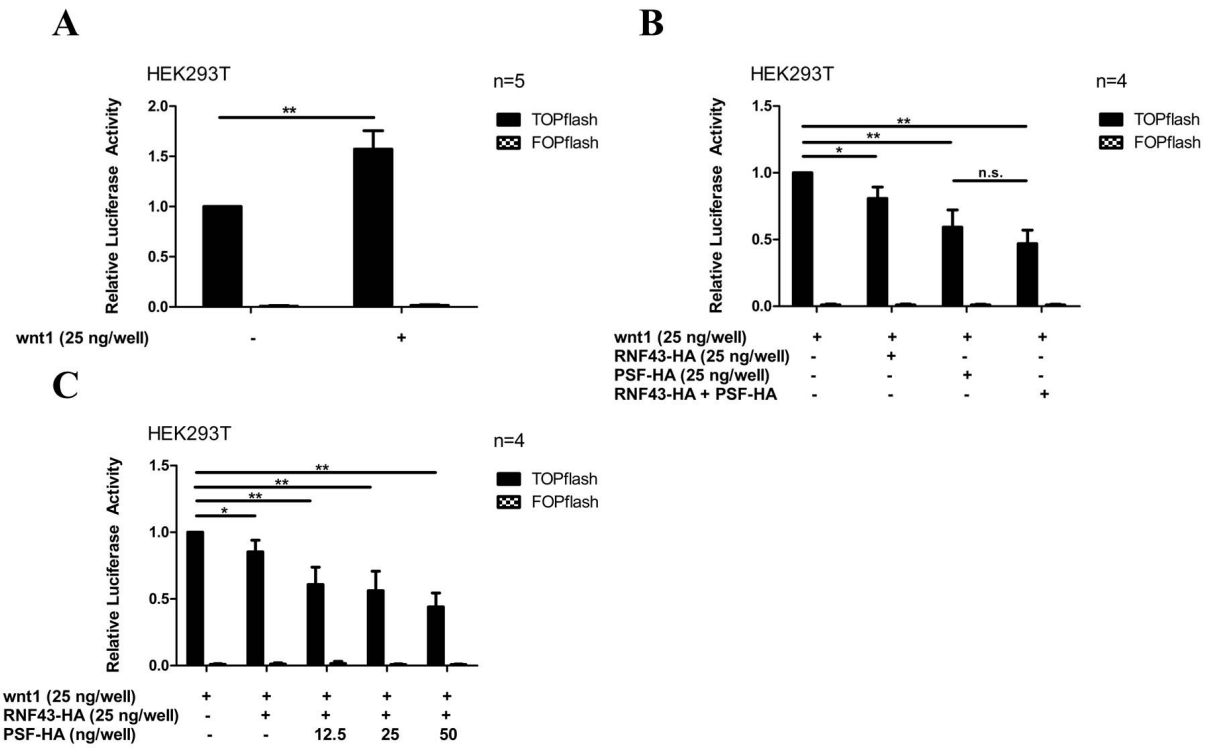

Figure 41 PSF inhibits Wnt1-induced Wnt signaling activity in HEK293T cells.
HEK293T cells were transfected with pTOPflash or the control pFOPflash reporter plasmids and the indicated amounts of constructs expressing RNF43-HA and PSF-HA. The Wnt signaling pathway was stimulated by co-transfection of a construct expressing Wnt1. Data were normalized to Renilla values as well as to (A) the control without Wnt1 or (B, C) the Wnt-transfected control without RNF43-flag and PSF-HA. Data are means + S.D. of four (B, C) or five (A) independent experiments.

As illustrated in Figure 41, co-transfection of 25 ng Wnt1 plasmid (per well) resulted in an increase in Wnt signaling activity of approximately 65 % (Figure 41A). Co-transfection of either RNF43-HA or PSF-HA decreased Tcf4-mediated transcription (Figure 41B), indicating a previously unidentified inhibitory effect on Wnt signaling activity not only of RNF43, but also of PSF. In addition, co-transfection of both RNF43-HA and PSF-HA together reduced Wnt signaling activity even further (Figure 41B). Thus, although not significant, there is a synergistic effect between RNF43 and PSF regarding the inhibition of Wnt signaling activity.

Co-transfection of increasing amounts of PSF-HA together with RNF43-HA resulted in a dose-dependent reduction of Wnt signaling activity (Figure 41C), indicating that PSF acts downstream of RNF43 in the Wnt signaling cascade, or together with RNF43.

Thus, PSF is a previously unknown inhibitor of the Wnt signaling pathway, which performs its function downstream or together with RNF43 and intensifies the inhibitory effect of RNF43 on Wnt signaling activity.

3.3.4 Interaction of RNF43 and Tcf4

RNF43 was described to be occasionally located in the nucleoplasm in a study of Sugiura et al. (Sugiura, Yamaguchi et al. 2008). These data could be confirmed by Immunofluorescence stainings during this study. Since RNF43 was shown to act downstream or at the level of ß-catenin (Figure 27, Figure 29), we next aimed to investigate whether RNF43 performs its function as a part of the TCF transcription complex, which is responsible for the transcription of Wnt target genes.

The existence of RNF43/Tcf4-complexes in mammalian cells was evidenced by Co-Immunoprecipitation analysis of RNF43 and endogenous Tcf4. Therefore, HCT116 cells were transfected with wildtype or mutant RNF43-HA constructs, and 48 h after transfection, whole cell lysates containing equal protein amounts were immunoprecipitated with a Tcf4 monoclonal antibody or irrelevant rabbit IgG as a control.

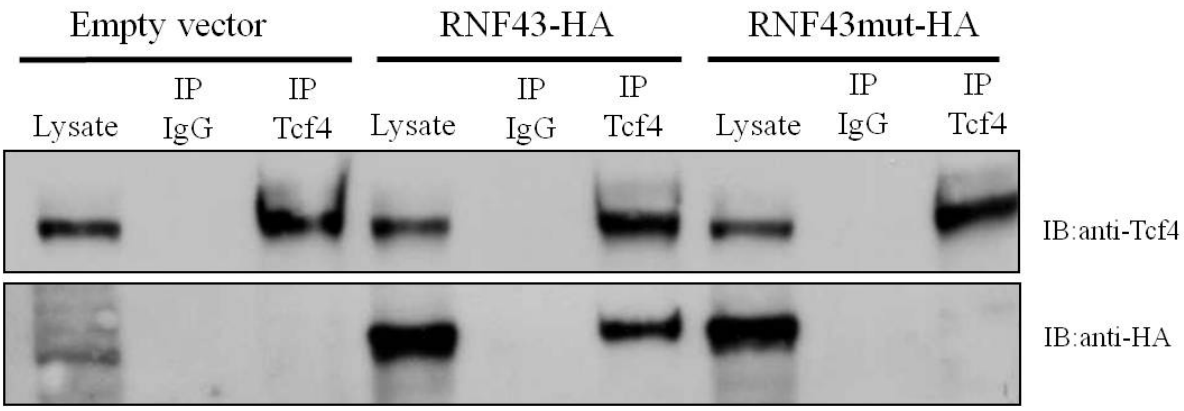

Figure 42 Association of Tcf4 and RNF43.
HCT116 cells were transfected with constructs expressing RNF43-HA and RNF43mut-HA as well as the empty vector and whole cell lysates were subjected to Immunoprecipitation analysis with monoclonal Tcf4 antibody or rabbit IgG as a control. The immunoprecipitates were analyzed by Western blot using the indicated antibodies.

Western blot analysis revealed a robust interaction between Tcf4 and wildtype RNF43 (Figure 42). In contrast, mutant RNF43 only very weakly co-immunoprecipitated with Tcf4 under the same conditions. The same results were obtained in DLD1 colon cancer cells (data not shown).

In order to confirm the results obtained by Co-Immunoprecipitations, the next aim was to investigate a putative colocalization of wildtype and mutant RNF43 and Tcf4 by Immunofluorescence stainings in HCT116 cells.

Therefore, HCT116 cells were transiently transfected with wildtype or mutant RNF43-flag and Tcf4-HA constructs, followed by IF stainings with anti-HA (mouse) and anti-flag (rabbit) antibodies as well as DAPI staining in order to visualize the nucleus. Images of planes of different depths within a single cell were taken.

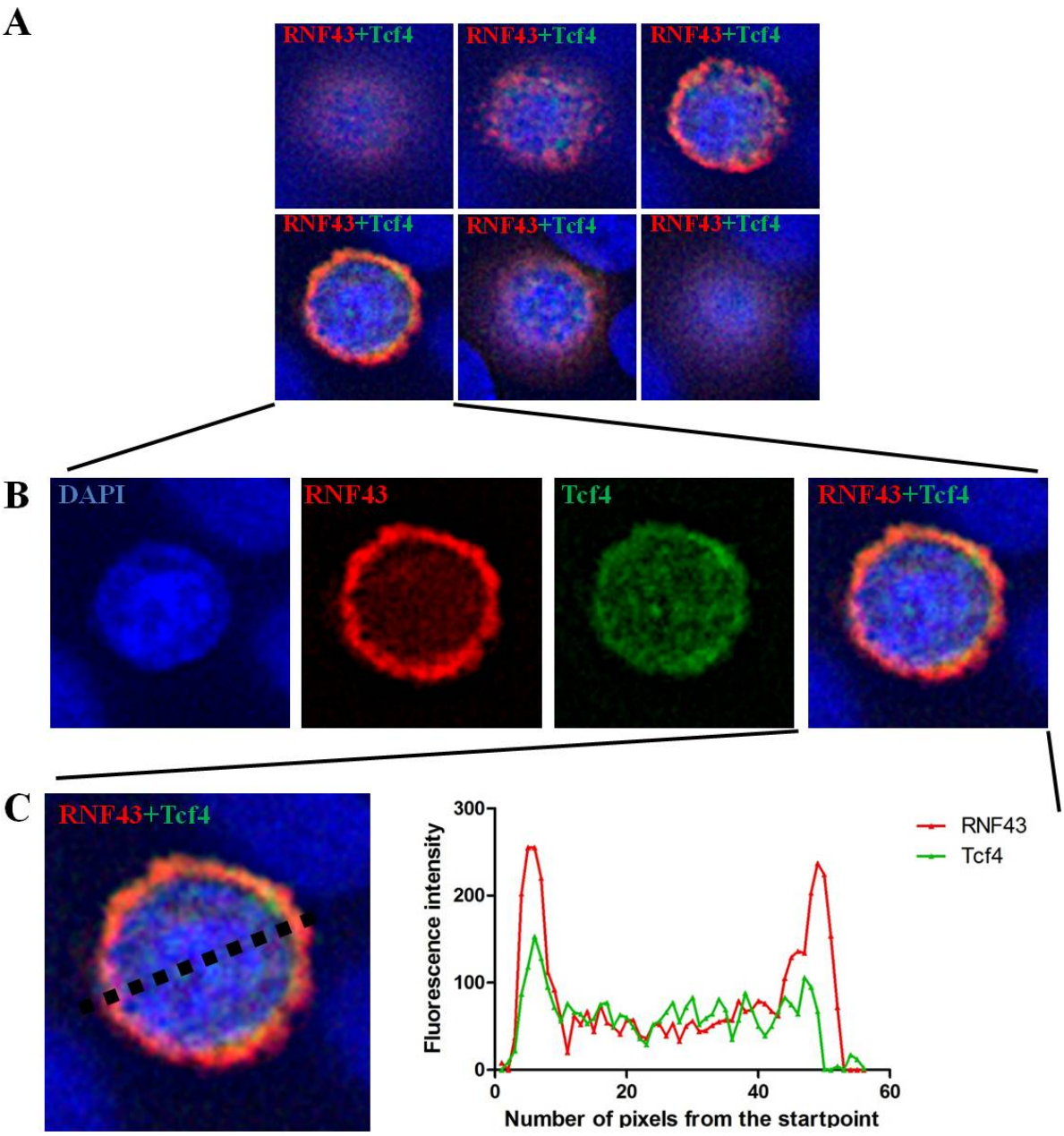

Figure 43 Overexpression of wildtype RNF43 and Tcf4 in HCT116 cells.
HCT116 cells were transiently transfected with RNF43-flag and Tcf4-HA constructs. Pictures of Immunofluorescence stainings illustrate DAPI (blue), anti-HA (green) and anti-flag (red) stainings. (A) Z-stack of one single cell transfected with both RNF43-flag and Tcf4-HA. (B) Magnification of a picture of the Z-stack illustrating the center of the nucleus of the cell. Single color channels are shown. (C) Illustration of the red and green fluorescence intensities of a cross section of the center of the nucleus.

As illustrated in Figure 43, wildtype RNF43 mainly localized to the nuclear rim, but small amounts were also detectable inside the nucleoplasm. Tcf4 mainly resided in small punctuate structures in the nucleoplasm, but small amounts of Tcf4 also localized to the nuclear membrane.

Therefore, only a slight colocalization of the two proteins was visible in Immunofluorescence microcopy pictures. Nevertheless, although large amounts of RNF43 were found at the nuclear rim, small amounts were also situated in the nucleoplasm. In addition, although the majority of Tcf4 was found inside the nucleoplasm, small amounts were detectable at the nuclear rim. Neither an interaction of RNF43 and Tcf4 inside the nucleoplasm, nor an interaction of the proteins at the nuclear membrane can be excluded. Thus, RNF43 may interact with Tcf4 either in the nucleoplasm or at the nuclear membrane.

Co-Immunofluorescence stainings of mutant RNF43 and Tcf4 are illustrated in Figure 44.

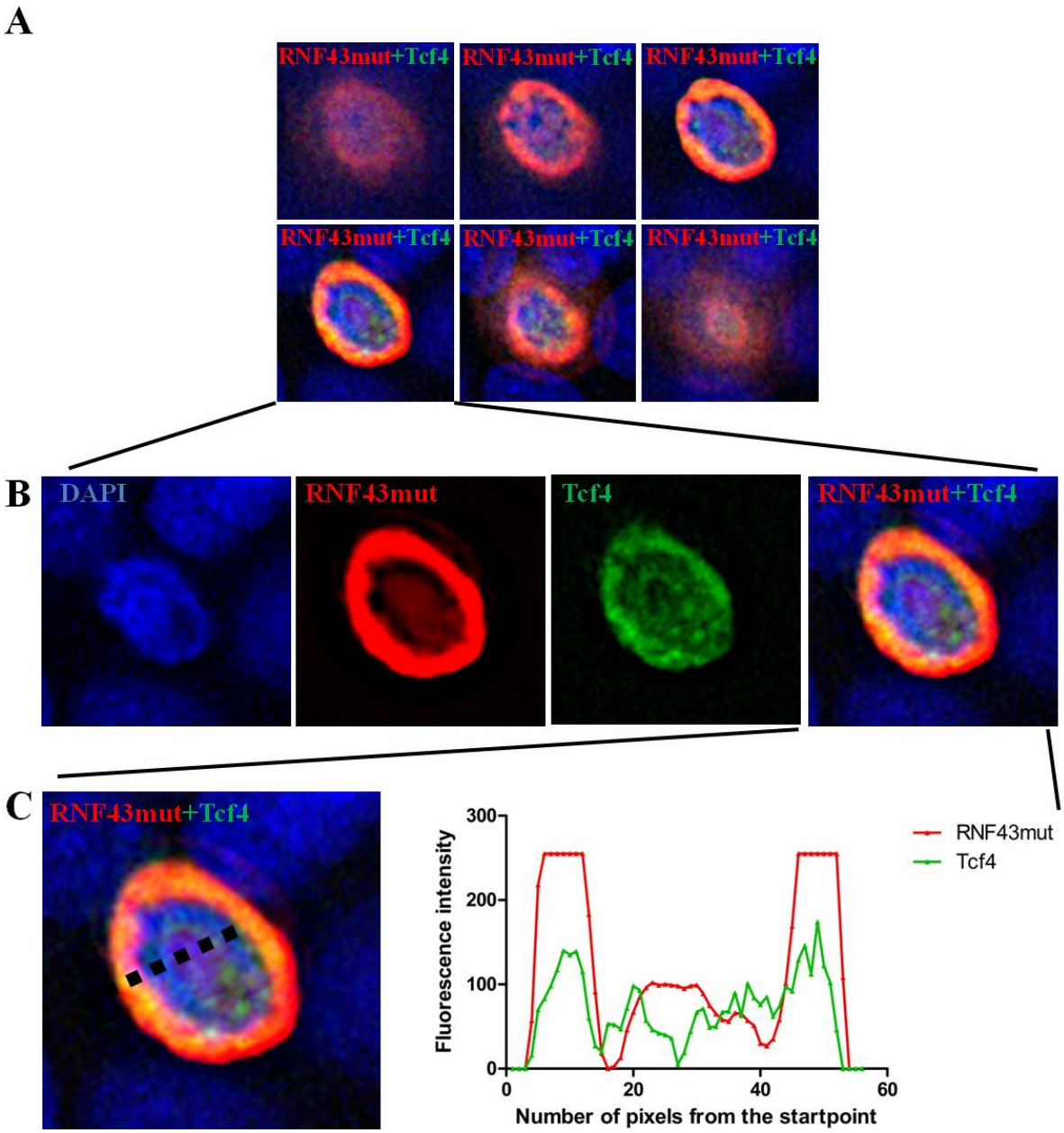

Figure 44 Overexpression of mutant RNF43 and Tcf4 in HCT116 cells.
HCT116 cells were transiently transfected with RNF43mut-flag and Tcf4-HA constructs. Pictures of Immunofluorescence stainings illustrate DAPI (blue), anti-HA (green) and anti-flag (red) stainings. (A) Z-stack of one single cell transfected with both RNF43mut-flag and Tcf4-HA. (B) Magnification of a picture of the Z-stack illustrating the center of the nucleus of the cell. Single color channels are shown. (C) Illustration of the red and green fluorescence intensities of a cross section of the center of the nucleus.

As illustrated in Figure 44, mutant RNF43 also exhibited a slight colocalization with Tcf4. Although only wildtype but not mutant RNF43 strongly co-immunoprecipitated with Tcf4, no differences of wildtype and mutant RNF43 could be observed regarding protein localizations. Like wildtype RNF43, mutant RNF43 slightly colocalized with Tcf4 in Co-Immunofluorescence stainings.

3.3.5 Interaction of RNF43 and CTBP

Since wildtype RNF43 was shown to interact with Tcf4, and Tcf4 is part of the transcription complex necessary for transcription of Wnt target genes, we next thought to investigate whether also other factors of the transcription complex are bound to wildtype or mutant RNF43.

Since TCF proteins have been shown to bind to C-terminal binding proteins (CTBP proteins), (Brannon, Brown et al. 1999; Valenta, Lukas et al. 2003; Hamada and Bienz 2004; Cuilliere-Dartigues, El-Bchiri et al. 2006), CTBP was assumed to possibly be another binding partner of RNF43 or RNF43mut.

CTBP is a protein that functions both as a gene-specific activator and as a repressor of the transcription of Wnt target genes. In the absence of Wnt signaling, it acts as a transcriptional co-repressor by binding to TCF or preventing ß-catenin from binding to TCF. In addition, the protein binds to enhancers and activates target gene expression in parallel with TCF upon Wnt stimulation. In this case, it is recruited to TCF binding sites or enhancers in a Wnt-dependent manner, where it increases ß-catenin transcriptional activation. Thus, CTBP both activates and represses Wnt target gene transcription (Fang, Li et al. 2006).

In order to determine whether wildtype and mutant RNF43 associate with CTBP, Co-Immunoprecipitation experiments were performed. Therefore, HCT116 cells and SW480 cells were transfected with constructs expressing wildtype or mutant RNF43-HA, or the empty vector as a control, and 48 h after incubation, whole cell lysates containing equal protein amounts were immunoprecipitated with a CTBP mouse (in HCT116 cells) or rabbit (in SW480 cells) antibody, or normal IgG as a control. The precipitated complexes were subjected to Western blot analysis with the indicated antibodies.

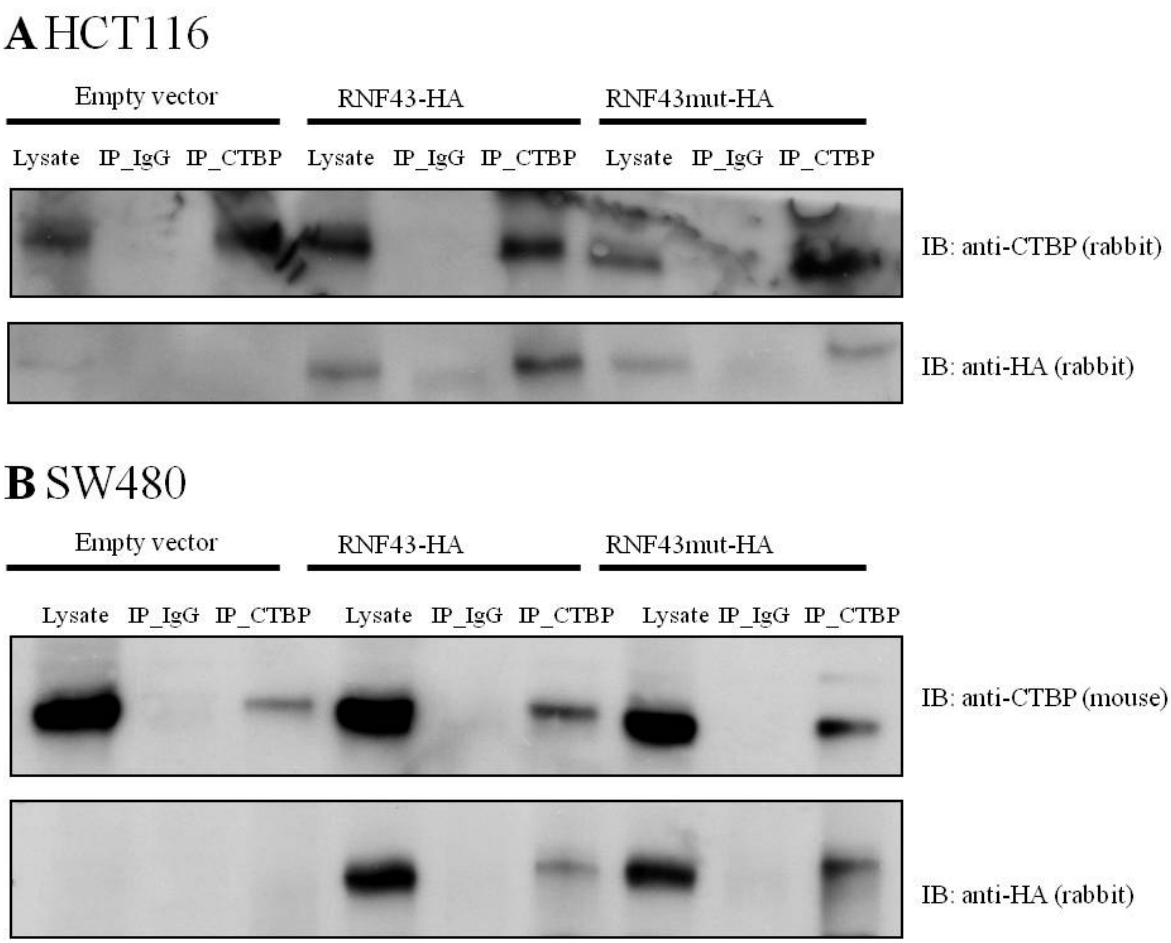

Figure 45 RNF43 and RNF43mut bind to CTBP.
(A) HCT116 cells and (B) SW480 cells were transfected with the indicated constructs expressing RNF43-HA, or the empty vector as a control. Whole cell lysates were subjected to Immunoprecipitation analysis with CTBP mouse (HCT116 cells) or rabbit (SW480 cells) antibody, or normal IgG as a control. The immunoprecipitates were analyzed by Western blot using the indicated antibodies.

In addition to the interaction of wildtype RNF43 and Tcf4, Co-Immunoprecipitation experiments revealed an interaction of wildtype RNF43 and CTBP (Figure 45). Similarly, in contrast to the only marginal binding of RNF43mut to Tcf4, a strong interaction of mutant RNF43 and CTBP was observed in HCT116 and SW480 colon cancer cells.

3.3.6 Effect of wildtype and mutant RNF43 on Tcf4 and CTBP proteins

RNF43 was shown to be a RING finger-dependent Ubiquitin E3-Ligase (Sugiura, Yamaguchi et al. 2008), suggesting that RNF43 ubiquitinates its specific target protein(s).

By ubiquitination, proteins can be marked for diverse fates (1.6). Upon monoubiquitination, target proteins can exhibit altered activities and signaling functions (reviewed in Pickart 2001). In contrast, upon multiubiquitination at K48 or K29, target proteins are typically

substrates for degradation by the proteasome (1.6). Chains of ubiquitin, which are linked through other lysine residues, like K63, represent distinct signals (reviewed in Pickart 2000).

In order to determine whether RNF43 is an Ubiquitin E3-Ligase that possibly mono- or polyubiquitinylates its interaction partners Tcf4 and CTBP, HCT116 cells were transfected with wildtype and mutant RNF43 constructs.

If RNF43 would multiubiquitinate Tcf4 or CTBP at K48 or K29, these proteins would be degraded by the proteasome, thus their protein levels would decrease upon ectopic expression of RNF43. If RNF43 would multiubiquitinate Tcf4 or CTBP at another lysine residue (K63), a smear would be detectable in Western blot analysis, which would be visible above the expected protein band. Monoubiquitination of Tcf4 or CTBP would result in an additional band in Western blot analysis, which would be 8 kDa larger than the band of the non-ubiquitinated protein.

As illustrated in Figure 46A, no changes in the protein levels of neither Tcf4 nor CTBP could be observed in Western blot analysis of whole cell extracts of HCT116 cells overexpressing wildtype or mutant RNF43. In addition, no smear or additional band above the Tcf4 or CTBP band could be observed upon ectopic expression of wildtype or mutant RNF43.

In order to exclude the possibility that the effect of RNF43 or RNF43mut overexpression on Tcf4 or CTBP protein levels was only marginal, the next aim was to block proteasomal degradation by inhibition of the proteasome. Inhibition of the proteasome would result in impaired degradation of proteins that are normally degraded by the proteasome. Thus, if either Tcf4 or CTBP would be marked for degradation by a chain of K48- or K29-linked ubiquitin residues by RNF43 or RNF43mut, treatment with the proteasome inhibitor would result in increased protein levels of these proteins and a higher molecular weight smear, detectable by Western blot analysis.

Therefore, wildtype and mutant RNF43 as well as the empty plasmid as a control were overexpressed in HCT116 cells and the proteasome was inhibited by treatment of the cells with the potent proteasome inhibitor MG132 (10 μM) for 12 h.

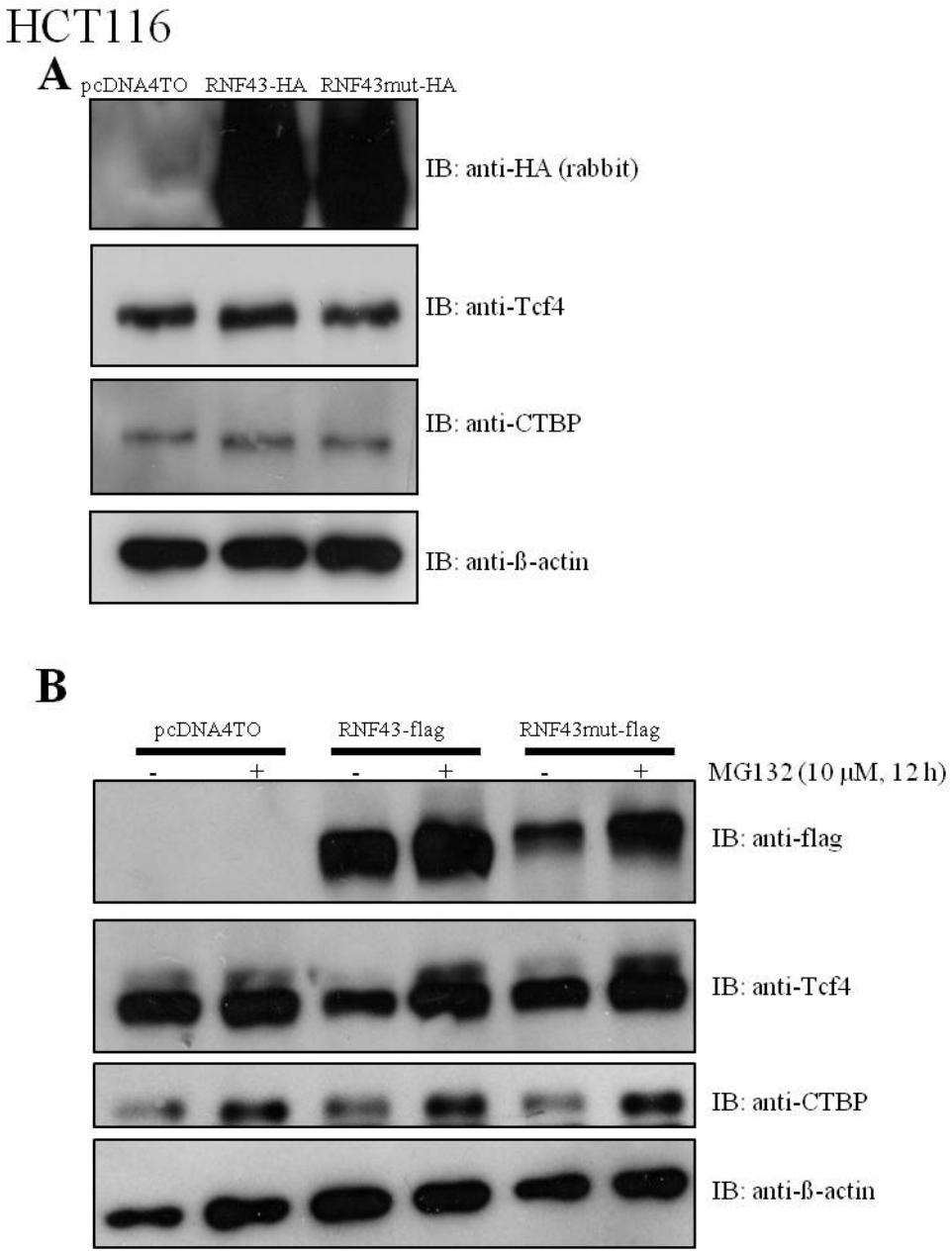

Figure 46 Effect of ectopic expression of wildtype and mutant RNF43 on Tcf4 and CTBP protein levels. (A) HCT116 cells were transfected with wildtype and mutant RNF43 as well as the empty vector as a control. (B) HCT116 cells were transfected with the empty vector, RNF43 or RNF43mut, followed by treatment with the proteasome inhibitor MG132 (10 µM) for 12 h. (A, B) Afterwards, cells were subjected to Western Blot analysis with the indicated antibodies. ß-actin was used as a loading control.

As visible in Figure 46A, no changes in the protein levels of Tcf4 or CTBP could be observed upon transfection of the cells with constructs expressing RNF43 or RNF43mut. Similarly, no higher molecular smears or bands were observed upon transfection of the cells with constructs expressing RNF43 or RNF43mut and additional treatment of the cells with MG132, as compared to the Tcf4 and CTBP bands upon transfection with the control plasmid and treatment with MG132 (Figure 46B).

Nevertheless, even in the sample transfected with the empty vector, treatment with MG132 resulted in elevated levels of Tcf4 and CTBP (Figure 46B), since both Tcf4 and CTBP are proteins that are degraded by the proteasomal pathway (Paliwal, Pande et al. 2006; Yamada 2006).

The double band which was visible in the Tcf4 blot (Figure 46B) represents post-translationally modified Tcf4, since Tcf4 is known to be a target of ubiquitination by NARF1 (Yamada 2006) as well as a target of sumoylation by PIAS family proteins (Yamamoto, Ihara et al. 2003).

In addition to the protein levels of Tcf4 and CTBP, which changed upon treatment with MG132, treatment of HCT116 cells overexpressing wildtype or mutant RNF43 with MG132 resulted in a profound increase in the protein levels of both wildtype and mutant RNF43 (Figure 46B). The same results were obtained in DLD1 colon cancer cells (Figure 47).

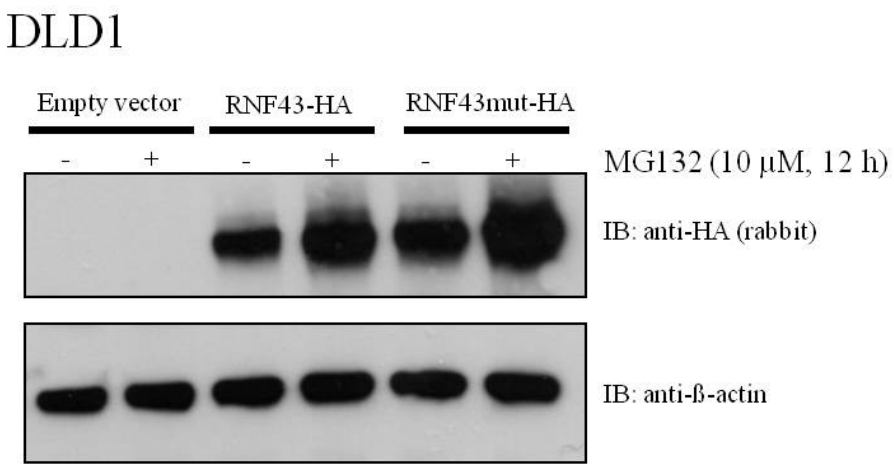

Figure 47 Wildtype and mutant RNF43 are subjected to proteasomal degradation.
DLD1 cells were transfected with the indicated plasmids pcDNA4TO, RNF43-HA and RNF43mut-HA. On the next day, cells were treated with the proteasome inhibitor MG132 (10 µM) for 12 h followed by Western blot analysis with the indicated antibodies.

As already observed in HCT116 cells (Figure 46), ectopic expression of RNF43 and RNF43mut followed by subsequent treatment of the cells with the proteasome inhibitor MG132 resulted in a strong increase in the protein levels of both wildtype and mutant RNF43 in DLD1 cells (Figure 47). Thus, both wildtype and mutant RNF43 are subjected to proteasomal degradation in the absence of MG132.

3.3.7 Autoubiquitination activity of RNF43

Autoubiquitination activity of RNF43 was observed by Sugiura et al. using an *E.coli* BL21 (DE3) strain (Sugiura, Yamaguchi et al. 2008). In order to investigate whether the autoubiquitination activity of RNF43 was also detectable in colon cancer cells, HCT116 colon cancer cells were co-transfected with wildtype or mutant RNF43-HA constructs and his-Ubiquitin. Cells were treated with the proteasome inhibitor MG132 (10 µM) for 12 h prior to cell lysis. 48 h after transfection, RNF43 and RNF43mut complexes were immunoprecipitated with an anti-HA (mouse) antibody or normal IgG as a control and the precipitated complexes were subjected to Western blot analysis with anti-His, anti-K63-linked polyubiquitin and anti-HA antibodies.

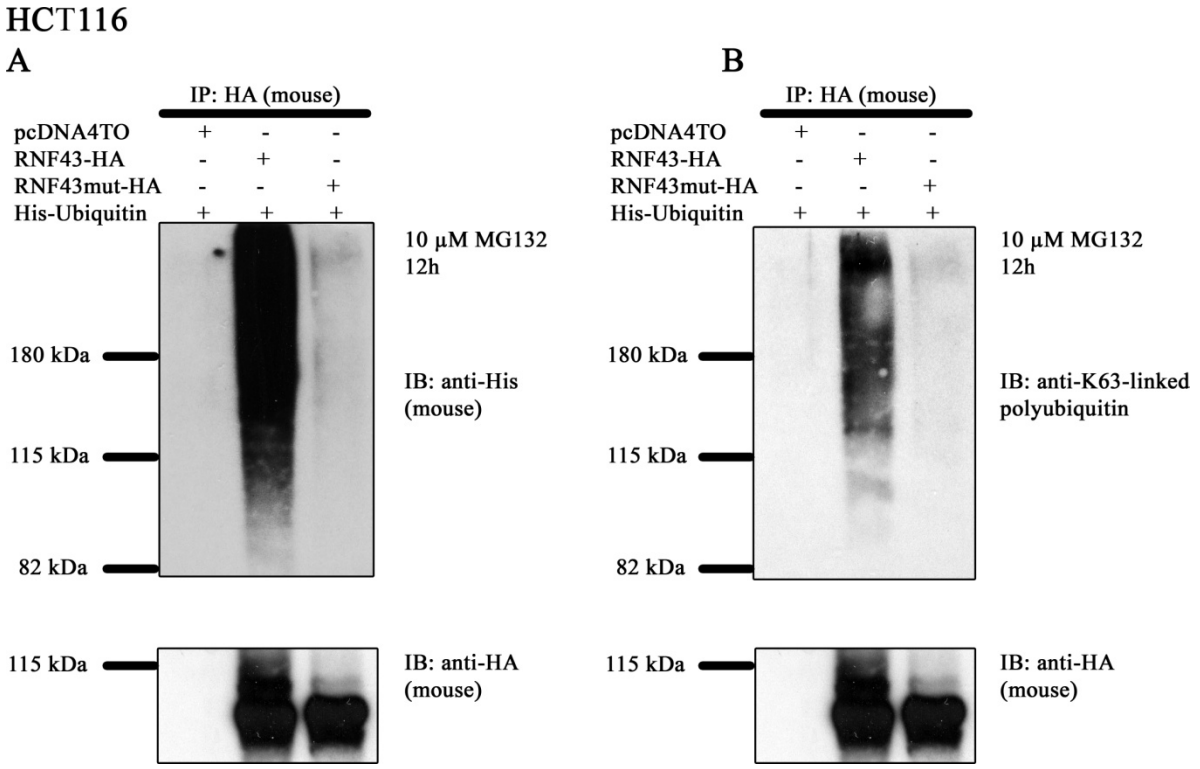

Figure 48 Analysis of RNF43 autoubiquitination.
HCT116 cells transfected with the RNF43-HA or RNF43mut-HA constructs as well as the empty vector. Cells were treated with 10 µM MG132 12 h prior to cell lysis. 48 h after transfection, whole cell lysates were generated and subjected to Immunoprecipitation with normal monoclonal anti-HA (mouse) antibody or mouse IgG as a control. The presence of polyubiquitin chains in precipitated complexes was determined by Western blot analysis with the indicated antibodies anti-his (mouse), anti-HA (mouse), and anti-K63-linked polyubiquitin (rabbit). The same membrane was used in (A) and (B).

As illustrated in Figure 48A, a high molecular smear, which represents polyubiquitinated forms of a protein, was detected for wildtype RNF43, but not for RNF43mut. Hence, wildtype RNF43 is subjected to autoubiquitination in HCT116 colon cancer cells. In contrast, mutant

RNF43, harboring inactivating mutations in the RING domain, did not exhibit autoubiquitination activity. Thus, a functional RING domain is essential for autoubiquitination of RNF43.

Additionally, K63-linked polyubiquitination, which is responsible for various biological functions other than proteasomal degradation, like regulatory purposes (1.6), was observed for wildtype RNF43 in Western blot analysis (Figure 48B).

In order to determine whether Tcf4 is a target protein of the Ubiquitin E3-Ligase RNF43 and thus ubiquitinated upon transfection of RNF43 or RNF43mut plasmids, ubiquitination assays were performed. Therefore, HCT116 colon cancer cells were co-transfected with Tcf4-HA as well as wildtype or mutant RNF43-flag and his-Ubiquitin constructs. Cells were treated with the proteasome inhibitor MG132 (10 µM) for 12 h prior to cell lysis. 48 h after transfection, Tcf4-HA complexes were immunoprecipitated and subjected to Western blot analysis with the indicated antibodies.

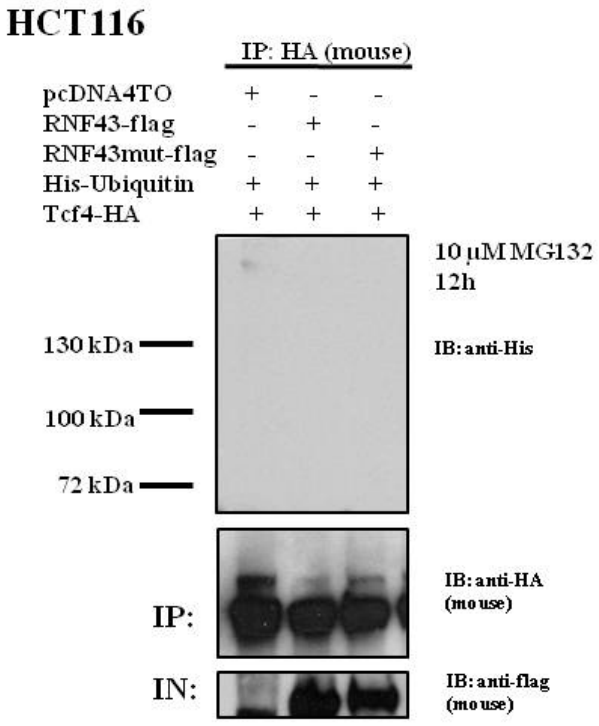

Figure 49 Analysis of Tcf4 ubiquitination.
HCT116 cells transfected with the RNF43-flag or RNF43mut-flag constructs as well as the empty vector. Cells were treated with 10 µM MG132 12 h prior to cell lysis. 48 h after transfection, whole cell lysates were generated and subjected to Immunoprecipitation with normal monoclonal anti-HA (mouse) antibody or mouse IgG as a control. The presence of polyubiquitin chains in precipitated complexes was determined by Western blot analysis with the indicated antibody anti-his (mouse). The presence of precipitated Tcf4-HA was proven by Western blot analysis with the indicated antibody anti-HA (mouse), and the presence of RNF43-flag and RNF43mut-flag in the transfected cells (input; IN; crude cell extract from HCT116 cells) was proven by Western blot analysis with the antibody anti-flag (mouse). One representative experiment is shown.

As illustrated in Figure 49, Tcf4 could never be shown to be ubiquitinated by RNF43. Upon precipitation of Tcf4-HA, no higher molecular smear above the Tcf4 band was detectable by the anti-His antibody in ubiquitination assays (Figure 49), as observed for wildtype RNF43 in autoubiquitination assays (Figure 48). Although no ubiquitination of Tcf4 was detectable, a higher molecular weight band was visible in the anti-HA blot, again indicating post-translational modification of Tcf4, as already observed (and described) in Figure 46.

Nevertheless, although Tcf4 could never be shown to be ubiquitinated by RNF43, the possibility that RNF43 ubiquitinates Tcf4 cannot be excluded. Tcf4 may possibly be ubiquitinated by RNF43, but the extent of ubiquitination may be low and thus below the Western blot detection limit. Similarly, only subsets of Tcf4 may possibly be ubiquitinated by RNF43. Therefore, further investigation using other methods will be necessary in order to investigate the ubiquitination of Tcf4 in detail.

3.3.8 The inhibitory effect of RNF43 on Wnt signaling activity is reversed by MG132

As shown in Figure 22, Wnt signaling activity in Cos7 cells can be induced by treatment with Lithium chloride. Subsequent transfection with constructs expressing RNF43 decreased Wnt signaling (Figure 24), and transfection with RNF43mut plasmids elevated Wnt signaling activity (Figure 25).

Although an interaction of RNF43 and Tcf4 as well as of RNF43 and CTBP could be detected, no ubiquitination of these proteins by RNF43 could be observed. Therefore, we next thought that another possible explanation for the negative effect of RNF43 on the Wnt signaling pathway could be that RNF43 possibly ubiquitinates a protein of the Wnt signaling pathway and therefore marks it for degradation. Since functional inactivation of the RING domain transactivates Wnt signaling, we thought that the target protein of RNF43 could possibly be an activator of the pathway.

In order to examine whether RNF43 ubiquitinates a positive regulator of the Wnt signaling pathway and marks it for degradation by the proteasome, TOP/FOP Luciferase reporter assays were performed and proteasomal degradation was inhibited by MG132. The effects of MG132 on the Wnt-inhibitory function of RNF43 as well as on the Wnt-transactivating function of RNF43mut were investigated (Figure 50).

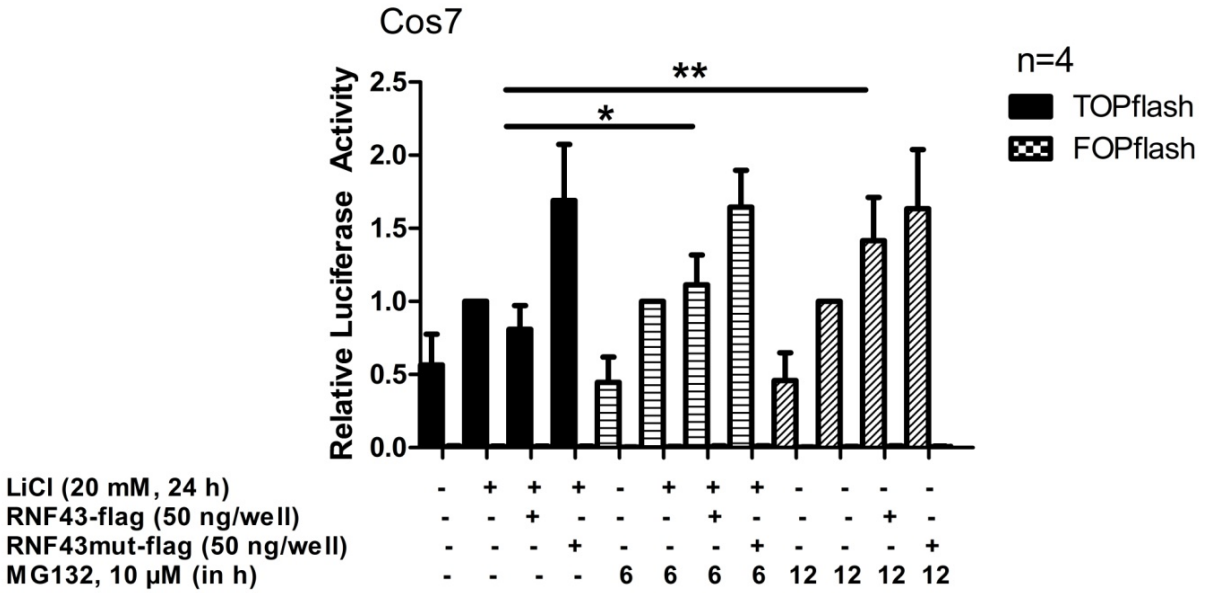

Figure 50 MG132 reverses the inhibitory effect of RNF43 in Cos7 cells.
Cos7 cells were transfected with pTOPflash or the control pFOPflash reporter plasmids and the indicated plasmids. Wnt signaling was induced by treatment with LiCl (20 mM, 24 h). Cells were treated with 10 µM MG132 for the indicated hours before cell lysis. Results were normalized to Renilla values and to LiCl induced controls without RNF43/RNF43mut. Data are means + S.D. of four independent experiments.

As illustrated in Figure 50, treatment with MG132 did not result in any alterations in the levels of TOPflash, FOPflash or Renilla values (data not shown). In contrast, treatment of RNF43-transfected Cos7 cells with MG132 significantly reversed the inhibitory effect of RNF43 on Wnt signaling after several hours, whereas the effect of RNF43mut on Wnt signaling did not significantly change upon treatment with MG132.

Thus, the inhibitory effect of RNF43 on Wnt signaling activity could be reversed by the proteasome inhibitor MG132 in a time-dependent manner, indicating that the function of RNF43 may possibly be to ubiquitinate an activator of the Wnt signaling pathway and hence mark it for degradation.

3.3.9 Effect of RNF43 on proliferation and cell growth

Since canonical Wnt signaling is known to stimulate proliferation (1.5), and since RNF43 is a strong negative regulator of the Wnt signaling pathway (Figure 24, Figure 26), the next aim was to investigate a possible effect of RNF43 on proliferation and cell growth. In addition, the effect of mutant RNF43, which was shown to strongly activate Wnt signaling (Figure 25), on proliferation and cell growth, was determined. Therefore, different methods were used.

3.3.9.1 Effect of knockdown of the *RNF43* gene

Knockdown of specific genes by transfection of small inhibitory RNAs (siRNAs) provides a valuable tool for studying gene functions. In order to investigate a possible effect of RNF43 on cell growth and Wnt signaling activity, *RNF43* gene expression should be knocked down in HT29 cells, which is the only cell line expressing RNF43 mRNA to a greater extent than all the other colon cancer cell lines investigated.

Therefore, three independent single strand siRNA oligonucleotides, designed to target the *RNF43* gene (OriGene), were used. They were referred to as siRNAs A, B and C, and their sequences are listed in 2.2.3.6. The siRNA sequences A and B are located approximately 150 and 300 bp upstream of the start codon ATG, and the siRNA sequence C is located approximately 350 bp downstream of the stop codon TGA in the RNF43 mRNA sequence.

The effectiveness of the three siRNA oligos was investigated by RT-PCR. Therefore, HT29 colon cancer cells were seeded in 6-well plates and on the next day, they were transfected with either control siRNA or different combinations of RNF43 siRNAs (final concentration: 10 nM) for 48 h (as described in 2.2.3.6). 48 h after transfection, mRNA extraction and cDNA synthesis were performed and endogenous RNF43 mRNA levels were subsequently determined by RT-PCR analysis. The effect of the siRNAs and siRNA combinations on *RNF43* gene expression is illustrated in Figure 51.

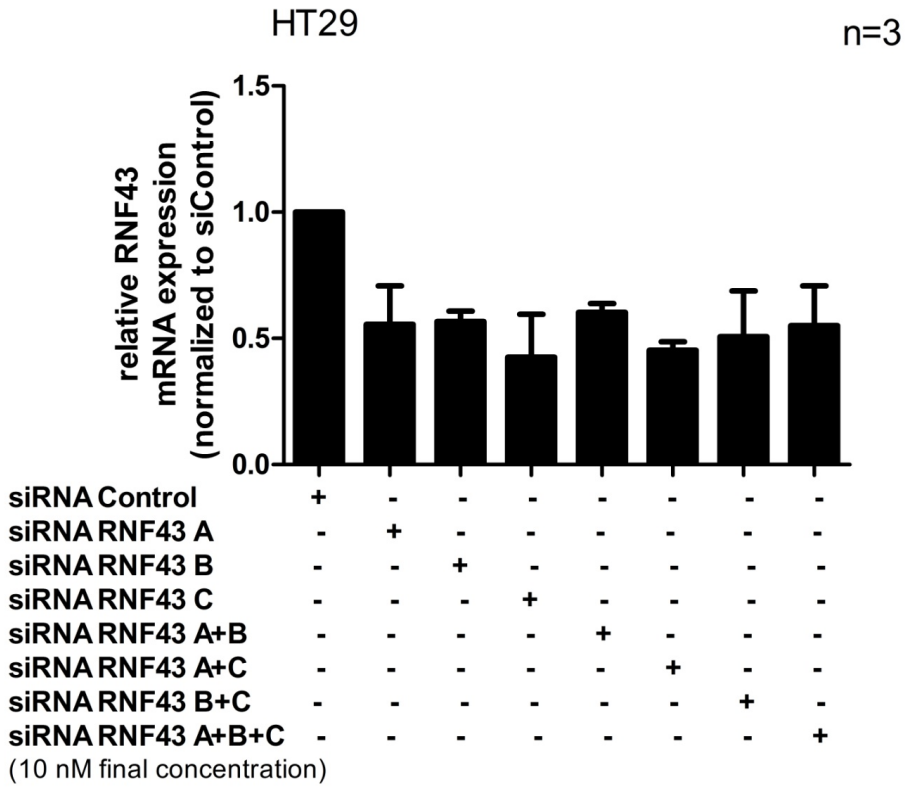

Figure 51 siRNA-mediated knockdown of *RNF43* gene expression.
RNF43 mRNA expression levels in HT29 cells upon transfection with control siRNA as well as upon transfection with different combinations of the three siRNA oligos A, B and C targeting *RNF43*. A final siRNA concentration of 10 nM was used. Data were normalized to RNF43 mRNA expression of HT29 cells transfected with control siRNA. Data are means + S.D. of three independent experiments.

Within the set of single stranded siRNA oligos, all three could knock down *RNF43* gene expression, but with different efficiencies. A knockdown of *RNF43* gene expression of approximately 50 % was observed in RNF43 siRNA transfected HT29 cells as compared to control siRNA transfected HT29 cells. Transfection of cells with a combination of the siRNA oligos A and C was the most effective and resulted in the strongest reduction of *RNF43* gene expression of approximately 55 %. Hence, all subsequent RNF43 knockdown experiments were carried out using a combination of RNF43 siRNAs A and C.

In order to investigate whether higher amounts of siRNA would result in a higher knockdown of *RNF43* gene expression, the final siRNA concentration was increased from 10 nM to 20 nM. Furthermore, the time between transfection and lysis was increased to 72 h (instead of 48 h). As visible in Figure 52, a higher final siRNA concentration and a longer transfection time resulted in an increase in siRNA-mediated knockdown of *RNF43* gene expression.

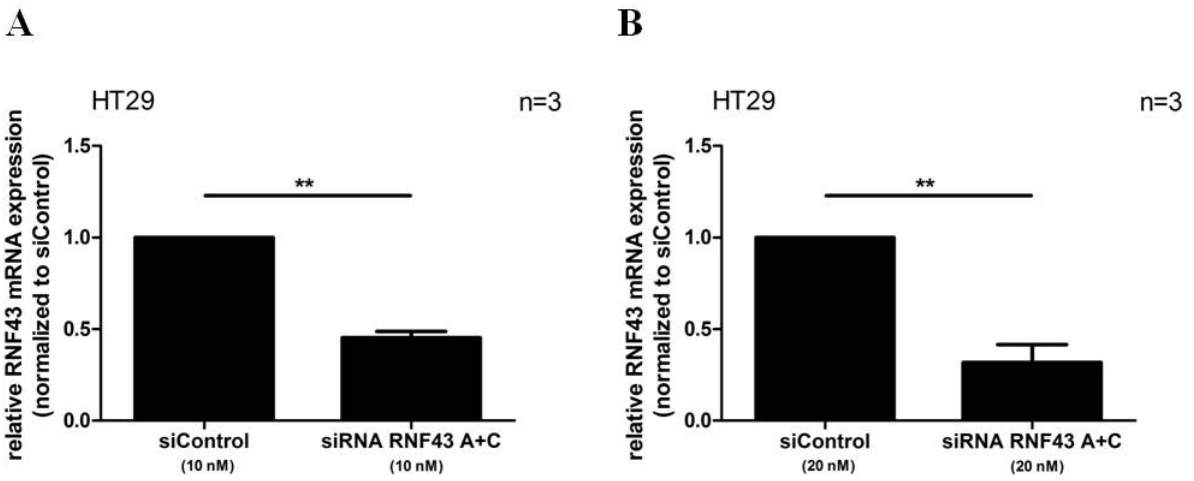

Figure 52 Effect of increase of final siRNA concentration and transfection time on siRNA-mediated knockdown of *RNF43* gene expression.
RNF43 mRNA expression levels in HT29 cells upon transfection with control siRNA or upon transfection with a combination of siRNAs A and C targeting *RNF43*. (A) A final siRNA concentration of 10 nM and a transfection time of 48 h were used. (B) A final siRNA concentration of 20 nM and a transfection time of 72 h were used. Data were normalized to RNF43 mRNA expression of HT29 cells transfected with control siRNA. Data are means + S.D. of three independent experiments.

As illustrated in Figure 52, knockdown of *RNF43* gene expression could be increased in HT29 cells upon elevation of the final siRNA concentration and transfection time. Transfection of HT29 cells with a final siRNA concentration of 20 nM for 72 h resulted in a reduction of *RNF43* gene expression of approximately 69 %. Hence, all subsequent RNF43 knockdown experiments were carried out using a final siRNA concentration of 20 nM and a transfection time of 72 h.

As shown in Figure 53, the knockdown of *RNF43* gene expression also strongly affected RNF43 protein levels.

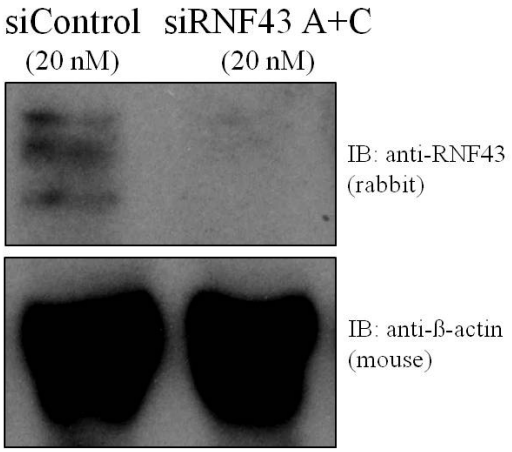

Figure 53 Effect of siRNA-mediated knockdown of *RNF43* gene expression on RNF43 protein levels.
RNF43 protein levels upon transfection with control siRNA as well as upon transfection with RNF43 siRNA oligos A+C targeting *RNF43* in HT29 cells. Cells were transfected with a final siRNA concentration of 20 nM for 72 h, followed by cell lysis and subsequent Western blot analysis with the indicated antibodies.

As visible in Figure 53, there was a strong effect of RNF43 siRNA transfection on RNF43 protein levels in HT29 colon cancer cells. Transfection of RNF43 siRNA oligos A+C resulted in a strong decrease in RNF43 protein levels. While several isoforms of RNF43 were clearly detectable upon transfection of control siRNA, only traces of RNF43 protein were detectable upon transfection of RNF43 siRNA.

Thus, transfection of HT29 cells with RNF43 siRNA not only resulted in a decrease in RNF43 mRNA levels, but also in a substantial reduction of RNF43 protein levels.

The HT29 colon cancer cell line was the only cell line expressing RNF43 mRNA to a greater extent (Figure 19) and by transfection with a combination of RNF43 siRNA oligonucleotides A and C, a decrease of *RNF43* gene expression of approximately 69 % was obtained (Figure 52). Furthermore, RNF43 protein levels were greatly reduced (Figure 53).

Therefore, HT29 cells were used to study the effect of RNF43 on proliferation and Wnt signaling activity by siRNA-mediated knockdown of *RNF43*.

For proliferation assays, HT29 colon cancer cells were seeded in 48-well plates and on the next day, they were transfected with either control siRNA or a combination of RNF43 siRNA oligos A+C for 72 h (as described in 2.2.3.6.). 72 h after transfection, proliferation rates were determined as described in section 2.2.9. In order to determine the effect of knockdown of *RNF43* gene expression on Wnt signaling activity, TOP/FOP Luciferase reporter assays were performed. Therefore, HT29 colon cancer cells were seeded in 24-well plates and on the next

day, they were transfected with pTOPflash or pFOPflash and Renilla plasmids (as described in 2.2.5). On the next day, cells were transfected with either control siRNA or a combination of RNF43 siRNA oligos A+C for 72 h (as described in 2.2.3.6.). 72 h after transfection with siRNAs, Wnt signaling activities were measured as described in section 2.2.5.

The effect of transfection of HT29 cells with siRNA on proliferation and Wnt signaling activity is illustrated in Figure 54.

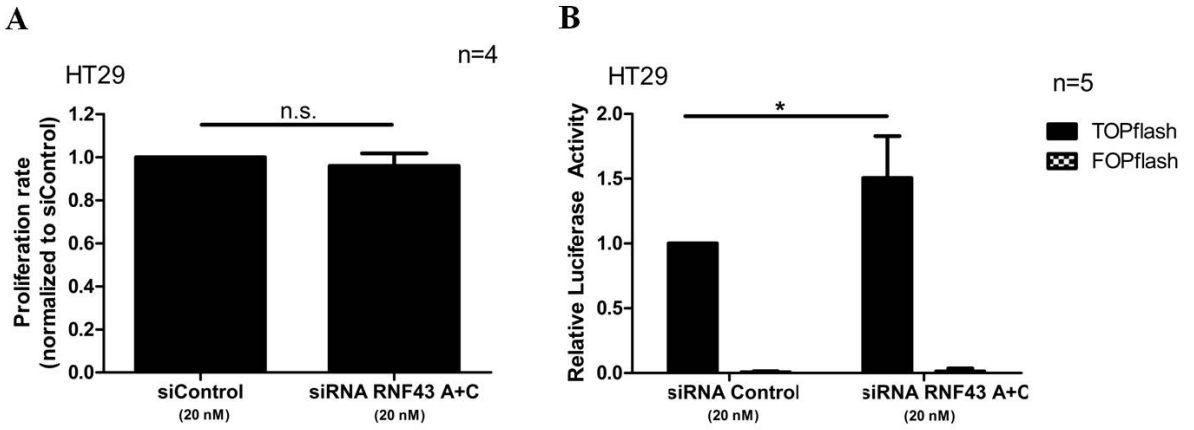

Figure 54 Effect of knockdown of *RNF43* gene expression on proliferation rate and Wnt signaling activity of HT29 cells.
(A) Effect of knockdown of *RNF43* gene expression on the proliferation rate. HT29 cells were transfected with 20 nM RNF43 siRNA or control siRNA 72 h before cell lysis and determination of the proliferation rate. Data were normalized to HT29 cells transfected with control siRNA. Data are means + S.D. of four independent experiments. (B) Effect of knockdown of *RNF43* gene expression on the Wnt signaling activity of HT29 cells. Wnt signaling activity was determined by TOP/FOP Luciferase reporter assays. HT29 cells were transfected with pTOPflash or the control pFOPflash reporter plasmids as well as the indicated siRNAs for 72 h. Results were normalized to Renilla values and to the sample transfected with control siRNA. Data are means + S.D. of five independent experiments.

As illustrated in Figure 54A, the proliferation rate of HT29 cells was not changed upon transfection with siRNA targeting the *RNF43* gene. HT29 cells transfected with RNF43 siRNA exhibited the same proliferation rate like HT29 cells transfected with control siRNA. Thus, although transfection of HT29 cells with RNF43 siRNA significantly decreased RNF43 mRNA and protein levels, no effects on proliferation rates were observed.

In contrast, siRNA-mediated knockdown of *RNF43* gene expression resulted in a significant increase in Wnt signaling activity of approximately 50 % in HT29 cells (Figure 54B), supporting the data showing that RNF43 negatively regulates Wnt signaling activity (3.2).

3.3.9.2 Effect of RNF43 ectopic expression on proliferation rates

Since knockdown of RNF43 did not affect proliferation rates, the next aim was to study the effect of ectopic expression of RNF43 and RNF43mut on proliferation. Therefore, HCT116 and Cos7 cells were used, since transfection efficiencies were very high in these cell lines. HCT116 and Cos7 cells were seeded in 96-well plated, transfected with RNF43-flag, RNF43mut-flag or the empty vector as described in 2.2.9, and proliferation rates were determined 48 h after transfections. The effect of ectopic expression of wildtype and mutant RNF43-flag on proliferation rates are illustrated in Figure 55.

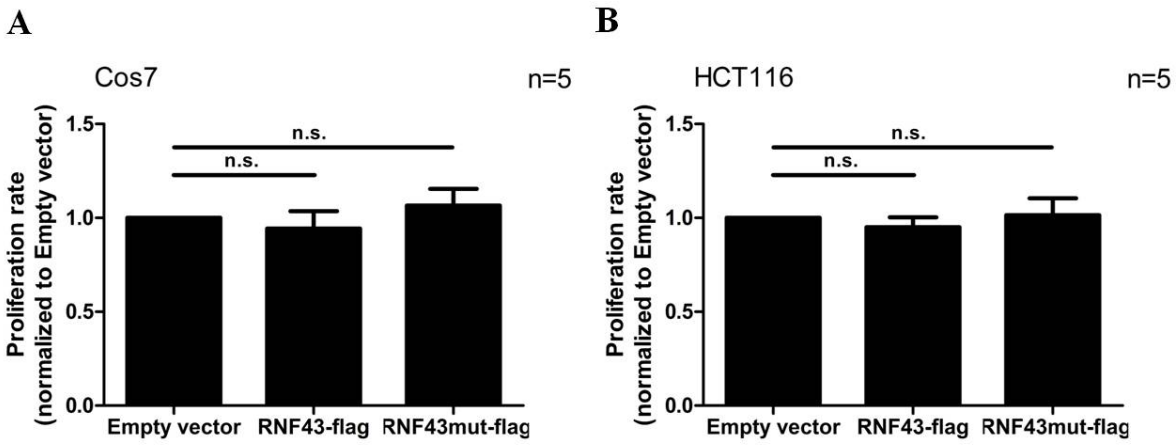

Figure 55 Effect of ectopic expression of wildtype and mutant RNF43 on proliferation rates.
Effects of overexpression of wildtype and mutant RNF43-flag as well as the empty vector on proliferation rates of (A) Cos7 and (B) HCT116 cells. Cells were transfected with the indicated constructs. 48 h after transfection, proliferation was measured. Data were normalized to proliferation of cells transfected with the empty vector. Data are means + S.D. of five independent experiments.

As illustrated in Figure 55, transfection of HCT116 and Cos7 cells with wildtype and mutant RNF43 did not result in a significant effect on proliferation rates of both cell lines. Proliferation was slightly decreased upon transient transfection with wildtype RNF43, but the effect was only marginal and insignificant. Proliferation upon transient transfection with mutant RNF43 resulted in a very little increase in proliferation. Again, the effect was only marginal and insignificant.

Thus, ectopic expression of neither wildtype nor mutant RNF43 significantly altered the proliferation rates of HCT116 and Cos7 cells.

3.3.9.3 Effect of wildtype and mutant RNF43 on colony formation ability

In order to explore the effects of overexpression of wildtype and mutant RNF43 on cell growth and viability, *in vitro* colony formation assays were conducted. Therefore, HCT116 cells were transfected with RNF43-flag, RNF43mut-flag and pcDNA4TO+Venus, as described in 2.2.12. The Zeocin resistance gene of the pcDNA4TO plasmid allowed the specific selection of transfected cells. Thus, following transfection, stable transfectants were selected for 2 weeks with Zeocin™. Following the selection period, cell colonies were stained with MTT, as described in 2.2.12. The experiment was performed three times. Images of one representative experiment are illustrated in Figure 56A.

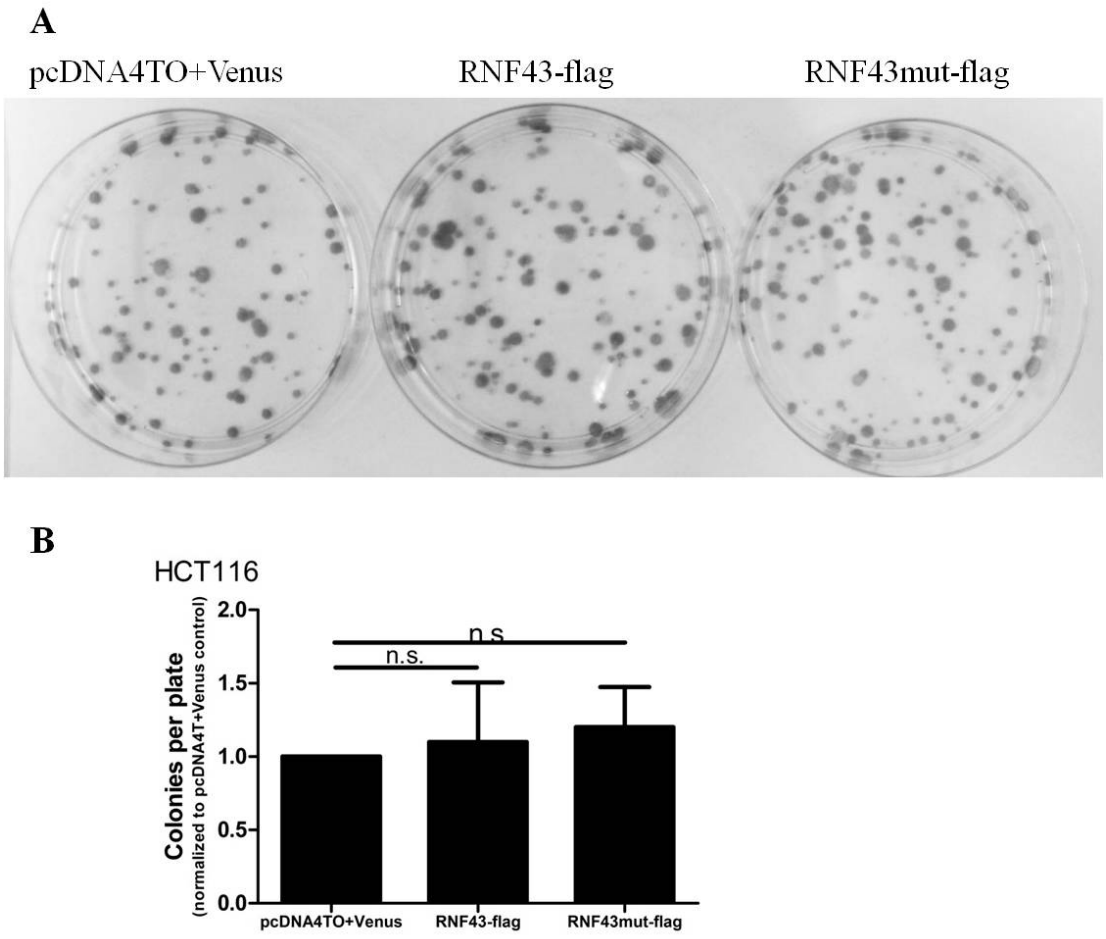

Figure 56 Effect of wildtype and mutant RNF43 on colony formation.
Colony formation assays were performed in HCT116 cells transfected with wildtype and mutant RNF43 followed by selection of transfected clones using Zeocin™. Colonies were stained using MTT. pcDNA4TO+Venus transfected cells were used as a control. (A) Images of one representative colony formation assay of three independent experiments. (B) Average numbers of colonies of three independent experiments. Results were normalized to colony numbers of pcDNA4TO+Venus transfected cells. Data represent the means + S.D. of three independent experiments.

As illustrated in Figure 56A, the number of colonies obtained from cells stably overexpressing wildtype or mutant RNF43 as compared to the number of colonies obtained from cells expressing a control plasmid did not significantly differ. In order to allow quantification of the data, three independent experiments were performed, and the combined data are shown in Figure 56B. No significant differences in the colony formation abilities were observed, neither between wildtype and mutant RNF43 transfected cells, nor between cells transfected with RNF43/RNF43mut and the control plasmid.

Thus, neither wildtype nor mutant RNF43 overexpression significantly decreased or increased cell growth and/or viability in *in vitro* colony formation assays.

3.4 Analysis of RNF43 deletion mutants

In order to study the functions of different parts of wildtype and mutant RNF43 proteins regarding their effects on Wnt signaling activity as well as their subcellular localizations, wildtype and mutant deletion mutants were generated.

For generation of RNF43 deletion mutants, the DNA sequence was obtained from NCBI (GENE ID: 54894 RNF43, NM_017763.4). The start codon ATG was inserted into each forward primer. In addition, all forward and reverse primers contained a restriction site, allowing the cloning of the amplified PCR products into the expression vector (2.1.8).

The deletion mutants lacking amino acids 1 - 244 of the full length protein (783 aa), termed RNF43(245-783) and RNF43mut(245-783), were generated during the master thesis project of Esther Wehrle (Wehrle 2010). The constructs harbor a C-terminal flag-tag for specific detection of the expressed constructs by Western blot analysis (Figure 57).

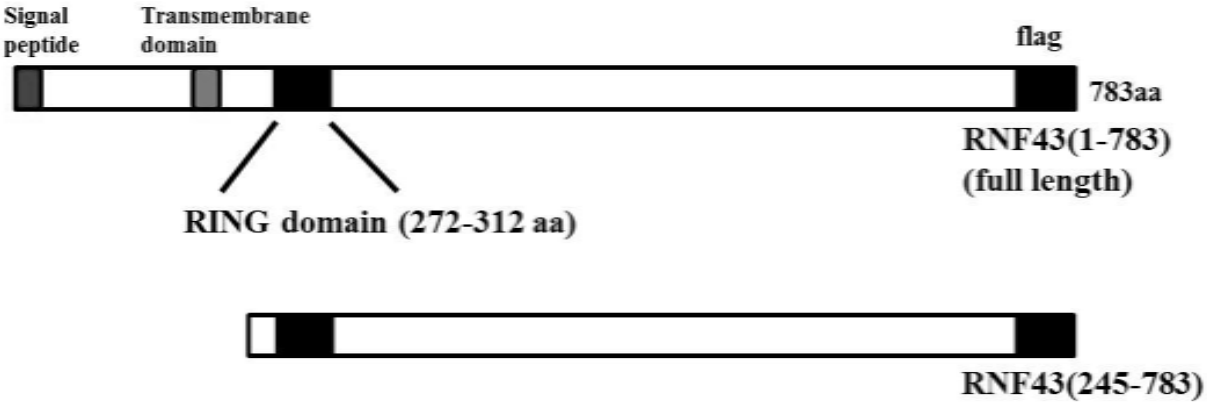

Figure 57 Scheme of the N-terminally truncated deletion mutant RNF43(245-783).

The expression of the constructs cloned by Esther Wehrle was verified during her work (Wehrle 2010). In order to determine whether the deletion of amino acids 1 - 244 leads to alterations in subcellular localizations of the proteins, Immunofluorescence stainings were performed.

Therefore, SW480, HCT116 and Cos7 cells were transiently transfected with RNF43(245-783) and RNF43mut(245-783) constructs, followed by Immunofluorescence co-stainings using the antibodies mentioned in the figure legend (Figure 58).

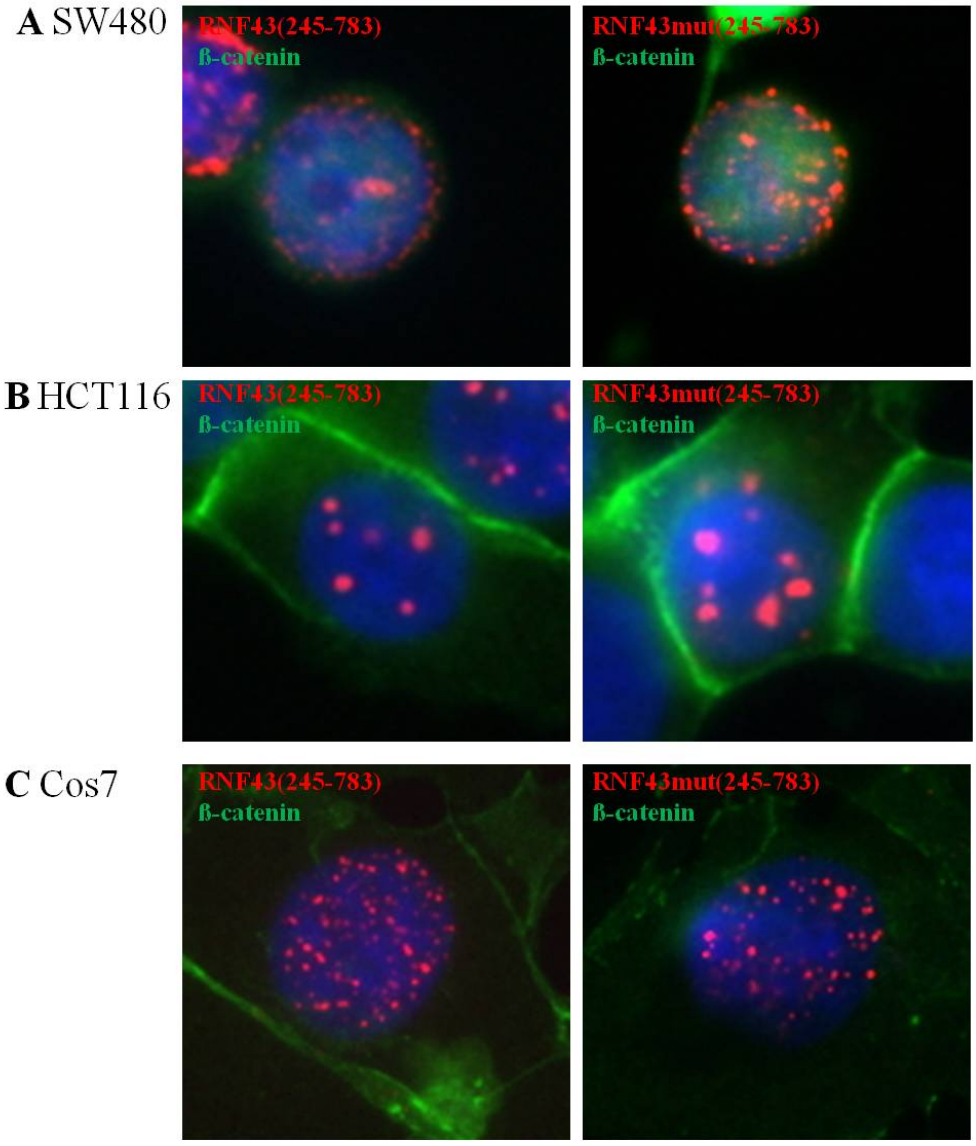

Figure 58 Immunofluorescence co-stainings of wildtype and mutant RNF43(245-783) N-terminal deletion mutants.
Immunofluorescence co-stainings of wildtype and mutant RNF43(245-783) and endogenous ß-catenin in (A) SW480, (B) HCT116 cells and (C) Cos7 cells. Cells were transiently transfected with wildtype or mutant RNF43(245-783) flag-tagged constructs. Pictures of Immunofluorescence stainings illustrate DAPI (blue), anti-flag (rabbit, red) and anti-ß-catenin (mouse, green) stainings.

As already observed by the master students working on RNF43 in our lab (Miriam Bognar (Bognar 2010), Esther Wehrle (Wehrle 2010) and Martina Grandl (Grandl 2011)), Immunofluorescence stainings of these constructs exhibited a strong expression of wildtype and mutant RNF43(245-783) in punctuate structures inside the nucleoplasm. Thus, since full length wildtype and mutant RNF43 mainly exhibited staining of the nuclear membrane with only very small protein amounts present in the nucleoplasm, there were substantial differences

in the localizations of full length RNF43 and RNF43(245-783) constructs. No differences between the localizations of wildtype and mutant RNF43(245-783) were observed.

In order to examine whether RNF43(245-783) and RNF43mut(245-783) deletion mutants also exhibit alterations in their functions as compared to full length proteins, TOP/FOP Luciferase reporter assays were performed in Cos7 cells. The Wnt signaling pathway was stimulated by LiCl treatment (20 mM, 24 h).

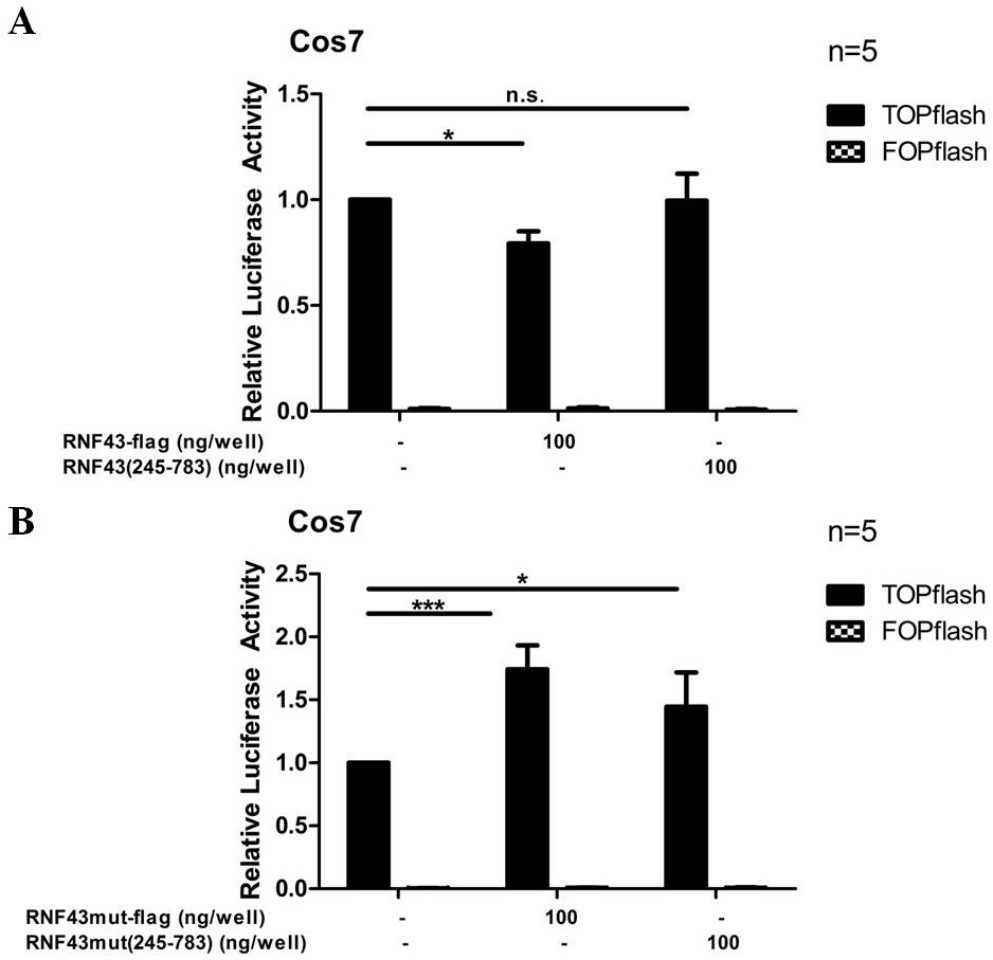

Figure 59 Effects of N-terminally truncated wildtype and mutant RNF43(245-783) on Wnt signaling activity.
Cos7 cells were transfected with pTOPflash or the control pFOPflash reporter plasmids and the indicated amounts of (A) RNF43-flag and RNF43(245-783) and (B) RNF43mut-flag and RNF43mut(245-783) plasmids. Wnt signaling was induced by LiCl (20 mM, 24 h). Results were normalized to Renilla values and to mock-transfected LiCl-induced cells. Data are means + S.D. of five independent experiments.

In contrast to the effect of full length RNF43, RNF43(245-783) did not result in a significant change of Wnt signaling activity. Nevertheless, transfection of the mutant construct, RNF43mut(245-783), still slightly increased Wnt signaling activity, although the activating effect was not as pronounced as the effect of full length RNF43mut.

Thus, the effect of wildtype RNF43 was completely reversed upon deletion of the amino acids 1 – 244. Since also mutant RNF43 exhibited markedly decreased function on Wnt signaling upon deletion of amino acids 1 - 244, as compared to the effects of mutant full length RNF43, these data indicate that the amino acids 1 - 244 of RNF43 are crucial for its function.

In order to study the specific region responsible for the change in the subcellular localization and ability of influencing Wnt signaling, further N-terminal deletion mutants lacking different parts of the N-terminus of RNF43/RNF43mut proteins were generated. In order to allow specific detection of the expressed constructs by antibodies used in Western blot analysis and Immunofluorescence stainings, each antisense primer included a sequence coding for a C-terminal flag-tag. The used primers are listed in 2.1.9.

The expression of the constructs was verified by Western Blot analysis, followed by characterization of the deletion mutants regarding their subcellular localization and their effect on Wnt signaling activity.

3.4.1 N-terminal deletion mutants

Several N-terminally truncated mutants of wildtype RNF43, as well as RNF43 mutated in the RING domain, were generated: RNF43(62-783), RNF43(121-783), RNF43(184-783), RNF43(229-783) and RNF43(245-783), as shown in Figure 60. All N-terminally truncated mutants still harbor a functional or non-functional RING domain, but the signal peptide is not present in these constructs, since it is located at the very N-terminus of the RNF43 sequence. The transmembrane membrane is still present in several constructs, which are RNF43(62-783), RNF43(121-783) and full length RNF43.

As described above, the RNF43(245-783) wildtype and mutant constructs were not generated during this work, but during the master thesis project of Esther Wehrle (Wehrle 2010).

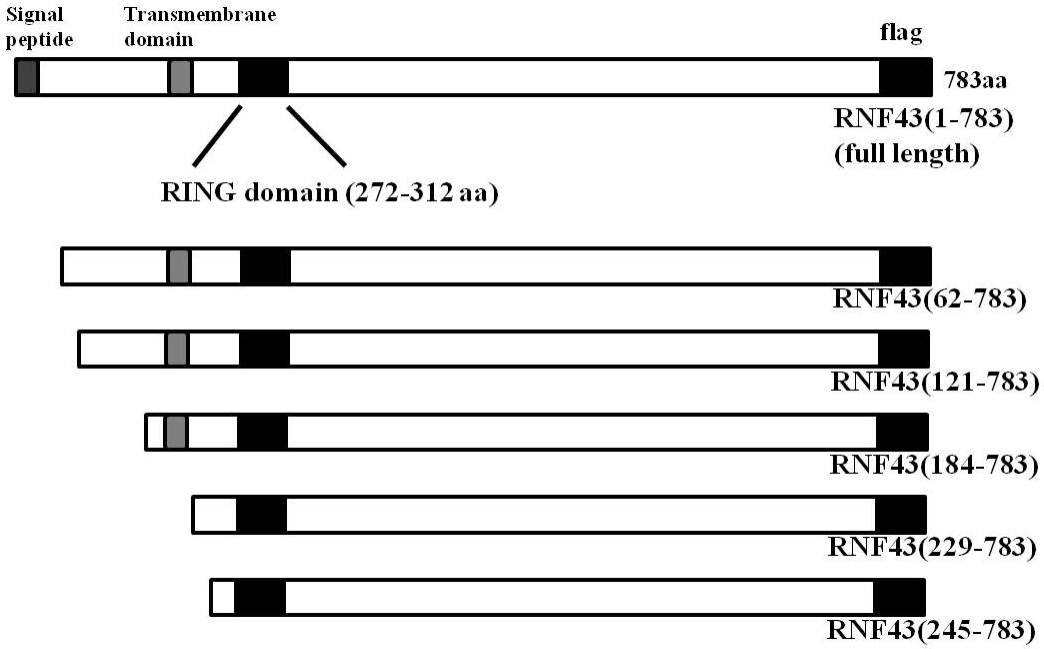

Figure 60 Scheme of the generated N-terminally truncated deletion mutants.

Expression of full length RNF43 and RNF43mut (which were generated by Markus Gerhard), and the N-terminal deletion mutants of RNF43 and RNF43mut, which were generated during this work, as well as the functionality of the attached C-terminal flag-tag, were investigated. Therefore, HCT116 cells were transiently transfected with the indicated constructs and 24 - 48 h after transfection, cell lysates were made, followed by Western blot analysis with an anti-flag antibody. ß-actin was used as an internal loading control.

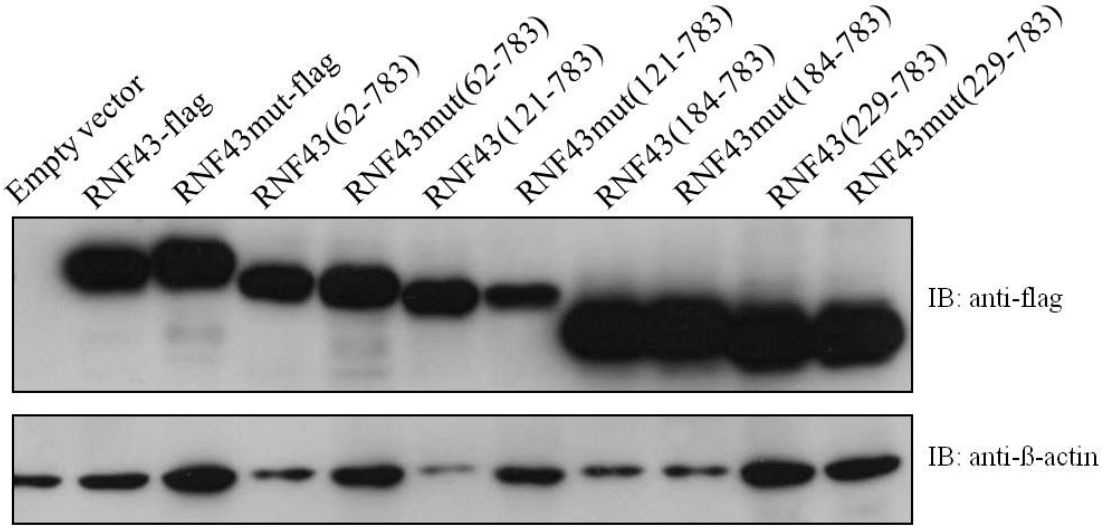

Figure 61 Expression of full length and N-terminally deleted mutants of wildtype and mutant RNF43.
HCT116 cells were transiently transfected with the full length and the generated N-terminally truncated RNF43 and RNF43mut mutants as well as the empty vector as a control, followed by cell lysis and subsequent Western blot analysis with the indicated antibodies.

As illustrated in Figure 61, all generated N-terminal deletion mutants, as well as the full length proteins, were strongly expressed in HCT116 cells upon transfection of the constructs and subsequent cell lysis and Western blot analysis.

In order to identify the region within the N-terminus of RNF43 responsible for the predominantly nuclear localization of wildtype and mutant RNF43(245-783), and in order to determine the subcellular localization of the newly generated N-terminal deletion mutants, Immunofluorescence stainings of the generated N-terminal deletion mutants were performed. Therefore, full length RNF43, RNF43(62-783), RNF43(121-783), RNF43(184-783) and RNF43(229-783) wildtype and mutant constructs were transiently transfected into HCT116 and SW480 colon cancer cells as well as Cos7 cells. The localization of the proteins was investigated by Immunofluorescence analysis, using antibodies directed against the flag-tag of the constructs (stained in red) and endogenous ß-catenin (visualized in green). The nucleus was visualized with DAPI staining (blue).

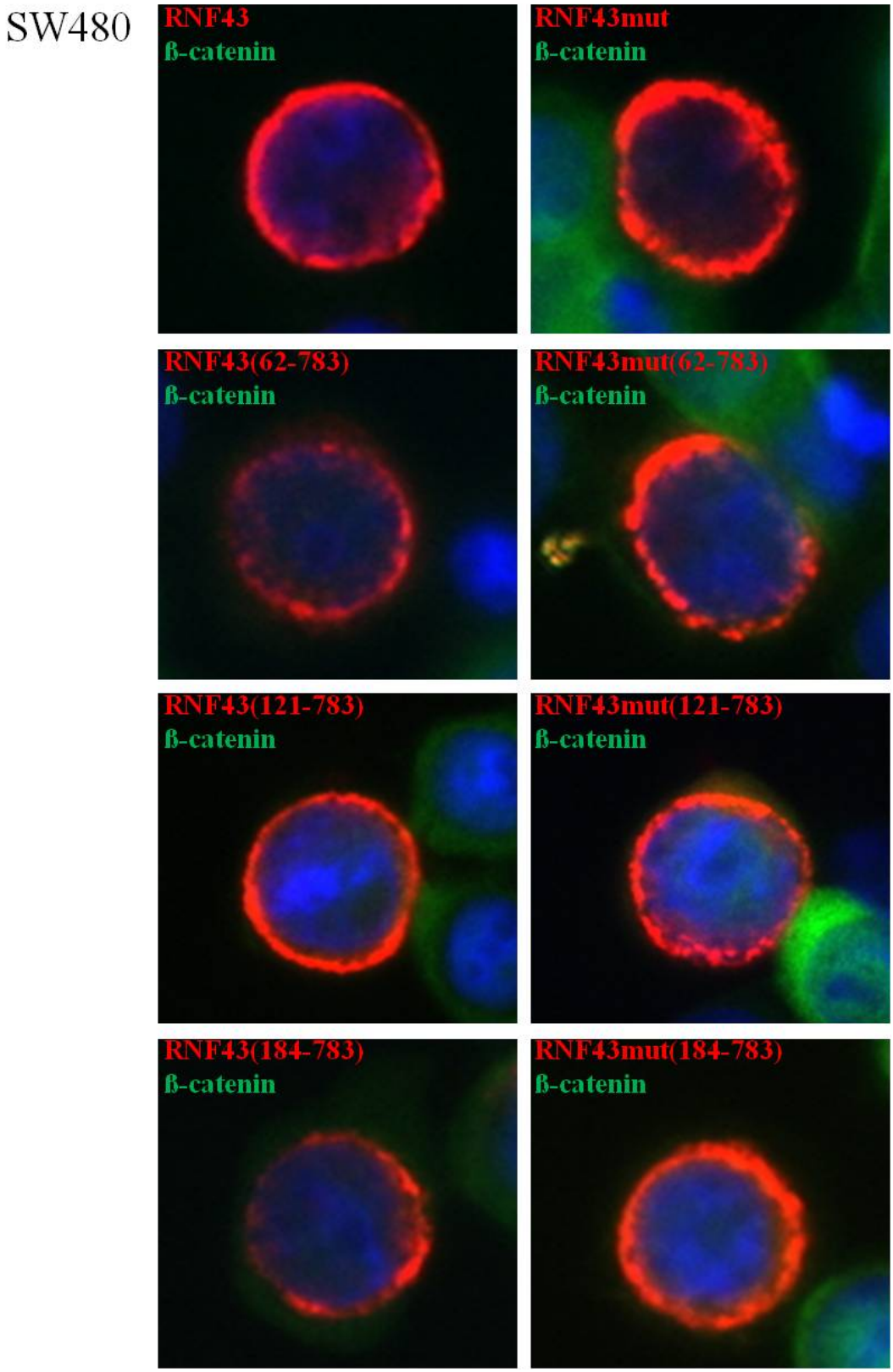

Figure 62 Immunofluorescence co-stainings of wildtype and mutant RNF43, RNF43(62-783), RNF43(121-783), RNF43(184-783) and endogenous ß-catenin in SW480 cells.
SW480 cells were transiently transfected with wildtype and the indicated RNF43-flag constructs. Pictures of Immunofluorescence stainings illustrate DAPI (blue), anti-flag (red) and anti-ß-catenin (green) stainings.

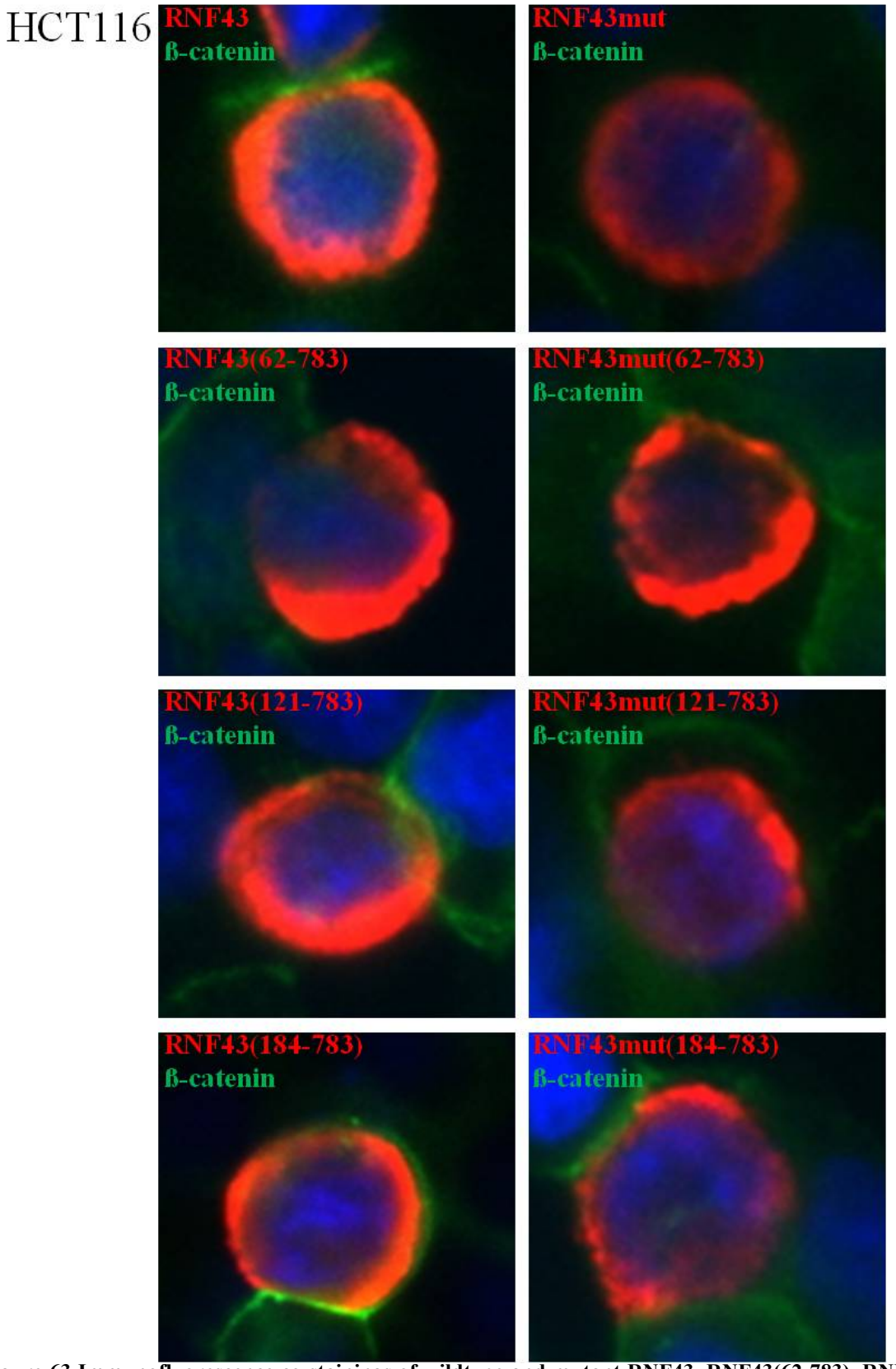

Figure 63 Immunofluorescence co-stainings of wildtype and mutant RNF43, RNF43(62-783), RNF43(121-783), RNF43(184-783) and endogenous ß-catenin in HCT116 cells.
HCT116 cells were transiently transfected with wildtype and the indicated RNF43-flag constructs. Pictures of Immunofluorescence stainings illustrate DAPI (blue), anti-flag (red) and anti-ß-catenin (green) stainings.

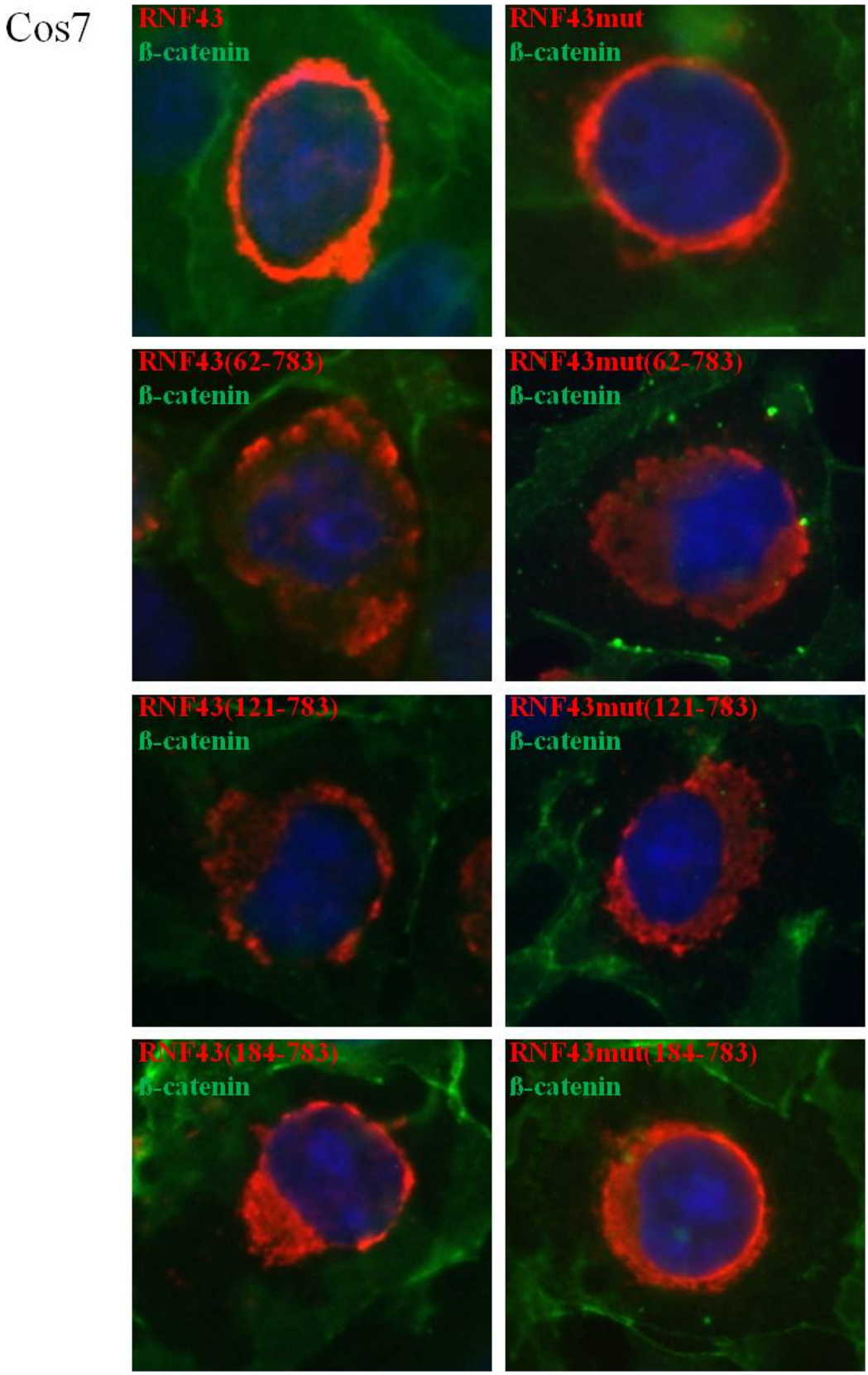

Figure 64 Immunofluorescence co-stainings of wildtype and mutant RNF43, RNF43(62-783), RNF43(121-783), RNF43(184-783) and endogenous ß-catenin in Cos7 cells.
Cos7 cells were transiently transfected with wildtype and the indicated RNF43-flag constructs. Pictures of Immunofluorescence stainings illustrate DAPI (blue), anti-flag (red) and anti-ß-catenin (green) stainings.

As illustrated in Figure 62, Figure 63 and Figure 64, truncations of different parts of the first 550 bp of the N-terminus of RNF43 and RNF43mut did not exhibit any alterations in the localizations of neither wildtype nor mutant RNF43. The N-terminally truncated proteins still localized mainly to the nuclear envelope as well as to ER/Golgi structures, as seen for full length RNF43. No differences in the localizations between the wildtype and the mutant proteins of these investigated N-terminally truncated constructs were observed.

In contrast, wildtype RNF43(229-783) did exhibit alterations in localizations in SW480, HCT116 and Cos7 cells (Figure 65).

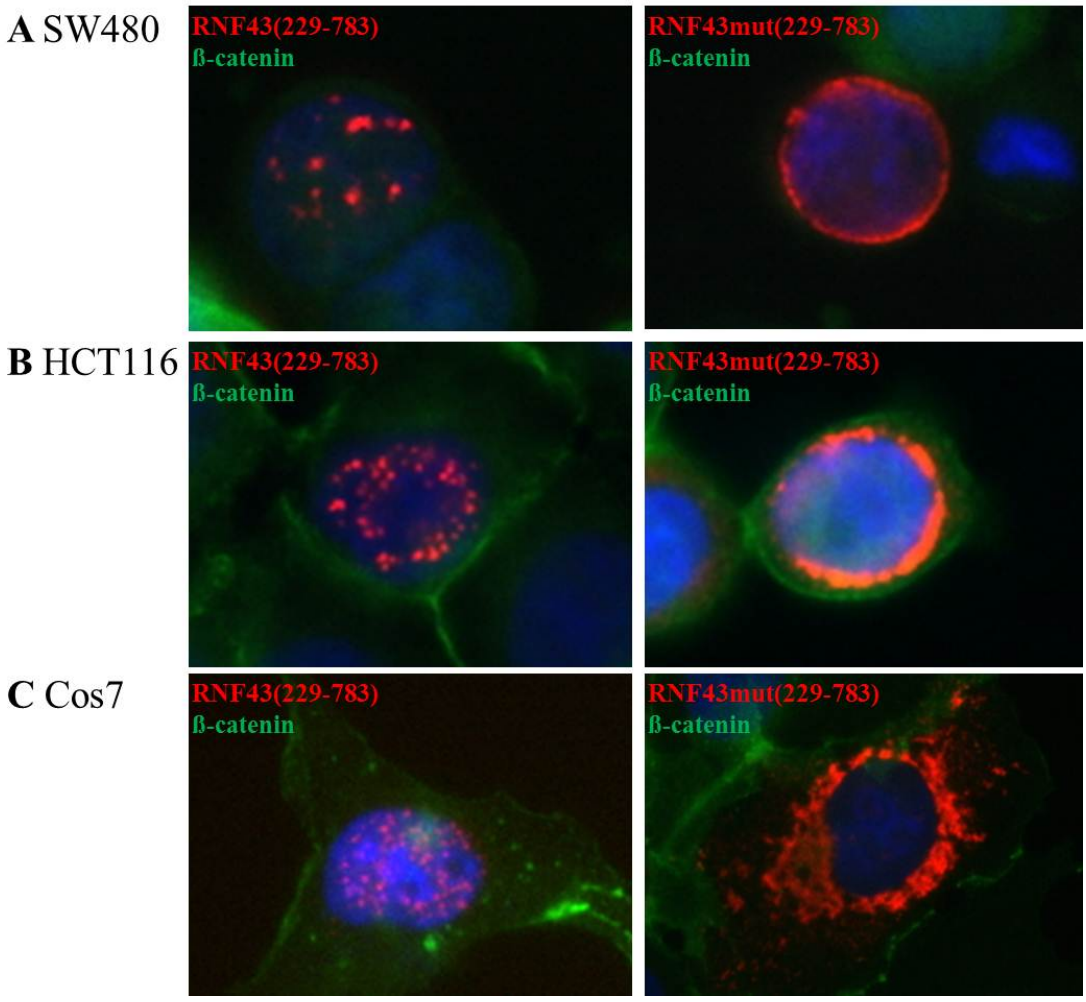

Figure 65 Immunofluorescence co-stainings of RNF43(229-783) and endogenous ß-catenin.
SW480 (A), HCT116 (B) and Cos7 (C) cells were transiently transfected with wildtype and mutant RNF43(229-783) constructs. Pictures of Immunofluorescence stainings illustrate DAPI (blue), anti-flag (red) and anti-ß-catenin (green) stainings.

As illustrated in Figure 65, wildtype RNF43(229-783) exhibited a more dominant nuclear localization pattern as compared to the other N-terminally deleted proteins in all three cell

lines. Wildtype RNF43(229-783) was only found in the nucleus, where it predominantly localized to punctuate structures inside the nucleoplasm.

In contrast to the wildtype, mutant RNF43(229-783) only localized to the nuclear membrane, as seen for the other N-terminal deletion mutants and full length RNF43 and RNF43mut. As visible in Figure 65, RNF43mut(229-783) did not localize to punctuate structures inside the nucleoplasm at all. These localization patterns of RNF43(229-783) and RNF43mut(229-783) were not only obtained in single cells, but visible in all cells that were transfected.

Thus, there is a difference in the localizations of wildtype and mutant RNF43(229-783) proteins. Whereas wildtype RNF43(229-783) only localized to the nucleoplasm, mutant RNF43(229-783) exhibited the same localization pattern as full length RNF43 and the N-terminally deleted mutants RNF43(61-783), RNF43(121-783), RNF43(184-783).

In order to determine whether the different localizations of wildtype and mutant RNF43(229-783) as well as the N-terminal truncations of RNF43(62-783), RNF43(121-783) and RNF43(84-783) influence the ability to modulate Wnt signaling as compared to the effect of full length proteins, TOP/FOP Luciferase reporter assay in Cos7 cells were performed. Wnt signaling was induced by treatment with LiCl (20 mM, 24 h).

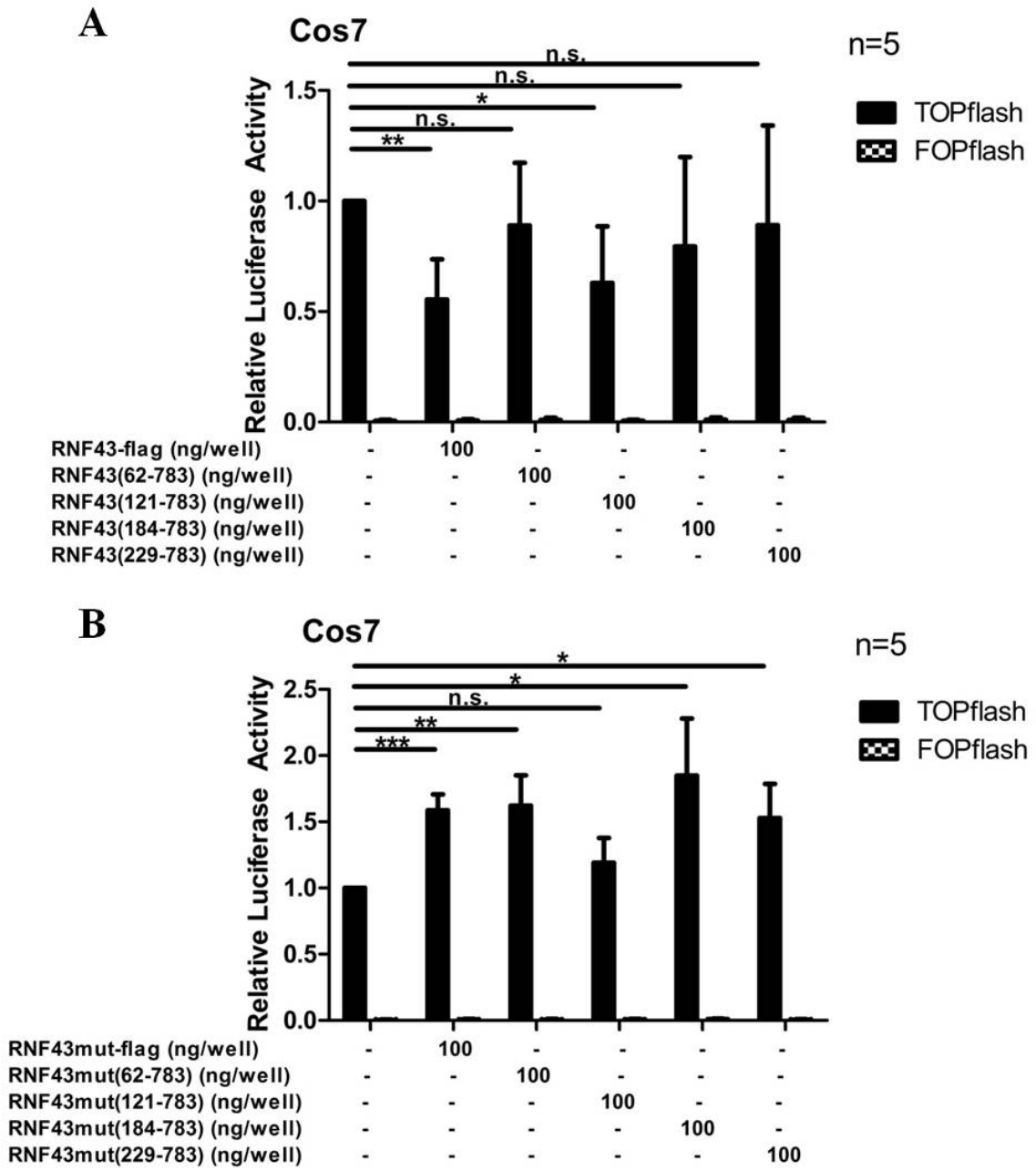

Figure 66 Effects of N-terminally truncated wildtype and mutant RNF43 on Wnt signaling activity.
Cos7 cells were transfected with pTOPflash or the control pFOPflash reporter plasmids and the indicated amounts of (A) RNF43-flag, RNF43(62-783), RNF43(121-783), RNF43(184-783) and RNF43(229-783) as well as (B) the mutant constructs RNF43mut-flag RNF43mut(62-783), RNF43mut(121-783), RNF43mut(184-783) and RNF43mut(229-783). Wnt signaling was induced by LiCl (20 mM, 24 h). Results were normalized to Renilla values and mock-transfected LiCl-induced cells. Data are means + S.D. of five independent experiments.

As illustrated in Figure 66, of the wildtype N-terminal deletion mutants investigated in TOP/FOP Luciferase reporter assays, only RNF43(121-783) exhibited a significant inhibitory effect on Wnt signaling activity (in addition to full length RNF43). Nevertheless, although the effects of several N-terminally truncated mutants on Wnt signaling activity were not

significant due to the high standard deviation, there was a tendency towards a better function of wildtype RNF43 in inhibiting Wnt signaling when the N-terminus was not truncated. All truncations at the N-terminus of RNF43 diminished the inhibitory effect of RNF43 on Wnt signaling activity, and the inhibitory function of RNF43 was reduced even more when the N-terminus was truncated to a greater extent. This was true for all wildtype RNF43 N-terminally truncated deletion mutants except RNF43(62-783), which for some unknown reasons did not exhibit any effect on Wnt signaling at all.

In contrast to the effects of N-terminally truncated wildtype proteins observed on Wnt signaling activity, which were greatly reduced as compared to the effects of full length wildtype RNF43, N-terminally truncated RNF43mut still exhibited a significant activating function on Wnt signaling, which was comparable to the effect of full length RNF43mut. This was true for all RNF43 N-terminally truncated mutants except RNF43mut(121-783). RNF43mut(121-783), for some unknown reasons, was the only N-terminal mutant that did not cause any effects on Wnt signaling activity.

Full length RNF43 strongly precipitated with Tcf4 in Co-IP experiments. Because of the relatively strong affinity of RNF43 for Tcf4, we next sought to identify the region of RNF43 responsible for mediating the protein-protein interaction. Therefore, several N-terminally truncated RNF43 constructs, namely RNF43(121-783), RNF43(184-783) and RNF43(245-783), were investigated in Co-IP experiments with endogenous Tcf4.

HCT116 cells were transfected with the N-terminally truncated RNF43-flag constructs, and 48 h after transfection, whole cell lysates containing equal amount of the proteins were immunoprecipitated with a Tcf4 monoclonal antibody or irrelevant rabbit IgG as a control. The precipitated complexes were subjected to Western Blot analysis with the indicated antibodies (Figure 67).

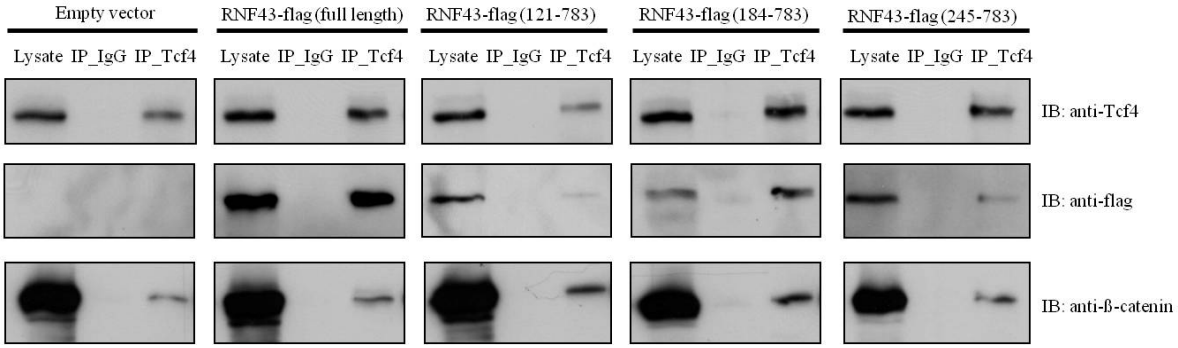

Figure 67 Tcf4 binds to N-terminally truncated RNF43.
HCT116 cells were transfected with the indicated RNF43 constructs as well as the empty vector. Whole cell lysates were subjected to Immunoprecipitation with monoclonal Tcf4 antibody or normal rabbit IgG as a control. The immunoprecipitates were analyzed by Western blot analysis with the indicated antibodies.

As illustrated in Figure 67, Immunoprecipitation of Tcf4 revealed an interaction of Tcf4 not only with full length RNF43, but also with the different N-terminally truncated mutants, suggesting that the region between the RING domain and the C-terminus of RNF43 is responsible for binding to Tcf4.

Further evidence for a possible interaction of RNF43 with Tcf4 via its region between the RING domain and the C-terminus was obtained by Immunofluorescence co-stainings, as shown in Figure 68 and Figure 69.

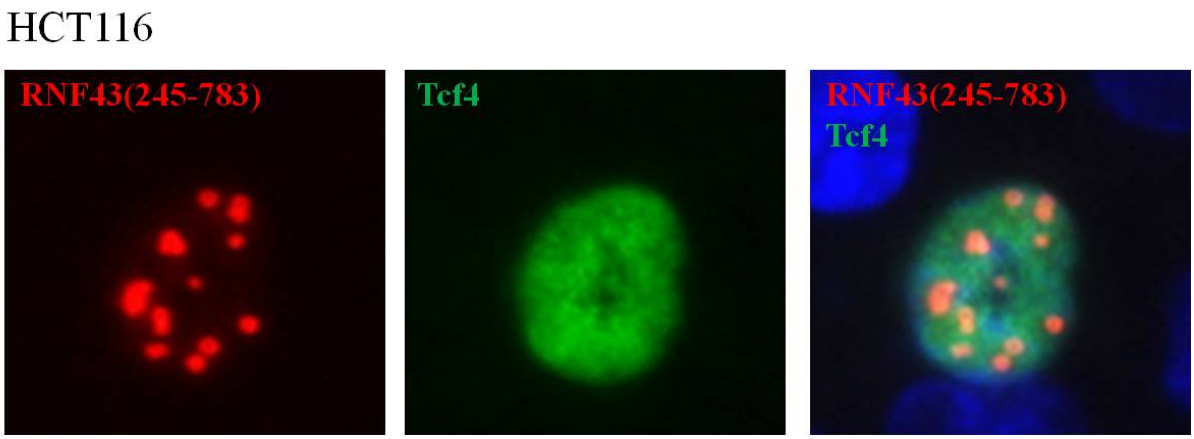

Figure 68 Immunofluorescence co-stainings of RNF43(245-783) and Tcf4 in HCT116 cells.
HCT116 cells were transiently transfected with RNF43(245-783)-flag and Tcf4-HA constructs. Pictures of Immunofluorescence stainings illustrate DAPI (blue), anti-flag (red) and anti-HA (green) stainings.

In Immunofluorescence co-stainings of RNF43(245-783) and Tcf4, RNF43(245-783) mainly localized to specific punctuate structures in the nucleoplasm. Tcf4 was randomly distributed throughout the nucleoplasm (Figure 68). RNF43(245-783) partially exhibited colocalization with Tcf4 inside the nucleus, further strengthening the data obtained by Co-Immunoprecipitation experiments (Figure 67).

Similarly, in Immunofluorescence co-stainings of wildtype RNF43(229-783) and Tcf4, RNF43(229-783) also mainly localized to specific punctuate structures inside the nucleoplasm, whereas Tcf4 was randomly distributed throughout the nucleoplasm (Figure 69).

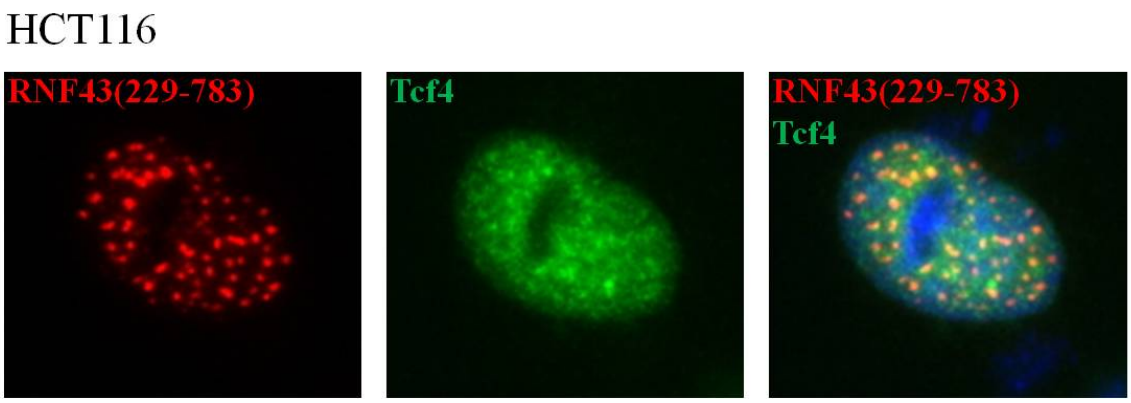

Figure 69 Immunofluorescence co-stainings of RNF43(229-783) and Tcf4 in HCT116 cells.
HCT116 cells were transiently transfected with RNF43(229-783)-flag and Tcf4-HA constructs. Pictures of Immunofluorescence stainings illustrate DAPI (blue), anti-flag (red) and anti-HA (green) stainings.

As already observed for RNF43(245-783), RNF43(229-783) also partially exhibited colocalization with Tcf4 inside the nucleus (yellow dots, Figure 69). The localization pattern visible in the stainings (Figure 68, Figure 69) suggests an interaction of RNF43 and Tcf4 inside the nucleoplasm.

Since RNF43 bound to Tcf4 via its region between the RING domain and the C-terminus in Co-Immunoprecipitation experiments (Figure 67), and since Immunofluorescence co-stainings of RNF43(245-783) and RNF43(229-783) exhibited colocalizations with Tcf4 inside the nucleoplasm, RNF43 is very likely to bind to Tcf4 via its region between the RING domain and C-terminus. Investigation of wildtype and mutant RNF43 deletion mutants lacking the C-terminus would give more information about the specific region of RNF43 binding to Tcf4.

3.4.2 Role of the signal peptide

The putative signal peptide sequence of RNF43 is located at the very N-terminus of the RNF43 sequence and comprises 69 bp (see 3.3.1). Thus, it is only present in the full length wildtype and mutant RNF43 constructs. All the other generated RNF43 constructs cloned so far, with truncations at the N-terminus, do not harbor the N-terminal signal peptide.

In order to examine a putative effect of the signal peptide on the localization of RNF43 and its function on the Wnt signaling pathway, new constructs were generated. The signal peptide sequence was attached to the N-terminus of wildtype and mutant RNF43(229-783), as well as to wildtype and mutant RNF43(245-783).

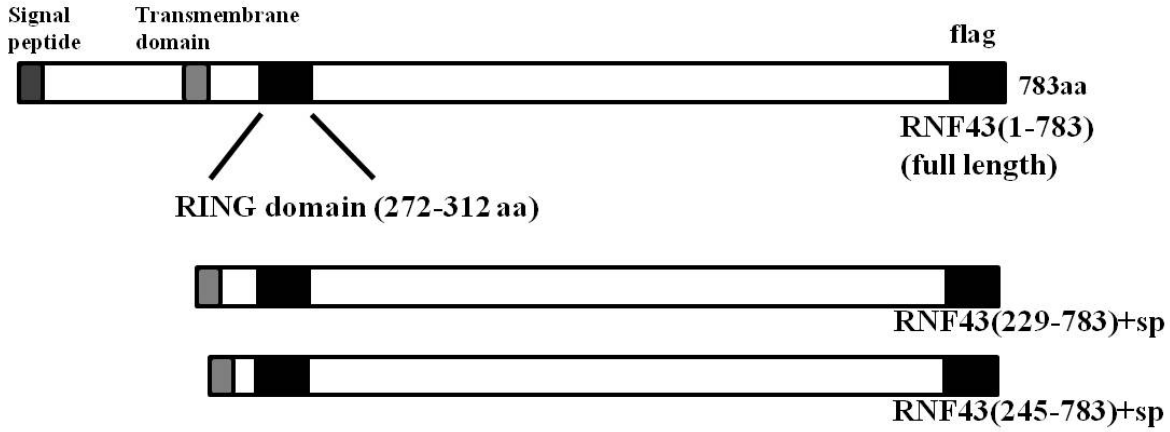

Figure 70 Scheme of the generated N-terminally truncated deletion mutants RNF43(229-783)+sp and RNF43(245-783)+sp.

The generated constructs harboring the signal peptide were termed RNF43(229-783)+sp, RNF43mut(229-783)+sp, RNF43(245-783)+sp and RNF43mut(245-783)+sp. Attachment of a C-terminal flag-tag allowed detection of the constructs. To verify the expression of the constructs, HCT116 cells were transiently transfected with the empty vector pcDNA4TO, as well as the wildtype and mutant RNF43(229-783)+sp and RNF43(245-783)+sp constructs, followed by cell lysis. Lysates were subjected to Western blot analysis with the indicated antibodies. ß-actin was used as an internal loading control.

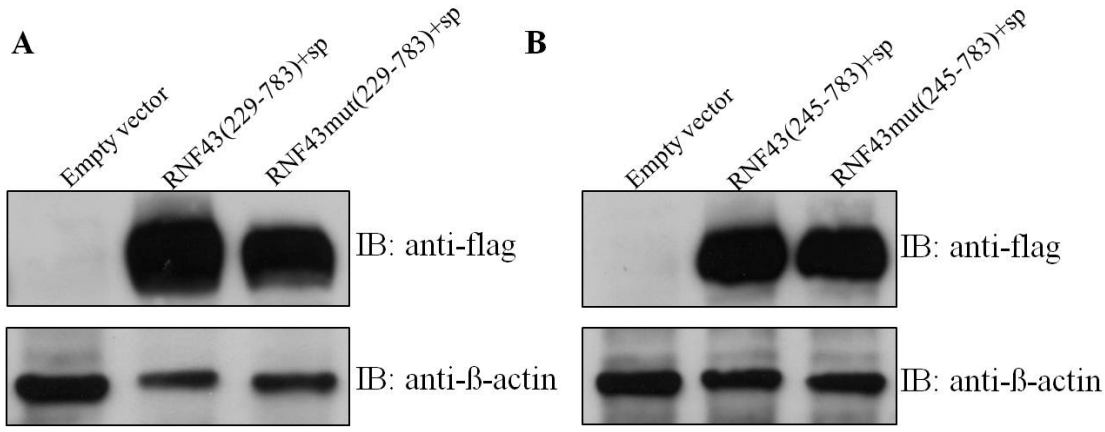

Figure 71 Expression of N-terminal deletion mutants harboring an N-terminal signal peptide.
HCT116 cells were transiently transfected with the generated N-terminally truncated (A) wildtype and mutant RNF43(229-783)+sp constructs as well as (B) wildtype and mutant RNF43(245-783)+sp constructs, followed by cell lysis and subsequent Western Blot analysis with the indicated antibodies.

As shown in Figure 71, wildtype and mutant RNF43(229-783)+sp as well as wildtype and mutant RNF43(245-783)+sp were expressed upon transfection of HCT116 cells.

The next aim was to investigate a putative effect of the N-terminal signal peptide sequence on the localization of the proteins. Wildtype RNF43(229-783) and wildtype and mutant RNF43(245-783), which do not harbor a signal peptide, were shown to predominantly exhibit nucleoplasmic localization (Figure 58 and Figure 65). A relocalization of these proteins to a specific compartment upon attachment of an N-terminal signal peptide, like to the nuclear membrane, would indicate a function of the signal peptide as a key factor essential for localization of RNF43 in the specific compartment.

Therefore, Immunofluorescence stainings were performed. SW480, HCT116 and Cos7 cells were transiently transfected with the indicated constructs, followed by stainings of the proteins using antibodies directed against the flag-tag of the constructs (stained in red) and endogenous ß-catenin (visualized in green). The nucleus was visualized with DAPI staining (blue).

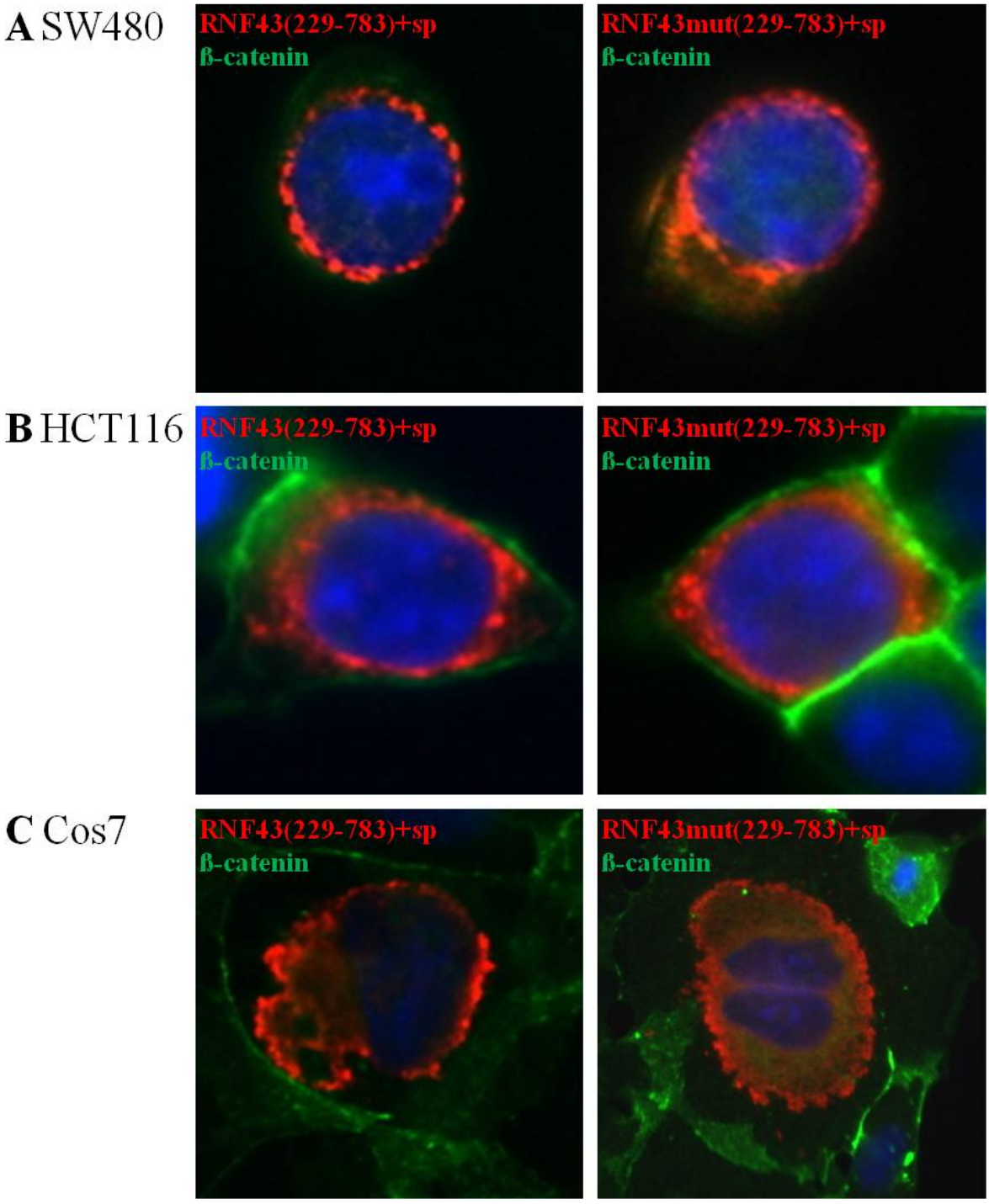

Figure 72 Immunofluorescence stainings of wildtype and mutant RNF43(229-783)+sp.
SW480 (A), HCT116 (B) and Cos7 (C) cells were transiently transfected with the indicated constructs. Pictures of Immunofluorescence stainings illustrate DAPI (blue), anti-flag (red) and anti-ß-catenin (green) stainings.

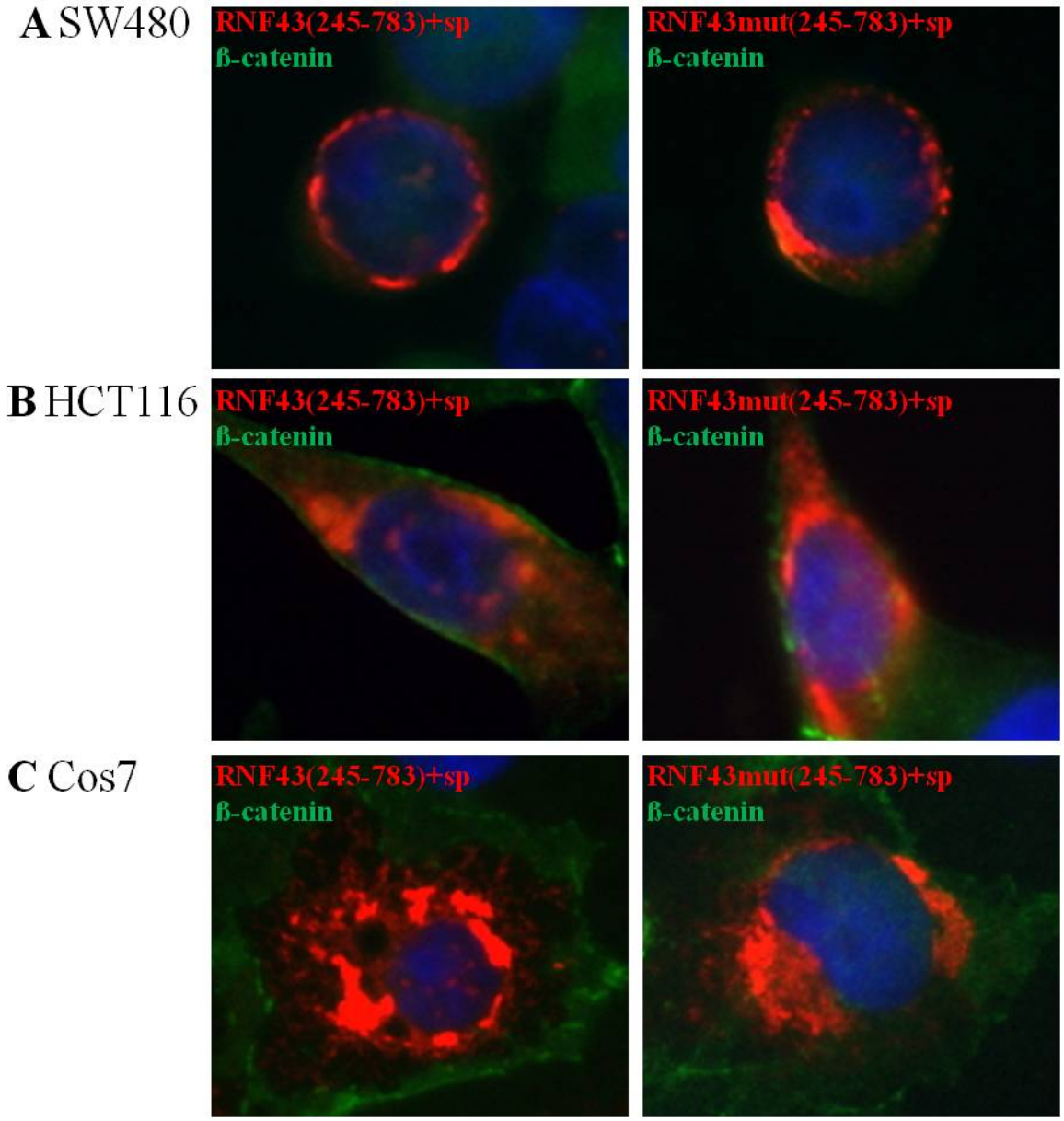

Figure 73 Immunofluorescence stainings of wildtype and mutant RNF43(245-783)+sp.
SW480 (A), HCT116 (B) and Cos7 (C) cells were transiently transfected with the indicated constructs. Pictures of Immunofluorescence stainings illustrate DAPI (blue), anti-flag (red) and anti-ß-catenin (green) stainings.

As illustrated in Figure 72 and Figure 73, expression of the 69 bp long signal peptide at the N-terminus resulted in a more predominant localization of wildtype and mutant RNF43(229-783)+sp and RNF43(245-783)+sp at the nuclear membrane in HCT116, SW480 and Cos7 cells. This localization patterns are in contrast to the exclusively nucleoplasmic localization patterns of wildtype RNF43(229-783) and wildtype and mutant RNF43(245-783) without signal peptide, as shown in Figure 58 and Figure 65.

Thus, attachment of the N-terminal signal peptide sequence to the N-terminally deleted RNF43 mutants RNF43(229-783) and RNF43(245-783) resulted in an amplified relocalization of the proteins from the nucleoplasm to the nuclear membrane and to the ER.

In order to examine whether the attachment of the N-terminal signal peptide to the N-terminally deleted RNF43 mutants RNF43(229-783) and RNF43(245-783) results in alterations in the effects on Wnt signaling activities as compared to the deletion mutants without the signal peptide, TOP/FOP Luciferase reporter assays in Cos7 cells were performed. Wnt signaling was induced by treatment with LiCl (20 mM, 24 h).

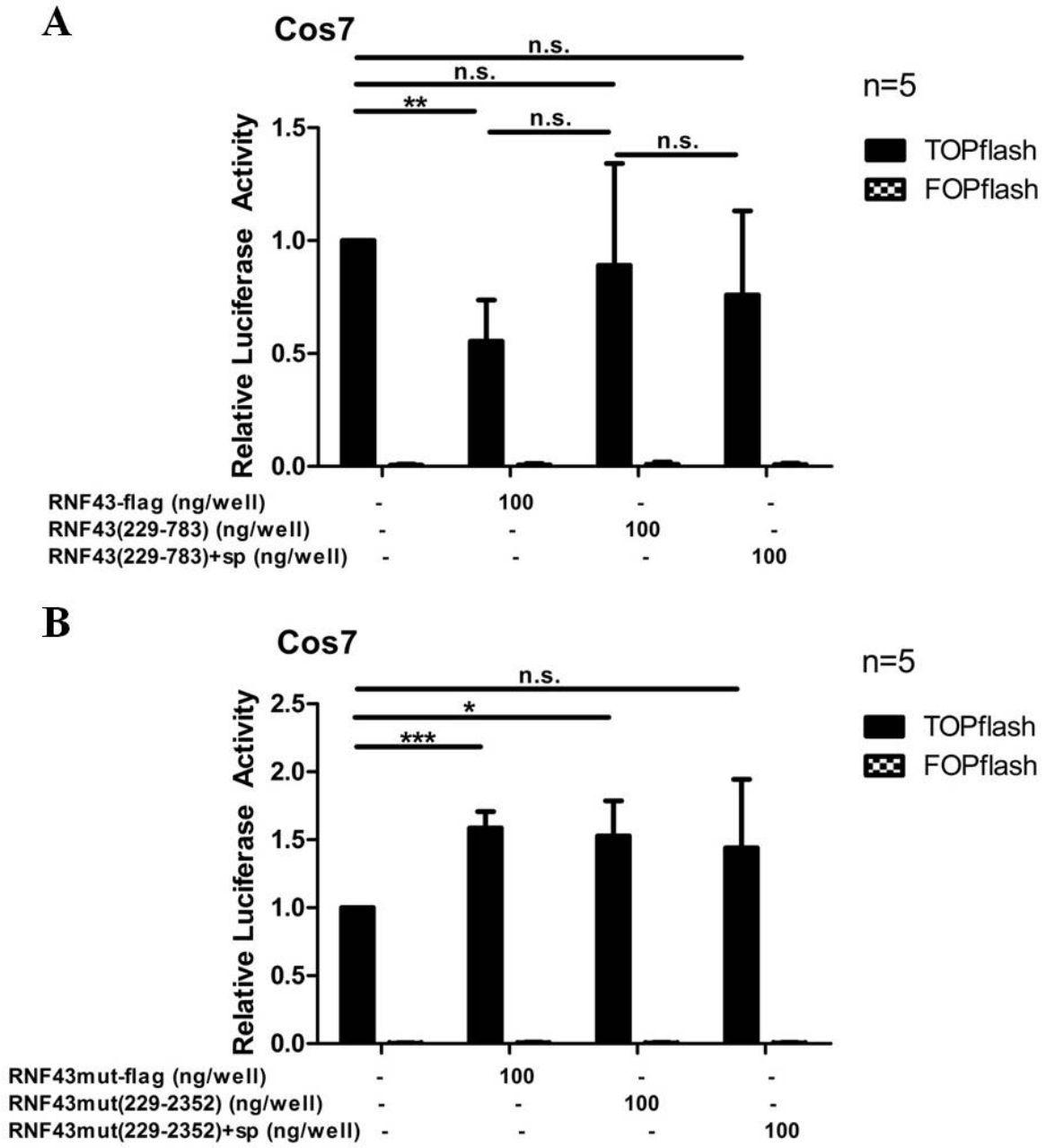

Figure 74 Effect of the attachment of the N-terminal signal peptide to wildtype and mutant RNF43(229-783) on Wnt signaling activity.
Cos7 cells were transfected with pTOPflash or the control pFOPflash reporter plasmids and the indicated amounts of (A) RNF43-flag, RNF43(229-783) and RNF43(229-783)+sp, and (B) RNF43mut-flag, RNF43mut(229-783) and RNF43mut(229-783)+sp plasmids. Wnt signaling was induced by LiCl (20 mM, 24 h). Results were normalized to Renilla values and to mock-transfected LiCl-induced cells. Data are means + S.D. of five independent experiments.

Although expression of the 69 bp long signal peptide at the N-terminus resulted in a predominant relocalization of wildtype RNF43(229-783)+sp to the nuclear membrane and the ER in HCT116, SW480 and Cos7 cells (Figure 72), only little changes in the effects on Wnt signaling activity were observed.

In TOP/FOP Luciferase reporter experiments, RNF43(229-783) without signal peptide was not functional, but RNF43(229-783)+sp exhibited a very small inhibitory effect on the Wnt signaling pathway. Nevertheless, the effect was only marginal, exhibited a high standard deviation and was not significant. Thus, although attachment of a signal peptide to the N-terminus of RNF43(229-783) resulted in a relocalization to the nuclear membrane, no difference in the effects on Wnt signaling activity were observed.

Mutant RNF43(229-783) localized to the nuclear membrane and so did mutant RNF43(229-783)+sp. Thus, the localization of the protein did not change upon attachment of the signal peptide sequence. Similarly to the effects on Wnt signaling observed for the wildtype protein, the difference in the effects of mutant RNF43(229-783) with and without signal peptide on Wnt signaling activity was only marginal, exhibited a high standard deviation and was not significant. Both proteins still slightly increased Wnt signaling activity, as did full length mutant RNF43. Nevertheless, the effects of mutant RNF43(229-783) with and without signal peptide were weaker than the effect of full length mutant RNF43, and due to the high standard deviation not significant for RNF43(229-783)+sp.

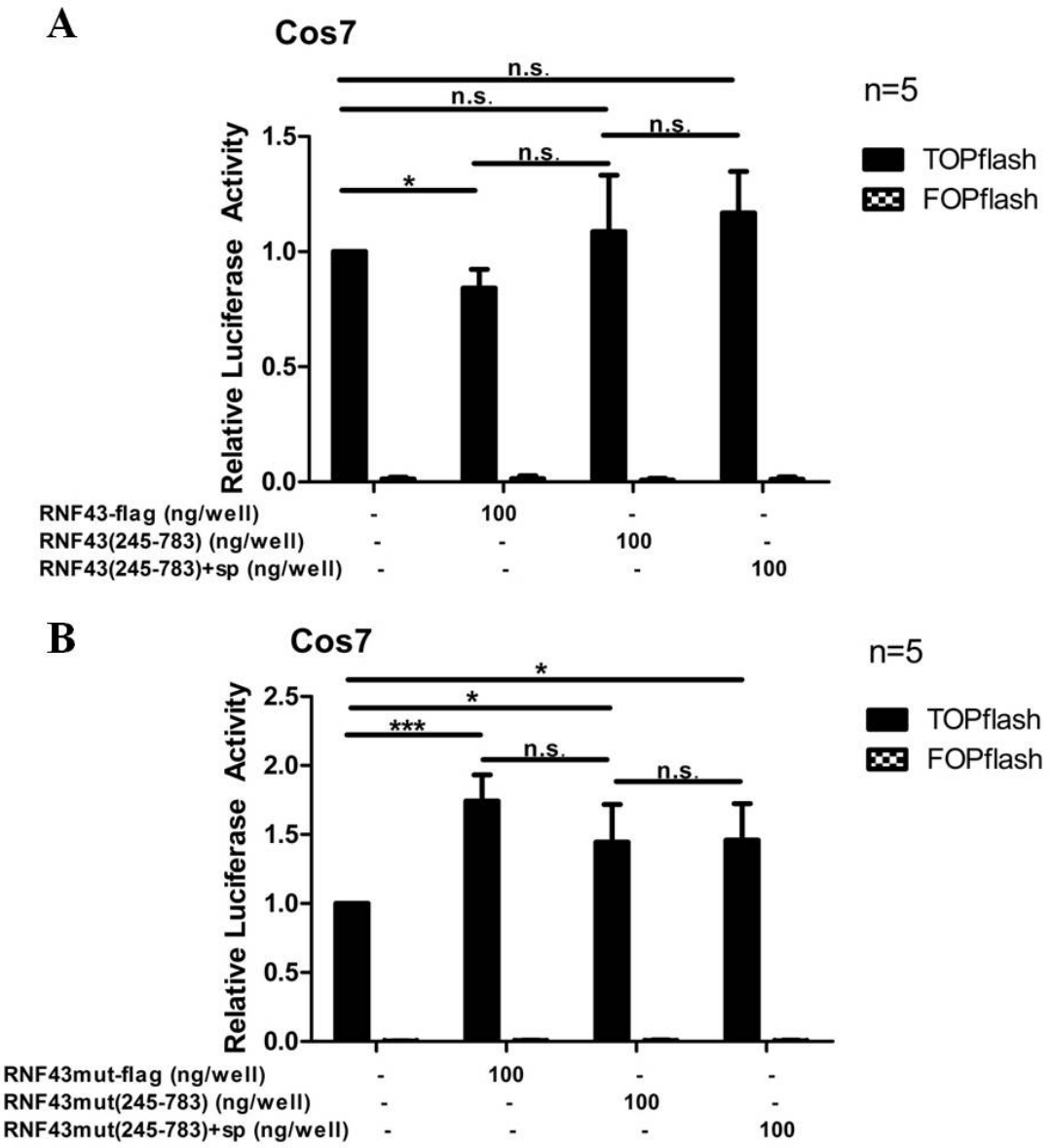

Figure 75 Effect of the attachment of the N-terminal signal peptide to wildtype and mutant RNF43(245-783) on Wnt signaling activity.
Cos7 cells were transfected with pTOPflash or the control pFOPflash reporter plasmids and the indicated amounts of (A) RNF43-flag, RNF43(245-783) and RNF43(245-783)+sp, and (B) RNF43mut-flag, RNF43mut(245-783) and RNF43mut(245-783)+sp plasmids. Wnt signaling was induced by LiCl (20 mM, 24 h). Results were normalized to Renilla values and to mock-transfected LiCl-induced cells. Data are means + S.D. of five independent experiments.

Although expression of the signal peptide at the N-terminus of wildtype and mutant RNF43(245-783) resulted in a predominant relocation to the nuclear membrane (Figure 73), an effect which was also observed for RNF43(229-783)+sp (Figure 72), no significant alterations in the effects on Wnt signaling activity as compared to RNF43(245-783) without signal peptide were observed. Wildtype RNF43(245-783) with/without signal peptide did not exhibit any effects on Wnt signaling activity, indicating that the inhibitory effect of full length

RNF43 was completely reversed upon deletion of the N-terminus. Mutant RNF43(245-783) with/without signal peptide still slightly increased Wnt signaling, but the effects of these two proteins were weaker than the effect of full length mutant RNF43.

Thus, although attachment of the N-terminal signal peptide resulted in a profound relocalization of the proteins, no significant effects on Wnt signaling activity were detected. Hence, these data suggest that the N-terminus is particularly important for the function of RNF43, whereas solely localization may possibly not be crucial for RNF43 function to the same extent.

3.4.3 RNF43 mutants lacking the transmembrane domain (Δaa191-228)

In contrast to the wildtype and mutant RNF43(184-783) proteins, wildtype RNF43(229-783) and RNF43(245-783) localized solely in punctuate structures inside the nucleoplasm. Thus, they exhibited a more dominant nuclear localization pattern as compared to the other generated N-terminally deleted proteins.

In order to identify putative transmembrane regions, which may be responsible for the diverging localizations of the proteins, sequence analysis using different transmembrane prediction tools was performed. The region between amino acids 199 and 219 was predicted to be a transmembrane region by the "DAS" Transmembrane Prediction server[11], the "TMHMM" server[12], as well as the "TMPred" program[13]. In accordance, the "Split" Membrane Protein Transmembrane Secondary Structure Prediction Server[14] also predicted a transmembrane region from amino acids 198 to 220.

Since we observed nucleoplasmic localization of RNF43(184-783), but predominantly nuclear membrane localization of RNF43(229-783), and since there was a putative transmembrane domain between amino acids 199 and 220, the next aim was to answer the question whether

[11] http://www.sbc.su.se/~miklos/DAS/

[12] http://www.cbs.dtu.dk/services/TMHMM/

[13] http://www.ch.embnet.org/software/TMPRED_form.html

[14] http://split.pmfst.hr/split/

the region between amino acids 184 and 228 is responsible for the localization of RNF43 to the nuclear envelope.

Therefore, wildtype and mutant RNF43 constructs lacking the transmembrane domain (amino acids 191 - 228) were cloned. The constructs, termed RNF43(Δ191-228) and RNF43mut(Δ191-228), harbor a C-terminal flag-tag which allows detection of the proteins. They both still harbor the RING domain as well as the N-terminal signal peptide.

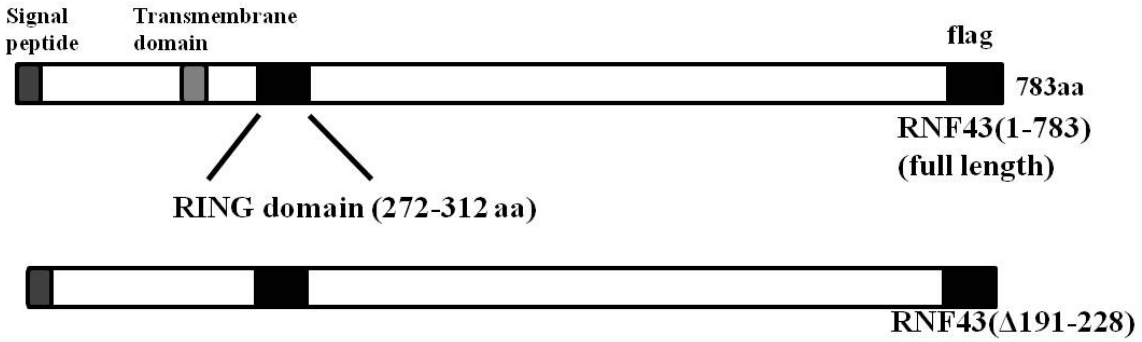

Figure 76 Scheme of the generated mutant RNF43(Δ191-228).

In order to investigate the expression of wildtype and mutant RNF43(Δ191-228), HCT116 cells were transiently transfected with the different constructs, followed by cell lysis and Western blot analysis with a flag antibody. ß-actin was used as an internal loading control.

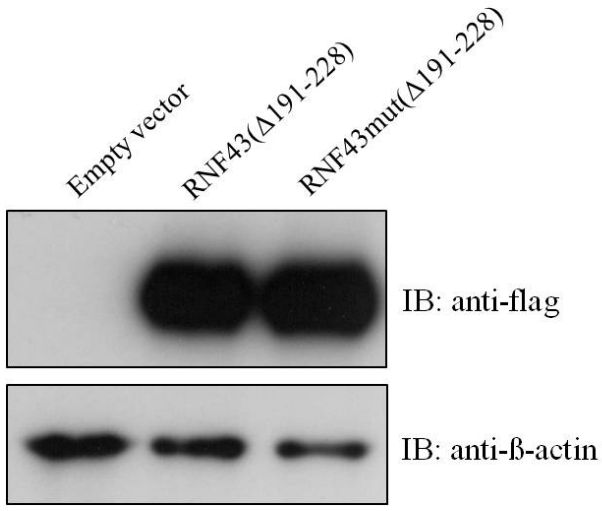

Figure 77 Expression of the deletion mutants RNF43(Δ191-228) and RNF43mut(Δ191-228), lacking the transmembrane domain.
HCT116 cells were transiently transfected with RNF(Δ191-228) and RNF43mut(Δ191-228), followed by cell lysis and subsequent Western Blot analysis with the indicated antibodies.

As shown in Figure 77, both wildtype and mutant RNF43(Δ191-228) were expressed upon transfection of HCT116 cells.

In order to investigate the subcellular localization patterns of wildtype and mutant RNF43(Δ191-228), Immunofluorescence stainings were performed. Therefore, SW480, HCT116 and Cos7 cells were transiently transfected with the indicated constructs, followed by stainings of the proteins using antibodies directed against the flag-tag of the constructs (stained in red) and endogenous ß-catenin (visualized in green). The nucleus was visualized with DAPI staining (blue).

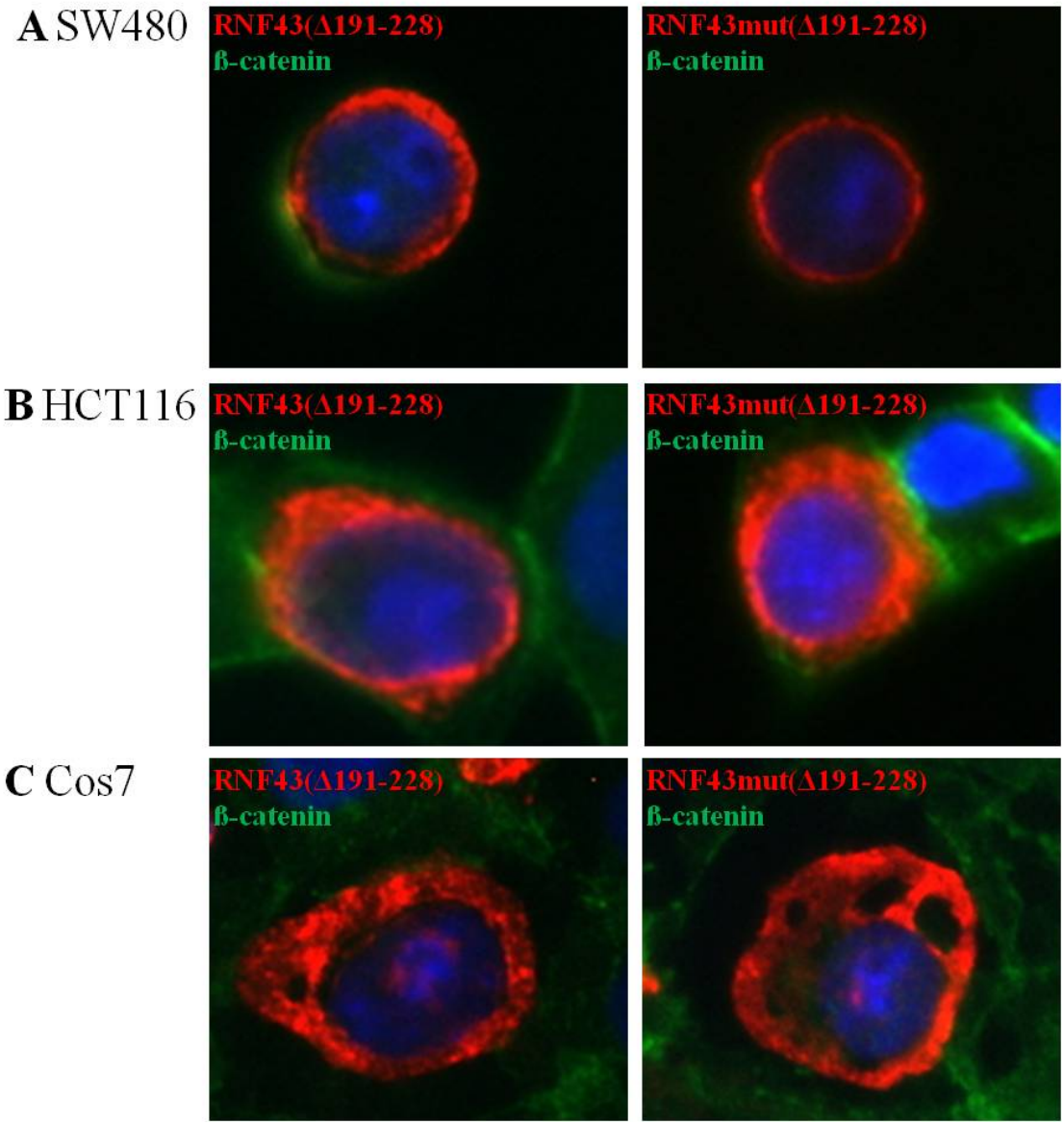

Figure 78 Immunofluorescence stainings of wildtype and mutant RNF43(Δ191-228).
SW480 (A), HCT116 (B) and Cos7 (C) cells were transiently transfected with the indicated constructs. Pictures of immunofluorescence stainings illustrate DAPI (blue), anti-flag (red) and anti-ß-catenin (green) stainings.

Both wildtype and mutant RNF43(Δ191-228) localized mainly to the nuclear membrane and the Golgi/ER structures, as observed for wildtype and mutant full length RNF43 proteins

(Figure 78). In addition, no differences between the localizations of wildtype and mutant proteins were observed. Thus, localization of RNF43 to the nuclear membrane was still observed upon deletion of the amino acids 191 - 228 of the RNF43 sequence. These data indicate that these amino acids are not the only amino acids that are crucial for localization of RNF43 to the nuclear envelope.

In order to examine whether the deletion of amino acids 191 - 228 of wildtype and mutant RNF43 results in alterations in the effect on Wnt signaling activity as compared to full length wildtype and mutant RNF43, TOP/FOP Luciferase reporter assays in Cos7 cells were performed. Wnt signaling was induced by treatment with LiCl (20 mM, 24 h).

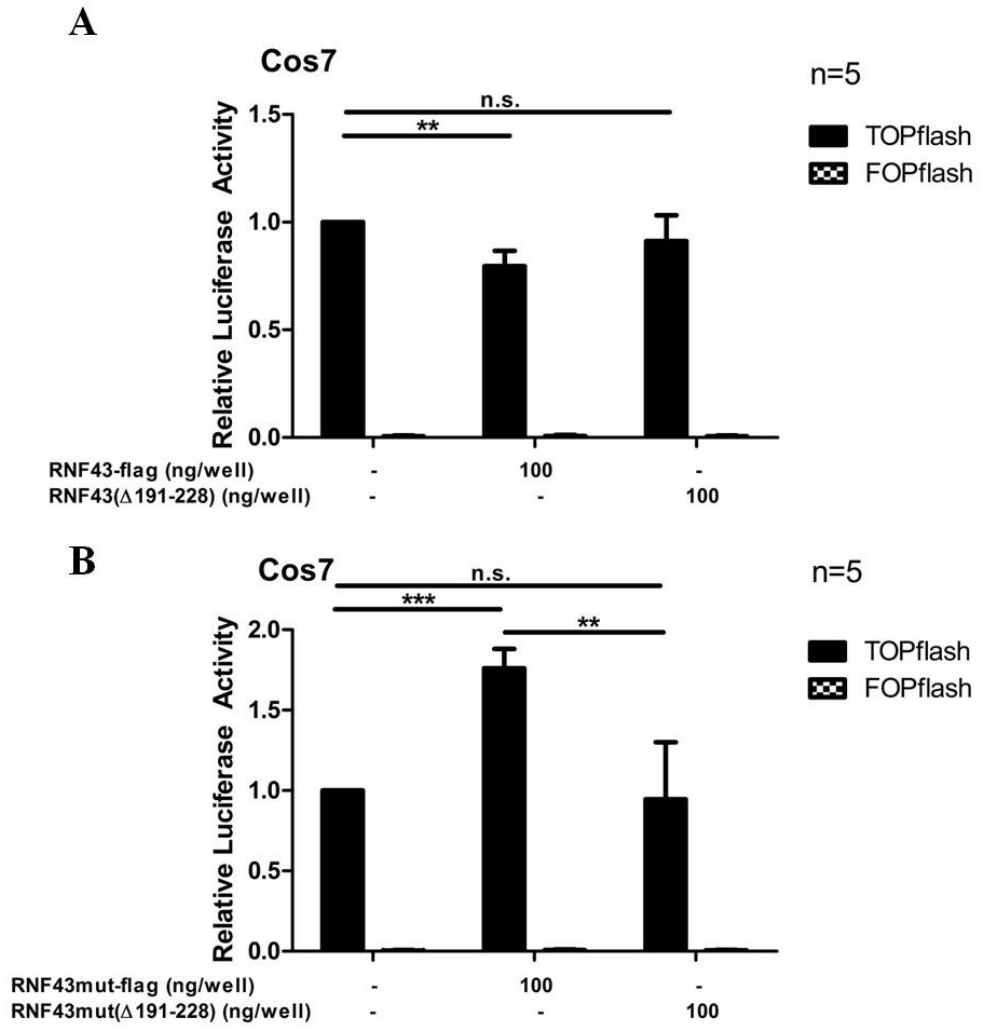

Figure 79 Effect of deletion of amino acids 191 - 228 of wildtype and mutant RNF43 on Wnt signaling activity.
Cos7 cells were transfected with pTOPflash or the control pFOPflash reporter plasmids and the indicated amounts of (A) RNF43-flag and RNF43(Δ191-228) as well as (B) RNF43mut-flag and RNF43mut(Δ191-228) plasmids. Wnt signaling was induced by treatment with LiCl (20 mM, 24 h). Results were normalized to mock-transfected LiCl-induced cells. Data are means + S.D. of five independent experiments.

As illustrated in Figure 79, deletion of amino acids 191 - 228 resulted in a complete reversal of the inhibitory effect of wildtype RNF43 as well as the activating effect of mutant RNF43 on LiCl-induced Wnt signaling activity. Wildtype RNF43(Δ191-228) did not exhibit any effect on Wnt signaling activity in TOP/FOP Luciferase reporter experiments, neither did mutant RNF43(Δ191-228). Thus, the amino acids 191 - 228 are essential for both the inhibitory function of wildtype RNF43, and the activating effect of mutant RNF43 on Wnt signaling activity.

The effects of wildtype and mutant truncated versions of RNF43, the effect of the signal peptide attached to wildtype and mutant RNF43(229-783) and RNF43(245-783), as well as the effects of wildtype and mutant RNF43 proteins lacking the transmembrane domain (Δ191-228), on Wnt signaling, which were described in this chapter (3.4), are summarized in Figure 80.

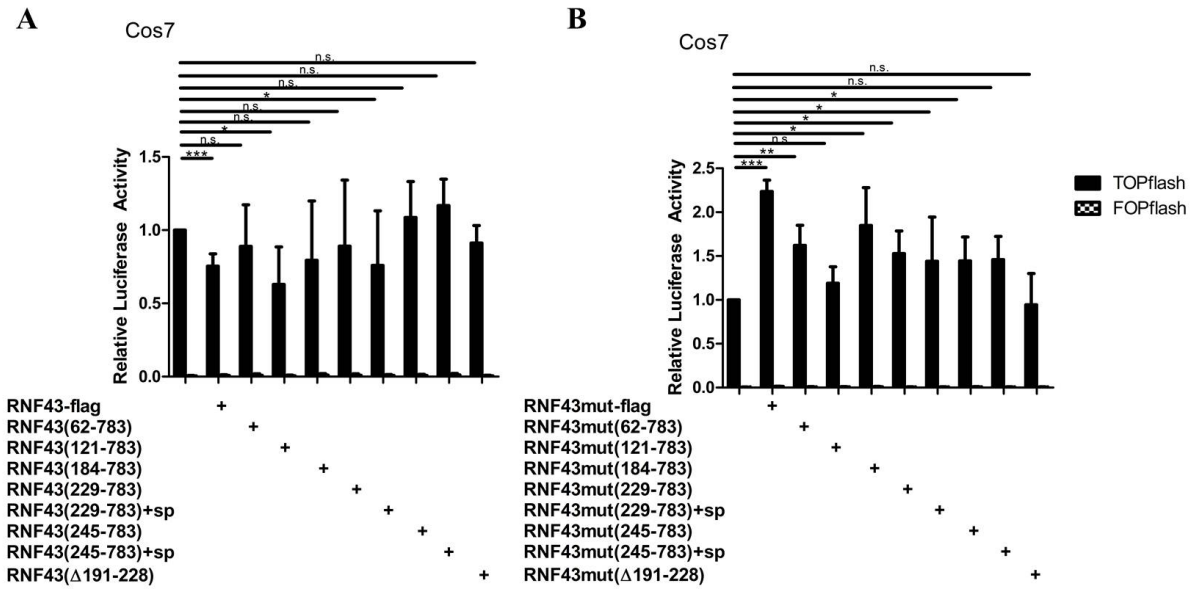

Figure 80 Summary of the effects of all the generated mutants on Wnt signaling activity.
A summary of the effects of wildtype and mutant truncated versions of RNF43, the effect of the signal peptide attached to wildtype and mutant RNF43(229-783) and RNF43(245-783) constructs, as well as the effects of wildtype and mutant RNF43 proteins lacking the transmembrane domain (Δ191-228), on Wnt signaling, as described in this chapter (3.4).

Thus, as visible in Figure 80, full length wildtype and mutant RNF43 exhibited the strongest effects on Wnt signaling activity. When compared to the effects of full length wildtype and mutant RNF43 on Wnt signaling activity, the effects of all other truncated versions of wildtype and mutant RNF43 on Wnt signaling were decreased.

Thus, these data indicate that the N-terminus is of particular importance for the inhibitory effect of RNF43 on the Wnt signaling pathway.

3.5 Clinical relevance

3.5.1 Transcriptional repression of RNF43 by CpG methylation in colon cancer cell lines

Apart from the known regulation of *RNF43* gene transcription as a target gene of the Wnt signaling pathway (1.9), the transcriptional regulatory mechanisms for RNF43 are entirely uncharacterized. Furthermore, the RNF43 mRNA levels determined in our experiments in colon cancer cell lines were very low in most cell lines, as shown in Figure 19. Therefore, we tested whether the expression of RNF43 is transcriptionally repressed. Transcriptional repression of genes often involves epigenetic alterations of the gene promoter such as CpG methylation (Jones, Veenstra et al. 1998). In order to investigate whether CpG methylation is involved in the transcriptional repression of RNF43, we tested whether 5-Aza-2'-Deoxycytidine (5-Aza-2'-dCyt), an inhibitor of CpG mehtyltransferases (Cameron, Bachman et al. 1999), could increase *RNF43* gene expression. Several colon cancer cell lines (HCT116, SW480, DLD1 and HT29) were subjected to treatment with 5-Aza-2'-dCyt. RNF43 mRNA levels of 5-Aza-2'-dCyt-treated and -untreated cells were determined by RT-PCR analysis.

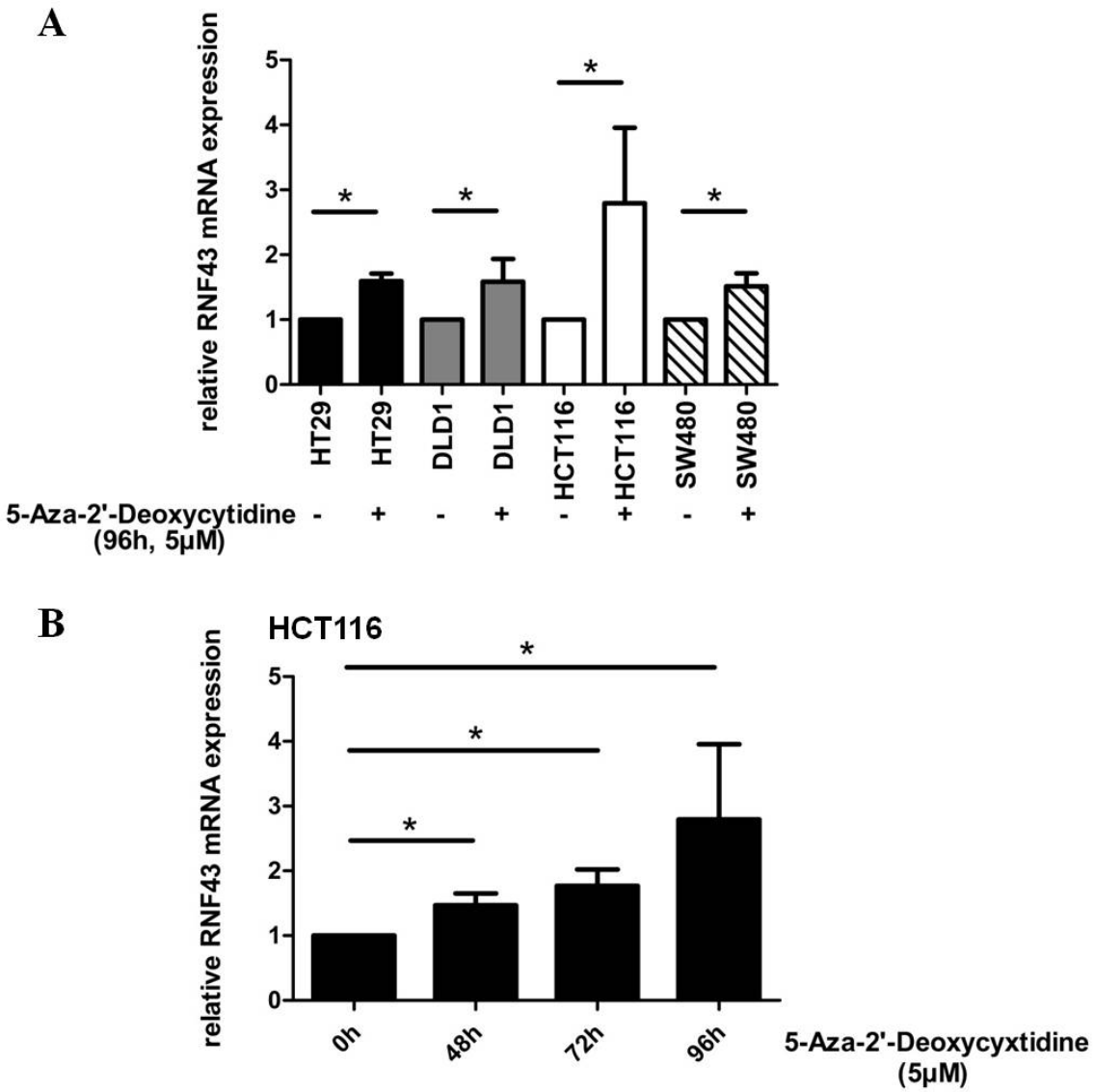

Figure 81 Transcriptional regulation of RNF43 by CpG methyltransferase.
(A) RT-PCR analysis from HCT116, SW480 and DLD1 colon cancer cell lines treated with 5-Aza-2'-Deoxycytidine (5 µM) for 96 h. RT-PCR data are means + S.D. of three (HT29, SW480), four (DLD1) or six (HCT116) independent experiments. (B) Time dependency of transcriptional regulation of RNF43 by CpG methyltransferase. RT-PCR analysis was conducted using RNAs from HCT116 cells treated with 5-Aza-2'-Deoxycytidine (5 µM). RT-PCR data are means + S.D. of three (48 h, 72 h) or six (96 h) independent experiments. (A, B) Data were normalized to GAPDH and to the untreated control.

As shown in Figure 81A, treatment of the colon cancer cell lines HT29, DLD1, HCT116 and SW480 with the agent 5-Aza-2'-Deoxycytidine blocking DNA methylation resulted in an increase in the levels of RNF43 mRNA in all tested cell lines. HCT116 cells were most responsive to the induction of RNF43 mRNA expression by 5-Aza-2'-dCyt. The increase in the level of RNF43 mRNA was time-dependent, as shown for HCT116 cells in Figure 81B.

Thus, an epigenetic alteration is involved in the transcriptional repression of *RNF43* gene.

3.5.2 High RNF43 mRNA expression is correlated with poor prognosis of tumor patients

As visible in Figure 19, RNF43 mRNA expression was low in normal muCos7a as compared to the expression in most colon cancer tumor samples. In contrast, tumor stage IV samples exhibited the highest levels of RNF43 expression. The expression of RNF43 in tumor stage II samples was variable and largely differed between the individual samples, indicating a more heterogeneous expression of RNF43 in tumor stage II samples.

The variation in tumor stage II samples regarding RNF43 mRNA expression was very high (Figure 82). RNF43 mRNA levels were elevated in only some tumor stage II samples, possibly due to present mutations in other proteins or deregulated signaling pathways. In order to further investigate the heterogeneous expression of RNF43 in tumor stage II samples and to perhaps identify a prevalent factor or deregulated signaling cascade, like a mutation in a tumor-associated protein or an upregulated signaling pathway that may influence RNF43 mRNA expression, a larger pool of tumor stage II samples was subjected to RNF43 mRNA expression analysis. Therefore, 186 colon cancer tumor stage II samples as well as four normal muCos7a samples were subjected to quantitative RT-PCR analysis using specific primers for RNF43 detection. Samples exhibiting abnormal melting curves, possibly through low quality of the cDNA, were excluded from the calculation, resulting in 142 tumor stage II samples suitable for analysis.

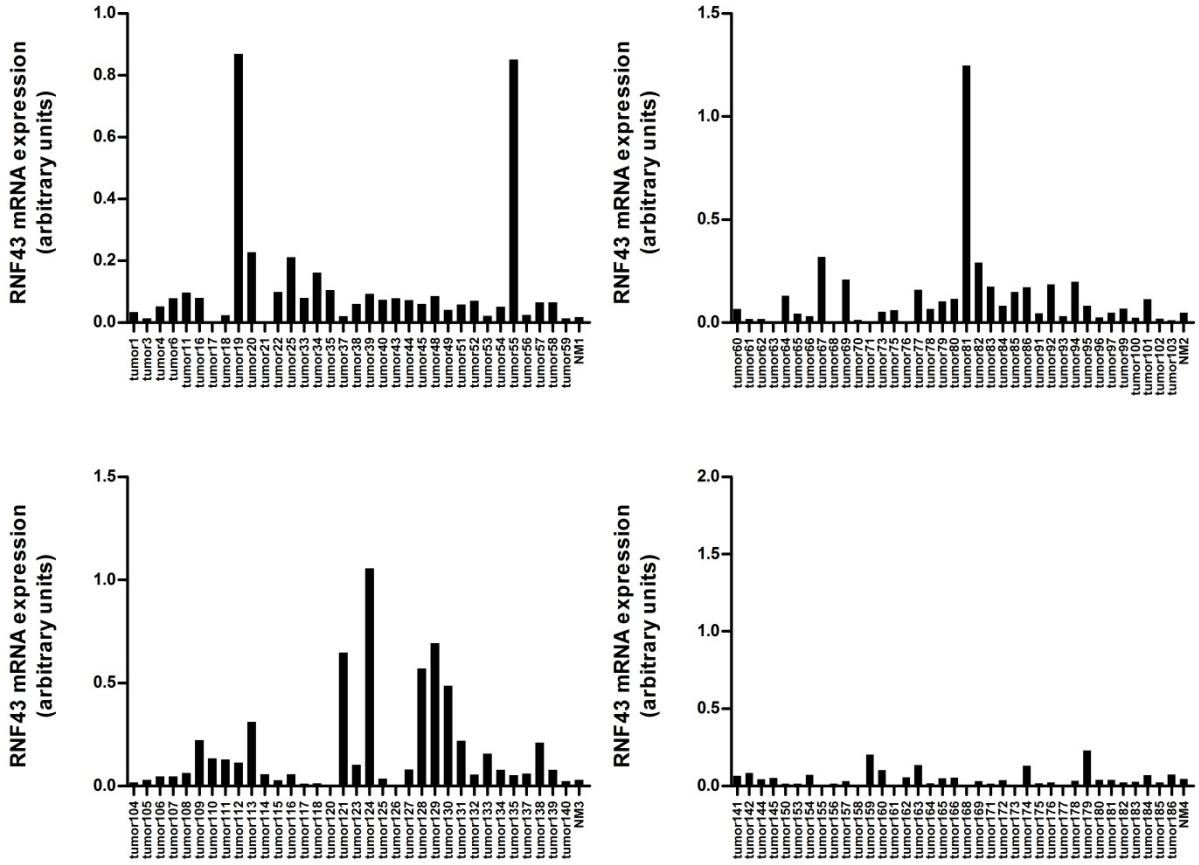

Figure 82 RNF43 mRNA expression in 142 human colon cancer stage II samples as well as in 4 normal muCos7a (NM) samples.
Quantitative RT-PCR analysis using specific primers for RNF43 and GAPDH detection was performed. Results were normalized to GAPDH expression. RT-PCR was performed two times and data shown are means + S.D. of two RT-PCRs.

In accordance with the heterogeneous RNF43 mRNA expression levels observed in tumor stage II samples illustrated in Figure 19, the expression of RNF43 mRNA in a larger pool of tumor stage II samples also exhibited large differences between the individual samples (Figure 82).

When comparing the RNF43 mRNA expression in tumor stage II samples of different grading, expression was higher in tumor stage II grade 2 and 3 samples as compared to grade 4 samples and samples of the normal muCos7a (Figure 83). Nevertheless, the differences between the individual samples of tumor stage II samples of the same grade were very high and thus exhibited a very high standard deviation (Figure 83).

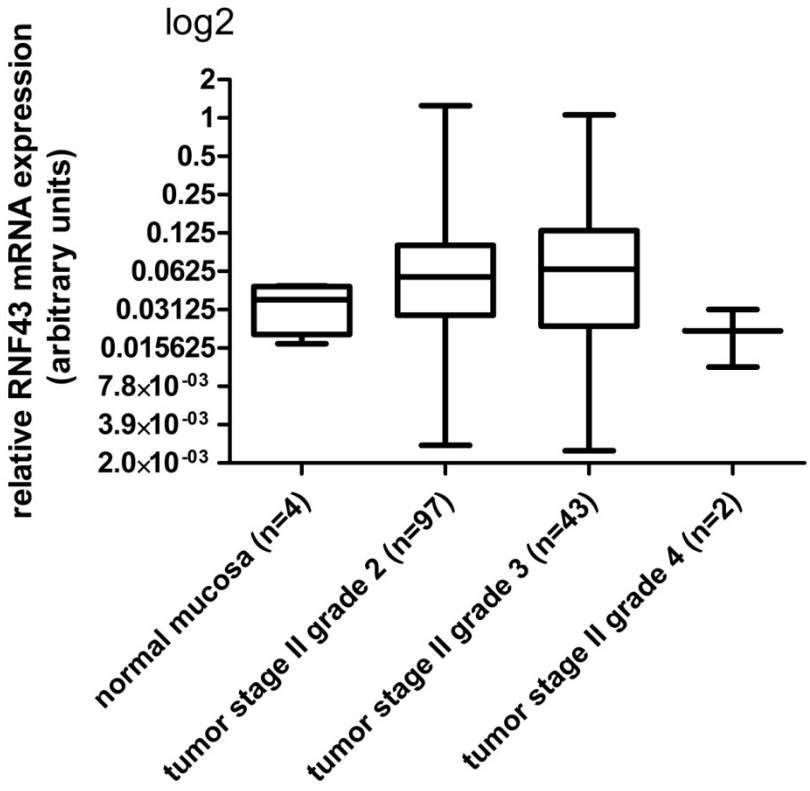

Figure 83 RNF43 mRNA expression in tumor stage II samples.
RNF43 mRNA expression in tumor stage II samples grade 2 (n = 97), grade 3 (n = 43) and grade 4 (n = 2) as well as normal muCos7a (n = 4) samples (log2 scale).

Due to the high variations in RNF43 mRNA levels in the individual samples of tumor stage II samples of the same grade, there was no statistically significant difference in the levels of RNF43 mRNA expression between early and advanced tumor stage II samples. Thus, other factors than grading, for instance mutations in various genes or deregulated signaling cascades, are likely to influence RNF43 expression levels in tumor stage II samples.

126 of the 142 RNF43 mRNA expression values of tumor stage II samples were subsequently subjected to statistical analysis by Dr. Ulrich Nitsche and Prof. Dr. Klaus-Peter Janssen.

In order to identify a possibly correlation between RNF43 mRNA expression and molecular as well as clinical markers, several parameters like age, sex, tumor grading, mutations in tumor markers and mismatch repair (MMR) status were examined applying the Spearman-Rho test, a non-parametric method for correlation. Analysis identified a significant ($p = 0.48$) positive correlation between RNF43 mRNA expression in tumor stage II samples and the sex of the patients. Female patients exhibited higher RNF43 mRNA expression in tumors than male patients. In contrast, RNF43 mRNA expression and molecular markers such as *BRAF* or

KRAS gene mutations, or mutations in MMR genes resulting in MSI, did not significantly correlate with RNF43 mRNA expression. Thus, no correlation of RNF43 mRNA expression with mutations of common oncogenes could be shown.

The 126 tumor stage II samples were subsequently subjected to conditional Monte Carlo testing. An estimated cutpoint was determined, and Kaplan-Meier analyses were performed in order to investigate a possible correlation between RNF43 mRNA expression and metastasis, survival and relapse after surgery (Figure 84).

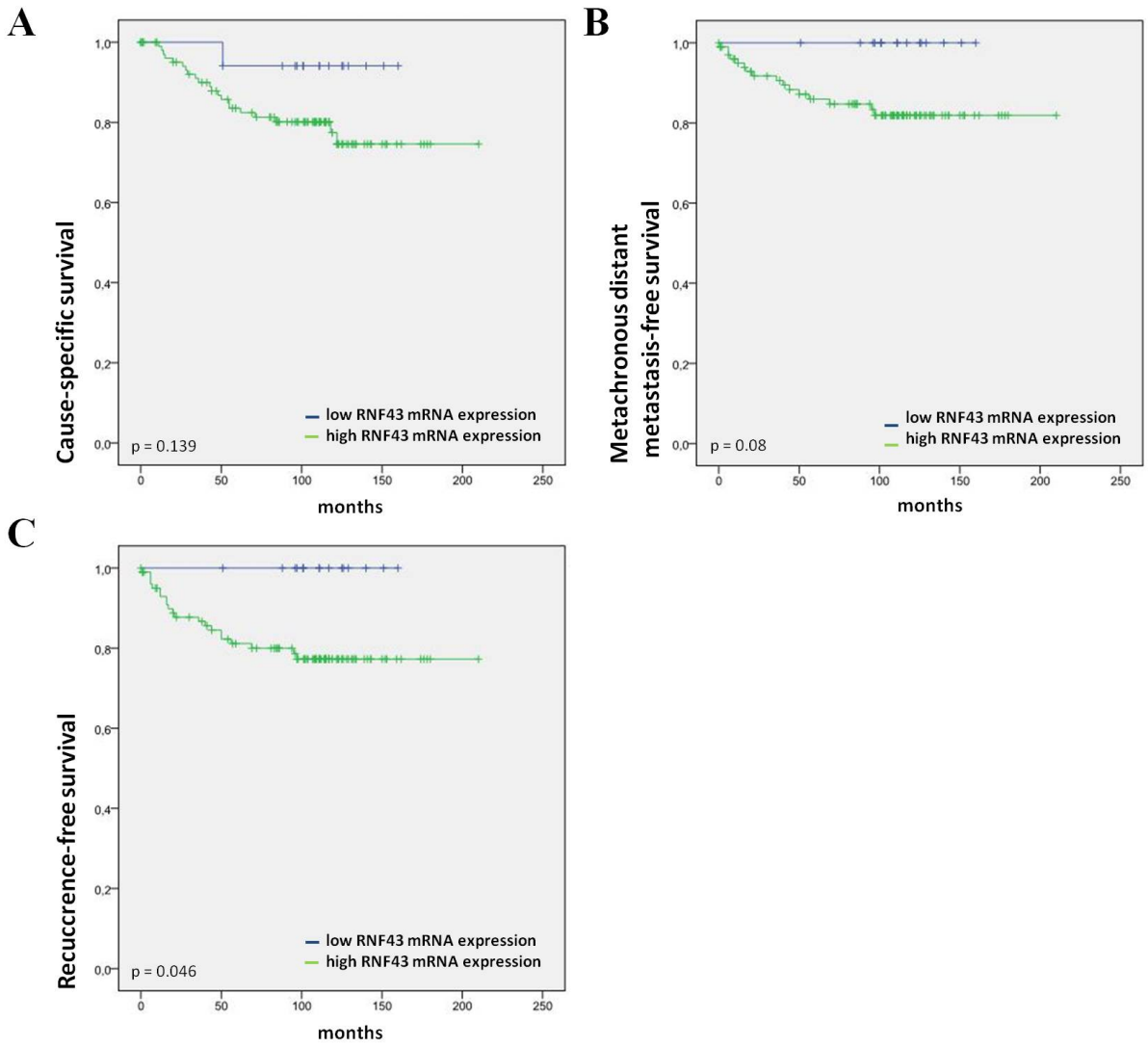

Figure 84 Poor prognosis of patients with tumors exhibiting high RNF43 mRNA expression levels. Kaplan-Meier analyses of the showing differences in (A) survival, (B) metachronic metastasis and (C) relapse after surgery between the low RNF43 mRNA expression group and the high RNF43 mRNA expression group of 126 patients. The p-value was calculated by the log-rank (Mantel-Cox) test.

As illustrated in Figure 84A and B, although no significance could be shown, there was a clear tendency towards lower survival rates and more frequent metachronic metastasis upon higher RNF43 mRNA expression levels in tumors.

In addition, there was a significant ($p = 0.046$) positive correlation between RNF43 mRNA expression and relapse after surgery. The higher RNF43 mRNA expression level was detected in tumor samples, the more often tumors recurred after surgery (Figure 84C).

Thus, there was a correlation between high RNF43 mRNA expression in tumors and poor prognosis of patients.

Since poor prognosis is commonly associated with high Wnt signaling activity, and since mutated RNF43 was shown to transactivate Wnt signaling (3.2.1), the presence of mutated RNF43 instead of wildtype RNF43 in these tumors would explain the poor prognosis of patients with tumors with high RNF43 mRNA levels. Thus, the next aim was to investigate the mutational status of the *RNF43* gene sequence in cell lines as well as in different tumor stage II and stage IV samples.

3.5.3 RNF43 is mutated in tumors

Recently, the *RNF43* gene was shown to exhibit inactivating mutations in several forms of neoplastic cysts (intraductal papillary mucinous neoplasms, IPMNs; mucinous cystic neoplasms, MCNs) in the pancreas. The mutations were base pair substitutions resulting in nonsense or missense codons, thus in truncated proteins, mostly in the N-terminal part of the *RNF43* gene. Wu et al. suggested that because of this preponderance of mutations resulting in inactive RNF43 protein, RNF43 may be a suppressor of both IPMNs and MCNs (Wu, Jiao et al. 2011). Furukawa et al. identified another mutation within the *RNF43* gene sequence. In IPMNs of the pancreas, they found an insertion of a nucleotide (cytosine) resulting in a frameshift at amino acid position 311, which is located inside the RING domain. (Furukawa, Kuboki et al. 2011).

Regarding mutations in colon cancer cell lines, Ivanov et al. found the *RNF43* gene sequence to be mutated in HCT116 and SW48 colon cancer cell lines. In both cell lines, they identified 3 deletions of 1 - 2 nucleotides in the *RNF43* sequence, resulting in frameshifts in amino acids 114 - 6, thus upstream of the RING domain, resulting in a fast nonsense-mediated degradation of RNF43 mRNA (Ivanov, Lo et al. 2007).

In addition, a mutation map of RNF43 was found at the "Tumor T cell antigen database (TANTIgen)"[15], which is a data source and analysis platform for cancer vaccine target discovery. The TANTIgen database illustrated five further mutations of the *RNF43* gene sequence (Figure 89).

Thus, there were several hints pointing towards a function of RNF43 as a tumor suppressor in normal tissue that may be lost upon mutations in pancreas (Furukawa, Kuboki et al. 2011; Wu, Jiao et al. 2011). Furthermore, an N-terminal frameshift was found in HCT116 colon cancer cells (Ivanov, Lo et al. 2007).

Therefore, the next aim was to investigate the *RNF43* gene sequence in colon cancer cell lines and in intestinal tumor samples, in order to identify additional putative mutations. Since *RNF43* was shown to be mainly mutated in the N-terminal region of the *RNF43* sequence in pancreas (Wu, Jiao et al. 2011), and since the N-terminus was evolutionary conserved to a higher extend than the C-terminus (Figure 15), mutation analysis of the first ~1000 nucleotides of the N-terminal sequence of *RNF43* was performed during this study.

Therefore, the N-terminal *RNF43* gene sequences were amplified by PCR from cDNA templates. Amplified sequences were cloned into pGEM®-T and sent for sequencing using T7 and SP6 primers, as described in 2.2.11. The resulting sequences were then analyzed by comparison of the obtained sequences with the annotated human *RNF43* sequence (NM_017763.4).

Using this approach, the N-terminal sequences of frequently used colon cancer cell lines (HCT116, LS174T, DLD1, SW480 and HT29) as well as HEK293T and Cos7 cells were investigated. In addition, several colon cancer samples (5 tumor stage II cDNA samples and 3 tumor stage IV cDNA samples) were included in the analysis.

Sequencing of *RNF43* gene sequences of cell lines revealed several previously unknown mutations, which are displayed in Figure 85.

[15] cvc.dfci.harvard.edu/cvccgi/tadb/displayFile.pl?FILE=RNF43

Cell lines

A LS174T

Wildtype, 5′→3′

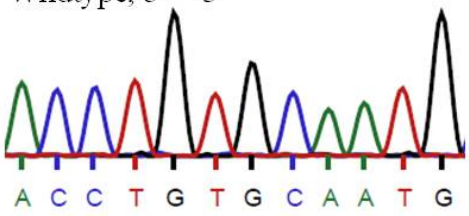

LS174T: p.**C**91**Y** (G272→A) 5′→3′

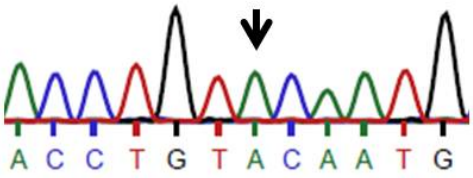

B DLD1

Wildtype, 5′→3′

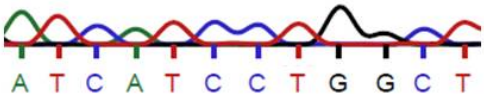

DLD1: p.**L**214**M** (C641→A) 5′→3′

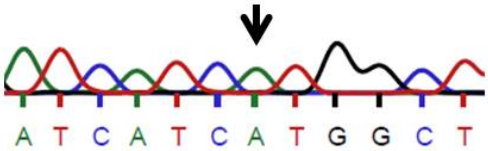

C SW480

Wildtype, 5′→3′ 3′→5′

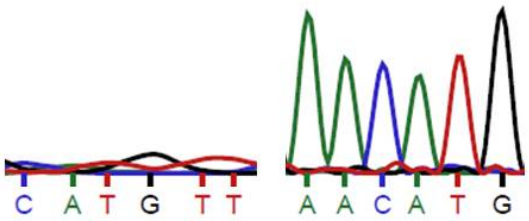

SW480: p.**M**313**I** (G939→A)
5′→3′ 3′→5′

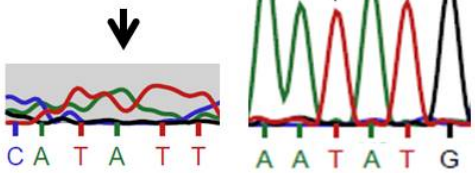

Wildtype, 5′→3′ 3′→5′

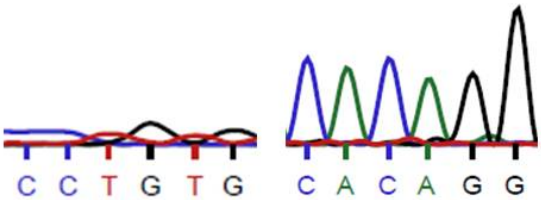

SW480: p.**P**270**P** (T810→G)
5′→3′ 3′→5′

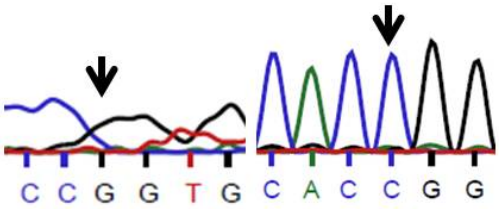

D HCT116

Wildtype, 5′→3′

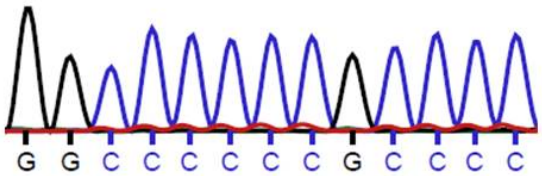

HCT116: 5′→3′
(del. of C in $(C)_6$ nt 343-8→
frameshift in aa114-6; p.**A**114-6**fs**)

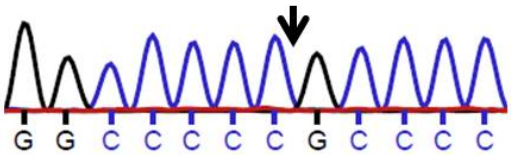

Wildtype, 5′→3′

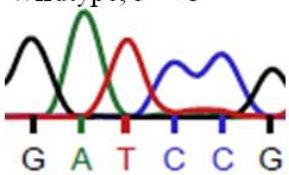

HCT116: p.**P**231**L** (C692→T) 5′→3′

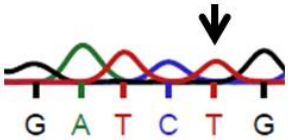

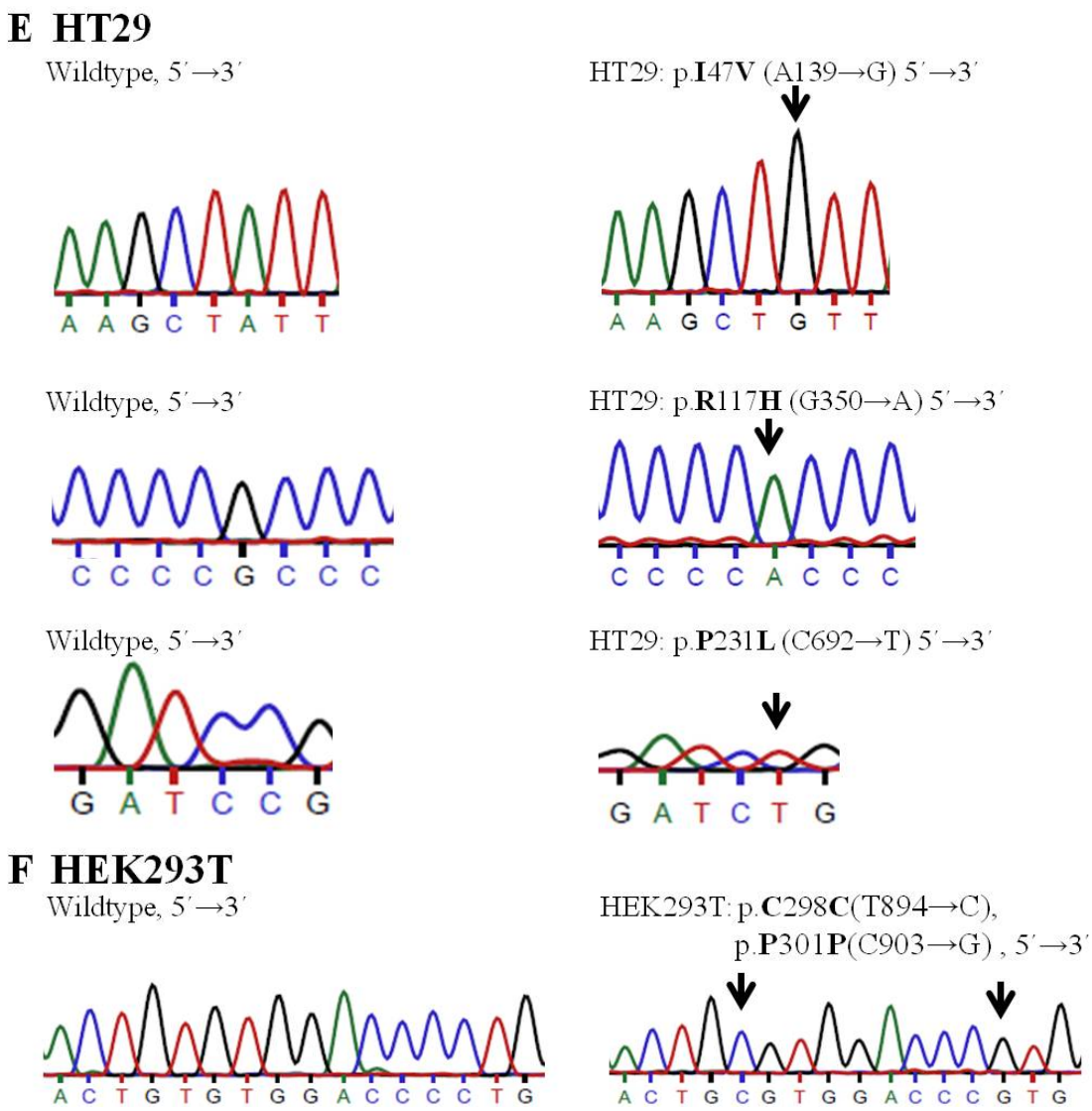

Figure 85 Mutations of the N-terminal *RNF43* gene sequence in different cell lines.

A huge variety of mutations was found in the *RNF43* gene sequence of different cell lines. In the colon cancer cell line DLD1, a nucleotide exchange in the RNF43 sequence from C to A at the nucleotide at position 641 resulted in an exchange of amino acid 214 from leucine (L) to methionine (M), p**L**214**M** (C641→A).

In SW480 colon cancer cells, two mutations were found. A nucleotide exchange from T to G at position 810 did not alter the amino acid proline (P) at position 270, p**P**270**P** (T810→G), but a second mutation, a nucleotide exchange from G to A at position 939 caused an exchange of amino acid 313 from M (methionine) to I (isoleucine), p**M**313**I** (G939→A) .

In LS174T colon cancer cells, a nucleotide exchange from G to A at position 272 resulted in an exchange of amino acid 91 from cysteine (C) to tyrosine (Y), p**C**91**Y** (G272→A).

In HCT116 colon cancer cells, a nucleotide exchange from C to T at position 692 caused an exchange of amino acid 231 from proline (P) to lysine (L). In addition, a deletion of nucleotide C in $(C)_6$ at position 343-8 introduced a frameshift at amino acids 114-6, p114-6**fs**.

In HEK293T human embryonic kidney cells, only one nucleotide exchange was found. This nucleotide exchange from T to C at position 894 did not alter the amino acid cysteine (C) at position 298, p**C**298**C** T894→C).

Although Cos7 cells were originally derived from African green monkey, and the sequence of the *RNF43* gene in African green monkey was not annotated so far, the sequence of *RNF43* in Cos7 cells was subjected to sequence analysis and compared to the annotated human *RNF43* gene sequence (NM_017763.4). Although sequences of humans and monkeys are usually very similar, there were several differences between the *RNF43* sequence in Cos7 cells and in humans. In addition to minor differences in the nucleotide sequence of *RNF43* in Cos7 cells, 110 nucleotides (nucleotides 573 - 682) were missing, when comparing the sequencing results to the annotated human *RNF43* sequence. The absent nucleotides were part of the human Exon 6 and were located N-terminally of the RING domain. Thus, the entire RNF43 RING domain was present in the *RNF43* sequence in Cos7 cells, and no differences were found between the RNF43 RING domain sequence between monkey and human, indicating evolutionary conservation. Nevertheless, a frameshift due to the absent nucleotides may cause an ablation of the RNF43 RING domain or a nonsense protein sequence, and the absence of a functional RNF43 protein in Cos7 cells cannot be excluded.

In HT29 colon cancer cells, different mutations in the *RNF43* gene sequence were found. cDNA amplification of the N-terminal 1000 basepairs, cloning into pGEM®-T and sequencing of 6 different obtained clones resulted in different *RNF43* gene sequence mutations.

In clones 1 and 4, a nucleotide exchange from C to T at position 692 caused an exchange of amino acid 231 from proline (P) to lysine (L), p**P**231**L** (C692→T), which was the same mutation found in the *RNF43* gene sequence of HCT116 cells.

In clones 2, 3, 5 and 6, a nucleotide exchange from A to T at position 139 caused an exchange of amino acid 47 from isoleucine (I) to valine (V), p**I**47**V** (A130→T). In addition, a nucleotide exchange from G to A at position 350 changed the amino acid at position 117 from arginine (R) to histidine (H), p**R**117**H** (G350→A).

Thus, in HT29 colon cancer cells either a p**P**231**L** (C692→T) mutation, or a p**I**47**V** (A130→T) mutation in combination with a p**R**117**H** (G350→A) mutation is prevalent in all investigated sequences, suggesting that the two alleles may possibly harbor different mutations in the *RNF43* gene sequence.

Since many mutations were found in the N-terminal part of the *RNF43* gene sequence of HT29 cells, it was further investigated whether there were more nonsense or missense mutations, or frameshifts in the residual C-terminal part of the *RNF43* gene sequence of HT29 cells. Therefore, the C-terminal part of the *RNF43* sequence was amplified by PCR, cloned into pGEM®-T and sequenced, as described in 2.2.11. Sequencing results showed that like in the N-terminus, neither frameshifts nor missense mutations were present in the C-terminal part of the *RNF43* gene sequence. Nevertheless, a nucleotide exchanges was identified, which caused an amino acid exchange at position 770. This amino acid exchange resulted from nucleotide exchange at position 2309, where a nucleotide exchange from G to A caused an amino acid exchange from glycine (G) to aspartic acid (D) at position 770, p**G**770**D** (G2309→A) (data not shown). Thus, in HT29 colon cancer cells, sequencing results revealed a high incidence of variations through mutations in the *RNF43* gene sequence.

In addition to the *RNF43* gene sequences in cell lines, N-terminal parts of the *RNF43* gene sequence of five tumor stage II samples and three tumor stage IV samples were analyzed. Sequencing of *RNF43* gene sequences of tumor samples exhibited several previously unknown as well as previously identified mutations, which are displayed in Figure 86 and Figure 88.

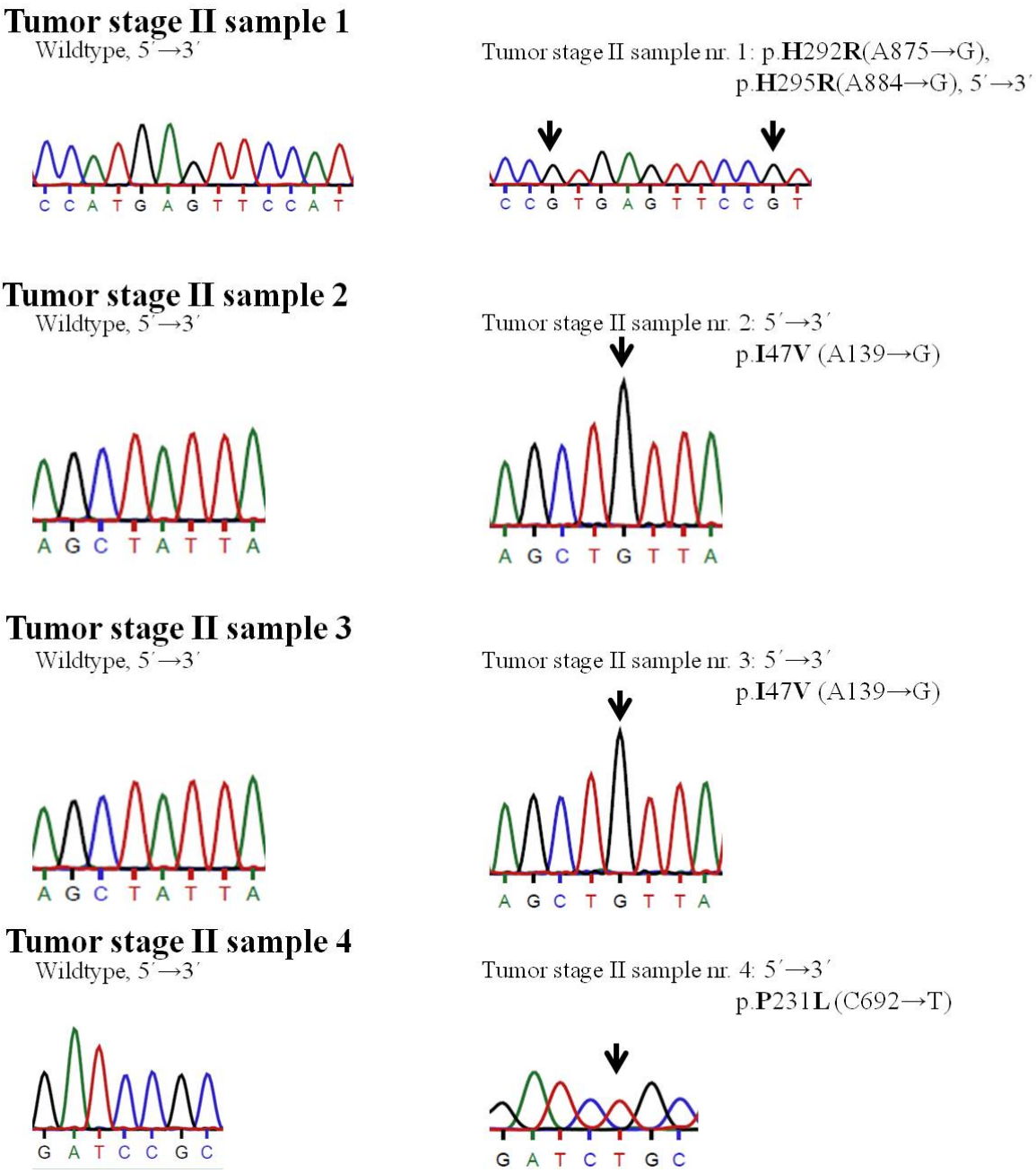

Figure 86 Mutations of the N-terminal *RNF43* gene sequence in tumor stage II samples.

In tumor stage II sample number 1, two mutations were found. The first mutation was a nucleotide exchange from A to G at nucleotide position 875, resulting in an amino acid exchange from histidine (H) to arginine (R) at amino acid position 292, p.**H**292**R** (A875→G). The second mutation was another nucleotide exchange from A to G at position 884, resulting in another amino acid exchange from histidine (H) to arginine (R) at amino acid position 295, p.**H**295**R** (A884→G). Interestingly, these two mutations are the same mutations that were introduced by mutagenesis into the *RNF43* sequence in order to functionally inactivate the

RING finger protein, indicating that the these mutations in the RNF43 sequence result in a protein which, in contrast to the wildtype protein, is functionally unable to negatively influence Wnt signaling activity, but rather transactivates Wnt signaling.

In order to confirm the mutations p.**H**292**R** and p.**H**295**R** found in the tumor stage II sample nr. 1 and in order to exclude the possibility that they originate from contaminations with a RNF43mut- plasmid during the PCR preparation process, the RING domain of RNF43 was again amplified from the cDNA using the primers 700se and 1391as. In addition, as a control, the same primers were used for amplification of the same region of an RNF43-flag wildtype plasmid. Internal negative controls (ddH_2O) were also included in the experiment, in order to be able to exclude unspecific amplification.

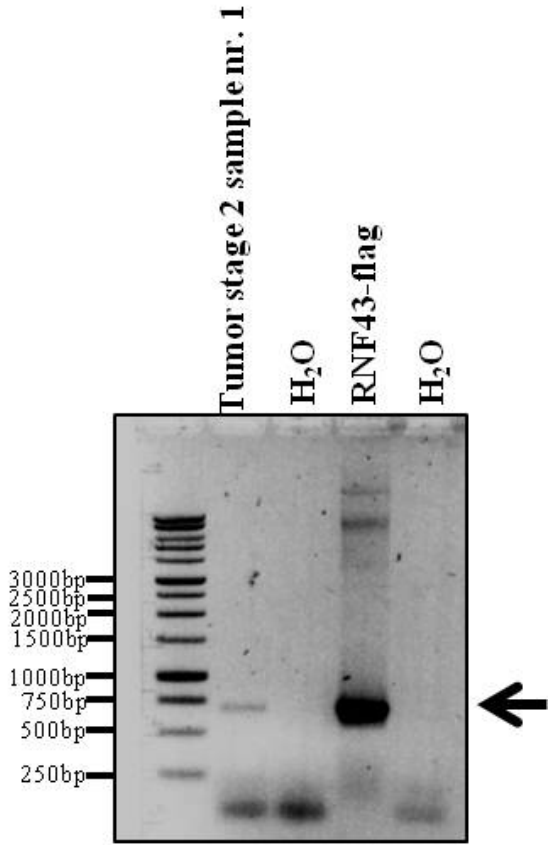

Figure 87 Agarose gel showing the amplified PCR products.
PCR products of a size of 691 bp (including the RING domain of RNF43), amplified from cDNA of tumor stage II sample nr. 1 (PCR 1) or a wildtype RNF43-flag plasmid (PCR 3) using the primers 700se and 1391as. Internal negative controls (ddH_2O) after PCR1 as well as after PCR 3 were included in the experiment (PCR 2 and PCR 4). PCR products were separated on a 1 % agarose gel.

No unspecific amplifications were observed in the negative controls (ddH_2O), but clearly visible PCR products appeared in the PCR samples where cDNA of tumor stage II sample nr. 1 and RNF43-flag were used as templates (Figure 87).

The two resulting PCR products (691 bp) in PCRs 1 and 3 (visible in Figure 87) were excised from the gel. DNA was extracted and subsequently cloned into pGEM®-T. Sequence analysis was performed as described in 2.2.11. Sequence analysis confirmed the p.**H**292**R** and p.**H**295**R** mutations in the tumor stage II sample nr. 1, whereas these mutations were not found in the RNF43-flag wildtype plasmid. Hence, the mutations identified in the tumor stage II sample nr. 1 could be confirmed and do not originate from a contamination.

Thus, the mutations that were introduced into the *RNF43* gene sequence *in vitro*, which resulted in an RNF43 mutant capable of activating Wnt signaling activity, were also identified *in vivo* in a tumor stage II sample.

In tumor stage II samples nr. 2 and 3 (Figure 86), a nucleotide exchange from A to T at position 139 resulted in an exchange of amino acid 47 from isoleucine (I) to valine (V), p**I**47**V** (A130→T). The same mutation was already observed in the *RNF43* gene sequence of HT29 cells.

In tumor stage II sample number 4, a nucleotide exchange from C to T at position 692 resulted in an exchange of amino acid 231 from proline (P) to lysine (L), p.**P**231**L** (C692→T), a mutation already observed in both HT29 and HCT116 colon cancer cell lines.

Tumor stage II sample number 5 did not exhibit any mutations in the N-terminal region of *RNF43*. Nevertheless, mutations cannot be excluded, since the C-terminal part was not investigated.

Thus, several mutations were identified in the N-terminus of the *RNF43* gene sequence of tumor stage II samples. Similarly, *RNF43* was frequently mutated in tumor stage IV samples. Mutations identified in the N-terminal part of the *RNF43* gene sequence observed in tumor stage IV samples are displayed in Figure 88.

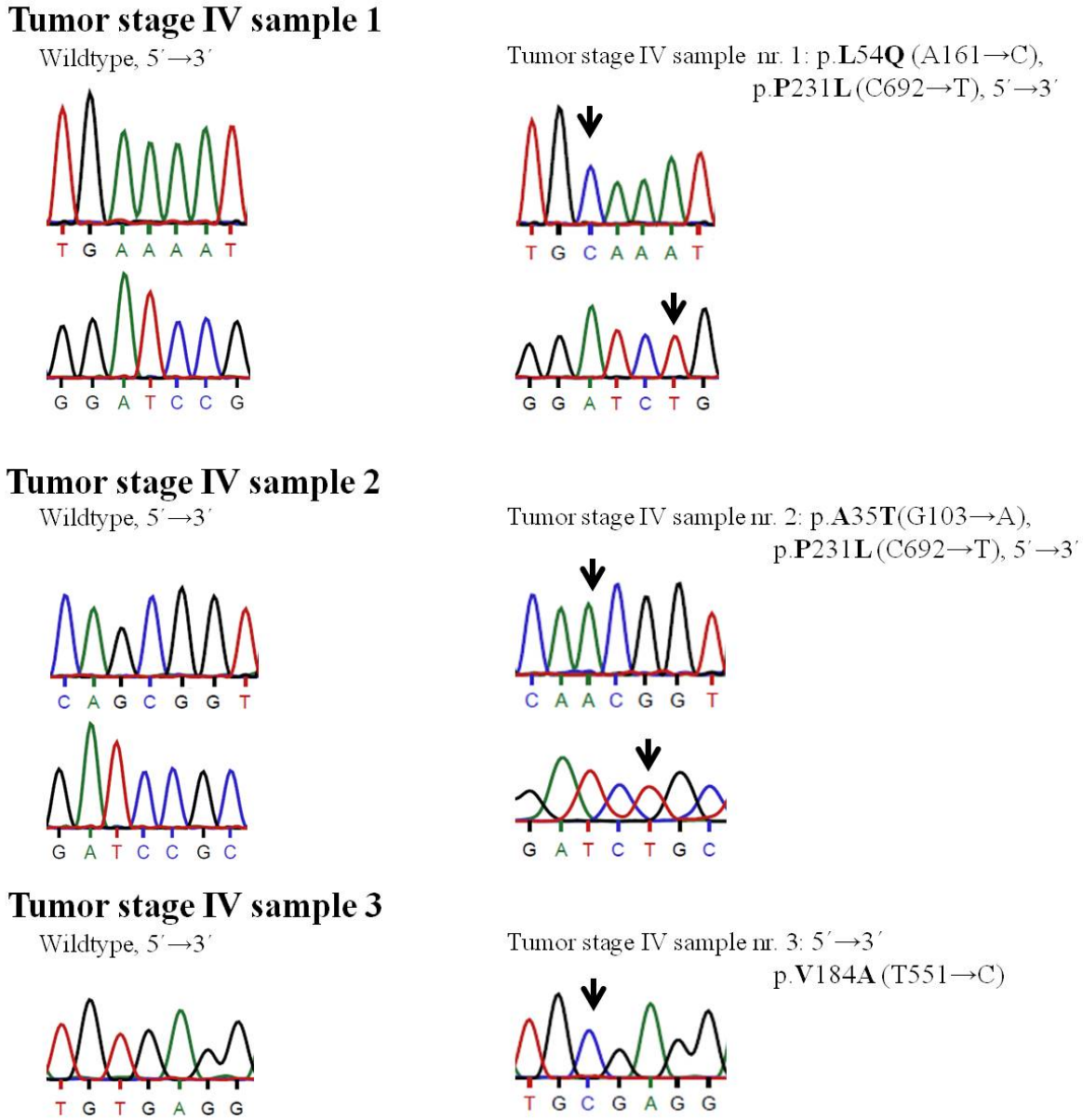

Figure 88 Mutations of the N-terminal *RNF43* gene sequence in tumor stage IV samples.

As illustrated in Figure 88, analysis of the *RNF43* gene sequence in tumor stage IV sample number 1 revealed two mutations. The first mutation was a nucleotide exchange from A to C at position 161, resulting in an amino acid exchange from lysine (L) to glutamine (Q) at position 54, p.**L**54**Q** (A161→C). The second mutation was a nucleotide exchange from C to T at position 692, resulting in an amino acid exchange from proline (P) to lysine (L) at position 231, p.**P**231**L** (C692→T).

In tumor stage IV sample number 2, two mutations were found. The first mutation was a nucleotide exchange from G to A at position 103, resulting in an amino acid exchange from alanine (A) to threonine (T) at position 35, p.**A**35**T** (G103→A). The second mutation was

again a nucleotide exchange from C to T at position 692, resulting in an amino acid exchange from proline (P) to lysine (L) at position 231, p.**P**231**L** (C692→T), a mutation already observed in HT29 cells, HCT116 cells, tumor stage II sample number 4 and tumor stage IV sample number 1.

Tumor stage IV sample number 3 exhibited only one mutation, a nucleotide exchange from T to C at position 551, which is a mutation causing an amino acid exchange from valine (V) to alanine (A), p.**V**184**A** (T551→C). This mutation was not found in any other cell line or tumor sample.

All *RNF43* mutations identified during this study, as well as mutations previously published by other groups, are illustrated in Figure 89.

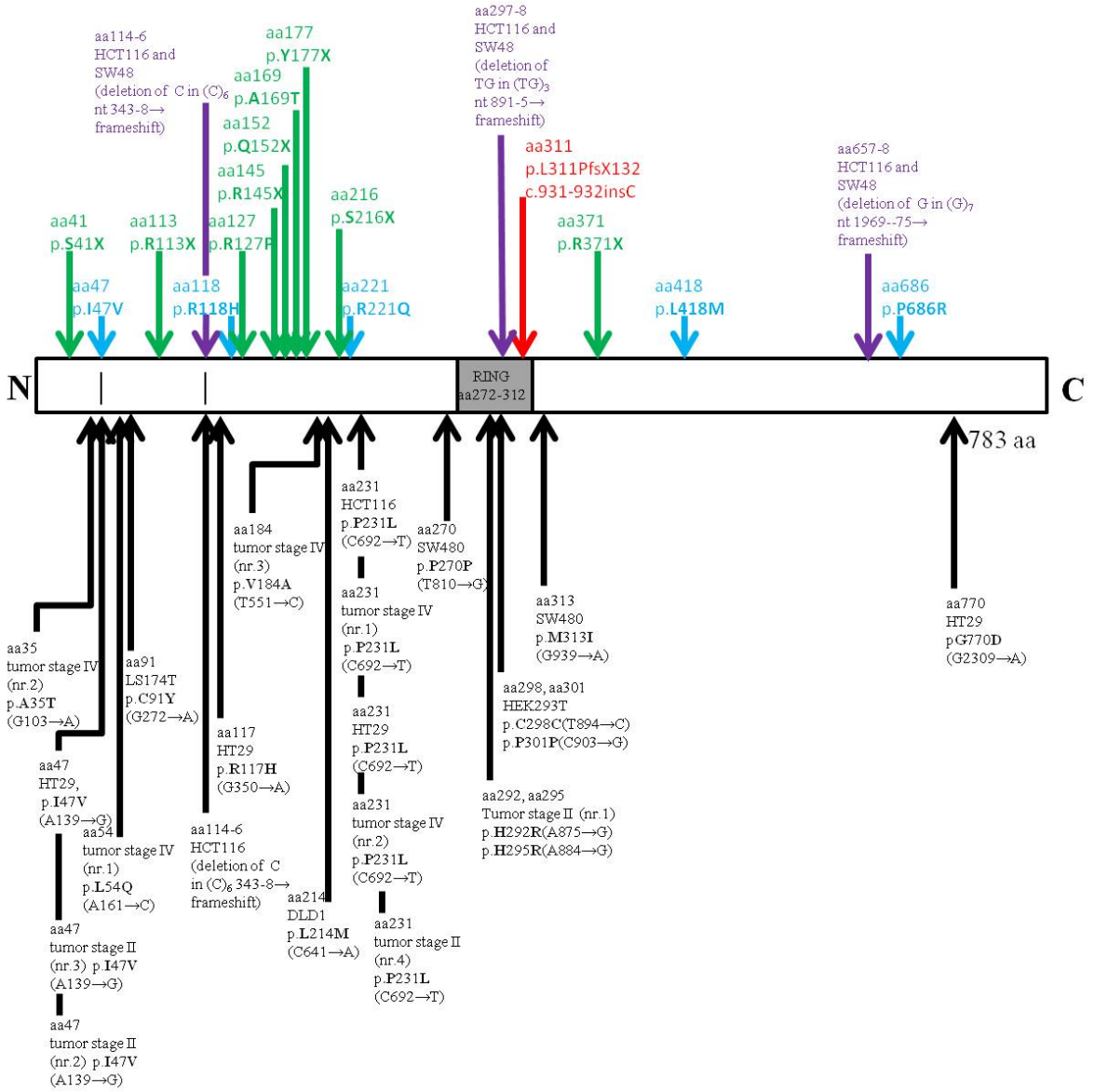

Figure 89 Mutation analysis of the *RNF43* gene sequence.
The *RNF43* mutations found during this study are highlighted with black arrows (mutations found in HCT116, SW480, DLD1, and HEK293T cell lines and in tumor stage II and IV samples). Mutations of the *RNF43* gene sequence found in colon cancer cell lines and pancreas neoplastic cysts and described in other studies are accentuated with green (Wu, Jiao et al. 2011), blue ("TANTIgen: Tumor T cell antigen database"[16]), red (Furukawa, Kuboki et al. 2011) or purple (Ivanov, Lo et al. 2007) arrows.

Two mutations in the *RNF43* gene sequence identified during this study correspond to mutations previously characterized in other studies. The first one, resulting in an isoleucine to valine exchange at amino acid position 47, which was found during this study in HT29 cells and in two tumor stage II samples, was described before in the previously mentioned

[16] cvc.dfci.harvard.edu/cvccgi/tadb/displayFile.pl?FILE=RNF43

"TANTIgen" mutation map of RNF43[17]. The other mutation that was identified during this study and corresponds to a previously published study (Ivanov, Lo et al. 2007), is a frameshift in the *RNF43* gene sequence of HCT116 cells resulting from a deletion of nucleotide C in $(C)_6$ at position 343 - 8. The deletion of the C nucleotide introduced a frameshift at amino acids 114 - 6, resulting in a fast nonsense-mediated RNF43 mRNA decay (Ivanov, Lo et al. 2007).

During this study, the mutation at amino acid position 231, resulting in an amino acid exchange from proline to lysine, was found in HT29 and HCT116 cells, and was additionally present in two tumor stage IV samples and one tumor stage II sample. Furthermore, the mutation resulting in an amino acid exchange at position 47 was found very frequently (in HT29 and in two tumor stage II samples) during this analysis. Together, these data indicate important functional roles for the amino acids 47 and 231 of RNF43.

Only in one out of five tumor stage II samples, no mutations could be found. Nevertheless, mutations could be downstream of the analyzed N-terminal 1000 nucleotides, which were not analyzed yet. Thus, except of one tumor stage II sample, all analyzed colon cancer cell lines and tumor stage II or IV samples harbored mutations in the N-terminal part of the *RNF43* gene sequence, whereas in HEK293T cells, no nucleotide exchanges resulting in amino acid alterations were found.

Thus, the *RNF43* gene is frequently mutated in colon cancer cell lines and in intestinal tumor samples, resulting in various amino acid exchanges, which may possibly alter protein function.

3.6 RNF43 mice

In addition to the *in vitro* experiments, a lot of work was done with mice in cooperation with Dr. Marlon Schneider (LMU Munich) and Dr. Behnam Kalali (TU Munich).

In cooperation with Dr. Marlon Schneider, a mouse model was generated for the *in vivo* study of the effect of RNF43 *knockout*. Therefore, Dr. Schneider has generated a pL451 construct in which exons 6 and 7 of RNF43 were flanked by loxP sites, followed by a FRT-flanked neomycin cassette. Exons 6 and 7 are the two exons that code for the RING domain. Figure

[17] http://cvc.dfci.harvard.edu/cvccgi/tadb/displayFile.pl?FILE=RNF43

90 illustrates a schematic representation of the strategy for the generation of RNF43 *knockout* mice.

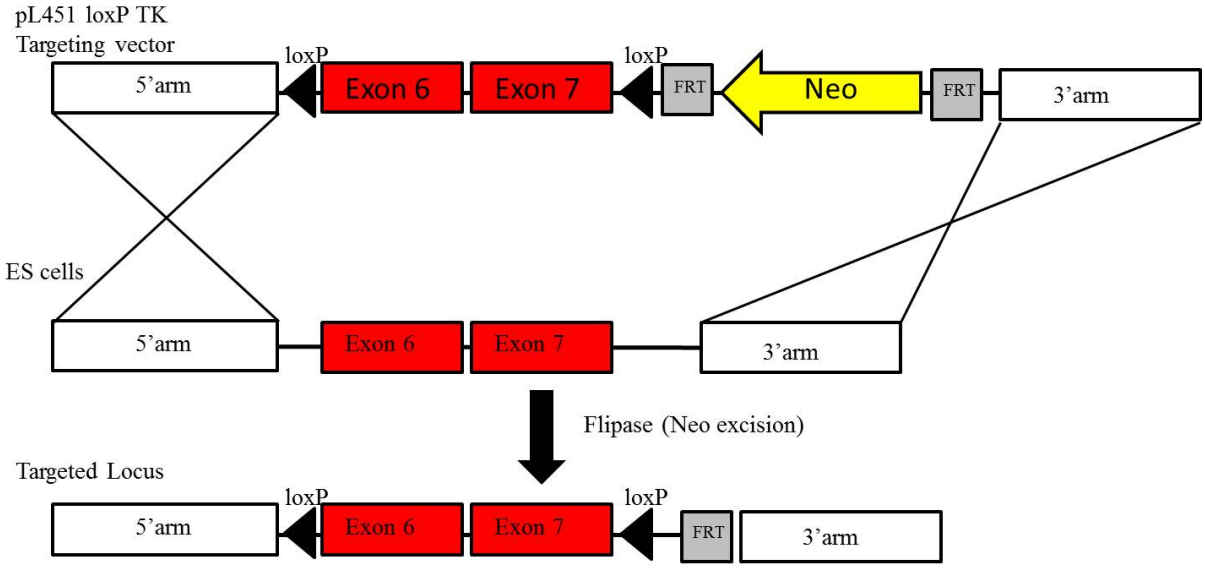

Figure 90 Schematic representation of the targeting strategy for the generation of RNF43 *knockout* mice.

After electroporation of embryonic stem cells (ES cells) using the targeting plasmid pL451, colonies were picked and a recombined clone was identified by PCR and Southern blot. Then, the *neo* cassette, which was inserted to allow selection of the transfected ES cells, was removed by a construct expressing flipase *in vitro*. After again evaluating a positive clone, the clone was used for blastocyst injection. Germline chimeras were obtained and their RNF43 fl/wt progeny were crossed with RNF43 fl/wt mice and Villin-Cre mice, which express a Cre recombinase under the control of a Villin promoter which is specifically active in the intestine (Madison, Dunbar et al. 2002).

Crossings of RNF43 fl/wt x RNF43 fl/wt mice did not result in any RNF43 fl/fl mice. In 7 litters, 37 progeny were obtained. Thereof, 13 RNF43 wt/wt and 24 RNF43 ft/wt mice, but no RNF43 fl/fl mice, were obtained, although 9.25 would have been expected (Table 10). (Expected genotypes: approximately 9.25 RNF43 wt/wt mice, 18.5 RNF43 fl/wt mice and 9.25 RNF43 fl/fl mice).

Actual and expected genotypes of progeny obtained by crossings of RNF43 fl/wt x RNF43 fl/wt mice are listed in Table 10.

CROSSING 1:				
RNF43 fl/wt x RNF43 fl/wt				
parent 1:	RNF43 fl/wt			
parent 2:	RNF43 fl/wt			
number of litters:	7			
genotype (weaning age)	**actual number:**	**actual percentage:**	**expected number:**	**expected percentage:**
RNF43 wt/wt	13 mice	35.14 %	9.25 mice	25 %
RNF43 fl/wt	24 mice	64.86 %	18.5 mice	50 %
RNF43 fl/fl	0 mice	0 %	9.25 mice	25 %
total number of progeny:	**37 mice**			

Table 10 Actual and expected genotypes of progeny obtained by crossings of RNF43 fl/wt x RNF43 fl/wt mice.

Similarly, among the 4 litters and 32 progeny obtained by crossings of RNF43 fl/wt Cre -/- with RNF43 fl/wt Cre +/- mice, no RNF43 fl/fl mice, but 7 RNF43 wt/wt Cre -/- mice, 7 RNF43 fl/wt Cre -/- mice, 7 RNF43 wt/wt Cre +/- mice and 11 RNF43 fl/wt Cre +/- mice were obtained.

Actual and expected genotypes of progeny obtained by crossings of RNF43 fl/wt Cre -/- x RNF43 fl/wt Cre +/- mice are listed in Table 11.

CROSSING 2:				
RNF43 fl/wt, Cre -/- x RNF43 fl/wt, Cre +/-				
parent 1:	RNF43 fl/wt, Cre -/-			
parent 2:	RNF43 fl/wt, Cre +/-			
number of litters:	4			
genotype (weaning age)	**actual number:**	**actual percentage:**	**expected number:**	**expected percentage:**
RNF43 wt/wt, Cre -/-	7 mice	21.875 %	4 mice	12.5 %
RNF43 wt/wt, Cre +/-	7 mice	21.875 %	4 mice	12.5 %
RNF43 fl/wt, Cre -/-	7 mice	21.875 %	8 mice	25 %
RNF43 fl/wt, Cre +/-	11 mice	34.375 %	8 mice	25 %
RNF43 fl/fl, Cre -/-	0 mice	0 %	4 mice	12.5 %
RNF43 fl/fl, Cre +/-	0 mice	0 %	4 mice	12.5 %
total number of progeny:	**32 mice**			

Table 11 Actual and expected genotypes of progeny obtained by crossings of RNF43 fl/wt Cre -/- x RNF43 fl/wt Cre +/- mice.

The data illustrated in Table 11 indicate that even in the absence of a Cre recombinase, the phenotype of RNF43 fl/fl mice is likely to be lethal before birth.

In order to determine the stage of lethality of RNF43 loss, the genotypes of mouse embryos generated by crossings of RNF43 fl/wt x RNF43 fl/wt mice were investigated at different time points during embryonic development. Therefore, 50 embryos were removed from 5 mothers during the first days after fertilization at blastocyste stage together with Dr. Maik Dahlhoff.

Similarly, like in postnatal animals, the RNF43 fl/fl genotype was never observed in early embryos.

These data indicate that the homozygous presence of the knock-in allele leads to early embryonic lethality, possibly due to inactivation of the *RNF43* gene.

Thus, a conditional RNF43 *knockout* mouse model, allowing the deletion of *RNF43* in a time-specific manner will facilitate the investigation of the spatial and temporal roles of RNF43 in both normal development and disease.

3.7 Prospective

3.7.1 Function of RNF43 in cell division

While this thesis was in progress, a new antibody allowing detection of endogenous RNF43 in Immunofluorescence stainings became available (manufacturer: LS Bio).

HT29 cells exhibited the highest RNF43 mRNA expression levels among the colon cancer cell lines (Figure 19) and they were also shown to express endogenous RNF43 protein (Figure 20). Therefore, the subcellular localization of endogenous RNF43 in HT29 cells was investigated by Immunofluorescence stainings, using antibodies directed against endogenous RNF43 (stained in red) and endogenous ß-catenin (visualized in green).

In addition, HCT116, HEK293T and Cos7 cells were included into the experiment, since these cell lines exhibited low levels of RNF43 mRNA expression, and since HEK293T and Cos7 cells additionally did not exhibit any RNF43 protein expression detectable by Western blot analysis (Figure 20).

The antibody recognized an epitope of the RNF43 protein located in the middle of the RNF43 protein sequence, which comprises 783 aa (epitope: aa 504 - 553 of RNF43; amino acid sequence: DFDPLVYCSPKGDPQRVDMQPSVTSRPRSLDSVVPTGETQVSSHVHYHRH).

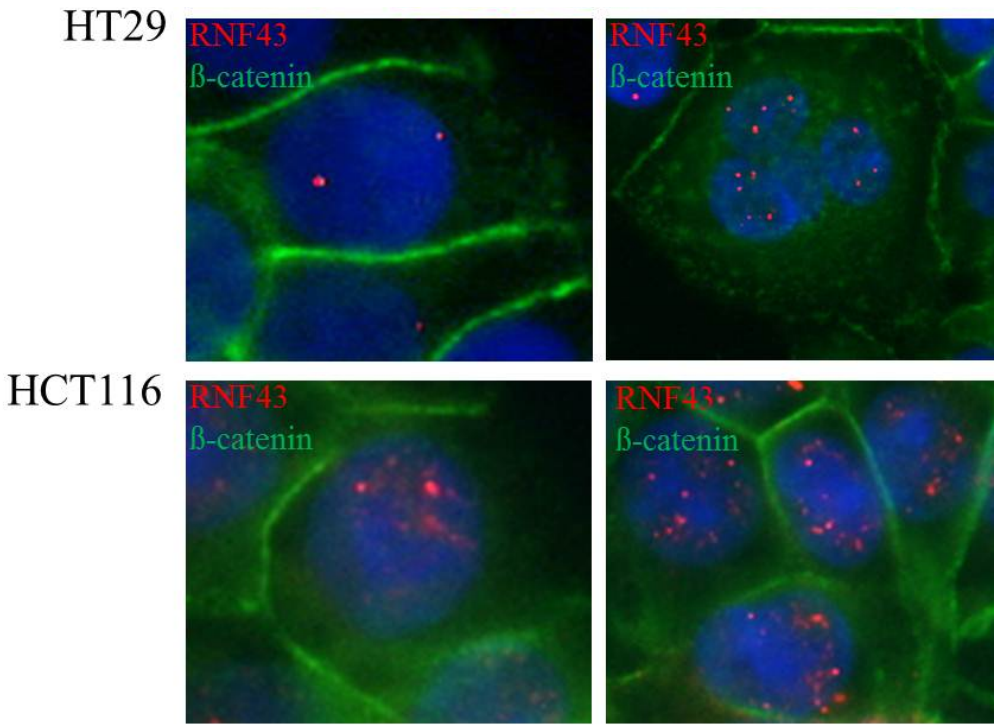

Figure 91 Immunofluorescence stainings of endogenous RNF43 in HT29 and HCT116 cells.
Pictures of Immunofluorescence stainings illustrate DAPI (blue), anti-RNF43 (red) and anti-ß-catenin (green) stainings.

As illustrated in Figure 91, in HT29 and HCT116 cells, endogenous RNF43 mainly localized to the nucleoplasm, where it was visible in two distinct dots, which may represent centrosomal regions. In addition, endogenous RNF43 was also detectable in small punctuate structures throughout the nucleoplasm. In contrast, the negative control (without primary antibody), did not exhibit any staining (data not shown).

Immunofluorescence stainings of endogenous RNF43 in HEK293T and Cos7 are illustrated in Figure 92.

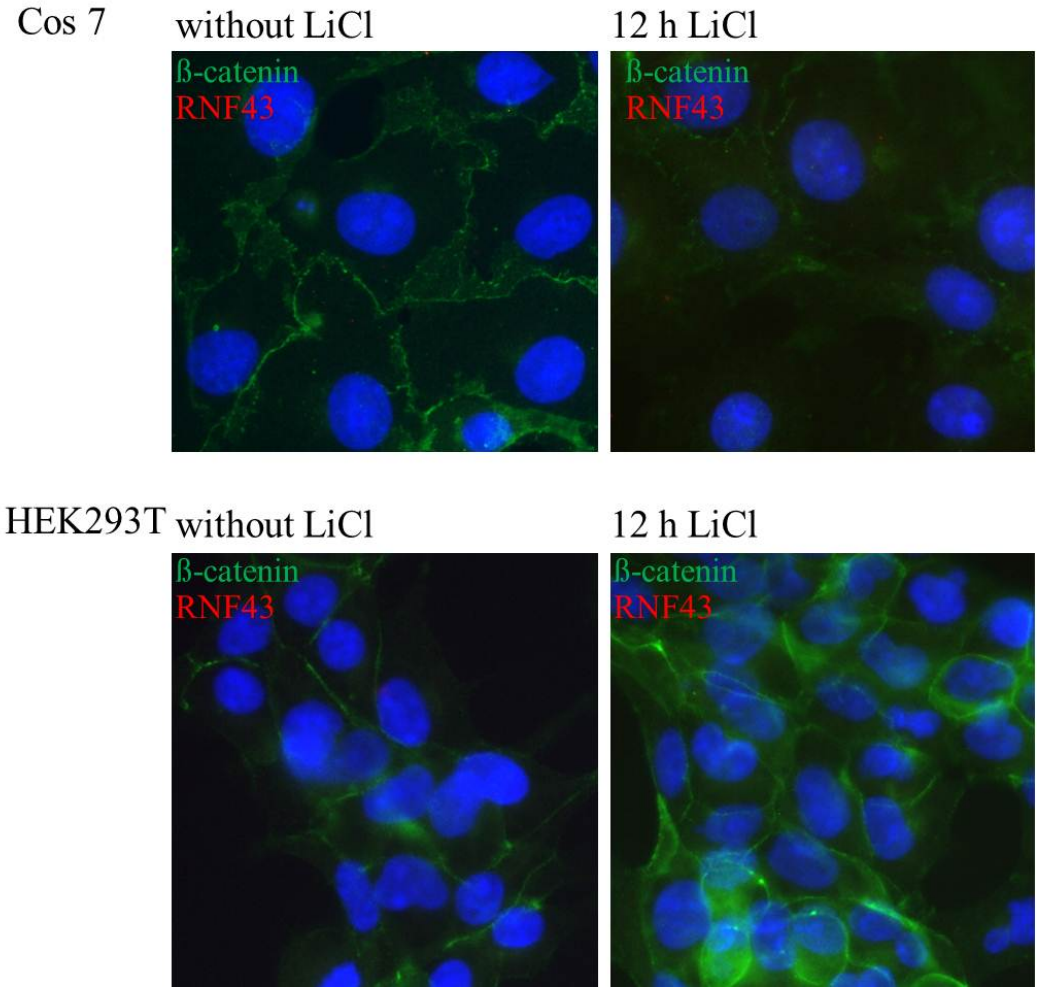

Figure 92 Immunofluorescence stainings of endogenous RNF43 in Cos7 and HEK293T cells with and without activation of the Wnt signaling pathway by LiCl.
For activation of the Wnt signaling pathway, HEK293T and Cos7 cells were treated with LiCl (final concentration: 40 mM) for 12 h. Pictures of Immunofluorescence stainings illustrate DAPI (blue), anti-RNF43 (red) and anti-ß-catenin (green) stainings.

In contrast to HT29 and HCT116 cells, no endogenous RNF43 staining was detectable in HEK293T and Cos7 cells in Immunofluorescence stainings (Figure 92). Thus, RNF43 is not, or only to a very low extent, at a level below the detection limit, expressed in HEK293T cells and Cos7 cells. These data are in accordance with data obtained by Western blot analysis (Figure 20), where endogenous RNF43 could be detected in all investigated colon cancer cell lines, but not in HEK293T and Cos7 cells.

Thus, RNF43 was detectable in HT29 and HCT116 cells, which both exhibit mutations in the Wnt signaling cascade, but not in HEK293T and Cos7 cells, which do not harbor any mutations in the pathway. The detectability solely in cell lines that harbor mutations in Wnt signaling suggested a correlation between Wnt signaling activity and endogenous RNF43

protein expression. In addition, RNF43 was shown to be a Wnt target gene (1.9). In order to investigate if the non-detectability of RNF43 in HEK293T and Cos7 cells was caused by the lack of mutations in the Wnt signaling cascade and thus very low Wnt signaling activities in these cell lines, Wnt signaling activities in HEK293T and Cos7 cells were increased by treatment with LiCl.

However, although treatment of cells with LiCl was shown to result in an increase in Wnt signaling activity in HEK293T and Cos7 cells (Figure 22, Figure 23), treatment of these cell lines with LiCl did not result in detectable levels of endogenous RNF43 (Figure 92).

In HT29 and HCT116 cells, the staining pattern observed in Immunofluorescence stainings using an antibody detecting endogenous RNF43 (Figure 91) was different from the staining pattern observed in Immunofluorescence stainings using antibodies detecting ectopically expressed RNF43 (Figure 30, Figure 31, Figure 33, Figure 34). Whereas overexpressed RNF43 was mainly visible at the nuclear envelope and only occasionally inside the nucleoplasm, only nucleoplasmic RNF43 was detected using an endogenous RNF43 antibody for stainings, indicating that the antibody detecting endogenous RNF43 only binds to a specific subform of RNF43, which exposes a specific epitope.

Nevertheless, the localization of endogenous RNF43, or possibly subforms of endogenous RNF43, in HT29 and HCT116 cells, in specific regions inside the nucleoplasm, suggests a previously uncharacterized role for RNF43 in cell cycle or cell division. Further investigation will be necessary in order to characterize a possible function of RNF43 in cell division and cell cycle in detail.

3.7.2 Investigation of the role of RNF43 in intestinal stem cells

RNF43 was shown to inhibit Wnt signaling activity *in vitro* and *in vivo* (Figure 24, Figure 26, Figure 27). Furthermore, RNF43 was shown to be expressed at sites of high Wnt signaling, like crypts and tumors (1.9). Therefore, a role of RNF43 in restricting Wnt signaling in intestinal stem cells was suggested.

In order to study the *in vivo* effect of RNF43 in intestinal stem cells and cancer, a mouse model was generated by Dr. Behnam Kalali. Therefore, Dr. Behnam Kalali has generated a pL254 targeting construct using a homologous recombination method. In the pL254 construct, RFP as well as an inducible Cre recombinase (CreERT2) were attached to the C-terminus of

the RNF43 protein, with 2A peptides in between RNF43, RFP and CreERT2. Thus, the three proteins are separated upon translation although all transcribed from the RNF43 promoter. In Figure 93, a schematic representation of the strategy for the generation of the RNF43 *knock in* mouse is shown.

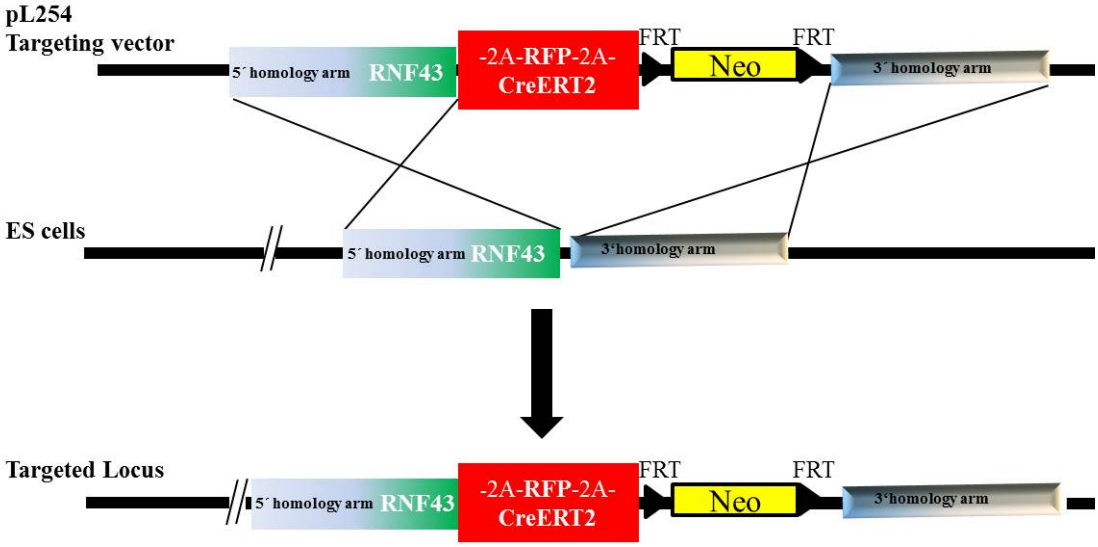

Figure 93 Schematic representation of the targeting strategy for the generation of RNF43 *knock in* mice.

After electroporation of embryonic stem cells (ES cells) using the targeting plasmid pL254, colonies were picked and a recombined clone was identified. The positive clone was used for blastocyst injection. A germline chimera was obtained and their RNF43 k.i./wt progeny were crossed with a Flipase mouse for removing the *neo* cassette. After deletion of the *neo* cassette, the expression of the RNF43-RFP-CreERT2 cassette was verified by PCR (data not shown).

Since RNF43 was shown to localize to putative stem cell positions in the intestine in *in situ* hybridizations (1.9), lineage-tracing experiments are planned in order to investigate the putative function of RNF43 in intestinal stem cells. Therefore, crossings with Rosa-LacZ reporter mice are in process. Progeny will be treated with tamoxifen, and lineage-tracing experiments according to Barker et al. (Barker and Clevers 2010) will be performed in order to confirm the putative expression of RNF43 in intestinal stem cells.

In addition, crossings with APC flox/flox mice are ongoing. Induction of the Cre recombinase in RNF43 k.i APC fl/fl mice will induce tumor formation within several days, if Cre recombinase is expressed. Hence, this experiment can be used for investigation of the function of the Cre recombinase. At the moment, RNF43 k.i/wt APC fl/wt heterozygous mice are bred to homozygosity, and crossings with Rosa-LacZ mice and APC flox mice are ongoing.

Thus, the RNF43-2A-RFP-2A-CreERT2 mice will provide a useful tool for investigating the *in vivo* functions of RNF43 in intestinal stem cells and intestinal cancer.

4 Discussion

RNF43 is a RING finger protein, which was recently described to be implicated in cancer. It was identified as an oncogene upregulated in colon cancer (Takemasa, Higuchi et al. 2001; Uchida, Tsunoda et al. 2004; Yagyu, Furukawa et al. 2004; Sugiura, Yamaguchi et al. 2008) as well as in pre-cancerous colon adenomas (Sugiura, Yamaguchi et al. 2008). In addition, it was recently shown to be mutated in several forms of pancreatic cancer (Wu, Jiao et al. 2011). These findings suggested a role for RNF43 in carcinogenesis. Nevertheless, the mechanisms of function of RNF43 remained elusive.

Alignment of protein sequences of RNF43 of different species revealed that not only the RING domain, but also the rest of the protein sequence of RNF43 is evolutionary conserved among species to a very high extent (Figure 15). Thus, since there is a correlation between protein conservation and functional importance, RNF43 is likely to be an essential or at least crucial protein in various species.

4.1 Expression of RNF43 in mice and humans

Analysis of the expression of RNF43 in mouse embryos by whole mount *in situ* hybridizations (Figure 16) revealed a posterior expression pattern at 8.5 dpc, which is typical for Wnt target genes. At 9.5 dpc, RNF43 was strongly expressed throughout the endoderm derived tissues and the trunk region. Since Galceran et al. showed that the Wnt genes TCF and LEF are strongly expressed in the primitive streak in mouse embryos (Galceran, Farinas et al. 1999), the expression of RNF43 in the tail region further strengthened the data showing that RNF43 is a target gene of the Wnt signaling pathway (1.9).

Real-time PCR analysis revealed that in mouse embryos (14.5 dpc and 18.5 dpc), RNF43 is mainly expressed in the intestine and stomach (Figure 17). These results are in accordance with the data obtained by whole mount *in situ* hybridizations (Figure 16), which indicate that in mouse embryos, RNF43 is mainly expressed in endoderm-derived tissues.

Similarly, in adult mice, RNF43 mRNA was also strongly expressed in endoderm-derived tissues like the stomach, intestine and liver, whereas less RNF43 mRNA expression was detectable in the brain as well as in the spleen (Figure 18).

Since the key component of the Wnt signaling pathway, ß-catenin, was found to promote the development of the endoderm and to be essential for this process (Imai, Takada et al. 2000), and since increased ß-catenin expression results in increased transcription of Wnt target genes, elevated gene expression in endoderm-derived tissues is typically observed for Wnt target genes. Thus, in addition to the expression of RNF43 in the tail region, the expression of RNF43 in endoderm-derived tissues is also in accordance with previous data showing that RNF43 is a target gene of the Wnt signaling cascade (1.9).

Investigation of RNF43 mRNA expression levels in tumor samples (Figure 19) revealed a high expression in intestinal tumor stage IV samples, indicating that RNF43 expression increases with the progression of the tumor. In contrast, the expression levels were low in normal muCos7a samples. The low RNF43 mRNA expression in normal muCos7a samples may reflect the small amount of cells at the crypt base expressing RNF43. The expression of RNF43 mRNA in tumor stage II samples largely differed between the individual samples. These data indicate that mutations or signaling pathways in specific tumors may possibly influence RNF43 mRNA expression. Thus, RNF43 mRNA levels may be elevated in only some tumor stage II samples, which may exhibit specific mutations, or deregulated signaling cascades.

Additionally, the mRNA expression levels of RNF43 in colorectal cancer cell lines were investigated (Figure 19). RT-PCR analysis revealed low expression levels in most of the colorectal cancer cell lines tested. In contrast to the low expression levels in HCT116, DLD1, SW480, CaCo2 and LS174T cells, the RNF43 mRNA expression level in HT29 adenocarcinoma cells was at a level comparable to RNF43 mRNA expression in tumors.

RNF43 mRNA was not detectable in cell lines HEK293T and Cos7. Similarly, in Western blot analysis using an endogenous anti-RNF43 antibody (Figure 20), RNF43 protein was not detectable in these cell lines, whereas several distinct bands were visible on RNF43-Western blots of whole cell lysates of the colon cancer cell lines DLD1, HCT116, HT29, SW480 and LS174T. The bands are likely to represent several isoforms of RNF43, since 4 different isoforms with a molecular weight of 85722 Da, 81229 Da, 72106 Da and 95038 Da were described to exist on protein level ("NeXtProt")[18]. Thus, whereas endogenous RNF43 was not

[18] http://www.nextprot.org/db/entry/NX_Q68DV7/localisation?isoforms=NX_Q68DV7-1

detectable in HEK293T and Cos7 cells, RNF43 was detectable in all investigated colon cancer cells.

Since RNF43 was shown to be a target gene of the Wnt signaling pathway (1.9), and since HEK293T and Cos7 cells were the only investigated cell lines without mutations in the Wnt signaling cascade, these data indicate that mutations in the Wnt signaling cascade, resulting in increased levels of endogenous Wnt signaling activity, may be necessary for RNF43 expression at detectable levels.

The expression of RNF43 observed in HCT116 cells (Figure 20) is in contrast to data of Ivanov et al.. In their study, they suggested that in this cell line, deletion of a nucleotide results in a homozygous frameshift mutation at the N-terminus of the protein (Ivanov, Lo et al. 2007). Nevertheless, since RNF43 was clearly detectable in Western blot analysis by an antibody recognizing a specific epitope located downstream of the frameshift mutation in the *RNF43* gene sequence, the frameshift mutation may possibly only affect one of the two alleles.

4.1.1 Correlation of RNF43 expression and endogenous Wnt signaling activity

In order to investigate a possible correlation between RNF43 expression levels and endogenous Wnt signaling activities, TOP/FOP Luciferase reporter assays were performed in HT29, HCT116, DLD1, SW480, HEK293T and Cos7 cells. In TOP/FOP Luciferase reporter assays, no correlation between RNF43 mRNA expression levels and endogenous Wnt signaling activities of these cell lines could be observed. Similarly, no correlation between RNF43 protein expression and endogenous Wnt signaling activity could be determined. Thus, RNF43 is possibly not the only parameter influencing the levels of endogenous Wnt signaling activities of these cell lines. Other parameters, e.g. their mutations in the Wnt signaling cascade, may also influence endogenous Wnt signaling activities.

HCT116 cancer cells harbor a mutation in the gene coding for ß-catenin (*CTNNB1*), and SW480 and DLD1 cancer cells both exhibit mutations in the *APC* gene, as described in 3.2.3. In addition, HT29 cells also harbor mutations in the *APC* gene resulting in truncated APC protein (Morin, Vogelstein et al. 1996).

Hence, all colon cancer cell lines (HCT116, SW480, DLD1 and HT29) that have been examined in TOP/FOP Luciferase reporter assays in order to determine their endogenous Wnt

signaling activities harbor activating mutations in the Wnt signaling pathway. These mutations, either in the *APC* or in the *CTNNB1* gene, are responsible for an increased endogenous Wnt signaling activity as compared to Cos7 and HEK293T cells, which do not harbor any described mutations in Wnt signaling genes.

Nevertheless, although the effects of APC, ß-catenin or mutated forms of these proteins on endogenous Wnt signaling activities may be larger than the effect of RNF43 due to the high abundance of these proteins and their key functions in the pathway, and although no correlation between RNF43 expression and endogenous Wnt signaling activities could be observed, RNF43, or mutated forms in RNF43, may also influence endogenous Wnt signaling activity.

4.2 Role of RNF43 in the Wnt signaling pathway

In a recent study, Shinada et al. suggested that in colorectal carcinogenesis, RNF43 may regulate cell growth and apoptosis via NEDL, a protein that binds and regulates p53, and via p53, which is one of the important tumor suppressors since it induces G1 cell cycle arrest (Shinada, Tsukiyama et al. 2011). Nevertheless, the expression of RNF43 selectively at sites of high Wnt activity, like intestinal adenomas and crypts, suggested to further investigate a possible correlation of RNF43 and the Wnt signaling pathway. Chromatin-IP experiments (Markus Gerhard and Pantelis Hatzis, unpublished data) further confirmed the assumed correlation of Wnt signaling and RNF43, showing that RNF43 is indeed a direct Wnt target gene, which harbors several Tcf4 binding sites in the introns and the promoter region of the *RNF43* gene. The finding that RNF43 is a target gene of the ß-catenin/Wnt signaling pathway was recently confirmed by other studies (Van der Flier, Sabates-Bellver et al. 2007; van der Flier, van Gijn et al. 2009; Hao, Xie et al. 2012).

The next aim was to investigate the putative function of the Wnt target gene *RNF43* on the Wnt signaling activity itself. Although no correlation of RNF43 expression with endogenous Wnt signaling activities of colon cancer cell lines could be determined, RNF43 was shown to be a strong inhibitor of Wnt signaling both *in vitro* and *in vivo*. *In vitro*, in TOP/FOP Luciferase reporter assays, RNF43 strongly inhibited LiCl-induced Wnt signaling activities in Cos7 and HEK293T cells (Figure 24) and endogenous Wnt signaling activities in HCT116

and SW480 cells (Figure 27), and *in vivo*, in *Xenopus laevis* axis duplication assays, RNF43 nearly completely inhibited the double axis formation induced by Wnt1 (Figure 26). These findings are in accordance with a recent study published by Hao et al.. As described for ZNRF3 (3.3.2), Hao et al. also suggested a negative function of RNF43 on Wnt signaling activity (Hao, Xie et al. 2012).

Functional inactivation of RNF43 by introduction of two point mutations into the RING domain (causing amino acid exchanges at positions 292 and 295 from histidine to arginine) resulted in a complete loss of the inhibitory effect on Wnt signaling (Figure 25, Figure 27, Figure 26). Thus, a functional RING domain, which is necessary for the coordination of the Zn^{2+} atoms, is essential for the function of RNF43 as a negative modulator of the Wnt signaling activity. Functional inactivation of the RING domain not only reversed the inhibitory effect of wildtype RNF43, but also transactivated Wnt signaling. These results indicate that the coordination of Zn^{2+} atoms and the function of RNF43 as an Ubiquitin E3-Ligase are crucial for its role as a negative regulator of the Wnt signaling pathway.

RNF43 still inhibited Wnt signaling in cells lines exhibiting elevated levels of Wnt signaling due to mutations in the Wnt signaling cascade, like in SW480 and HCT116 cells, which harbor activating mutations in the *APC* gene or the ß-catenin gene *CTNNB1*, indicating that RNF43 acts downstream or at the level of these mutations (Figure 27). In addition, mutant RNF43 still activated Wnt signaling in these cell lines. Furthermore, both proteins still performed their functions in cells exhibiting Wnt signaling activity induced by a stabilized form of ß-catenin (Figure 29), again indicating a role of RNF43 downstream or at the level of the mutation, thus downstream or at the level of ß-catenin.

The fact that ß-catenin is commonly known to perform its function inside the nucleoplasm suggested a role for RNF43 at the transcription complex. Alternatively, a function of RNF43 at the nuclear rim could not be excluded, since ß-catenin was also described to be regulated by proteins located in the nuclear membrane. For instance, the inner nuclear membrane protein Emerin inhibits ß-catenin activity by restricting its accumulation in the nucleus, since it facilitates its export (Markiewicz, Tilgner et al. 2006). Thus, a function of RNF43 downstream or at the level of ß-catenin indicated a localization of RNF43 either inside the nucleoplasm or at the nuclear membrane.

4.2.1 Subcellular localization of RNF43

The next aim was to investigate the function of RNF43 more precisely. Since there is often a correlation of proteins between their localizations and their functions and in order to evaluate where exactly RNF43 performs its function in the Wnt signaling cascade, the subcellular localization of the protein was investigated in more detail.

In all investigated cell lines (HCT116, SW480, Cos7), both wildtype and mutant RNF43 mainly localized to the inner nuclear membrane, the Endoplasmatic reticulum (ER) and the Golgi apparatus. Frequently, small amounts were also detectable in the nucleoplasm (Figure 30, Figure 31, Figure 33, Figure 34, Figure 35).

Since we observed RNF43 to mainly localize to the nuclear envelope, the results obtained during this study are in contrast to the data of Yagyu et al., which suggested a localization of RNF43 in spotty granules inside the cytoplasm (Yagyu, Furukawa et al. 2004). In our study, neither RNF43 nor RNF43mut were ever detected inside the cytoplasm.

Similarly, although Yagyu et al. described RNF43 to be a secreted protein (Yagyu, Furukawa et al. 2004), we could never confirm the extracellular localization of the protein (Figure 32), and neither could any other study. An explanation for the detection of RNF43 in the culture media of cells, which was observed by Yagyu et al., could be that as a result of transfection, cells became apoptotic or dead and hence released proteins, including RNF43, into their environment. These apoptotic or dead cells could also result from maintaining Cos7 cells in only 0.5 % FCS.

Although the RNF43 subcellular localization data obtained during this study are in contrast to data from Yagyu et al., they are in accordance with other publications, suggesting that RNF43 mainly localized to the nuclear rim (Miyamoto, Sakurai et al. 2008; Sugiura, Yamaguchi et al. 2008), with occasional staining in the nucleoplasm (Sugiura, Yamaguchi et al. 2008).

During this study, additionally to the localization of wildtype and mutant RNF43 in the nucleoplasm and at the nuclear rim, both proteins were also detected in the ER/Golgi compartment upon overexpression (Figure 34, Figure 35). The colocalization of RNF43 with the ER marker Calnexin is also in accordance with data published by Suguira et al., suggesting that apart from its predominant localization to the nuclear rim and occasionally to the nucleoplasm, RNF43 is also localized to the ER in Cos71, Cos7 and HeLa cells (Sugiura,

Yamaguchi et al. 2008), as well as with data presented in a study by Miyamoto et al. (Miyamoto, Sakurai et al. 2008).

The data regarding subcellular RNF43 localization obtained during this study are also mainly in accordance with calculations from the protein localization prediction tools. PSORTII predicted a localization of RNF43 in the nucleus, which is in compliance with our stainings. In addition, PSORTII calculated that RNF43 is a type 1b transmembrane protein. Since type 1b transmembrane proteins are often found in the ER, these calculations also fit to the results obtained during this study by co-stainings with the ER marker protein Calnexin (Figure 34).

Euk-mPLoc2.0 predicted a localization of RNF43 in the nucleus, the cytoplasm and the ER. Apart from the calculated RNF43 localization in the cytoplasm, which could not be observed during this study, these calculations are also in accordance with our observations.

Closer investigation of the nucleus using the Subnuclear Compartments Prediction System predicted RNF43 to localize to the nuclear lamina. This calculation also corresponds to the RNF43 localization observed during this study.

4.2.2 RNF43 is a homologue of ZNRF3

In a recent study, Hao et al. suggested a localization of an RNF43-GFP fusion protein in the plasma membrane (Hao, Xie et al. 2012; data not shown). RNF43 was never described to localize to the plasma membrane in any other published study. Similarly, in our study, RNF43 was only detected there upon attachment of CFP or Cherry fluorescent proteins (Figure 36). Since RNF43 fused to CFP or Cherry exhibited altered localization as compared to RNF43 fused to smaller tags like HA or flag, the different localization of RNF43-GFP may possibly also result from the fusion with the GFP-tag, which may influence the localization pattern. Thus, it is likely that the localization of RNF43 in the plasma membrane, which was suggested by Hao et al., does not depict the actual localization of RNF43 but is an artifact caused by the attachment of GFP to the RNF43 protein. Additionally, since attachment of the fluorescent proteins CFP and Cherry resulted in functional inactivation of RNF43 (Figure 37), it is also likely that attachment of GFP may additionally have caused functional alterations of RNF43.

Sequence alignment of the human RNF43 protein sequence and the human ZNRF3 protein sequence showed that the sequences are only conserved to a very low extent (Figure 38),

suggesting that although RNF43 was described to be a homologue of ZNRF3, the function of the two proteins may not necessarily be the same. Although ZNRF3 may act at the plasma membrane responsible for the degradation of LRP6 and Frizzled in the absence of R-spondin, RNF43 may possibly have additional functions in the Wnt signaling cascade.

4.2.3 Interaction partners of RNF43

In previous studies, RNF43 was shown to interact with HAP95, a protein of the nuclear envelope, which is associated to chromatin (Sugiura, Yamaguchi et al. 2008). Furthermore, RNF43 was shown to interact with NEDL1, a protein that binds and regulates p53, and also with p53, which is one of the important tumor suppressors (Shinada, Tsukiyama et al. 2011).

Additionally, RNF43 was shown to interact with the tumor suppressor PSF, which is part of the PSF/p54nrb heterodimer (Miyamoto, Sakurai et al. 2008). Miyamoto et al. suggested that upon co-expression of PSF, RNF43 is relocalized from the perinuclear region to the cytoplasm, resulting in a profound colocalization of RNF43 with PSF in the nucleoplasm of Cos71 cells. In contrast, during our study, a relocalization of RNF43 was never observed upon co-expression of PSF-HA. Co-transfection with PSF-HA did not result in a relocalization of RNF43 to the nucleoplasm (Figure 39). In contrast to the diverging data obtained by Immunofluorescence analysis, the interaction of PSF and RNF43 could be observed during this study (Figure 40). Nevertheless, since in addition to the nuclear rim staining of RNF43 very small amounts of RNF43 were also frequently detected in the nucleoplasm, and since PSF localized to the nuclear membrane and to the nucleoplasm, it remains elusive whether RNF43 and PSF interact at the nuclear membrane or inside the nucleoplasm.

Additionally, PSF was identified as a previously unknown strong inhibitor of the Wnt signaling pathway, which performs its function downstream or together with RNF43 and intensifies the inhibitory effect of RNF43 on Wnt signaling activity (Figure 41). Further investigation will be necessary in order to understand the effect of PSF on Wnt signaling activity in detail.

Since RNF43 was shown to inhibit Wnt signaling downstream or at the level of ß-catenin (Figure 27, Figure 29), the next aim was to elucidate a possible interaction of RNF43 with

proteins of the transcription complex. Indeed, wildtype RNF43 could be shown to strongly interact with the transcription factor Tcf4 (Figure 42). In contrast, mutant RNF43 only very weakly interacted with Tcf4, indicating that a functional RING domain is essential for a strong association of RNF43 and Tcf4. The results could be confirmed by Martina Grandl, a master student of our lab. She could show an interaction of RNF43 and Tcf4 in DLD1 colon cancer cells (Grandl 2011).

In Co-Immunofluorescence stainings, RNF43 mainly localized to the nuclear envelope, and Tcf4 was detectable there too (Figure 43). Both proteins also localized to the nucleoplasm, Tcf4 to a greater extend then RNF43. Since RNF43 mainly localized to the nuclear rim, with only small protein amounts detectable in the nucleoplasm, while Tcf4 was primarily present inside the nucleoplasm, only marginal colocalization of the two proteins was visible in Immunofluorescence microcopy pictures. Nevertheless, a colocalization of RNF43 and Tcf4 either at the nuclear membrane or inside the nucleoplasm cannot be excluded.

The data obtained by Immunofluorescence analysis, indicating that not only RNF43 but also Tcf4 is -beside its nucleoplasmic localization- also localized to the nuclear membrane, is in accordance with literature. It was previously shown that Tcf4 interacts with a large variety of proteins of the nuclear pore complex (NPC), where it is sumoylated by RanBP2, and sumoylation of Tcf4 enhances its ability to bind to ß-catenin. Additionally, expression of NPCs increases the transcriptional activity of Tcf4 (Shitashige, Satow et al. 2008). Furthermore, the nuclear envelope has been described to be implicated in transcriptional activation as well as transcriptional repression. Nuclear pores have been implicated in transcriptional activation, since many transcribed genes were found to associate with the nuclear pore complex, whereas silenced heterochromatin was found to be located in between nuclear pore complexes (reviewed in Akhtar and Gasser 2007; Schneider and Grosschedl 2007; Mekhail and Moazed 2010)

Since Tcf4 was described to interact with proteins of the nuclear pore complex (Shitashige, Satow et al. 2008), the nuclear envelope was suggested to be implicated in transcriptional activation and repression (reviewed in Akhtar and Gasser 2007; Schneider and Grosschedl 2007; Mekhail and Moazed 2010), and Immunofluorescence co-stainings revealed a localization of both Tcf4 and RNF43 at the nuclear membrane, the interaction of RNF43 and Tcf4 may possibly occur at the nuclear membrane. Nevertheless, the possibility that the interaction takes place inside the nucleoplasm cannot be excluded. Thus, according to

Immunofluorescence pictures (Figure 43), an interaction of RNF43 and Tcf4, either at the nuclear membrane or inside the nucleoplasm, would be possible.

Although no differences between localizations of wildtype and mutant RNF43 were detected by Immunofluorescence stainings, only wildtype RNF43 strongly associated with Tcf4 (Figure 42). These data indicate that wildtype and mutant RNF43 may perhaps exhibit slightly different subcellular localization patterns. Alternatively, wildtype RNF43 may possibly cause a translocation of Tcf4 or the whole transcription complex. Nevertheless, no differences were visible, possibly due to the detection limit of the Immunofluorescence staining method.

Another indication for the function of RNF43 at the transcription complex was the interaction with CTBP (Figure 45), a protein described to act both as a positive and negative regulator on Wnt signaling activity by interacting with the transcription complex (Fang, Li et al. 2006). Both wildtype and mutant RNF43 were shown to interact with CTBP during this study. The results could be confirmed by Martina Grandl, a master student of our lab, who could show an interaction of RNF43 and CTBP in DLD1 colon cancer cells (Grandl 2011).

The binding of wildtype RNF43 to the Tcf4- transcription complex as well as to CTBP may possibly indicate a function of RNF43 in linking the repressor complex (containing CTBP) to the transcription complex, causing an inhibition of Tcf4-mediated transcription and thus Wnt signaling activity.

Overexpression of wildtype or mutant RNF43 did not change the levels of neither Tcf4 nor CTBP (Figure 46). Thus, the proteins Tcf4 and CTBP were not marked for degradation by neither wildtype nor mutant RNF43 as a result of multiubiquitination at K48 or K29. Furthermore, no smear or additional band above the Tcf4 or CTBP band could be observed upon ectopic expression of wildtype or mutant RNF43, indicating that these two proteins are neither multiubiquitinated at K63 nor monoubiquitinated by wildtype or mutant RNF43.

Additionally, no higher molecular smears or bands became visible upon ectopic expression of wildtype or mutant RNF43 and treatment with MG132, again indicating that these proteins are no targets of ubiquitination by wildtype or mutant RNF43.

Nevertheless, the possibility that these two proteins are ubiquitinated by the Ubiquitin E3-Ligase RNF43 and thus are targets of RNF43 ubiquitination cannot be excluded. The extent of ubiquitination may possibly be below the Western blot detection limit, or maybe only small amounts of Tcf4, e.g. Tcf4 at the active chromatin, may be ubiquitinated by RNF43. Thus, RNF43 may possibly interact with Tcf4 at the active chromatin, where it may perhaps alter the binding of Tcf4 to its target genes. Chromatin-IP assays using a Tcf4 antibody would yield further information regarding a possible function of RNF43 at the transcription complex.

4.3 Function of RNF43 as an Ubiquitin E3-Ligase

RNF43 was shown to exhibit RING finger-dependent Ubiquitin E3-Ligase activity (Sugiura, Yamaguchi et al. 2008). Since substrates are still uncharacterized for many E3 ligases, and binding sites are not very conserved among these proteins, both substrates and binding sites are still uncharacterized for many E3 ligases. In addition, the potential need for post-translational modifications of E2 and E3 proteins necessary for interactions are unknown (van Wijk, de Vries et al. 2009). Thus, no common preferences regarding the substrate specificity of RNF43, that would facilitate the identification of the RNF43 substrate, could be assumed. Although several proteins, like HAP95 (Sugiura, Yamaguchi et al. 2008), PSF (Miyamoto, Sakurai et al. 2008) and NEDL1 (Shinada, Tsukiyama et al. 2011) were described as interaction partners of RNF43, none of these factors was shown to be ubiquitinated by the Ubiquitin E3-Ligase RNF43.

In addition to the function of RNF43 as an Ubiquitin E3-Ligase, RNF43 was shown to exhibit autoubiquitination activity in *E.coli* autoubiquitination experiments (Sugiura, Yamaguchi et al. 2008). Autoubiquitination of RNF43 could be confirmed during this study (Figure 48). In HCT116 cells, wildtype but not mutant RNF43 was shown to be autoubiquitinated. Thus, the autoubiquitination activity of RNF43 is dependent on its active RING domain.

Since also K63-linked polyubiquitination was observed for wildtype RNF43 in Western blot analysis (Figure 48B), wildtype RNF43 may also be autoubiquitinated for regulatory purposes. Since RNF43 is known to be degraded by the proteasome (Figure 46B, Figure 47), this different form of ubiquitination is likely to occur additionally to the autoubiquitination which marks the protein for degradation. Thus, it cannot be excluded, that RNF43 also marks its target protein with K63-linked polyubiquitination for regulatory purposes.

In experiments where MG132 treatment was coupled to Western blot analysis, the levels of both wildtype and mutant RNF43 proteins increased in HCT116 (Figure 46B) and DLD1 cells (Figure 47) upon treatment with MG132. These data indicate that not only wildtype, but also mutant RNF43 is subjected to degradation by the proteasome in the absence of MG132.

This is in accordance with a study of Sugiura et al., suggesting that RNF43 is ubiquitinated in HEK293T cells, and that a mutant harboring mutations at amino acids 290 and 292 (p**C**290**S** and p**H**292**S**), thus a mutant with an inactivate RING domain, also undergoes ubiquitination (Sugiura, Yamaguchi et al. 2008).

The stabilizing effect of MG132 treatment on wildtype RNF43 can be explained by its autoubiquitinating activity mediated by its active RING domain, which was described previously (Sugiura, Yamaguchi et al. 2008). Since mutant RNF43 is also stabilized upon treatment with MG132 but does not comprise an active RING domain and thus is not proficient of ubiquitinating itself, the data suggest that RNF43 is possibly ubiquitinated and marked for degradation by the proteasome by another yet unknown protein. Another possibility would be that the low levels of endogenous RNF43, capable of ubiquitination since harboring an active RING domain, are sufficient for ubiquitinating ectopically expressed mutated RNF43.

In order to determine whether RNF43 ubiquitinates Tcf4, ubiquitination assays were performed. Analysis of Tcf4 ubiquitination (Figure 49) indicated that Tcf4 was not ubiquitinated by the Ubiquitin E3-Ligase RNF43, or the extent of ubiquitination was very low and thus below the Western blot detection limit.

Since the Tcf4 protein levels did not change upon overexpression of RNF43, and since ubiquitination assays indicated that Tcf4 is not ubiquitinated by the Ubiquitin E3-Ligase RNF43, RNF43 may possibly have other targets for ubiquitination, which may perhaps also be part of the Tcf4 transcription complex. Alternatively, RNF43 may possibly have other functions apart from its putative role at the Tcf4 transcription complex.

We next hypothesized that the function of RNF43 may possibly be to mark an important activator of the Wnt signaling pathway for degradation. In contrast, the mutant form of RNF43 would not be able to keep the levels of this activator low, thus causing increased levels of Wnt signaling. This hypothesis was strengthened by an experiment in which

treatment of an inhibitor of the proteasome (MG132) completely reversed the inhibitory effect of RNF43 on the Wnt signaling pathway, whereas it did not influence the effect of mutant RNF43 (Figure 50).

These data indicate that the function of RNF43 may possibly indeed be to ubiquitinate a protein, which is of particular importance for the activation of canonical Wnt signaling activity, and mark it for subsequent proteasomal degradation. Thus, RNF43 may be responsible for keeping the levels of this activator low, resulting in an inhibition of Wnt signaling. The ubiquitination-deficient mutant may not be proficient of keeping the levels of the activator low, resulting in increased protein levels of the activator and hence a transactivation of Wnt signaling.

Alternatively, the reversion of the inhibitory effect of RNF43 on Wnt signaling upon treatment with MG132 may possibly be due to increased ß-catenin levels, since ß-catenin was shown to be a protein degraded by the proteasome and is therefore stabilized upon treatment with proteasome inhibitors (Aberle, Bauer et al. 1997). Nevertheless, since no changes in the Wnt signaling activities were observed upon transfection of RNF43mut- or mock-plasmids and treatment with MG132, it is very unlikely that the reversion of the inhibitory effect of RNF43 on Wnt signaling results from increased ß-catenin levels.

Since ubiquitination of Tcf4 by RNF43 could never be observed, the identity of the activator of Wnt signaling possibly marked for ubiquitination by RNF43 remains elusive. Nevertheless, it cannot be excluded that Tcf4 is this activator, and the target of RNF43 ubiquitination, since the extent of ubiquitination may be below the Western blot detection limit.

4.4 Effect of knockdown of the *RNF43* gene on cell growth and Wnt signaling activity

A possible effect of RNF43 on proliferation rate and Wnt signaling activity was investigated by knockdown of *RNF43* gene expression using specific siRNA targeting the *RNF43* gene. *RNF43* gene expression was knocked down in HT29 cells, which is the only cell line expressing RNF43 mRNA at higher levels. Transfection of cells with a combination of the siRNA oligonucleotides A and C (20 nm final concentration; 72 h) was the most effective and resulted in a reduction of *RNF43* gene expression of approximately 69 % (Figure 52). In addition, transfection resulted in greatly reduced endogenous RNF43 protein levels (Figure

53). Nevertheless, no effect of RNF43 siRNA on the proliferation rate was observed in HT29 cells as compared to HT29 cells transfected with control siRNA (Figure 54A).

These data indicate that either RNF43 does not have an effect on proliferation rates of HT29 cells, or that the effect of siRNA-mediated knockdown of the *RNF43* gene expression was not sufficient for observing an effect on proliferation. The remaining 31 % of *RNF43* gene expression could still be enough for allowing the cells to proliferate normally.

In contrast, a significant increase in Wnt signaling activity of approximately 50 % was observed in TOP/FOP Luciferase reporter assays upon siRNA-mediated knockdown of *RNF43* gene expression in HT29 cells (Figure 54B). These data are in accordance with data showing that RNF43 negatively regulates Wnt signaling activity (3.2).

4.5 Effect of ectopic expression of RNF43 on proliferation rates and cell growth

In accordance with the data obtained by siRNA-mediated knockdown of *RNF43* gene expression, ectopic expression of wildtype and mutant RNF43 did not significantly affect proliferation rates in Cos7 and HCT116 cells (Figure 55). These data indicate that either wildtype or mutant RNF43 do not have an effect on proliferation rates of these two cell lines, or that transient transfection is not sufficient for investigating the effect of wildtype or mutant RNF43 on proliferation rates, since only few cells are transfected. Therefore, stable RNF43/RNF43mut- expressing clones would be a better model for the investigation of the effects of ectopic expression on wildtype and mutant RNF43 on proliferation.

Similarly, in *in vitro* colony formation assays, overexpression of neither wildtype nor mutant RNF43 resulted in any alterations in cell growth and/or viability.

Together, these results indicate that wildtype and mutant RNF43 do not exhibit any effects on proliferation, neither upon knockdown of RNF43, nor upon overexpression of the protein.

These results are in contrast to data obtained by Yagyu et al.. In their study, they suggested a growth-promoting effect for wildtype RNF43, since they observed a higher colony-formation ability of cells upon ectopic expression of RNF43 in colony formation assays (Yagyu, Furukawa et al. 2004). However, a growth promoting effect of wildtype RNF43 was never observed in this study.

4.6 Function of truncated versions of RNF43

In order to investigate the function of specific regions of RNF43 in detail and in order to obtain more information about the regions of RNF43 responsible for the localization in specific subcellular compartments, truncated versions of wildtype and mutant RNF43 were generated (Figure 60, Figure 70, Figure 76).

Immunofluorescence stainings of both wildtype and mutant N-terminally truncated RNF43(245-783) constructs exhibited strong expression in punctuate structures inside the nucleoplasm (Figure 58). The results could be confirmed by several master students of our lab (Miriam Bognar (Bognar 2010), Esther Wehrle (Wehrle 2010) and Martina Grandl (Grandl 2011)).

Since full length wildtype and mutant RNF43 exhibited a different localization pattern (3.3.1), these data indicate that the region responsible for localization in the membrane is missing in these truncated versions of RNF43, and that the N-terminal amino acids 1 - 244 of RNF43 are necessary for the localization of the protein in the nuclear membrane.

The effect of wildtype RNF43 on LiCl-induced Wnt signaling activity in Cos7 cells was completely reversed in RNF43(245-783) constructs, thus upon deletion of amino acids 1 - 244 (Figure 59). Since also mutant RNF43 exhibited markedly decreased function on Wnt signaling upon deletion of amino acids 1 - 244, as compared to the effects of full length mutant RNF43, these findings indicate that the amino acids 1 - 244 of RNF43 are crucial for the function of RNF43. Since both wildtype and mutant RNF43(245-783) localized inside the nucleoplasm and both lost their function, the localization of RNF43 at the nuclear membrane, as observed for full length RNF43 and RNF43mut, may be necessary for the function of the protein in the Wnt signaling cascade. The interactions with other proteins may be impaired or altered upon relocalization to the nucleoplasm. Alternatively, the localizations of other proteins may possibly be changed upon relocalization of RNF43 to the nucleoplasm, or responsible of its relocalization.

In contrast to wildtype and mutant RNF43(245-783), wildtype and mutant RNF43(62-783), RNF43(121-783), RNF43(184-783) as well as RNF43(Δ191-232) all exhibited a subcellular localization pattern identical to the expression pattern of full length proteins (Figure 62, Figure 63, Figure 64). Since these N-terminally truncated mutants are also lacking the signal

peptide, which comprises 69 bp (23 aa) and is located at the very N-terminus (as described in 3.3.1), the presence of the signal peptide is unlikely to be the reason for the localization of full length RNF43, RNF43(62-783), RNF43(121-783), RNF43(184-783) and RNF43(Δ191-232) in the nuclear membrane.

All these constructs (wildtype and mutant RNF43(62-783), RNF43(121-783), RNF43(184-783) and RNF43(Δ191-232)) exhibited the same localization pattern that was observed for full length proteins, but their effects on Wnt signaling activity, as compared to the effects of full length proteins, were weaker (Figure 66).

For an unknown reason, the localization patterns of wildtype and mutant RNF43(229-783) proteins were not identical (Figure 65). The wildtype RNF43(229-783) protein exclusively localized to the nucleoplasm, whereas the mutant RNF43(229-783) protein exhibited a subcellular localization pattern identical to the expression pattern of full length proteins. Additionally, the effects on Wnt signaling activity of these two proteins were strongly decreased.

The different localization patterns of the two proteins indicate that they may possibly also attach to distinct interaction partners. A specific protein may possibly only bind to wildtype RNF43(229-783) and may relocate it from the nuclear envelope to the nucleoplasm. Since a strong colocalization of RNF43(229-783) and Tcf4 was observed (Figure 69), Tcf4 could be the protein responsible for the relocation of wildtype RNF43(229-783). Further investigation will be necessary in order to identify binding partners of wildtype and mutant RNF43(229-783), and in order to completely understand the distinct localization patterns of wildtype and mutant RNF43(229-783).

The next aim was to determine a possible role of the signal peptide, which is present at the N-terminus of RNF43 full length proteins, in protein localization and function. In order to investigate whether the attachment of the RNF43 signal peptide to the N-terminally truncated proteins, which exhibited nucleoplasmic localization, could relocalize these proteins to the nuclear membrane, the signal peptide sequence was attached to the N-terminus of RNF43(229-783) and RNF43(245-783). The resulting proteins, termed RNF43(229-783)+sp and RNF43(245-783)+sp, as well as their mutant forms, exhibited an amplified relocalization

from the nucleoplasm to the nuclear membrane (Figure 72, Figure 73). These results indicate that the signal peptide either is a key factor for the transport of proteins out of the nucleoplasm, or for the localization of proteins to the nuclear membrane. Since various other mutants generated during this work also localized to the nuclear membrane (Figure 62, Figure 63, Figure 64) but do not harbor a signal peptide sequence, other sequences apart from the N-terminal signal sequence found at the N-terminus of RNF43 are likely to be responsible for the localization of RNF43 to the nuclear membrane. Nevertheless, although expression of the signal peptide at the N-terminus resulted in a predominant relocation of wildtype RNF43(229-783)+sp as well as wildtype and mutant RNF43(245-783)+sp to the nuclear membrane in HCT116, SW480 and Cos7 cells, only little effects on the Wnt signaling activity were observed (Figure 74, Figure 75).

The next aim was to investigate a possible role of the predicted transmembrane domain, which is located between amino acids 199 and 219 of RNF43, in protein localization and function. Although the localizations of wildtype and mutant RNF43(Δ191-228) proteins were not changed as compared to full length proteins (Figure 78), deletion of the transmembrane domain revealed an essential function of the transmembrane domain for both the inhibitory function of full length wildtype RNF43, and the activating effect of mutant RNF43 on the Wnt signaling activity. Deletion of the amino acids 191 - 228 resulted in a complete abolishment of the effects of both proteins (Figure 79). Since the localizations of these proteins remained unchanged, these data indicate that the removed amino acids possibly provide a binding site for RNF43 interaction partners, or possibly these amino acids are part of a catalytic center mediating protein interactions or providing structural preconditions for functions of RNF43. Alternatively, this region may possibly harbor amino acids, which are targets of post-translational modification. Since Tcf4 was still associated with RNF43(245-783) in Immunoprecipitation experiments, the possibility that the binding of Tcf4 to this specific region (aa 191 - 228) is the crucial event which makes it especially important for functionality can be excluded.

In summary, these data indicate that all amino acids of RNF43, which were deleted during this study, are important for the function of full length wildtype as well as mutant RNF43. All investigated truncated versions of wildtype and mutant RNF43, independently of their

localizations, exhibited weaker effects on Wnt signaling activities, either in inhibiting Wnt signaling, as described for wildtype RNF43, or in increasing Wnt signaling, as described for mutant RNF43 (Figure 80). These data are in accordance with results from Martina Grandl, a master student in our lab. She investigated the localization patterns and functions of several constructs generated during this study, and could confirm the results obtained in this study (Grandl 2011).

The data, suggesting that the N-terminus is of particular importance for the function of the protein, are in accordance with the data obtained by sequence alignment analysis (Figure 15), indicating that especially the N-terminus of RNF43 is evolutionarily highly conserved among species. Thus, it can be concluded that truncations or deletions of RNF43 are not permissible for achieving an effective function.

Investigation of C-terminally truncated RNF43 deletion mutants will yield further information about the regions of RNF43 necessary for its localization and function.

4.7 Role of RNF43 in tumors

RNF43 was shown to be overexpressed in tumors. Nevertheless, the levels of RNF43 mRNA expression in colon cancer cell lines were low, indicating transcriptional repression of RNF43 in colon cancer cell lines. Indeed, treatment of cells with 2-Aza-5'dCyt increased RNF43 mRNA expression levels in HCT116, HT29, SW480 and DLD1 cells, indicating that in colon cancer cell lines, RNF43 levels are downregulated by a mechanism involving epigenetic silencing.

So far, it remains elusive whether RNF43 is also transcriptionally silenced in tumors. Exploration of the methylation status of RNF43 in tumor samples would yield further information about a possible transcriptional repression of RNF43 in tumors. Nevertheless, RNF43 expression was shown to be high in intestinal tumors, especially as tumors progressed (Figure 19), suggesting that transcriptional repression of RNF43 expression in tumors to a great extend is unlikely. Thus, RNF43 may possibly be either transcriptionally repressed only to a lower extent, or in only some tumors.

Since RNF43 expression was shown to be high in intestinal tumors (Figure 19), the next aim was to investigate the function of RNF43 in tumors more precisely. Analysis of RNF43

mRNA levels of intestinal tumor stage II samples revealed very high variations among RNF43 mRNA expression in tumor samples of the same grade (Figure 83). Thus, other factors than grading, e.g. mutations in various genes or deregulated signaling cascades, are likely to influence RNF43 expression levels in tumor stage II samples.

Statistical analysis revealed a correlation between patients with tumors exhibiting high RNF43 expression levels and poor prognosis. In particular, a correlation between patients with tumors exhibiting high RNF43 expression levels and survival, metachronic metastasis and relapse after surgery was identified.

These data indicate that RNF43 is highly expressed in cells responsible for metastasis and relapse. The cells responsible for metastasis and relapse are referred to as cancer stem cells (reviewed in Reya and Clevers 2005; Vermeulen, Sprick et al. 2008; Clevers 2011), indicating that RNF43 mRNA expression may possibly be higher in cancer stem cells that in other cells of the tumor. RNF43 may perhaps be a marker for cancer stem cells, and the presence of more cancer stem cells in tumors exhibiting high RNF43 expression levels would be an explanation for poor prognosis of these patients. Nevertheless, the RNF43 protein levels in cancer stem cells as well as the functionality of the protein in cancer stem cells remain elusive.

There is often a correlation between poor prognosis of patients and tumors with high Wnt signaling, and the expression of the Wnt inhibitor RNF43 was found to correlate with poor prognosis. Therefore, we next thought that a possible functional inactivation of RNF43 in intestinal tumors would be an explanation. An increase in Wnt signaling resulting from inactivated RNF43 would be a possible explanation for the obtained results, and would logically explain the correlation between patients with high RNF43 expression in tumors and poor prognosis, as well as the occurrence of high RNF43 expression at sites of high Wnt signaling like tumors. According to this hypothesis, the high RNF43 levels in tumors would not represent wildtype RNF43, but functionally inactive RNF43. Since functional inactivation of RNF43 was shown to increase levels of Wnt signaling (Figure 25), functionally inactive RNF43 would, according to the hypothesis, be correlated with the high levels of Wnt signaling activity at sites of RNF43 expression.

In order to strengthen this hypothesis, and since RNF43 was found to be frequently mutated in pancreatic cancer (Furukawa, Kuboki et al. 2011; Wu, Jiao et al. 2011), sequence analysis of the *RNF43* gene sequence was performed, and various mutations were identified in all investigated colon cancer cell lines as well as in several intestinal tumor stage II and IV

samples (Figure 85, Figure 86, Figure 88, Figure 89). Mutations found in HT29 colon cancer cells indicate that the two alleles may possibly harbor different mutations in the *RNF43* gene sequence (Figure 85).

Thus, sequence analysis revealed a high level of mutations in colon cancer cells and colon cancer samples. Frequent mutations are likely to impair gene function. Therefore, the mutations in the *RNF43* gene sequence in tumor cells are likely to impair the function of RNF43 and thus promote tumorigenesis, most likely through transactivation of the Wnt signaling pathway.

It could also be possible that in several tumors, mutations in RNF43 not necessarily transactivate Wnt signaling, but rather result in an impaired inhibitory function of the protein. Truncated RNF43 protein versions were shown to completely loose or to exhibit at least weaker inhibitory function on the Wnt signaling pathway (Figure 80). Thus, *in vivo*, these truncated RNF43 proteins, although without transactivating function, would possibly result in abnormal high levels of Wnt signaling due to an impaired inhibitory function of the protein, and these deregulated levels of Wnt signaling would be implicated in the development or progression of tumors.

For example, a high incidence of variations through mutations in the *RNF43* gene sequence was found in HT29 colon cancer cells. Thus, the RNF43 protein is mutated in these cells. Nevertheless, since RNF43 siRNA-mediated knockdown of RNF43 in HT29 resulted in increased levels of Wnt signaling activity (Figure 54B), RNF43 is unlikely to be functionally inactive in HT29 cells. However, an impaired function of RNF43 in HT29 cells due to the mutations is likely.

Nevertheless, RNF43 is likely to be non-functional in at least some tumors, since the RNF43 mutant which was used during this study (p.**H**292**R** (A875→G) and p.**H**295**R**(A884→G)) and transactivated Wnt signaling *in vitro* (Figure 25), was also identified *in vivo* in a tumor stage II sample (Figure 86). Thus, this mutated and functionally inactive variant of RNF43 really exists *in vivo* and is likely to transactivate Wnt signaling not only *in vitro* but most likely also in tumors. Thus, poor prognosis of patients with high RNF43 mRNA expression levels in tumors may possibly result from mutated RNF43, causing increased levels of Wnt signaling activity. Functional analysis of some more mutant variants of RNF43 found in tumor samples regarding their effects on Wnt signaling activity would yield further information.

Thus, in the intestine, RNF43 is likely to function as a tumor suppressor, and functional impairment or inactivation of RNF43 through mutations may lead to abnormal high levels, or transactivation, of Wnt signaling activity and thus tumor progression. Since inactivating mutations of the *RNF43* gene sequence were also detected in several forms of neoplastic cysts in the pancreas (Wu, Jiao et al. 2011), RNF43 may possibly be functionally inactivated or impaired not only in intestinal tumors, but also in tumors of other tissues. Nevertheless, the detailed molecular mechanism of RNF43 remains elusive and further investigation is necessary in order to obtain more information about the function of RNF43.

Mutagenesis of the frequently mutated amino acids in RNF43 followed by investigation of the functions of the mutated constructs would yield further information about the importance of these amino acids regarding the effect on the Wnt signaling pathway.

4.8 RNF43 *knockout* mice

In order to investigate the function of RNF43 *in vivo*, an RNF43 *knockout* mouse line was established. In this mouse model, exons 6 and 7, the two exons that are coding for the RING domain in mice, were flanked by loxP sites. RNF43 fl/wt mice were crossed with RNF43 fl/wt as well as RNF43 fl/wt Villin-Cre +/- mice.

Even in the absence of Cre recombinase, no homozygous RNF43 fl/fl mice were obtained. The genotypes of progeny suggest that even in the absence of a Cre recombinase, the phenotype of RNF43 fl/fl mice is early embryonic lethal, indicating that the introns where the loxP sites were inserted may possibly contain important regulatory sequences for the expression of the *RNF43* gene, or other genes, in mice. Alternatively, insertion of the loxP sequence into the *RNF43* gene locus may possibly interfere with correct splicing of the RNF43 mRNA, rendering the *RNF43* gene non-functional.

A lethal effect of non-functional RNF43 gene copies on both alleles would indicate an essential function of RNF43. Since RNF43 was shown to be strongly expressed in embryonic stem cells of mice (Behnam Kalali, unpublished data), and since the RNF43 fl/fl genotype was never found at pre-implantation stage, an essential function of RNF43 very early in development is suggested.

4.9 The localization of endogenous RNF43 protein

Recently, while this work was in progress, a new antibody, detecting endogenous RNF43 in Immunofluorescence stainings, became available. The antibody recognized an epitope of the RNF43 protein located in the middle of the protein sequence, indicating that it should be able to detect all variants of RNF43, and not only several special splice variants of RNF43.

In HT29 and HCT116 colon cancer cells, endogenous RNF43 localized in punctuate structures inside the nucleoplasm. In some cells, RNF43 was only localized to nucleoplasmic regions, indicating that RNF43 may probably have a function in cell division or cell cycle.

Interestingly, the staining pattern observed in Immunofluorescence stainings using an antibody detecting endogenous RNF43 (Figure 91) was different from the staining pattern observed in Immunofluorescence stainings using antibodies detecting ectopically expressed RNF43 (Figure 30, Figure 31, Figure 33, Figure 34). Overexpressed RNF43 was mainly detectable at the nuclear envelope and only occasionally in the nucleoplasm, whereas only nucleoplasmic RNF43 was detected using an endogenous RNF43 antibody for stainings.

A possible explanation for the distinct Immunofluorescence staining pattern could be that the antibody detecting endogenous RNF43 may perhaps only bind to a specific subform of RNF43, which is folded differently and may expose a specific epitope. Alternatively, the RNF43 antibody may possibly only bind to specific mutated forms of RNF43, since RNF43 was shown to be mutated in both HT29 and HCT116 cells.

As already observed in Western blot analysis (Figure 20), endogenous RNF43 was detectable in HCT116 cells in Immunofluorescence stainings (Figure 91), although a deletion of a nucleotide in HCT116 cells was described to result in a homozygous frameshift mutation in the RNF43 open reading frame (Ivanov, Lo et al. 2007). Although the mutation was also found in our sequence analysis (Figure 85), the detectability of RNF43 in both Western blot analysis and Immunofluorescence stainings in this cell line indicates that the frameshift in the RNF43 open reading frame may possibly only be present in one of the two alleles.

Endogenous RNF43 was not detectable in HEK293T and Cos7 cells (Figure 92), which do not harbor any mutations in the pathway. The detectability of endogenous RNF43 only in cell lines exhibiting mutations in the Wnt signaling cascade, as well as its identification as a Wnt target gene (1.9) suggested a correlation between Wnt signaling activity and endogenous RNF43 protein expression. In order to investigate a possible effect of Wnt signaling activity

on the detectability of endogenous RNF43, Wnt signaling activities in HEK293T and Cos7 cells were increased by treatment with LiCl. However, although treatment of cells with LiCl results in an increase in Wnt signaling activity in HEK293T and Cos7 cells (Figure 22, Figure 23), treatment of these cell lines with LiCl did not result in detectable endogenous RNF43 (Figure 92).

Treatment with LiCl may possibly not have increased Wnt signaling to an extent that would be required for elevating the transcription of the Tcf4 target gene RNF43 to a detectable level. Alternatively, differences between RNF43 protein folding between different cell lines may possibly exist, resulting in detectable endogenous RNF43 protein in colon cancer cell lines, but in non-detectable, differently folded endogenous RNF43 in HEK293T and Cos7 cells.

4.10 Another mechanism of RNF43 function

In accordance with the data obtained during this thesis, in August 2012, few days before the submission of this thesis, a new study of Koo et al. suggested an additional role for RNF43 as a negative regulator of the Wnt signaling (Koo, Spit et al. 2012).

In their study, RNF43 abolished the response to Wnt3A in HEK293T cells, whereas functional inactivation of RNF43 by inserting inactivating point mutations into the RING domain enhanced Wnt signaling. Furthermore, expression of RNF43 in HCT116 cells reversed the effect of Wnt3A. Thus, in accordance with data presented in this study, Koo et al. also suggested a role for RNF43 as a negative regulator of the canonical Wnt signaling pathway. Nevertheless, Koo et al. suggested that RNF43 is located at the plasma membrane, and that RNF43 blocks Wnt signaling by selectively ubiquitinating Frizzled receptors at the plasma membrane and thereby inducing endocytosis and degradation of the receptors, resulting in decreased Wnt signaling.

These data are in accordance with the data obtained by Hao et al., suggesting that RNF43 is located to the plasma membrane, responsible for the degradation of LRP6 and Frizzled in the absence of R-spondin (Hao, Xie et al. 2012). In contrast, we, and others (Miyamoto, Sakurai et al. 2008; Sugiura, Yamaguchi et al. 2008) never observed RNF43 to be located at the plasma membrane, but in the nuclear envelope, the ER and occasionally in the nucleoplasm.

Additionally, we observed RNF43 to inhibit Wnt signaling downstream or at the level of ß-catenin, and RNF43 was additionally found to interact with proteins of the transcription complex (Tcf4, CTBP) during this study.

These data indicate that RNF43 may possibly have two functional mechanisms. The mechanism described by Koo et al. and Hao et al. is likely to be another mechanism than of RNF43 being localized to the nuclear envelope and the nucleoplasm. Thus, two functional mechanisms, depending on protein localization, are suggested.

Koo et al. additionally identified RNF43 as a gene enriched in Lgr5-positive stem cells. They showed that, together with ZNRF3, RNF43 is responsible for the restriction of proliferation in the intestines of mice, since simultaneous conditional *knockout* of both genes resulted in an expansion of the proliferative compartment due to the abnormal high levels of Wnt signaling. Furthermore, simultaneous *knockout* of RNF43 and ZNRF3 resulted in adenoma formation, Wnt target gene expression and increased numbers of progenitor and Paneth cells. Thus, in accordance with our hypothesis, Koo et al. suggested that RNF43 is responsible for restricting the levels of Wnt signaling in the intestine, in order to prevent tumor formation and abnormal proliferation (Koo, Spit et al. 2012).

4.11 Future perspectives

4.11.1 Investigation of the role of RNF43 in intestinal stem cells

In addition to its role in intestinal tumors, RNF43 is likely to have an important function in intestinal stem cells. Van der Flier et al. found RNF43 to be upregulated in GFP-positive epithelial cells from crypts isolated from LGR5-GFP-ires-CreERT mice, indicating that RNF43 is part of the transcriptome of Lgr5 positive intestinal stem cells (van der Flier, van Gijn et al. 2009). Furthermore, Koo et al. identified RNF43 as a gene enriched in Lgr5-positive stem cells, and genetic removal of *ZNRF3* and *RNF43* resulted in abnormal expansion of the stem-cell zone (Koo, Spit et al. 2012). These data, showing that *RNF43* gene expression is upregulated in intestinal stem cells, make it an interesting candidate for further research in this field.

Further investigation is required in order to obtain more information about the molecular mechanism and function of RNF43 in intestinal stem cells. The RNF43-2A-RFP-2A-

CreERT2 mouse model will provide a powerful tool for investigating the *in vivo* functions of RNF43 in intestinal stem cells.

4.11.2 Investigation of the role of RNF43 in cell cycle and cell division

Other possible functions of RNF43, apart from its role in Wnt signaling, cannot be excluded. Since in HT29 and HCT116 cells endogenous RNF43 recently mainly localized to nucleoplasmic regions (Figure 91), RNF43 may probably have a function in cell division or cell cycle. Further investigation will be necessary, also in order to determine whether the localization of RNF43 to punctuate structures is associated with its function in Wnt signaling.

4.11.3 Role of RNF43 in a complex network of signaling pathways

In addition, the possibility that RNF43 is linked to other pathways apart from the Wnt signaling pathway cannot be excluded. There is growing evidence that Wnt signaling cooperates with Notch signaling. For instance, Li et al. suggested that activation of the Notch pathway positively influences the activities of the Wnt signaling pathway through elevation of RNA levels of transcription factors, in order to prime them for being able to rapidly respond upon activation of their pathway (Li, Hibbs et al. 2012). It was also shown that there is a link between Notch signaling and stem cells, since activation of the Notch pathway expands the pool of neural stem cells and has been shown to play a critical role during development and homeostasis of several stem cell compartments (reviewed in Chiba 2006; Li, Hibbs et al. 2012). Thus, a complex network of signaling cascades that regulate single cell fate decisions is suggested. Therefore, investigation of the role of RNF43 in other signaling pathway would be necessary and would yield further information about the detailed function of RNF43 in development, tumorigenesis and homeostasis.

4.12 Closing remarks

With the identification of RNF43 as a novel negative regulator of the canonical Wnt signaling pathway, a novel interesting approach for cancer treatment has been identified. Since commonly known Wnt inhibitors act upstream of the oncogenic mutations found in colon cancer, thus upstream of *APC* and the ß-catenin gene *CTNNB1*, these inhibitors are not able to block the pathway in cancer cells bearing APC or ß-catenin mutations. Therefore, new

inhibitors are needed which act downstream of the oncogenic mutations. Thus, the novel inhibitory function of RNF43 may pave the way for the development of new therapeutic approaches.

5 References

Aberle, H., A. Bauer, et al. (1997). "beta-catenin is a target for the ubiquitin-proteasome pathway." EMBO J **16**(13): 3797-3804.

Abreu, M. T. (2010). "Toll-like receptor signalling in the intestinal epithelium: how bacterial recognition shapes intestinal function." Nat Rev Immunol **10**(2): 131-144.

Adler, P. N. (2002). "Planar signaling and morphogenesis in Drosophila." Dev Cell **2**(5): 525-535.

Ahmed, F. E. (2005). "Molecular markers that predict response to colon cancer therapy." Expert Rev Mol Diagn **5**(3): 353-375.

Akhtar, A. and S. M. Gasser (2007). "The nuclear envelope and transcriptional control." Nat Rev Genet **8**(7): 507-517.

Alonso, L. and E. Fuchs (2003). "Stem cells in the skin: waste not, Wnt not." Genes Dev **17**(10): 1189-1200.

Arnason, T. and M. J. Ellison (1994). "Stress resistance in Saccharomyces cerevisiae is strongly correlated with assembly of a novel type of multiubiquitin chain." Mol Cell Biol **14**(12): 7876-7883.

Austinat, M., R. Dunsch, et al. (2008). "Correlation between beta-catenin mutations and expression of Wnt-signaling target genes in hepatocellular carcinoma." Mol Cancer **7**: 21.

Bafico, A., G. Liu, et al. (2001). "Novel mechanism of Wnt signalling inhibition mediated by Dickkopf-1 interaction with LRP6/Arrow." Nat Cell Biol **3**(7): 683-686.

Barker, N. and H. Clevers (2010). "Lineage tracing in the intestinal epithelium." Curr Protoc Stem Cell Biol **Chapter 5**: Unit5A 4.

Barker, N., M. van de Wetering, et al. (2008). "The intestinal stem cell." Genes Dev **22**(14): 1856-1864.

Barker, N., J. H. van Es, et al. (2007). "Identification of stem cells in small intestine and colon by marker gene Lgr5." Nature **449**(7165): 1003-1007.

Behrens, J., J. P. von Kries, et al. (1996). "Functional interaction of beta-catenin with the transcription factor LEF-1." Nature **382**(6592): 638-642.

Berg, J. M. (1990). "Zinc fingers and other metal-binding domains. Elements for interactions between macromolecules." J Biol Chem **265**(12): 6513-6516.

Bergink, S. and S. Jentsch (2009). "Principles of ubiquitin and SUMO modifications in DNA repair." Nature **458**(7237): 461-467.

Bienz, M. and H. Clevers (2000). "Linking colorectal cancer to Wnt signaling." Cell **103**(2): 311-320.

Bilic, J., Y. L. Huang, et al. (2007). "Wnt induces LRP6 signalosomes and promotes dishevelled-dependent LRP6 phosphorylation." Science **316**(5831): 1619-1622.

Bjerknes, M. and H. Cheng (1981). "The stem-cell zone of the small intestinal epithelium. I. Evidence from Paneth cells in the adult mouse." Am J Anat **160**(1): 51-63.

Bjerknes, M. and H. Cheng (1981). "The stem-cell zone of the small intestinal epithelium. III. Evidence from columnar, enteroendocrine, and mucous cells in the adult mouse." Am J Anat **160**(1): 77-91.

Bjerknes, M. and H. Cheng (1999). "Clonal analysis of mouse intestinal epithelial progenitors." Gastroenterology **116**(1): 7-14.

Bognar, M. (2010). Charakterisierung von Deletionsmutanten von RNF43, einem Negativregulator des Wnt Signalweges. Klinikum Rechts der Isar, II. Medical Department. Munich, Technical University Munich.

Boland, C. R. and A. Goel (2010). "Microsatellite instability in colorectal cancer." Gastroenterology **138**(6): 2073-2087 e2073.

Booth, C. and C. S. Potten (2000). "Intestine instincts: thoughts on intestinal epithelial stem cells." J Clin Invest **105**(11): 1493-1499.

Borden, K. L. (2000). "RING domains: master builders of molecular scaffolds?" J Mol Biol **295**(5): 1103-1112.

Botteri, E., S. Iodice, et al. (2008). "Smoking and colorectal cancer: a meta-analysis." JAMA **300**(23): 2765-2778.

Boutros, M., N. Paricio, et al. (1998). "Dishevelled activates JNK and discriminates between JNK pathways in planar polarity and wingless signaling." Cell **94**(1): 109-118.

Brabletz, S., O. Schmalhofer, et al. (2009). "Gastrointestinal stem cells in development and cancer." The Journal of Pathology **217**(2): 307-317.

Brannon, M., J. D. Brown, et al. (1999). "XCtBP is a XTcf-3 co-repressor with roles throughout Xenopus development." Development **126**(14): 3159-3170.

Burt, R. W., M. F. Leppert, et al. (2004). "Genetic testing and phenotype in a large kindred with attenuated familial adenomatous polyposis." Gastroenterology **127**(2): 444-451.

Cabrera, C. V., M. C. Alonso, et al. (1987). "Phenocopies induced with antisense RNA identify the wingless gene." Cell **50**(4): 659-663.

Cadigan, K. M. and R. Nusse (1997). "Wnt signaling: a common theme in animal development." Genes Dev **11**(24): 3286-3305.

Cameron, E. E., K. E. Bachman, et al. (1999). "Synergy of demethylation and histone deacetylase inhibition in the re-expression of genes silenced in cancer." Nat Genet **21**(1): 103-107.

Capili, A. D., E. L. Edghill, et al. (2004). "Structure of the C-terminal RING finger from a RING-IBR-RING/TRIAD motif reveals a novel zinc-binding domain distinct from a RING." J Mol Biol **340**(5): 1117-1129.

Cavallo, R. A., R. T. Cox, et al. (1998). "Drosophila Tcf and Groucho interact to repress Wingless signalling activity." Nature **395**(6702): 604-608.

Chau, V., J. W. Tobias, et al. (1989). "A multiubiquitin chain is confined to specific lysine in a targeted short-lived protein." Science **243**(4898): 1576-1583.

Cheng, H. (1974). "Origin, differentiation and renewal of the four main epithelial cell types in the mouse small intestine. IV. Paneth cells." Am J Anat **141**(4): 521-535.

Cheng, H. and C. P. Leblond (1974). "Origin, differentiation and renewal of the four main epithelial cell types in the mouse small intestine. I. Columnar cell." Am J Anat **141**(4): 461-479.

Cheng, H. and C. P. Leblond (1974). "Origin, differentiation and renewal of the four main epithelial cell types in the mouse small intestine. V. Unitarian Theory of the origin of the four epithelial cell types." Am J Anat **141**(4): 537-561.

Chiba, S. (2006). "Notch signaling in stem cell systems." Stem Cells **24**(11): 2437-2447.

Chinnadurai, G. (2002). "CtBP, an unconventional transcriptional corepressor in development and oncogenesis." Mol Cell **9**(2): 213-224.

Clevers, H. (2006). "Wnt/beta-catenin signaling in development and disease." Cell **127**(3): 469-480.

Clevers, H. (2011). "The cancer stem cell: premises, promises and challenges." Nature Medicine: 313-319.

Cong, F. and H. Varmus (2004). "Nuclear-cytoplasmic shuttling of Axin regulates subcellular localization of beta-catenin." Proc Natl Acad Sci U S A **101**(9): 2882-2887.

Cuilliere-Dartigues, P., J. El-Bchiri, et al. (2006). "TCF-4 isoforms absent in TCF-4 mutated MSI-H colorectal cancer cells colocalize with nuclear CtBP and repress TCF-4-mediated transcription." Oncogene **25**(32): 4441-4448.

Daniels, D. L., K. Eklof Spink, et al. (2001). "beta-catenin: molecular plasticity and drug design." Trends Biochem Sci **26**(11): 672-678.

Daniels, D. L. and W. I. Weis (2005). "Beta-catenin directly displaces Groucho/TLE repressors from Tcf/Lef in Wnt-mediated transcription activation." Nat Struct Mol Biol **12**(4): 364-371.

Davidson, G., W. Wu, et al. (2005). "Casein kinase 1 gamma couples Wnt receptor activation to cytoplasmic signal transduction." Nature **438**(7069): 867-872.

de Santa Barbara, P., G. R. van den Brink, et al. (2003). "Development and differentiation of the intestinal epithelium." Cell Mol Life Sci **60**(7): 1322-1332.

Fagotto, F., U. Gluck, et al. (1998). "Nuclear localization signal-independent and importin/karyopherin-independent nuclear import of beta-catenin." Curr Biol **8**(4): 181-190.

Fang, M., J. Li, et al. (2006). "C-terminal-binding protein directly activates and represses Wnt transcriptional targets in Drosophila." EMBO J **25**(12): 2735-2745.

Fang, S., K. L. Lorick, et al. (2003). "RING finger ubiquitin protein ligases: implications for tumorigenesis, metastasis and for molecular targets in cancer." Semin Cancer Biol **13**(1): 5-14.

Fearon, E. R. and B. Vogelstein (1990). "A genetic model for colorectal tumorigenesis." Cell **61**(5): 759-767.

Fedi, P., A. Bafico, et al. (1999). "Isolation and biochemical characterization of the human Dkk-1 homologue, a novel inhibitor of mammalian Wnt signaling." J Biol Chem **274**(27): 19465-19472.

Finch, P. W., X. He, et al. (1997). "Purification and molecular cloning of a secreted, Frizzled-related antagonist of Wnt action." Proc Natl Acad Sci U S A **94**(13): 6770-6775.

Finley, D., S. Sadis, et al. (1994). "Inhibition of proteolysis and cell cycle progression in a multiubiquitination-deficient yeast mutant." Mol Cell Biol **14**(8): 5501-5509.

Fisk, H. A. and M. P. Yaffe (1999). "A role for ubiquitination in mitochondrial inheritance in Saccharomyces cerevisiae." J Cell Biol **145**(6): 1199-1208.

Fodde, R., R. Smits, et al. (2001). "APC, signal transduction and genetic instability in colorectal cancer." Nat Rev Cancer **1**(1): 55-67.

Fortunel, N. O., H. H. Otu, et al. (2003). "Comment on " 'Stemness': transcriptional profiling of embryonic and adult stem cells" and "a stem cell molecular signature"." Science **302**(5644): 393; author reply 393.

Freemont, P. S. (1993). "The RING finger. A novel protein sequence motif related to the zinc finger." Ann N Y Acad Sci **684**: 174-192.

Freemont, P. S. (2000). "RING for destruction?" Curr Biol **10**(2): R84-87.

Freemont, P. S., I. M. Hanson, et al. (1991). "A novel cysteine-rich sequence motif." Cell **64**(3): 483-484.

Furukawa, T., Y. Kuboki, et al. (2011). "Whole-exome sequencing uncovers frequent GNAS mutations in intraductal papillary mucinous neoplasms of the pancreas." Sci Rep **1**: 161.

Galan, J. M. and R. Haguenauer-Tsapis (1997). "Ubiquitin lys63 is involved in ubiquitination of a yeast plasma membrane protein." EMBO J **16**(19): 5847-5854.

Galceran, J., I. Farinas, et al. (1999). "Wnt3a-/--like phenotype and limb deficiency in Lef1(-/-)Tcf1(-/-) mice." Genes Dev **13**(6): 709-717.

Giles, R. H., J. H. van Es, et al. (2003). "Caught up in a Wnt storm: Wnt signaling in cancer." Biochim Biophys Acta **1653**(1): 1-24.

Giovannucci, E. (2002). "Modifiable risk factors for colon cancer." Gastroenterol Clin North Am **31**(4): 925-943.

Glinka, A., W. Wu, et al. (1998). "Dickkopf-1 is a member of a new family of secreted proteins and functions in head induction." Nature **391**(6665): 357-362.

Gordon, M. D. and R. Nusse (2006). "Wnt signaling: multiple pathways, multiple receptors, and multiple transcription factors." J Biol Chem **281**(32): 22429-22433.

Grandl, M. I. (2011). Analysis of RING finger protein 43 deletion mutants: from subcellular localization to function. Facultry of Chemistry, Department of Biotechnology. Munich, Technical University Munich.

Gregorieff, A., D. Pinto, et al. (2005). "Expression pattern of Wnt signaling components in the adult intestine." Gastroenterology **129**(2): 626-638.

Groden, J., A. Thliveris, et al. (1991). "Identification and characterization of the familial adenomatous polyposis coli gene." Cell **66**(3): 589-600.

Habas, R. and I. B. Dawid (2005). "Dishevelled and Wnt signaling: is the nucleus the final frontier?" J Biol **4**(1): 2.

Habas, R., I. B. Dawid, et al. (2003). "Coactivation of Rac and Rho by Wnt/Frizzled signaling is required for vertebrate gastrulation." Genes Dev **17**(2): 295-309.

Habas, R., Y. Kato, et al. (2001). "Wnt/Frizzled activation of Rho regulates vertebrate gastrulation and requires a novel Formin homology protein Daam1." Cell **107**(7): 843-854.

Hall, P. A., P. J. Coates, et al. (1994). "Regulation of cell number in the mammalian gastrointestinal tract: the importance of apoptosis." J Cell Sci **107 (Pt 12)**: 3569-3577.

Hamada, F. and M. Bienz (2004). "The APC tumor suppressor binds to C-terminal binding protein to divert nuclear beta-catenin from TCF." Dev Cell **7**(5): 677-685.

Hampel, H., W. L. Frankel, et al. (2008). "Feasibility of screening for Lynch syndrome among patients with colorectal cancer." J Clin Oncol **26**(35): 5783-5788.

Hanahan, D. (1983). "Studies on transformation of Escherichia coli with plasmids." J Mol Biol **166**(4): 557-580.

Hao, H. X., Y. Xie, et al. (2012). "ZNRF3 promotes Wnt receptor turnover in an R-spondin-sensitive manner." Nature **485**(7397): 195-200.

Harland, R. and J. Gerhart (1997). "Formation and function of Spemann's organizer." Annu Rev Cell Dev Biol **13**: 611-667.

Heath, J. P. (1996). "Epithelial cell migration in the intestine." Cell Biol Int **20**(2): 139-146.

Hedgepeth, C. M., L. J. Conrad, et al. (1997). "Activation of the Wnt signaling pathway: a molecular mechanism for lithium action." Dev Biol **185**(1): 82-91.

Heisenberg, C. P., M. Tada, et al. (2000). "Silberblick/Wnt11 mediates convergent extension movements during zebrafish gastrulation." Nature **405**(6782): 76-81.

Henderson, B. R. (2000). "Nuclear-cytoplasmic shuttling of APC regulates beta-catenin subcellular localization and turnover." Nat Cell Biol **2**(9): 653-660.

Hermiston, M. L., R. P. Green, et al. (1993). "Chimeric-transgenic mice represent a powerful tool for studying how the proliferation and differentiation programs of intestinal epithelial cell lineages are regulated." Proc Natl Acad Sci U S A **90**(19): 8866-8870.

Hershko, A. and A. Ciechanover (1998). "The ubiquitin system." Annu Rev Biochem **67**: 425-479.

Hochstrasser, M. (1996). "Ubiquitin-dependent protein degradation." Annu Rev Genet **30**: 405-439.

Hofmann, R. M. and C. M. Pickart (1999). "Noncanonical MMS2-encoded ubiquitin-conjugating enzyme functions in assembly of novel polyubiquitin chains for DNA repair." Cell **96**(5): 645-653.

Hsieh, J. C., L. Kodjabachian, et al. (1999). "A new secreted protein that binds to Wnt proteins and inhibits their activities." Nature **398**(6726): 431-436.

Imai, K., N. Takada, et al. (2000). "(beta)-catenin mediates the specification of endoderm cells in ascidian embryos." Development **127**(14): 3009-3020.

Ionov, Y., M. A. Peinado, et al. (1993). "Ubiquitous somatic mutations in simple repeated sequences reveal a new mechanism for colonic carcinogenesis." Nature **363**(6429): 558-561.

Ivanov, I., K. C. Lo, et al. (2007). "Identifying candidate colon cancer tumor suppressor genes using inhibition of nonsense-mediated mRNA decay in colon cancer cells." Oncogene **26**(20): 2873-2884.

Ivanova, N. B., J. T. Dimos, et al. (2002). "A stem cell molecular signature." Science **298**(5593): 601-604.

Jasperson, K. W., T. M. Tuohy, et al. (2010). "Hereditary and familial colon cancer." Gastroenterology **138**(6): 2044-2058.

Jemal, A., F. Bray, et al. (2011). "Global cancer statistics." CA Cancer J Clin **61**(2): 69-90.

Joazeiro, C. A. and A. M. Weissman (2000). "RING finger proteins: mediators of ubiquitin ligase activity." Cell **102**(5): 549-552.

Johnson, G. L. and K. Nakamura (2007). "The c-jun kinase/stress-activated pathway: regulation, function and role in human disease." Biochim Biophys Acta **1773**(8): 1341-1348.

Jones, P. L., G. J. Veenstra, et al. (1998). "Methylated DNA and MeCP2 recruit histone deacetylase to repress transcription." Nat Genet **19**(2): 187-191.

Joslyn, G., D. S. Richardson, et al. (1993). "Dimer formation by an N-terminal coiled coil in the APC protein." Proc Natl Acad Sci U S A **90**(23): 11109-11113.

Kawano, Y. and R. Kypta (2003). "Secreted antagonists of the Wnt signalling pathway." J Cell Sci **116**(Pt 13): 2627-2634.

Kazanskaya, O., A. Glinka, et al. (2004). "R-Spondin2 is a secreted activator of Wnt/beta-catenin signaling and is required for Xenopus myogenesis." Dev Cell **7**(4): 525-534.

Kikkert, M., R. Doolman, et al. (2004). "Human HRD1 is an E3 ubiquitin ligase involved in degradation of proteins from the endoplasmic reticulum." J Biol Chem **279**(5): 3525-3534.

Kim, B. M., J. Mao, et al. (2007). "Phases of Canonical Wnt Signaling During the Development of Mouse Intestinal Epithelium." Gastroenterology **133**(2): 529-538.

Kim, K. A., M. Kakitani, et al. (2005). "Mitogenic influence of human R-spondin1 on the intestinal epithelium." Science **309**(5738): 1256-1259.

Kinzler, K. W., M. C. Nilbert, et al. (1991). "Identification of FAP locus genes from chromosome 5q21." Science **253**(5020): 661-665.

Kishida, S., H. Yamamoto, et al. (1999). "DIX domains of Dvl and axin are necessary for protein interactions and their ability to regulate beta-catenin stability." Mol Cell Biol **19**(6): 4414-4422.

Klaus, A. and W. Birchmeier (2008). "Wnt signalling and its impact on development and cancer." Nat Rev Cancer **8**(5): 387-398.

Klein, P. S. and D. A. Melton (1996). "A molecular mechanism for the effect of lithium on development." Proc Natl Acad Sci U S A **93**(16): 8455-8459.

Komiya, Y. and R. Habas (2008). "Wnt signal transduction pathways." Organogenesis **4**(2): 68-75.

Koo, B. K., M. Spit, et al. (2012). "Tumour suppressor RNF43 is a stem-cell E3 ligase that induces endocytosis of Wnt receptors." Nature **488**(7413): 665-669.

Korinek, V. (1997). "Constitutive Transcriptional Activation by a beta -Catenin-Tcf Complex in APC-/- Colon Carcinoma." Science **275**(5307): 1784-1787.

Korinek, V., N. Barker, et al. (1998). "Depletion of epithelial stem-cell compartments in the small intestine of mice lacking Tcf-4." Nat Genet **19**(4): 379-383.

Kuhl, M. (2002). "Non-canonical Wnt signaling in Xenopus: regulation of axis formation and gastrulation." Semin Cell Dev Biol **13**(3): 243-249.

Kuhl, M., L. C. Sheldahl, et al. (2000). "The Wnt/Ca2+ pathway: a new vertebrate Wnt signaling pathway takes shape." Trends Genet **16**(7): 279-283.

Levanon, D., R. E. Goldstein, et al. (1998). "Transcriptional repression by AML1 and LEF-1 is mediated by the TLE/Groucho corepressors." Proc Natl Acad Sci U S A **95**(20): 11590-11595.

Levkowitz, G., H. Waterman, et al. (1999). "Ubiquitin ligase activity and tyrosine phosphorylation underlie suppression of growth factor signaling by c-Cbl/Sli-1." Mol Cell **4**(6): 1029-1040.

Leyns, L., T. Bouwmeester, et al. (1997). "Frzb-1 is a secreted antagonist of Wnt signaling expressed in the Spemann organizer." Cell **88**(6): 747-756.

Li, Y., M. A. Hibbs, et al. (2012). "Genome-Wide Analysis of N1ICD/RBPJ Targets in vivo Reveals Direct Transcriptional Regulation of Wnt, SHH, and Hippo Pathway Effectors by Notch1." Stem Cells.

Lin, G., N. Xu, et al. (2008). "Paracrine Wingless signalling controls self-renewal of Drosophila intestinal stem cells." Nature **455**(7216): 1119-1123.

Liu, J. and A. Lin (2005). "Role of JNK activation in apoptosis: a double-edged sword." Cell Res **15**(1): 36-42.

Liu, P., M. Wakamiya, et al. (1999). "Requirement for Wnt3 in vertebrate axis formation." Nat Genet **22**(4): 361-365.

Liu, W., X. Dong, et al. (2000). "Mutations in AXIN2 cause colorectal cancer with defective mismatch repair by activating beta-catenin/TCF signalling." Nat Genet **26**(2): 146-147.

Livak, K. J. and T. D. Schmittgen (2001). "Analysis of relative gene expression data using real-time quantitative PCR and the 2(-Delta Delta C(T)) Method." Methods **25**(4): 402-408.

Logan, C. Y. and R. Nusse (2004). "The Wnt signaling pathway in development and disease." Annu Rev Cell Dev Biol **20**: 781-810.

Lorick, K. L., J. P. Jensen, et al. (1999). "RING fingers mediate ubiquitin-conjugating enzyme (E2)-dependent ubiquitination." Proc Natl Acad Sci U S A **96**(20): 11364-11369.

Lovering, R., I. M. Hanson, et al. (1993). "Identification and preliminary characterization of a protein motif related to the zinc finger." Proc Natl Acad Sci U S A **90**(6): 2112-2116.

Luo, J., J. Chen, et al. (2007). "Wnt signaling and human diseases: what are the therapeutic implications?" Lab Invest **87**(2): 97-103.

Lynch, H. T. and A. de la Chapelle (2003). "Hereditary colorectal cancer." N Engl J Med **348**(10): 919-932.

Madison, B. B., L. Dunbar, et al. (2002). "Cis elements of the villin gene control expression in restricted domains of the vertical (crypt) and horizontal (duodenum, cecum) axes of the intestine." J Biol Chem **277**(36): 33275-33283.

Mao, B., W. Wu, et al. (2002). "Kremen proteins are Dickkopf receptors that regulate Wnt/beta-catenin signalling." Nature **417**(6889): 664-667.

Mao, B., W. Wu, et al. (2001). "LDL-receptor-related protein 6 is a receptor for Dickkopf proteins." Nature **411**(6835): 321-325.

Mao, J., J. Wang, et al. (2001). "Low-density lipoprotein receptor-related protein-5 binds to Axin and regulates the canonical Wnt signaling pathway." Mol Cell **7**(4): 801-809.

Markiewicz, E., K. Tilgner, et al. (2006). "The inner nuclear membrane protein emerin regulates beta-catenin activity by restricting its accumulation in the nucleus." EMBO J **25**(14): 3275-3285.

Marlow, F., J. Topczewski, et al. (2002). "Zebrafish Rho kinase 2 acts downstream of Wnt11 to mediate cell polarity and effective convergence and extension movements." Curr Biol **12**(11): 876-884.

Marshman, E., C. Booth, et al. (2002). "The intestinal epithelial stem cell." Bioessays **24**(1): 91-98.

McMahon, A. P. and A. Bradley (1990). "The Wnt-1 (int-1) proto-oncogene is required for development of a large region of the mouse brain." Cell **62**(6): 1073-1085.

Mekhail, K. and D. Moazed (2010). "The nuclear envelope in genome organization, expression and stability." Nat Rev Mol Cell Biol **11**(5): 317-328.

Miller, J. R., A. M. Hocking, et al. (1999). "Mechanism and function of signal transduction by the Wnt/beta-catenin and Wnt/Ca2+ pathways." Oncogene **18**(55): 7860-7872.

Miyaki, M., M. Konishi, et al. (1994). "Characteristics of somatic mutation of the adenomatous polyposis coli gene in colorectal tumors." Cancer Res **54**(11): 3011-3020.

Miyamoto, K., H. Sakurai, et al. (2008). "Proteomic identification of a PSF/p54nrb heterodimer as RNF43 oncoprotein-interacting proteins." Proteomics **8**(14): 2907-2910.

Miyoshi, Y., H. Ando, et al. (1992). "Germ-line mutations of the APC gene in 53 familial adenomatous polyposis patients." Proc Natl Acad Sci U S A **89**(10): 4452-4456.

Molenaar, M., M. van de Wetering, et al. (1996). "XTcf-3 transcription factor mediates beta-catenin-induced axis formation in Xenopus embryos." Cell **86**(3): 391-399.

Moon, R. T., J. D. Brown, et al. (1997). "WNTs modulate cell fate and behavior during vertebrate development." Trends Genet **13**(4): 157-162.

Moon, R. T., A. D. Kohn, et al. (2004). "WNT and beta-catenin signalling: diseases and therapies." Nat Rev Genet **5**(9): 691-701.

Moran, A., P. Ortega, et al. (2010). "Differential colorectal carcinogenesis: Molecular basis and clinical relevance." World J Gastrointest Oncol **2**(3): 151-158.

Morin, P. J., A. B. Sparks, et al. (1997). "Activation of beta-catenin-Tcf signaling in colon cancer by mutations in beta-catenin or APC." Science **275**(5307): 1787-1790.

Morin, P. J., B. Vogelstein, et al. (1996). "Apoptosis and APC in colorectal tumorigenesis." Proc Natl Acad Sci U S A **93**(15): 7950-7954.

Nicolas, P., K. M. Kim, et al. (2007). "The stem cell population of the human colon crypt: analysis via methylation patterns." PLoS Comput Biol **3**(3): e28.

Nieuwkoop, P. D., Faber, J. (1967). "Normal tables of Xenopus laevis (Daudin)." Elsevier North Holland Biomedical Press, Amsterdam.

Nishisho, I., Y. Nakamura, et al. (1991). "Mutations of chromosome 5q21 genes in FAP and colorectal cancer patients." Science **253**(5020): 665-669.

Novelli, M., A. Cos7su, et al. (2003). "X-inactivation patch size in human female tissue confounds the assessment of tumor clonality." Proc Natl Acad Sci U S A **100**(6): 3311-3314.

Nusse, R. (2008). "Wnt signaling and stem cell control." Cell Research **18**(5): 523-527.

Nusse, R. and H. E. Varmus (1982). "Many tumors induced by the mouse mammary tumor virus contain a provirus integrated in the same region of the host genome." Cell **31**(1): 99-109.

Nusse, R. and H. E. Varmus (1992). "Wnt genes." Cell **69**(7): 1073-1087.

O'Brien, W. T., A. D. Harper, et al. (2004). "Glycogen synthase kinase-3beta haploinsufficiency mimics the behavioral and molecular effects of lithium." J Neurosci **24**(30): 6791-6798.

Paliwal, S., S. Pande, et al. (2006). "Targeting of C-terminal binding protein (CtBP) by ARF results in p53-independent apoptosis." Mol Cell Biol **26**(6): 2360-2372.

Parkin, D. M. (2004). "International variation." Oncogene **23**(38): 6329-6340.

Parr, B. A. and A. P. McMahon (1994). "Wnt genes and vertebrate development." Curr Opin Genet Dev **4**(4): 523-528.

Parr, B. A. and A. P. McMahon (1995). "Dorsalizing signal Wnt-7a required for normal polarity of D-V and A-P axes of mouse limb." Nature **374**(6520): 350-353.

Patton, J. G., E. B. Porro, et al. (1993). "Cloning and characterization of PSF, a novel pre-mRNA splicing factor." Genes Dev **7**(3): 393-406.

Peltomaki, P. (2001). "Deficient DNA mismatch repair: a common etiologic factor for colon cancer." Hum Mol Genet **10**(7): 735-740.

Pickart, C. M. (2000). "Ubiquitin in chains." Trends Biochem Sci **25**(11): 544-548.

Pickart, C. M. (2001). "Mechanisms underlying ubiquitination." Annu Rev Biochem **70**: 503-533.

Pickart, C. M. (2001). "Ubiquitin enters the new millennium." Mol Cell **8**(3): 499-504.

Pinto, D. and H. Clevers (2005). "Wnt control of stem cells and differentiation in the intestinal epithelium." Exp Cell Res **306**(2): 357-363.

Pinto, D., A. Gregorieff, et al. (2003). "Canonical Wnt signals are essential for homeostasis of the intestinal epithelium." Genes Dev **17**(14): 1709-1713.

Polakis, P. (2000). "Wnt signaling and cancer." Genes Dev **14**(15): 1837-1851.

Polesskaya, A., P. Seale, et al. (2003). "Wnt signaling induces the myogenic specification of resident CD45+ adult stem cells during muscle regeneration." Cell **113**(7): 841-852.

Potten, C. S. (1977). "Extreme sensitivity of some intestinal crypt cells to X and gamma irradiation." Nature **269**(5628): 518-521.

Potten, C. S., C. Booth, et al. (1997). "The intestinal epithelial stem cell: the muCos7al governor." Int J Exp Pathol **78**(4): 219-243.

Potten, C. S., L. Kovacs, et al. (1974). "Continuous labelling studies on mouse skin and intestine." Cell Tissue Kinet **7**(3): 271-283.

Potten, C. S. and M. Loeffler (1990). "Stem cells: attributes, cycles, spirals, pitfalls and uncertainties. Lessons for and from the crypt." Development **110**(4): 1001-1020.

Potten, C. S., G. Owen, et al. (2002). "Intestinal stem cells protect their genome by selective segregation of template DNA strands." J Cell Sci **115**(Pt 11): 2381-2388.

Powell, S. M., N. Zilz, et al. (1992). "APC mutations occur early during colorectal tumorigenesis." Nature **359**(6392): 235-237.

Radtke, F. and H. Clevers (2005). "Self-renewal and cancer of the intestine: two sides of a coin." Science **307**(5717): 1904-1909.

Ramalho-Santos, M., S. Yoon, et al. (2002). ""Stemness": transcriptional profiling of embryonic and adult stem cells." Science **298**(5593): 597-600.

Reya, T. and H. Clevers (2005). "Wnt signalling in stem cells and cancer." Nature **434**(7035): 843-850.

Reya, T., A. W. Duncan, et al. (2003). "A role for Wnt signalling in self-renewal of haematopoietic stem cells." Nature **423**(6938): 409-414.

Rijsewijk, F., M. Schuermann, et al. (1987). "The Drosophila homolog of the mouse mammary oncogene int-1 is identical to the segment polarity gene wingless." Cell **50**(4): 649-657.

Roose, J., M. Molenaar, et al. (1998). "The Xenopus Wnt effector XTcf-3 interacts with Groucho-related transcriptional repressors." Nature **395**(6702): 608-612.

Rosin-Arbesfeld, R., F. Townsley, et al. (2000). "The APC tumour suppressor has a nuclear export function." Nature **406**(6799): 1009-1012.

Roth, K. A., M. L. Hermiston, et al. (1991). "Use of transgenic mice to infer the biological properties of small intestinal stem cells and to examine the lineage relationships of their descendants." Proc Natl Acad Sci U S A **88**(21): 9407-9411.

Rubinfeld, B., P. Robbins, et al. (1997). "Stabilization of beta-catenin by genetic defects in melanoma cell lines." Science **275**(5307): 1790-1792.

Rubinfeld, B., B. Souza, et al. (1993). "Association of the APC gene product with beta-catenin." Science **262**(5140): 1731-1734.

Saadeddin, A., R. Babaei-Jadidi, et al. (2009). "The links between transcription, beta-catenin/JNK signaling, and carcinogenesis." Mol Cancer Res **7**(8): 1189-1196.

Sangiorgi, E. and M. R. Capecchi (2008). "Bmi1 is expressed in vivo in intestinal stem cells." Nature Genetics **40**(7): 915-920.

Saurin, A. J., K. L. Borden, et al. (1996). "Does this have a familiar RING?" Trends Biochem Sci **21**(6): 208-214.

Schneider, R. and R. Grosschedl (2007). "Dynamics and interplay of nuclear architecture, genome organization, and gene expression." Genes Dev **21**(23): 3027-3043.

Scoville, D. H., T. Sato, et al. (2008). "Current view: intestinal stem cells and signaling." Gastroenterology **134**(3): 849-864.

Semenov, M. V., K. Tamai, et al. (2001). "Head inducer Dickkopf-1 is a ligand for Wnt coreceptor LRP6." Curr Biol **11**(12): 951-961.

Shav-Tal, Y. and D. Zipori (2002). "PSF and p54(nrb)/NonO--multi-functional nuclear proteins." FEBS Lett **531**(2): 109-114.

Shih, J. and R. Keller (1992). "Patterns of cell motility in the organizer and dorsal mesoderm of Xenopus laevis." Development **116**(4): 915-930.

Shinada, K., T. Tsukiyama, et al. (2011). "RNF43 interacts with NEDL1 and regulates p53-mediated transcription." Biochemical and Biophysical Research Communications **404**(1): 143-147.

Shitashige, M., R. Satow, et al. (2008). "Regulation of Wnt signaling by the nuclear pore complex." Gastroenterology **134**(7): 1961-1971, 1971 e1961-1964.

Smith, J. C., F. L. Conlon, et al. (2000). "Xwnt11 and the regulation of gastrulation in Xenopus." Philos Trans R Soc Lond B Biol Sci **355**(1399): 923-930.

Snippert, H. J. and H. Clevers (2011). "Tracking adult stem cells." EMBO Rep **12**(2): 113-122.

Sokol, S. Y. (1999). "Wnt signaling and dorso-ventral axis specification in vertebrates." Curr Opin Genet Dev **9**(4): 405-410.

Spence, J., S. Sadis, et al. (1995). "A ubiquitin mutant with specific defects in DNA repair and multiubiquitination." Mol Cell Biol **15**(3): 1265-1273.

Spirio, L., S. Olschwang, et al. (1993). "Alleles of the APC gene: an attenuated form of familial polyposis." Cell **75**(5): 951-957.

Sporle, R. and K. Schughart (1998). "Paradox segmentation along inter- and intrasomitic borderlines is followed by dysmorphology of the axial skeleton in the open brain (opb) mouse mutant." Dev Genet **22**(4): 359-373.

Stadeli, R., R. Hoffmans, et al. (2006). "Transcription under the control of nuclear Arm/beta-catenin." Curr Biol **16**(10): R378-385.

Stappenbeck, T. S., J. C. Mills, et al. (2003). "Molecular features of adult mouse small intestinal epithelial progenitors." Proc Natl Acad Sci U S A **100**(3): 1004-1009.

Stappenbeck, T. S., M. H. Wong, et al. (1998). "Notes from some crypt watchers: regulation of renewal in the mouse intestinal epithelium." Curr Opin Cell Biol **10**(6): 702-709.

Stark, K., S. Vainio, et al. (1994). "Epithelial transformation of metanephric mesenchyme in the developing kidney regulated by Wnt-4." Nature **372**(6507): 679-683.

Stoffel, E., B. Mukherjee, et al. (2009). "Calculation of risk of colorectal and endometrial cancer among patients with Lynch syndrome." Gastroenterology **137**(5): 1621-1627.

Su, L. K., B. Vogelstein, et al. (1993). "Association of the APC tumor suppressor protein with catenins." Science **262**(5140): 1734-1737.

Sugiura, T., A. Yamaguchi, et al. (2008). "A cancer-associated RING finger protein, RNF43, is a ubiquitin ligase that interacts with a nuclear protein, HAP95." Experimental Cell Research **314**(7): 1519-1528.

Takemasa, I., H. Higuchi, et al. (2001). "Construction of preferential cDNA microarray specialized for human colorectal carcinoma: molecular sketch of colorectal cancer." Biochem Biophys Res Commun **285**(5): 1244-1249.

Thibodeau, S. N., G. Bren, et al. (1993). "Microsatellite instability in cancer of the proximal colon." Science **260**(5109): 816-819.

Thomas, K. R. and M. R. Capecchi (1990). "Targeted disruption of the murine int-1 proto-oncogene resulting in severe abnormalities in midbrain and cerebellar development." Nature **346**(6287): 847-850.

Tian, H., B. Biehs, et al. (2011). "A reserve stem cell population in small intestine renders Lgr5-positive cells dispensable." Nature **478**(7368): 255-259.

Uchida, N., T. Tsunoda, et al. (2004). "Ring finger protein 43 as a new target for cancer immunotherapy." Clin Cancer Res **10**(24): 8577-8586.

Valenta, T., J. Lukas, et al. (2003). "HMG box transcription factor TCF-4's interaction with CtBP1 controls the expression of the Wnt target Axin2/Conductin in human embryonic kidney cells." Nucleic Acids Res **31**(9): 2369-2380.

van de Wetering, M., R. Cavallo, et al. (1997). "Armadillo coactivates transcription driven by the product of the Drosophila segment polarity gene dTCF." Cell **88**(6): 789-799.

van de Wetering, M., E. Sancho, et al. (2002). "The beta-catenin/TCF-4 complex imposes a crypt progenitor phenotype on colorectal cancer cells." Cell **111**(2): 241-250.

van der Flier, L. G. and H. Clevers (2009). "Stem cells, self-renewal, and differentiation in the intestinal epithelium." Annu Rev Physiol **71**: 241-260.

Van der Flier, L. G., J. Sabates-Bellver, et al. (2007). "The Intestinal Wnt/TCF Signature." Gastroenterology **132**(2): 628-632.

van der Flier, L. G., M. E. van Gijn, et al. (2009). "Transcription Factor Achaete Scute-Like 2 Controls Intestinal Stem Cell Fate." Cell **136**(5): 903-912.

van Wijk, S. J., S. J. de Vries, et al. (2009). "A comprehensive framework of E2-RING E3 interactions of the human ubiquitin-proteasome system." Mol Syst Biol **5**: 295.

Varshavsky, A. (1997). "The ubiquitin system." Trends Biochem Sci **22**(10): 383-387.

Veeman, M. T., J. D. Axelrod, et al. (2003). "A second canon. Functions and mechanisms of beta-catenin-independent Wnt signaling." Dev Cell **5**(3): 367-377.

Vermeulen, L., M. R. Sprick, et al. (2008). "Cancer stem cells – old concepts, new insights." Cell Death and Differentiation **15**(6): 947-958.

Voog, J. and D. L. Jones (2010). "Stem cells and the niche: a dynamic duo." Cell Stem Cell **6**(2): 103-115.

Wallingford, J. B., S. E. Fraser, et al. (2002). "Convergent extension: the molecular control of polarized cell movement during embryonic development." Dev Cell **2**(6): 695-706.

Wallingford, J. B., B. A. Rowning, et al. (2000). "Dishevelled controls cell polarity during Xenopus gastrulation." Nature **405**(6782): 81-85.

Wang, S., M. Krinks, et al. (1997). "Frzb, a secreted protein expressed in the Spemann organizer, binds and inhibits Wnt-8." Cell **88**(6): 757-766.

Wehrle, E. (2010). Development, verification and functional analysis regarding Wnt.signaling of RNF43/RNF43 H292 deletion mutants. Lehrstuhl für Medizintechnik. Munich, Technical University Munich.

Weissman, A. M. (2001). "Themes and variations on ubiquitylation." Nat Rev Mol Cell Biol **2**(3): 169-178.

Wells, J. M. and D. A. Melton (1999). "Vertebrate endoderm development." Annu Rev Cell Dev Biol **15**: 393-410.

Wharton, K. A., Jr. (2003). "Runnin' with the Dvl: proteins that associate with Dsh/Dvl and their significance to Wnt signal transduction." Dev Biol **253**(1): 1-17.

White, B. D., N. K. Nguyen, et al. (2007). "Wnt signaling: it gets more humorous with age." Curr Biol **17**(21): R923-925.

Winter, C. G., B. Wang, et al. (2001). "Drosophila Rho-associated kinase (Drok) links Frizzled-mediated planar cell polarity signaling to the actin cytoskeleton." Cell **105**(1): 81-91.

Wodarz, A. and R. Nusse (1998). "Mechanisms of Wnt signaling in development." Annu Rev Cell Dev Biol **14**: 59-88.

Wong, D. J., H. Liu, et al. (2008). "Module map of stem cell genes guides creation of epithelial cancer stem cells." Cell Stem Cell **2**(4): 333-344.

Wong, H. C., A. Bourdelas, et al. (2003). "Direct binding of the PDZ domain of Dishevelled to a conserved internal sequence in the C-terminal region of Frizzled." Mol Cell **12**(5): 1251-1260.

Worman, H. J., C. D. Evans, et al. (1990). "The lamin B receptor of the nuclear envelope inner membrane: a polytopic protein with eight potential transmembrane domains." J Cell Biol **111**(4): 1535-1542.

Worman, H. J., J. Yuan, et al. (1988). "A lamin B receptor in the nuclear envelope." Proc Natl Acad Sci U S A **85**(22): 8531-8534.

Wu, J., Y. Jiao, et al. (2011). "Whole-exome sequencing of neoplastic cysts of the pancreas reveals recurrent mutations in components of ubiquitin-dependent pathways." Proc Natl Acad Sci U S A **108**(52): 21188-21193.

Yagyu, R., Y. Furukawa, et al. (2004). "A novel oncoprotein RNF43 functions in an autocrine manner in colorectal cancer." Int J Oncol **25**(5): 1343-1348.

Yamada, M. (2006). "NARF, an Nemo-like Kinase (NLK)-associated Ring Finger Protein Regulates the Ubiquitylation and Degradation of T Cell Factor/Lymphoid Enhancer Factor (TCF/LEF)." Journal of Biological Chemistry **281**(30): 20749-20760.

Yamamoto, H., M. Ihara, et al. (2003). "Sumoylation is involved in beta-catenin-dependent activation of Tcf-4." EMBO J **22**(9): 2047-2059.

Yamamoto, H., H. Komekado, et al. (2006). "Caveolin is necessary for Wnt-3a-dependent internalization of LRP6 and accumulation of beta-catenin." Dev Cell **11**(2): 213-223.

Yamamoto, H., H. Sakane, et al. (2008). "Wnt3a and Dkk1 regulate distinct internalization pathways of LRP6 to tune the activation of beta-catenin signaling." Dev Cell **15**(1): 37-48.

Yang, Y., S. Fang, et al. (2000). "Ubiquitin protein ligase activity of IAPs and their degradation in proteasomes in response to apoptotic stimuli." Science **288**(5467): 874-877.

Yokouchi, M., T. Kondo, et al. (1999). "Ligand-induced ubiquitination of the epidermal growth factor receptor involves the interaction of the c-Cbl RING finger and UbcH7." J Biol Chem **274**(44): 31707-31712.

Yost, C., M. Torres, et al. (1996). "The axis-inducing activity, stability, and subcellular distribution of beta-catenin is regulated in Xenopus embryos by glycogen synthase kinase 3." Genes Dev **10**(12): 1443-1454.

Zeng, X., K. Tamai, et al. (2005). "A dual-kinase mechanism for Wnt co-receptor phosphorylation and activation." Nature **438**(7069): 873-877.